Project details

Project title	Biomass Gasification Polygeneration – Polygeneration of heat, power and bioSNG in a Danish smart-grid context
Project identification (program abbrev. and file)	ForskVE 12205 (transferred to EUDP during the project period)
Name of the programme which has funded the project	ForskVE
Project managing company/institution	Technical University of Denmark, Department of Chemical and Biochemical Engineering, CHEC centre, Risø division. Building 313, Frederiksborgvej 399, 4000 Roskilde.
Project partners	Technical University of Denmark (DTU-KT + DTU-MEK) Danish Gas Technology Center Dall Energy
CVR (central business register)	30060946
Date for submission	November 7th 2018

Table of Contents

1. Short description of project objective and results

This project investigates a *polygeneration* concept that can either produce or consume power, and store electricity as biofuels. Specifically, the project analyzed the coupling of the TwoStage Viking gasifier with solid oxide cells and the upscaling potential of the gasifier. It is found that the gasifier can be integrated with a SOFC and utilize oxygen (instead of air) without any major modifications and that the performance is state-of-the-art. A thermoeconomic analysis of the polygeneration concept highlights the benefits of polygeneration. Several >10MW_{th} TwoStage gasifier designs have been generated and a significant potential is found.

Dette projekt undersøger et *polygeneration* koncept, der enten kan producerer eller forbruge el og samtidig lagre el i biobrændstoffer. Specifikt analyserer projektet koblingen mellem To-trins Viking forgasseren og fast-oxid celler, samt forgasserens opskaleringspotentiale. Det er påvist at forgasseren kan integreres med både SOFC og anvende iltblæsning (fremfor luft) uden nogen større modifikationer og at systemets performance er state-of-the-art. En termo-økonomisk analyse af konceptet fremhævede fordelene ved polygeneration. Adskillige >10MW_{th} To-trins forgasningsdesign blev genereret og der ses et markant potentiale.

2. Executive summary

This study investigates a proposed *polygeneration* concept that can either produce or consume power, and store electricity as biofuels. The concept consist of a joint platform of thermal biomass gasification and solid oxide cell technologies that form a very efficient and flexible system. This system has two operational states: 1) The gasifier operates with air and the resulting product gas is fed to the solid oxide fuel cell (SOFC) for power production; 2) The cells are now operated as electrolysis cells (SOEC), converting power and steam into H_2 and O_2, which is then fed to the gasifier that produces a N_2-free gas suited for biofuel synthesis. The polygeneration study is centered around the state-of-the-art TwoStage gasification concept. This project seeks to provide the foundation for future polygeneration plants by performing experimental proof-of-concepts and analysis for the two operational states, and provide theoretical investigations of large-scale configurations of the gasification system. The project is divided into four main parts.

The first part of the project studies the coupling of the 80kW_{th} TwoStage Viking pilot gasifier plant and an 800W_e SOFC stack from Topsoe Fuel Cell for power production. The coupling has been suggested as highly efficient and competitive, and the aim of this study is therefore to assess the performance characteristics of this coupling. This was done during two experimental campaigns respectively. Initially, the SOFC was operated with product gas at part-load performance down to 55% flow rate and is found to maintain its electric efficiency. The peak electric efficiency is found to 46% gas-to-power, which is the highest reported value in the literature for product gas operation. The performance correlates to ≈40% biomass-to-power efficiency for the entire system, which is in line with previous investigations. In the second campaign the impact of applying minimal or no gas cleaning between the gasifier and SOFC is studied along with operational characteristics. Initially, tests were performed with an air-blown product gas at SOFC operating temperatures of 700^{o}C and 800^{o}C. A power and efficiency increase of 8-11% and 4%-points respectively is found at 800^{o}C. Afterwards, the gas cleaning were bypassed, no short-term changes in operational voltage was seen with 1.5-2.8ppm sulphur in the feed gas.

The second part of the project performs a comparative study of the Viking pilot plant, where air-blown operation were changed to O_2-CO_2-blown. The purpose is to achieve an N_2-free gas and analyze the gasifier operation, performance and gas quality. Thermodynamic modeling was initially applied, where it is seen that the operational characteristics are within range of air if 21v% O_2-in-CO_2 is applied and nearly identical parameters at 30v% O_2. The pilot plant was then modified and prepared and an experimental campaign was carried out with air, 21v% O_2–in-CO_2 and 25v% O_2–in-CO_2. The results validated the tendencies of the modeling studies, as operation temperatures were seen to slightly decrease at 21v% O_2-in-CO_2: the partial oxidation temperature by 52-69^{o}C and grate temperature by 31-36^{o}C. As expected, 25v% O_2 showed characteristics between these value and air-operation. Detailed gas analysis showed that the tar and sulphur concentrations of a few mg/Nm^3 and <3ppm respectively, are similarly low across the gasification media and that the N_2-content is reduced to a few percentages.

The third part consists of a thermoeconomic analysis of the proposed polygeneration concept described above. Thermodynamic modeling and simulation of the polygeneration plant is performed to calculate the energy efficiency of each operating mode, and to size the different components in terms of energy output. The analysis showed that the electricity production mode achieves a biomass to electricity efficiency of 46% and when including heat production, the total efficiency is 90%. The electricity storage mode or biofuel production mode achieves a biomass + electricity to biofuel efficiency of 69% and a total efficiency of 85%.
The economic analysis indicated that polygeneration systems are more attractive than single mode systems because higher capacity factors are achieved and the investment in the polygeneration system is lower than the combined investment of two single mode systems. Furthermore, the operation of the polygeneration system depends greatly on the future electricity prices: in some scenarios, the system operates most in electricity production mode while in others most in electricity storage mode. The advantage with polygeneration is found to be greatest when electricity prices are volatile.

The fourth part of the project analyzed the possibility of developing large-scale plant designs of >10MW$_{th}$ based on the TwoStage gasification concept and to investigate whether they could be integrated in a polygeneration context respectively. In the initial study, the project analyses the potential for wood-based fixed bed and fluid bed systems. Amongst several, two noteworthy new design features was implemented in the concepts: 1) applying a pyrolysis reactor with recirculation of gas for utilizing available heat sources indirectly and avoid dilution; 2) applying subsequent cooling of the hot partial oxidation gases with drying steam. These two features led to three main design concepts, which were shown to achieve very high cold gas efficiencies and are expected to require minimal tar removal downstream. The three concepts achieved cold gas efficiencies of 88-93%. The concept with two updraft reactors proved to be especially interesting. While still in the developmental phase, the cold gas efficiencies were found to be 6-22%-points higher than current state-of-the-art gasifiers, whilst applying minimal or very simple gas cleaning in comparison. In the second study, the aim was to design systems capable of polygeneration with air and 50v% O_2-H_2O. Three different plant configurations are presented: all apply fluid bed gasification reactors, but with either an updraft, slow fluid bed or fast fluid bed pyrolysis coupling. In order to expand the analysis, the use of wood and straw fuels are investigated. The results show relatively stable plant operation and cold gas efficiencies of 83-88%. In line with the initial study, the concepts are found to have significant potential and be – on a technical basis - competitive with current state-of-the-art gasifier with regards to cold gas efficiency, gas cleaning equipment and fuel flexibility.

3. Project objectives

3.1 Overall aim

This project investigates the technical feasibility and potential of a biomass based poly-generation plant incorporating storage of electricity from fluctuating sources – see Figure 1.

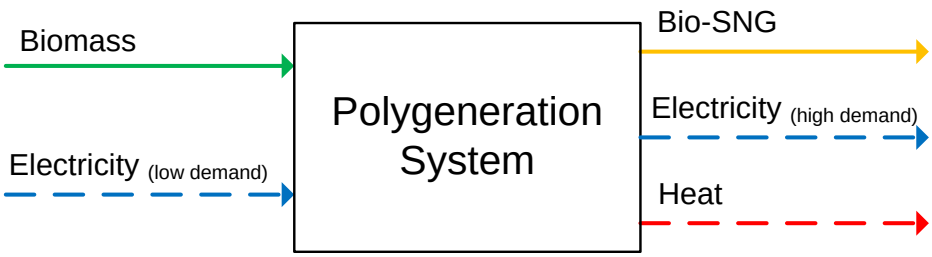

Figure 1 – Simplified diagram of the proposed polygeneration plant

The proposed polygeneration plant produces heat, power and synthetic natural gas (bioSNG) with very high overall efficiency. In addition to high efficiency conversion of biomass, the poly-generation plant is also able to store large amounts of energy in the form of bioSNG by up-grading the synthesis gas (syngas) from the biomass gasifier with electrolytic hydrogen. With these characteristics, the proposed polygeneration plant will be very well suited for a future Danish energy system with a high penetration of fluctuating electricity production from wind and solar. The plant will produce power and heat when the electricity price and demand is high and it will store electricity, in the form of bioSNG sent to the gas grid, when the electricity price and demand is low. The grid thus provides a buffer capacity and the bioSNG can be stored until the demand for electricity is high, or it can be used in the transportation sector in Gas Driven Vehicles (GDVs) or simply replace natural gas in existing infrastructure.The gasification unit of the proposed polygeneration plant is based on the principles of the TwoStage Gasification process developed at DTU.

In addition to the gasifier, the plant also includes a synthesis reactor for the conversion of gasi-fication syngas to bioSNG, and solid oxide cells (SOC) for the conversion of electricity to fuel (Solid Oxide Fuel Cells - SOFC), or vice versa (Solid Oxide Electrolysis Cells - SOEC).

3.2 Milestones

The projects work packages and there relations are shown in Figure 2.

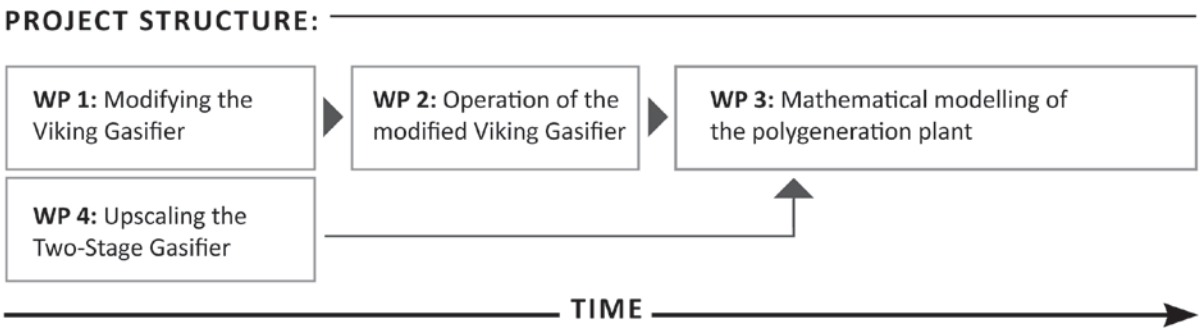

Figure 2 – Project structure showing how the work packages are connected to each other.

The original specific work packages and their milestones and status are:

WP 1: Modifying the Viking Gasifier

The Viking Gasifier will be modified in two ways:

- By changing from air-blown operation to oxygen-steam-blown operation
- By integration of a steam dryer up-stream of the gasifier

Milestone 1: End of modifications to experimental setups.
Status: Completed, but slightly altered as CO_2 and not steam were applied with the oxygen. See Section 3.3.

WP 2: Oxygen Blown Operation of the modified Viking Gasifier

Related to WP 1, the modifications done to the gasifier will be tested and investigated. Specifically, the changes in operating characteristics between air- and oxygen-steam-blown operation regarding:

- Temperatures
- Pressures and gas flows
- Gas analysis: composition, tars, inorganics
- Gasifier performance
- Difference in SOFC performance when gases are applied as fuel

Milestone 2: Successful oxygen-blown operation of the modified Viking Gasifier.
Status: Completed.

WP 3: Mathematical modelling of the polygeneration plant

The complete polygeneration plant is analysed and optimized mathematically. The analysis will consider:

- Energy and exergy
- Economic cost
- Sustainability indicators e.g. greenhouse gas emissions

The results from this WP will include; optimum configurations for the proposed polygeneration plant given specific boundaries of the energy system, and hour-by-hour optimization of the operation of the polygeneration plant.

Milestone 3: Evaluation of the optimized design of the polygeneration plant complete.
Status: Completed.

WP 4: Development of large-scale TwoStage Gasifier concepts

In WP 4, concepts for a medium- to large-scale version of the TwoStage Gasifier will be generated and evaluated. The aim of is to develop concepts that can:

- Scale to at least 10-50 MW_{th}
- Produce a very clean gas suitable for fuel synthesis
- Utilize fuels other than wood

Milestone 4: Concepts for a medium- to large-scale version of the TwoStage Gasifier generated.
Status: Completed.
Milestone 5: Evaluation of large-scale concepts complete.
Status: Completed.

3.3 Development of project

The overall project has developed organically and according to plan. There were however three mentionable developments in the project:

- There were some delay in WP 1. This was related to finding the right equipment and seller. While the original plan was to initially operate the gasifier with an O_2-CO_2 mixture and then an O_2-H_2O mixture, the reduced time available forced us to only apply O_2-CO_2 during tests.
- As the analytical work progressed in WP 4, the interest amongst the participants increased due to promising initial results. This caused the WP's share to increase and hence included additional studies related to the overall polygeneration concept. Besides two scientific publications, this WP also resulted in a patent application.
- While tests with an SOFC were planned in WP 2, additional SOFC tests were included with air-blown product gas. These tests included load variations, peak performance and longer operating results (up to 62 hours). These tests supports the analysis of the polygeneration concepts operating conditions and laid a foundation for the tests in WP 2.

4. Dissemination of results

4.1 Scientific peer-reviewed publications – all 6 publications are attached in the Annex.

1. **Solid oxide fuel cells powered by biomass gasification for high-efficiency power generation**; Rasmus Ø. Gadsbøll, Jesper Thomsen, Christian Bang-Møller, Jesper Ahrenfeldt, Ulrik B. Henriksen. Published in Energy (2017) vol. 131, p. 198-206.

2. **Solution for the future smart energy system: a polygeneration plant based on reversible solid oxide cells and biomass gasification producing either electrofuel or power**; Hafthor Æ. Sigurjonsson, Lasse R. Clausen. Published in Applied Energy (2018) vol. 216, p. 323-337.

3. **Solid oxide fuel cell stack coupled with an oxygen-blown TwoStage gasifier using minimal gas cleaning**; Rasmus Ø. Gadsbøll, Adrian Vivar Garcia, Jesper Ahrenfeldt, Ulrik B. Henriksen. In review: Energy.

4. **Oxygen-blown operation of the TwoStage gasifier**; Rasmus Ø. Gadsbøll, Zsuzsa Sárossy, Lars Jørgensen, Jesper Ahrenfeldt, Ulrik B. Henriksen. Publiashed in Energy (2018) vol. 158, p. 495-503.

5. **Thermodynamic analysis of upscaled TwoStage gasifier concepts**; Rasmus Ø. Gadsbøll, Lasse R. Clausen, Jesper Ahrenfeldt, Ulrik B. Henriksen. In review: Fuel processing

6. **Flexible TwoStage biomass gasifier designs for polygeneration operation**; Rasmus Ø. Gadsbøll, Lasse R. Clausen, Tobias Pape Thomsen, Jesper Ahrenfeldt, Ulrik B. Henriksen. In review: Fuel.

4.2 Other publications

1. **Polygeneration – hvad er nu det for noget?**; Biopress nr. 52, 2015. http://www.biopress.dk/PDF/polygeneration-2013-hvad-er-nu-det-for-noget

Special courses for students:

1. 5 ECTS-point special course: **SOFC operation on biomass producer gas**, Technical University of Denmark, 2015

2. 5 ECTS-point special course: **Two-stage gasification of sewage sludge**, Technical University of Denmark, 2016

3. 5 ECTS-point special course: **Fluidization of char for tar conversion**, Technical University of Denmark, 2016

4. 5 ECTS-point special course: **SOFC operation with oxygen-blown TwoStage Viking gasifier**, Technical University of Denmark, 2018

4.3 Conference and workshop presentations

Oral presentations

1. **Experimental analysis of a solid oxide fuel cell stack coupled with biomass gasification**; Rasmus Ø. Gadsbøll, Jesper Thomsen, Christian Bang-Møller, Jesper Ahrenfeldt, Ulrik B. Henriksen. European Biomass Conference & Exhibition, Vienna, Austria, 2015

2. **Experimental analysis of a solid oxide fuel cell stack coupled with biomass gasification**; Rasmus Ø. Gadsbøll, Jesper Thomsen, Christian Bang-Møller, Jesper Ahrenfeldt, Ulrik B. Henriksen. DTU Sustain conference, Lyngby, Denmark, 2015

3. **Design and analysis of upscaled TwoStage biomass gasifiers**; Rasmus Ø. Gadsbøll, Lasse R. Clausen, Jesper Ahrenfeldt, Ulrik B. Henriksen. European Biomass Conference & Exhibition, Copenhagen, Denmark, 2018

4. **5 presentations at internal DTU seminars**; Rasmus Ø. Gadsbøll et al. Technical University of Denmark, 2015-2018

Posters

1. **Biomass Gasification Polygeneration**; Rasmus Ø. Gadsbøll, Jesper Thomsen, Christian Bang-Møller, Jesper Ahrenfeldt, Ulrik B. Henriksen. CHEC research day, Technical University of Denmark, 2016

2. **Design and analysis of a large-scale TwoStage updraft biomass gasifier**; Rasmus Ø. Gadsbøll, Lasse R. Clausen, Jesper Ahrenfeldt, Ulrik B. Henriksen. CHEC annual day, Technical University of Denmark, 2017

4.4 Thesis

1. **Biomass Gasification Polygeneration**; Rasmus Ø. Gadsbøll. PhD thesis, Technical University of Denmark. PhD defence pending.

4.5 Patents

1. **A gasification unit, a method for producing a product gas and use of such a method**. Danish patent application no. PA2017 70775. Filed October 2017. Rasmus Ø. Gadsbøll, Jesper Ahrenfeldt, Ulrik B. Henriksen.

5. Project results

All of the project results are included in the six publications listed in Section 4.1. The results are summarized here, but more details can be found in the publications.
The main body of work has been performed by DTU. Danish Gas Technology Center has participated by performing detailed gas analysis on several occasions on site and in the lab, been active in gas data interpretation and provided an external stay for a PhD during the project. Dall Energy has been involved in the process of upscaling the TwoStage gasifier (WP4) and has also provided feedback on other occasions. All project partners has been active participants in project meetings.

5.1 Coupling the TwoStage gasifier with a solid oxide fuel cell stack (Additional SOFC tests [see Section 3.3] and WP 2)

5.1.1 Coupling the TwoStage gasifier with a SOFC for power generation

The aim of this study is to examine the commercial operation system potential of the joint gasification and SOFC technology platform. Investigations are done by combining the commercial TwoStage Viking gasifier developed at the Technical University of Denmark and a state-of-the-art SOFC stack from Topsoe Fuel Cell for high efficiency power generation.

Methods and materials

The experimental work was carried out over 3 campaigns for a total operating time of 145 hours with product gas as described in [1]. An overview of reported tests is shown in Table 1.

Test #	Gas flow* [l/min]	Duration [hours]	Range of current values for tests [A]
1	15.9	1.5	0 - 15.1
2	22.5	3.5	0 – 23.1
3	23.0	7	0 – 24.1
4	28.8	2	10.0 - 25.1
5	22.4	62**	20.1

*Table 1 - Overview of tests performed. *Flow measured at 20ºC and atmospheric pressure.*

A flow diagram of the Viking gasifier is shown in Figure 3. The gasifier is operated at atmospheric pressure levels. Pine wood chips of ≈40% humidity are fed into an externally heated screw conveyor that dries and pyrolyzes the fuel up to 600ºC. The screw conveyor is heated using superheated engine exhaust. The pyrolysis products are led to the second reactor and are partially oxidized by air, raising the temperature above 1100ºC. Hereby, the tar content is reduced by 99%. The gas and char then pass through a hot fixed char bed, where the char is gasified and the temperature is subsequently lowered to 800ºC at the bed outlet. The hot char bed acts as a tar cleaning unit, removing 99% of the remaining tars [2][3], yielding a near tar-free gas. The obtained product gas then flows through a series of heat exchangers and a bag house filter that removes small amounts of particles, tars and water. Afterwards, the gas enters a mixing tank, where a slipstream of about 2 kW_{th} was directed to the fuel cell setup.

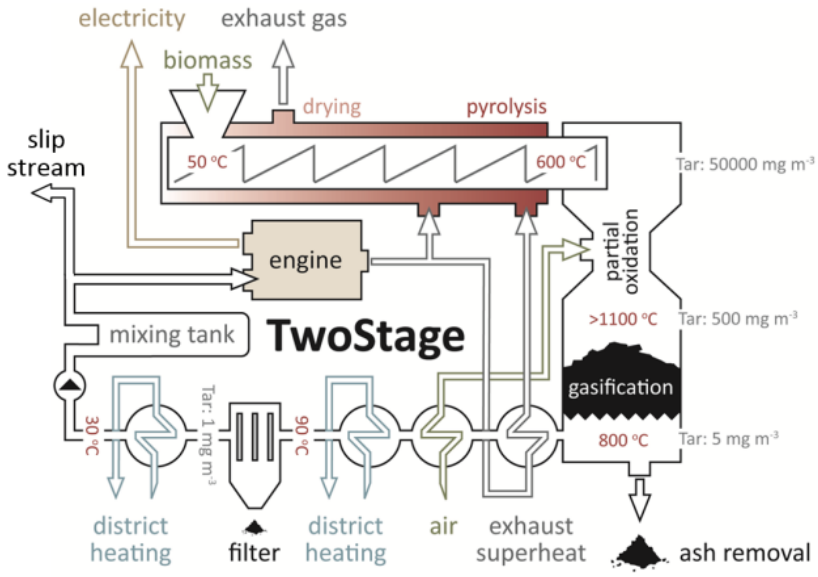

Figure 3 - Flow diagram of TwoStage gasification with an engine.

The product gas initially flowed through two active carbon filters to remove inorganic compounds and tars. Afterwards, the gas passed through an electrically heated water spray tower. The humidification temperature was 60ºC, which correspond to a water molar fraction of about 19.5% in the humidified product gas. The humid product gas was electrically heated to 245ºC and led through a fixed guard bed with ZnO pellets that removed remaining sulphur compounds. An overview of the gas conditioning is shown in Figure 4.

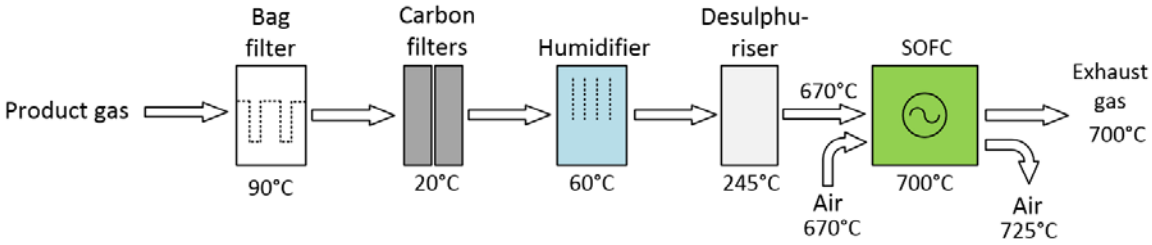

Figure 4 - Overview of fuel cell gas conditioning with operating temperatures.

The SOFC stack is produced by Topsoe Fuel Cell. The stack is made of 50 planar, anode supported cells and the anode is made of yttrium-stabilized zirconia (YSZ), nickel catalysts and a mechanical support structure. The electrolyte is made of YSZ and the cathode of lanthanum strontium manganite. The stack is an 'S 1-02' type, with a footprint of 12x12 cm and a nominal capacity of 800 W_e. The SOFC stack was placed in an electrically heated oven at 700ºC, as the stack was not insulated. A picture of the mounted SOFC stack is shown in Figure 5.

Figure 5 - SOFC stack mounted in oven

Results

The performance of the SOFC stack is evaluated based on power output, voltage and electric efficiency (power to fuel input [LHV]). The FU is an appropriate dimensionless base of comparison value across fuel flows and gas compositions. The FU is defined in Equation 1. N_c is the number of cells in the stack and F is Faradays constant.

$$FU = \frac{\frac{I}{2 \cdot F} N_c}{n_{H2-eq}}$$

Equation 1

During the campaigns, only small fluctuations in the product gas composition from the TwoStage gasifier were seen. Average gas compositions during the tests are shown in Table 2.

Test #	CH_4 [vol%]	CO [vol%]	CO_2 [vol%]	H_2 [vol%]	N_2 (rest) [vol%]	Sum [vol%]	Gas energy flow (LHV)* [W]
1	0.6	15.2	15.4	27.2	41.6	100.0	1245
2	0.7	14.1	15.1	26.3	43.8	100.0	1723
3	0.7	15.6	14.1	26.7	42.8	99.9	1826
4	0.5	14.9	15.3	26.0	43.3	100.0	2200
5	0.6	13.3	16.0	24.8	45.3	100.0	1588

Table 2 - Overview of average dry product gas compositions during the different tests. Compositions are calculated as average values over 3-10 minutes. Nitrogen content is calculated by difference.

The SOFC performance was tested in a large operating area in order to simulate part- and full-load conditions. Voltage, power density and voltage standard deviation as a function of current density for Test 2 is shown in Figure 6 and the power outputs of the SOFC stack for Test 1-4 are shown in Figure 7. The corresponding electric efficiencies for Test 1-4 are shown in Figure 8.

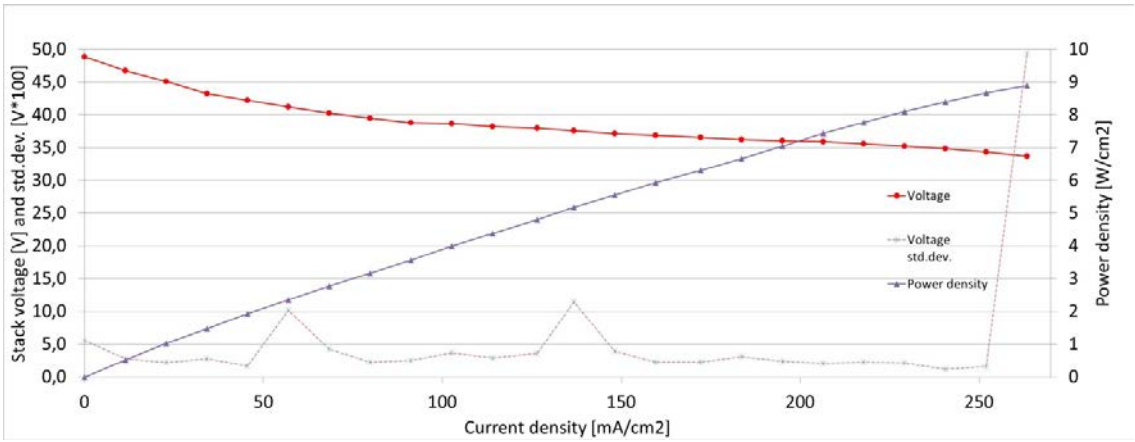

Figure 6 - SOFC stack voltage with standard deviation and power density as a function of current density for Test 2.

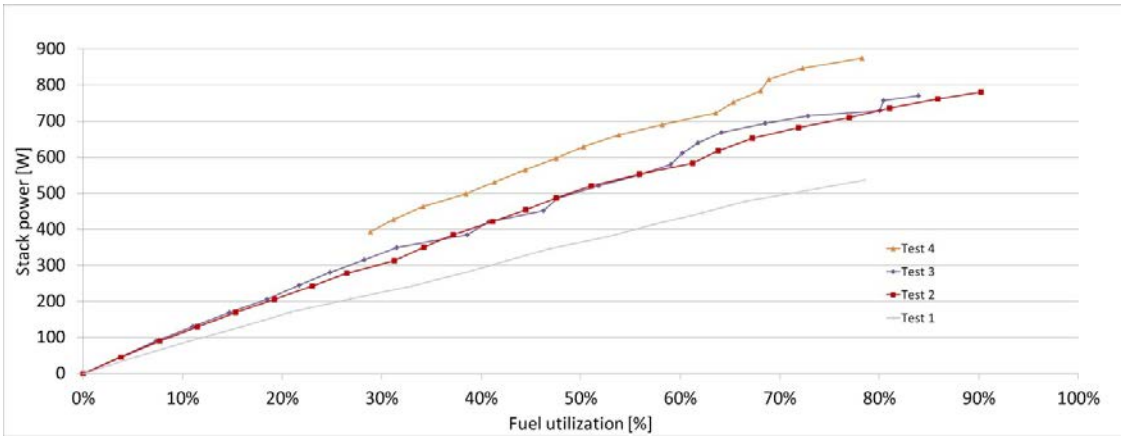

Figure 7 - SOFC stack power output shown as a function of fuel utilisation for Test 1-4.

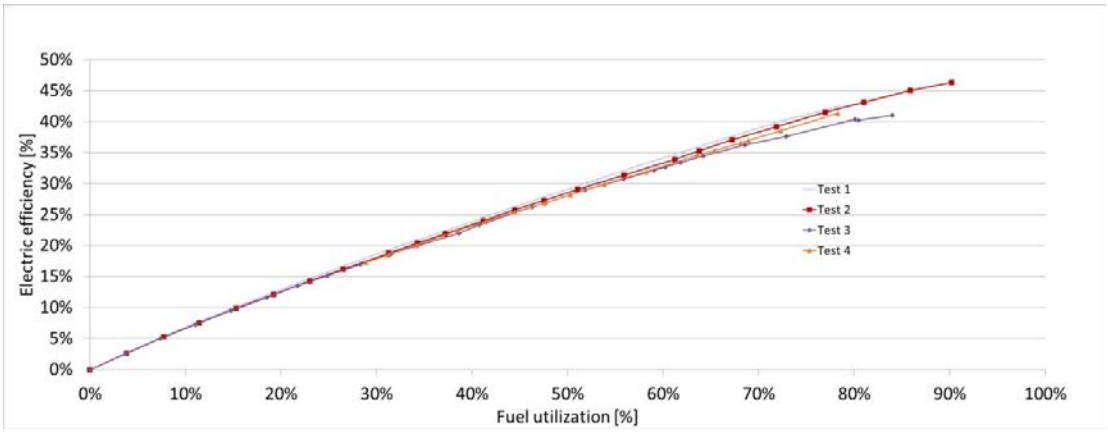

Figure 8 - SOFC stack electric efficiencies shown as a function of fuel utilisation for Test 1-4.

Even though the FU was up to 90.2%, there was no significant decline in power in following tests due to internal losses in the stack (see Figure 7) and tests at different flows yielded nearly equal electrical efficiencies across FU. This means that part-load operation down to 55% flow (Test 1 compared to Test 4) does not reduce the efficiency of the stack, which is an important factor in an energy system with large fluctuations from e.g. wind and solar power.

The peak values for Test 1-4 are shown in Table 2, showing the data for the measurements at max FU. The maximum efficiency value (46.4%), power (875W) and FU (90.2%) achieved are, to the authors knowledge, the highest values found in literature for product gas operation at the time. These efficiencies are markedly higher than previous tests in which 38% was reached [4][5]. Previous tests with the TwoStage gasifier and a single-cell SOFC showed electric effi-

ciency of 24% at a fuel utilization of 30% [6], which is higher than the roughly 18% obtained here at the same FU. Even though the gas was similar it should be noted that the previous test operated at 850°C and a current density of 260mA/cm^2 – compared to 700°C and ≈50-100 mA/cm^2 (depending on test and gas flow).

Test #	Flow compared to Test 4 [%]	Power [W]	Electric efficiency [%]	FU [%]
1	55.2	537	42.6	78.5
2	78.1	780	46.4	90.2
3	79.9	771	41.0	84.0
4	100	875	41.4	78.3

Table 3 - Data for max fuel utilisation (FU) measurements. Data are taken as averages over 60 min.

Considering the gasifier-SOFC system, a plant efficiency η_{plant} can be estimated based on the present results. Using Equation 2, the combinations of SOFC efficiency at maximum FU and gasification efficiency gives TwoStage-SOFC electrical efficiencies of 38-43%. TwoStage cold gas efficiency is denoted with η_{cg} and the SOFC stack efficiency with η_{SOFC}. The range of this approximation is confirmed through mathematical modeling of the system [7].

$$\eta_{\text{plant}} = \eta_{cg} \cdot \eta_{SOFC}$$

Equation 2

The TwoStage-SOFC system is thought as a decentralised constellation in the <10MW$_{th}$ range. The efficiencies of this system are significantly higher than typical competing decentralised biomass power plants at 18-33% [8]. The obtained efficiencies are comparable with those of biomass power plants with capacities >100MW$_{th}$ [8]. Gasification systems typically have electrical efficiencies of 18-33% [9], similar to those of decentralised power plants, with the typically engine operated TwoStage gasifier of 29% (gross) [2]. Two of the most efficient demonstrated biomass gasification systems, not using fuel cells, are the Värnamo combined cycle and Skive engine plants. These plants reach electrical efficiencies of 33% and 30% respectively [10][11] and are significantly outperformed in comparison to these tests.
In order to investigate any decline in the performance of the SOFC stack when continuously using product gas, a 62 hour-test (Test 5) have been performed. No significant drop-off in performance due to product gas use was seen.

Conclusion
The 4 tests displayed the SOFC stacks excellent part-load performance down to 55% flow, without loss of efficiency. The tests achieved the highest reported values of such a system globally, with a SOFC stack electric efficiency of 46.4% at 90% fuel utilisation. A gasifier-SOFC system electric efficiency was estimated to be around 40%, which is considerably higher than those from traditional decentralised biomass power plants and showcases the systems intriguing potential. A total of 145 hours of operation was achieved without significant losses in SOFC performance.

5.1.2 Coupling an oxygen-blown TwoStage gasifier with a SOFC using minimal gas cleaning

The coupling of biomass gasification and solid oxide cell technologies is very intriguing due to its high efficiency and flexibility potential. One of the key challenges in order to realize a gasifier-SOFC system design is a clean quality gas that can meet the strict requirements of the SOFC. This study presents the result of an experimental campaign with the TwoStage Viking biomass gasifier and a Topsoe Fuel Cell SOFC stack connected via a carbon filter and a

desulphurizer. The stack is operated with both air- and O_2-CO_2-blown product gas, at 700°C and 800°C, and tests without any gas cleaning was conducted.

Methods and materials

Tests was carried out over 3 days in which the SOFC stack was coupled to the TwoStage Viking gasifier plant. The first day featured air-blown operation of the gasifier and the last to featured 21v% O_2 in CO_2 as gasification medium – gasification tests are described in detail in Section 5.2. On Day 1 and 2, the operation conditions were changed by varying the SOFC operation temperature and gas composition, whilst using an active carbon filter and a desulphurizer at the SOFC setup. On Day 3, the gas cleaning equipment at the SOFC setup was removed and product gas was fed directly to the stack. An overview of the tests is shown in Table 3.

Test #	Time	Gasification media	SOFC operating temperature [°C]	SOFC current range [A]	Gas cleaning
1	Day 1 12:25-15:53	Air	≈700	0-20	Yes
2	Day 1 16:42-18:54	Air	≈800	0-20	Yes
3	Day 2 12:22-15:20	21v% O_2 in CO_2	≈700	0-20	Yes
4	Day 3 13:33-17:02	21v% O_2 in CO_2	≈700	0-20	No

Table 4 – Overview of tests

The experimental setup was very similar to the study described in Section 5.1.1. The gasifier and SOFC were the same. The key difference was: 1) the gasifier was modified to operate in both an air- and oxygen-blown configuration (see Section 5.2) and; 2) a change in the gas cleaning train, which now only consisted of a carbon filter and a desulphurizer – see Figure 9.

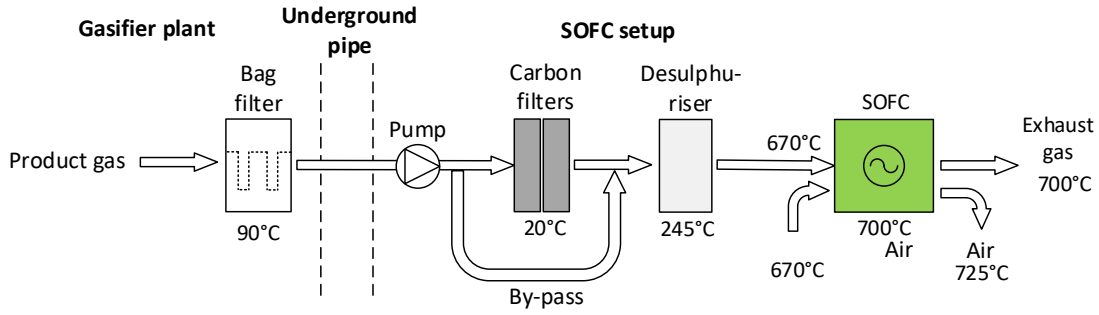

Figure 9 – Overview of gas cleaning from the char gasification reactor to the SOFC. The underground pipe includes a water separator. The by-pass around the carbon filter is controlled by a valve and the filters are only by-passed in Test 5.

Operating temperatures and gas flows during the tests are given in Table 5.

Test #	Product gas [°C]	Exhaust gas [°C]	Air in [°C]	Air out [°C]	Gas flow[a] [l/min]
1	650-674	669-694	653-671	677-735	25.0
2	756-778	765-788	732-754	787-823	25.0
3	650-673	672-692	653-667	686-734	24.8
4	648-673	668-696	654-670	673-736	24.0

Table 5 – Gas temperature measurement ranges and average gas pump flow.

Results

The average gas compositions for Test 1-3 are shown in Table 6. It was not possible to take a sample for gas composition during Test 4, but operating conditions were almost identical to Test 3 at the reactor outlet (714-692°C in Test 3 and 708°C in Test 4) and the moisture content were within 1% on 4 occasions, hence the gas composition is therefore expected to very similar.

	Day - time	Test #	H_2 [v%]	CO_2 [v%]	CO [v%]	CH_4 [v%]	N_2 [v%]	SUM
Air	1 – 12:45-15:53	1	27.8	14.9	15.1	0.2	41.3	99.3
	1 - 16:42-18:45	2	26.1	14.5	15.6	0.2	42.9	99.3
21v% O_2-CO_2	2 – 13:20	3	21.2	43.2	24.9	0.2	4.7	94.2
	2 – 13:22	3	20.6	44.3	25.8	0.2	4.6	95.5

Table 6 – Average online gas analysis for air and single-sample gas chromatography data from gas pipette samples for O_2-CO_2-blown product gas.

Four SPA samples from the air-blown operation only showed 0-3mg/nm^3 of pyrene before and after the bag filter, while three SPA samples during O_2-CO_2 operation showed only 0-1mg/nm^3 of pyrene. No other tar components were found. Sulphur results sampled at the gasifier are shown in Table 12. The low levels of up to 3ppm is very similar to previous tests with the system [12][6][13]. See Section 5.2 for more details.

Air-blown product gas operation: 700°C vs 800°C

SOFC data for the air-blown Tests 1 and 2 are given in Figure 10. Stack voltage and power density were increased up to +11% and are at +8% at 20A when comparing 800°C to 700°C. Only minimal changes in gas composition is seen between the tests (Table 6). The results for 700°C are in line with previous tests (Section 5.1.1) [12].

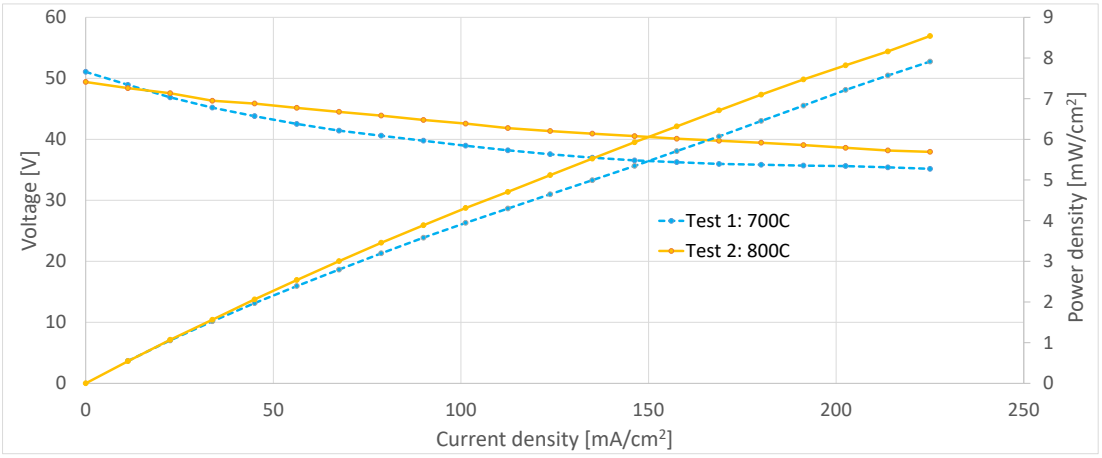

Figure 10 – Stack voltage and power density as a function of applied current at 700°C and 800°C using air-blown product gas.

O_2-CO_2 product gas operation: with and without gas cleaning

SOFC data for the 700°C Tests 1 and 3 are given in Figure 11. Differences in stack voltage and power density were fluctuating between -2.0% and +2.5%. Small differences in operation between the tests are seen, the key being the difference in gas composition as the CO content is significantly higher in Test 3 (25.4v% vs 15.1v% in Test 1). While the molar hydrogen equivalent (Equation 1) is 7.5% higher in Test 3, CO causes a higher overpotential/loss during conversion due to its lower diffusion rate [14][15][16], which lowers the voltage.

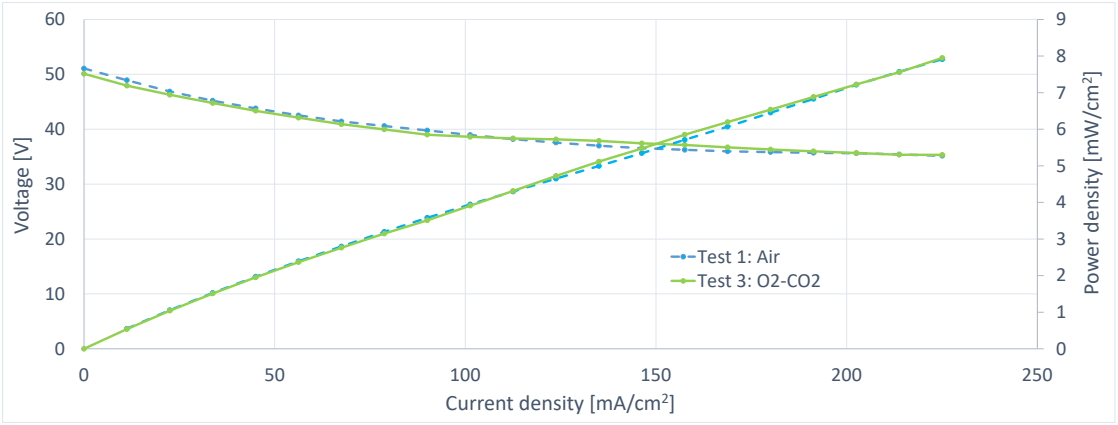

Figure 11 – Stack voltage and power density vs. current at 700°C using air- and O_2-CO_2-blown product gas.

In Test 4, the ZnO pellets were removed from the desulphurizer and the reactor was vacuum cleaned thoroughly – see Figure 12. The setup was then started up as usual (see Section 2.5) with Formier10gas. While no gas composition measurements were taken during Test 4, the operating temperatures of the gasifier were very stable – see Figure 14. Product gas was added through the carbon filters to the setup at OCV, and after 30min of stable operation the carbon filters were by-passed. Following 30min of operation without gas cleaning, it can be seen on Figure 13 that the impact was negligible. The sulphur content into the system was 1.5-2.8ppm sulphur (Table 12). Therefore it was decided to ramp up the current to investigate any possible effects at higher current densities.

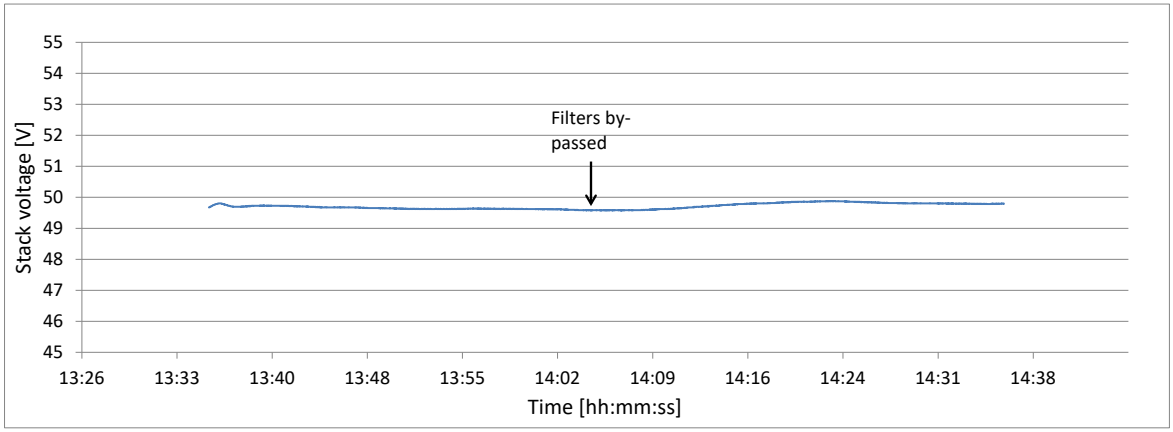

Figure 12 – SOFC open-circuit voltage with carbon filters and by-passed filters

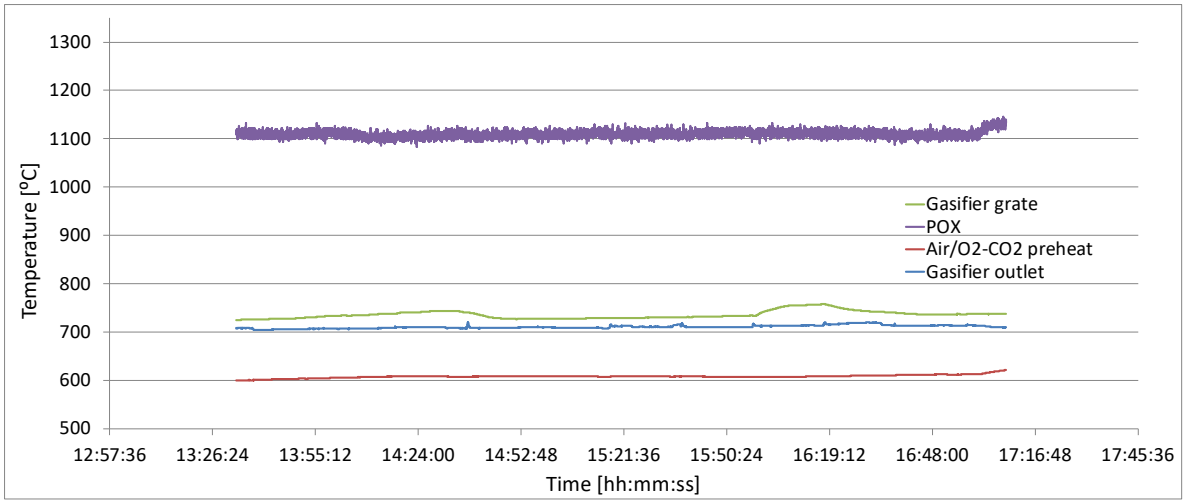

Figure 13 – Operating temperatures of the gasifier during Test 4

SOFC data for the O_2-CO_2-blown Tests 3 and 4 (with and without gas cleaning respectively) are given in Figure 15. Differences in stack voltage and power density are down to -5.2% and are at -2.5% at 20 A. One difference in operation between the tests were that the pump flow was 3.2% lower in Test 4, which indicates the change in performance with and without gas cleaning is negligible.

Following Test 4, the current was ramped down to 0A and the system was stabilized for 5min. The average voltage over the following 15min was 50.3V. For comparison, the average voltage in Figure 13 was 49.7V, which indicates no significant damage to the stack. This is however somewhat inconclusive as no hard data for situational gas composition and only a short evaluation period were given.

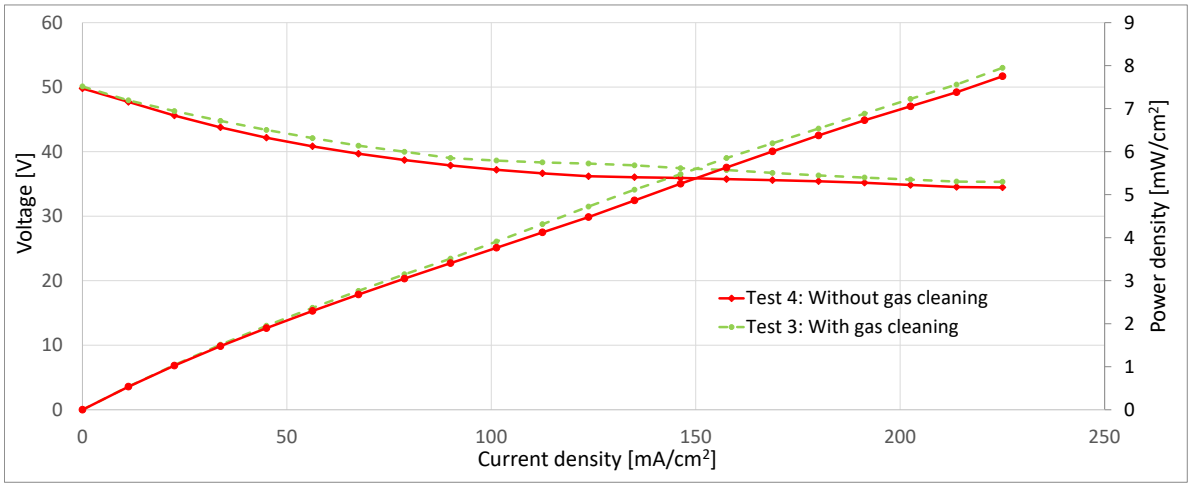

Figure 14 - Stack voltage and power density as a function of applied current at 700°C with and without gas cleaning using O_2-CO_2-blown product gas.

Stack efficiencies

The FU is defined in Equation 1. The average gas compositions from Table 6 are used for the calculation – Test 3 as an average of the latter two compositions. The gas temperature at the gas pump is assumed to be 15°C. The values at peak performance for Test 1-3 are given in Table 7 along with the corresponding electric (gas-to-power) efficiencies.

	Test 1	Test 2	Test 3
FU [%]	67.3	69.2	63.0
η_{SOFC}^{a} [%]	35.8	39.6	32.6

Table 7 – Fuel utilization and electric efficiencies for Test 1-3 at 20A.

Conclusions

The study presented successful operation of a relatively simple TwoStage gasifier-SOFC system. Only minimal gas cleaning was applied with a 90°C bag filter, room-temperature carbon filter and a desulphurizer separating the gasifier and the SOFC. Gas-to-power efficiencies reached up to 39.6% at fuel utilizations up to 69.2%. An 8-11% increase in power and 3.8% increase in efficiency was seen when increasing the SOFC operating temperature from 700°C to 800°C. Changing air- to O_2-CO_2-blown product gas was seen to effect the performance, as the SOFC efficiency was seen to decrease due to the lower performance of CO compared to H_2. As the carbon filter and desulphurizer were bypassed, no short-term changes in operational voltage was seen with 1.5-2.8ppm sulphur in the feed gas. This indicates that the gasifier design can be a key feature when constructing gas cleaning trains for gasifier-SOFC systems, as in-situ gas cleaning can reduce the downstream cleaning significantly.

5.2 Oxygen-blown operation of the TwoStage gasifier (WP 1 and 2)

In order to optimize the TwoStage gasification process, it is suggested to apply an O_2-CO_2 gas mixture as gasification medium, instead of air, to limit N_2-dilution of the product gas.

Modeling

A smaller modeling study of the oxygen-blown Viking was carried out. As seen in Table 8 the direct substitution of CO_2 for N_2 with 21v% O_2 will cause a decline in gasifier performance with lower temperatures and subsequent carbon conversion and efficiency. Namely the higher heat capacity is responsible for this decline, as the gasifier exhaust will have a higher content of sensible heat. In order to keep the efficiency and POX temperature at similar levels, a ≈12% larger volume flow is required. Generally it is seen that the efficiency and POX

temperature are in the same range as for the air-blown mode.
In line with the literature review, it is seen that an O_2-concentration of 30v% obtain very similar parameters to those of the air-blown mode. As an extreme case, pure oxygen might be added to the process, which is seen to obtain higher performance across parameters, as the otherwise large amounts of N_2/CO_2 does not need to be heated and carried through the system. Increasing the O_2 concentration for higher cold gas efficiency is in line with experimental studies e.g. [17][18]. The use of pure oxygen on the plant might however be challenging with regards to the present plant design (temperatures, materials, gas flows etc.) and highly dependent on the fuel moisture levels in order to avoid hot spots. Therefore it is seen as reasonable to blend the oxygen with a carrier gas in order to make the system more robust and allow dryer fuels and potential other fuels with a lower volatile fraction that both will increase the POX temperature.

	Unit	Air	O_2-CO_2	O_2-CO_2	O_2-CO_2	O_2
Oxygen fraction	[v%]	**21**	**21**	**21**	30	100
Gas/fuel flow	[m3[a]/kg(dry)]	**1.13**	**1.13**	1.26	0.80	0.22
Gas preheat to 450°C	[kW_{th}[b]]	2.6	3.6	4.0	2.6	0.5
POX temperature	[°C]	1191	1085	1144	1197	1307
Carbon conversion	[%]	**99.0**	90.2	**99.0**	**99.0**	**99.0**
Cold gas efficiency	[%](dry,LHV)	89.1	80.9	87.8	89.2	91.0
H_2	[v%(dry)]	36	30	28	36	52
CO	[v%(dry)]	17	25	26	27	25
CO_2	[v%(dry)]	17	46	46	37	23
CH_4	[v%(dry)]	0	0	0	0	0
N_2	[v%(dry)]	30	0	0	0	0
LHV_{mass}	[MJ/kg]	6.4	5.1	5.1	6.6	10.8
LHV_{vol}	[MJ/Nm^3]	5.8	6.1	6.1	7.0	8.5

Table 8 – Model comparison using air or O2-CO2. [a]At 20°C, 1bar. [b]Based on 80kW_{th} fuel input (LHV).

Based on the literature and modeling studies presented, the TwoStage Viking gasifier plant was modified and experimental campaigns were carried out over 3 days. The campaign details are presented in the following sections.

Methods and materials

The TwoStage Viking gasifier (Figure 3) was modified for the tests. A steam dryer has been installed on the Viking plant. This will enable the use of fuel with high moisture contents up to ≈60-70% and also enable separation of the high-temperature pyrolysis heat exchanger area as shown in scaled up designs [19]. The steam dryer utilizes a steam loop, where it is moved and heated by a blower and an electrical heater. As seen on Figure 16, the steam is then passed through a screw conveyer where the fuel moisture evaporates. The main fraction of the steam is then recirculated via a blower and reheated, while the produced moisture-steam is carried with the dry fuel to the pyrolyzer. The inlet steam temperature to the steam dryer was 173°C. The plant is described in Section 5.1.1.

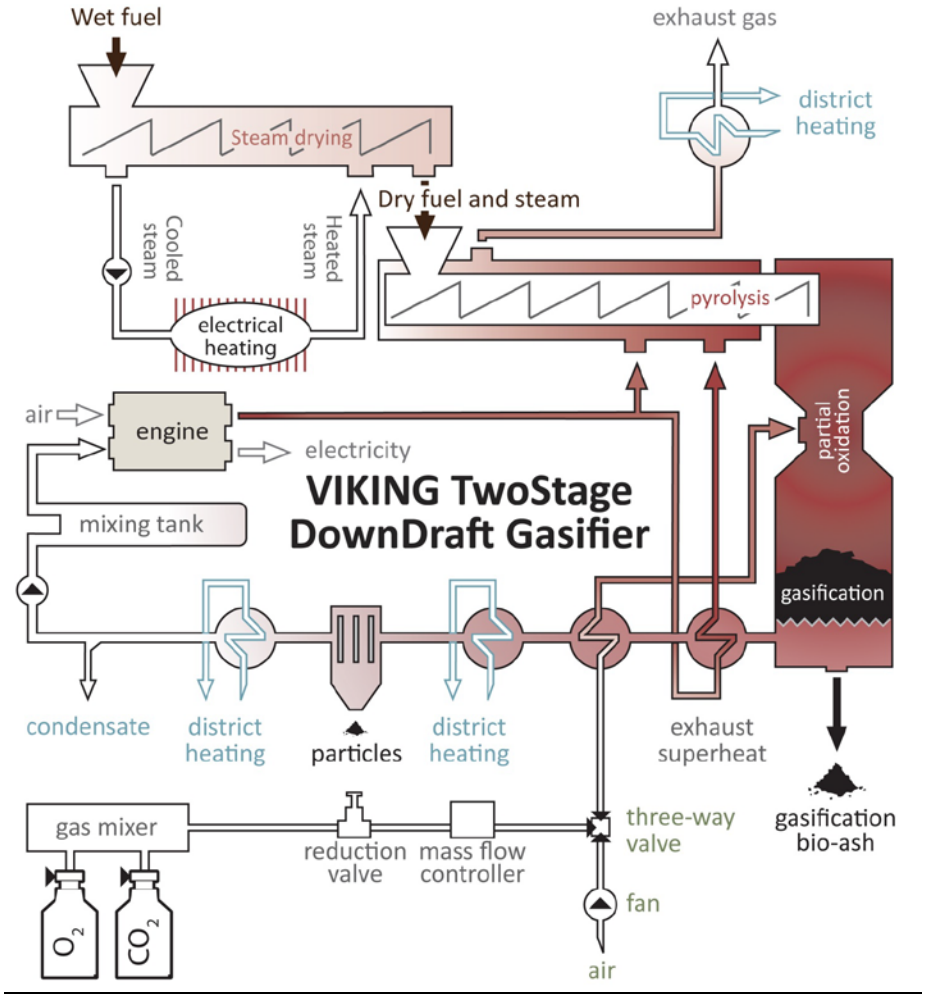

Figure 15 – Schematic overview of the Viking gasifier with an installed steam dryer and O_2-CO_2 mixing setup.

The standard gasification medium is atmospheric air that is delivered to the system via a blower. Replacing the air injection with an O_2-CO_2 mixture is done via the following setup. The O_2 and CO_2 are supplied via gas bottles, reduced to 10 bar via reduction valves and led to a gas mixer (Dansensor MAP Mix Provectus.) The gas mixer is based on two mass flow controllers, which secure the correct composition within 1%. The mixer feeds a 100L buffer tank with a reduction valve, that secures a stable outlet pressure at 3 bar. The system feeds a thermal mass flow controller (Aalborg Model GFC) that uses the original air blower signal from the PLC (Siemens Step7) to dose the mixture near atmospheric pressure levels. The flow controller has an accuracy of ±1%. The mixture composition is manually set at the mixer and has been thoroughly tested beforehand. The equipment is shown in Figure 17.

Figure 16 – Experimental setup for converting the air-blown gasifier to O_2-CO_2-blown. Left: Gas bottles. Upper right: gas mixer. Lower right: mass flow controller.

The 25v% oxygen-mix volume flow is set to match the absolute oxygen flow, meaning a smaller total gas flow is applied.

Results

The reported tests were carried out over 3 following days: Day 1 - air-blown, Day 2 – 21 and 25v% O_2-CO_2-blown, Day 3 - 21v% O_2-CO_2-blown. Time dependent temperature data for air and O_2-CO_2 operation is shown in Figure 18 and Figure 19. Temperature measurements were taken after the air preheater, at the POX zone, just above the gasifier grate and at the reactor outlet and all parameters showed satisfying process stability.

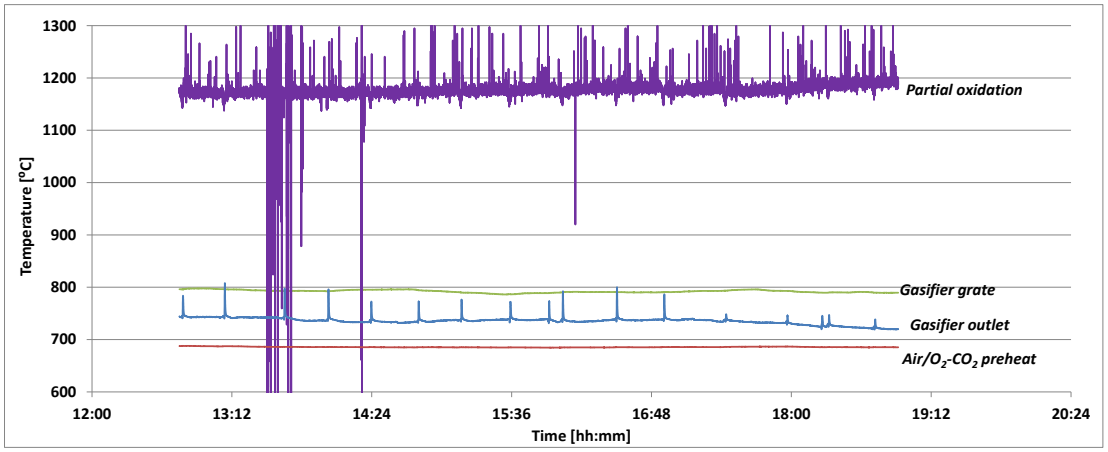

Figure 17 – Operating temperatures for air-blown operation during Day 1.

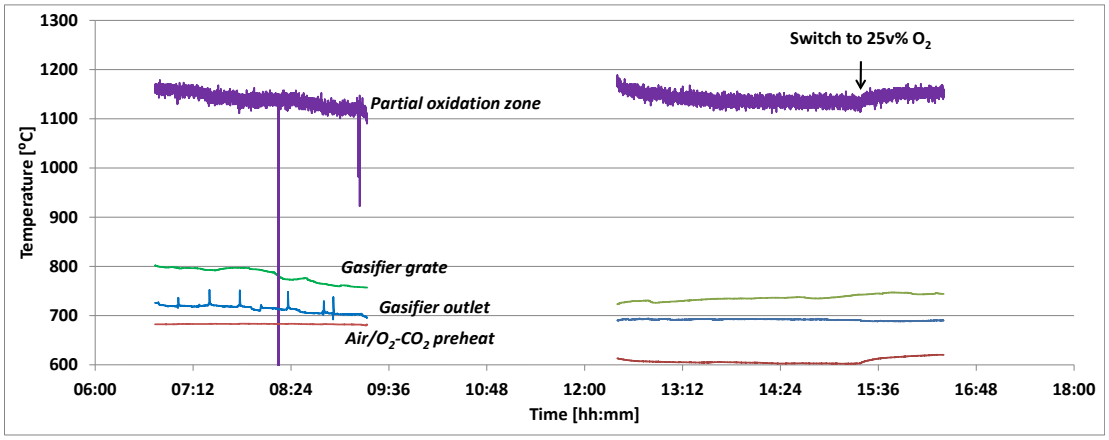

Figure 18 – Operating temperatures for 21v% and 25v% O_2-CO_2-blown operation during the time of testing. The two periods before the switch to 25v% O_2-CO_2 is 21v% O_2-CO_2 day 2.

The operating temperatures and gas compositions are summarized as averages in Table 9 and gas pipette gas compositions are given in Table 6. As discussed in the modeling study, it is seen that the general trend is that the temperatures are decreasing in the gasifier as the process is switched from air to 21v% O_2-CO_2: a POX temperature reduction of 52-69°C with grate temperatures decreasing with 31-36°C. The preheating temperature is generally somewhat lower, which is expected as the heat capacity is significantly higher compared to air. At 25v% oxygen, both preheat, POX and grate temperatures are increased and are more similar to air-blown data.

Test Time period	Day	$T_{preheat}$ [°C]	T_{POX} [°C]	T_{grate} [°C]	T_{outlet} [°C]
Air 12:45-18:45	1	686	1177	792	736
Air #2[a] 0:00-6:13	2	680	1188	766	719
21v% O_2-CO_2 6:44-9:20	2	683	1137	730	714
21v% O_2-CO_2 13:05-15:24	2	604	1136	735	692
25v% O_2-CO_2 15:24-16:24	2	616	1149	745	689
Air #3[a] 0:00-6:23	3	640	1183	766	695
21v% O_2-CO_2 10:42-17:00	3	595	1114	731	708

Table 9 – Day-by-day Averaged temperature and online gas data for the test campaigns. [a]Test data for overnight operation without gas analysis.

	Day - time	H_2 [v%]	CO_2 [v%]	CO [v%]	CH_4 [v%]	N_2 [v%]	SUM
Air	1 – 12:45-18:45	27.0	14.7	15.3	0.4	42.1	99.5
21v% O_2-CO_2	2 – 11:15	24.0	42.6	26.9	0.05	4.6	98.2
	2 – 13:20	21.2	43.2	24.9	0.16	4.7	94.2
	2 – 13:22	20.6	44.3	25.8	0.22	4.6	95.5
25v% O_2-CO_2	2 – 15:50	21.2	39.3	18.6	0.04	3.8	82.9
	2 – 16:50	22.8	39.4	20.6	0.09	4.6	87.5

Table 10 – Data from online gas analysis (air) and gas chromatography data from gas pipette samples (21v% and 25v% O_2-in-CO_2).

Tar measurements are shown in Table 11. For air-blown operation, the results show expected low results in the low mg/m^3-range with only PAH compounds present. The particle filter is seen to not cause any significant reduction in tar concentration, however on day 1 no tars could be measured after the filter. While the relative difference between tar concentrations in the air and O_2-CO_2 samples is high, the absolute difference is seen to be very small. Hence no significant difference is seen between the two states.

Time	Location	Gasifier medium	Pyrene	Naphthalene	Sum [mg/Nm^3]	Sum [ppm]
Pre-liminary	Before filter	Air	4.9 ±0.2	0	**4.9**	**N/A**
Pre-liminary	After filter	Air	4.2 ±0.5	0	**4.2**	**N/A**
10:29 Day 1	Before filter	Air	2.8	0	**2.8**	**0.003**
11:00 Day 1	Before filter	Air	3	0	**3**	**0.003**
10:05 Day 1	After filter	Air	0	0	**0**	**0**
10:17 Day 1	After filter	Air	0	0	**0**	**0**
Preliminary	Before filter	21v% O_2-CO_2	5.7 ±0.8	3.5 ±2.5	**9.2**	**N/A**
Preliminary	After filter	21v% O_2-CO_2	3.8 ±0.2	6.5 ±0.4	**10.3**	**N/A**
13:53 Day 2	Before filter	21v% O_2-CO_2	0	0	**0**	**0**
13:42 Day 2	After filter	21v% O_2-CO_2	1	0	**1**	**0.001**
13:47 Day 2	After filter	21v% O_2-CO_2	0	0	**0**	**0**

Table 11 – Tar measurements [mg/Nm^3] before and after the bag filter of the gasifier. Preliminary samples were taken during the initial tests of the system 2 months prior to the main experimental work that is reported here – operation conditions were very similar.

Gas samples were taken during Day 1 and 3 to assess the sulphur load and results are shown in Table 12. The range of 0.6-2.8 ppm total sulphur is within previous measurements of the gasifier of 3.7 ppm of COS (no H_2S) [12], 0.17-0.28 ppm of COS (no H_2S) [6] and <2ppm H_2S + COS [13], which is also in line with the sulphur content of the applied wood fuels and is similar to previous analysis of wood fuel for the Viking [2]. It was expected that the bag filter might capture some of the sulphur species, as it will be partially coated with char from the gasifier and hence act as a carbon filter. It is however seen that this is not the case, as the filters' capture, if

any, is negligible. The sampling and analysis were carried out by Danish Gas Technology Center and the relative uncertainty was estimated based on experiences to 40% for the first three samples in Table 12 and 25% for the remaining samples.
Between the media, the difference in sulphur species is negligible, with an additional 1ppm extra on average for the O_2-CO_2 blend. This is due to additional COS, that could be slightly promoted with the given gas composition. As mentioned, previous tests have shown higher COS levels when air was applied, and hence the difference might also be due to small variations in operation from Day 1 to 3.

Samplingtime	Location	Gasification media	H_2S [ppm]	COS [ppm]	Total S [ppm]
Day 1 12:20	Before filter	Air	0.1	0.6	0.7
Day 1 12:23	After filter	Air	0.1	0.5	0.6
Day 1 12:27	Before filter	Air	0.1	1.0	1.1
Day 1 12:32	Before filter	Air	0.4	1.1	1.5
Day 1 12:36	After filter	Air	0.4	1.0	1.4
Day 3 10:52	Before filter	21v% O_2-CO_2	0.3	1.8	2.1
Day 3 10:57	After filter	21v% O_2-CO_2	0.4	2.4	2.8
Day 3 11:36	Before filter	21v% O_2-CO_2	0.2	1.6	1.8
Day 3 11:41	After filter	21v% O_2-CO_2	0.2	1.3	1.5
Day 3 12:07	Before filter	21v% O_2-CO_2	0.2	1.8	2.0
Day 3 12:12	After filter	21v% O_2-CO_2	0.2	1.3	1.5

Table 12 – Measurements for sulphur in the product gas.

Conclusions

The Viking gasifier has been successfully converted from its original air-blown configuration to using O_2-CO_2 as gasification medium. Literature, modeling and experimental studies showed that operating conditions were expected to be in the range of air-blown values at 21-30v% O_2-in-CO_2, with partial oxidation and grate temperatures reduced by 52-69°C and 31-36°C respectively at 21v% O_2. Detailed gas analysis for tar and sulphur species showed that the gas qualities during O_2-CO_2 operation were comparable to the very high standards of the typical air-blown mode at <11mg/Nm^3 and <3ppm respectively – without any downstream gas cleaning equipment.
Hence the system can be successfully converted to operate with an O_2-CO_2 blend without ma-

jor additions to existing design. Compared to the more typically applied O_2-H_2O medium in the literature, applying CO_2 might be better suited for some applications, as the media can be: 1) conveniently recirculated back to the oxygen source without need for high evaporation heat; 2) be completely converted into biofuels by addition of electrolytic hydrogen downstream of the system.

5.3 Mathematical modeling of the polygeneration plant (WP 3)

Analytical framework

The analytical framework is constructed based on thermodynamic modeling using DNA software, which is a component-based thermodynamic modeling and simulation tool [20]. The techno-economic analysis was modeled in Python using process data from DNA, and the analysis was used to determine the total revenues required and net present value, given a range of bio-SNG and electricity prices.

The marginal cost of operation for both production modes is calculated by fuel and other running costs, along with the electricity market spot price, which determines the yearly running time of the system (capacity factor). To determine the yearly running time, three reference years were used to describe the electricity system development in Denmark. Figure 19 displays the current (2016) and projected (2025 and 2035) power price (€/MWh) cumulative curves in the Nordpool electricity market, based on analysis work by the Danish transmission system operator (TSO) Energinet.dk [21] using the energy system model SIFRE [22], as reported by Lythcke-Jørgensen et al. [23]. An alternative scenario is provided ("vol"), representing the increased volatility of power prices over the years. This scenario is constructed based on the 2016 curve, but has 2000 h of higher prices.

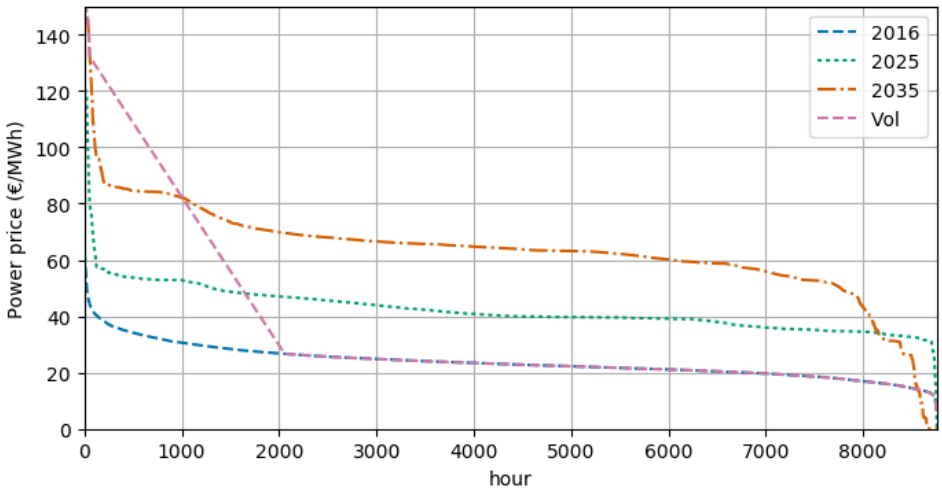

Figure 19 - Cumulative curves for current and predicted power prices.

Results

The electricity production mode modeling and simulation shows that the electrical efficiency is ~46%, while the district heat production efficiency is ~44%, resulting in an overall efficiency of 90% on a dry biomass basis. This can be compared with electricity production from biomass gasification cogeneration. In a review article by Ahrenfeldt et al. [24] regarding state-of-the-art and future perspectives, the overall efficiencies ranged from 80–97%, with electrical efficiency ranging from 6–50%. Part of the reason for the high efficiency of the system is the utilization of unconverted fuel from the SOFC by the gas engine, which increases the electrical efficiency

from 36–46%. Gas with a similar chemical composition to that of the unconverted fuel was tested in a gas engine for proof of concept, and the engine was run successfully.

The electricity storage mode modeling and simulation shows that the conversion efficiency from biomass and electricity to bio-SNG is 69%, while the heat production efficiency is 16%, resulting in an overall efficiency of 85%. Furthermore, it can be seen that bio-SNG methane content is 98.5%, which is more than required to supply it to the grid. Table 13 provides a summary of the production efficiencies in both the operation modes.

Electricity mode	
Electrical efficiency [MW electricity / MW biomass]	46%
District heat efficiency [MW heat / MW biomass]	44%
Total efficiency [(MW electricity + MW heat) / MW input]	90%
Bio-SNG mode	
Bio-SNG efficiency [MW bio-SNG / MW input]	69%
District heat efficiency [MW heat / MW input]	16%
Total efficiency [(MW bio-SNG + MW heat) / MW input]	85%
Electricity input fraction [MW electricity / MW input]	59%
Biomass input fraction [MW biomass / MW input]	41%

Table 13 - System production efficiencies and energy ratios in both electricity and bio-SNG operation modes. LHV on a dry basis is used.

Figure 21 illustrates Total Revenues Required (TRR) in €/MWh by the system as a function of the primary production capacity factor, where the revenues from district heating sales using the pricing scenarios introduced above are included. The bio-SNG mode results are provided for three electricity prices in order to highlight the importance of this parameter. Through comparison with the electricity price scenarios in Figure 19, it can be seen that the assumed electricity prices are relevant. DH zero, DH lower, DH upper and DH max, represent different price prediction of sold heat to the district heating system by the system based on prices payed in Denmark today, see Figure 20.

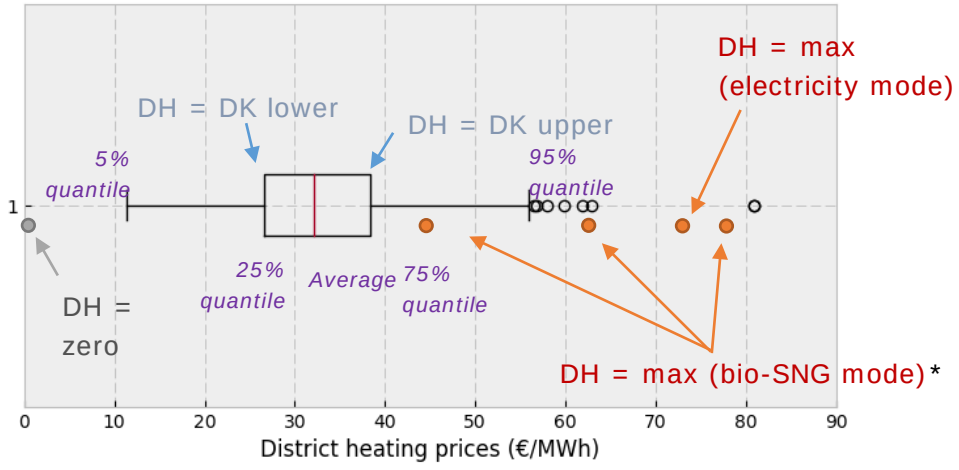

Figure 20 - Price of district heating produced by polygeneration system based on energy content allocation between produced products and true district heating production cost in Denmark by statistical distribution [25]. **Price is determined based on average electricity price in 2016, 2025, and 2035, i.e., 23.6 €/MWh, 42.5 €/MWh, and 63.0 €/MWh.*

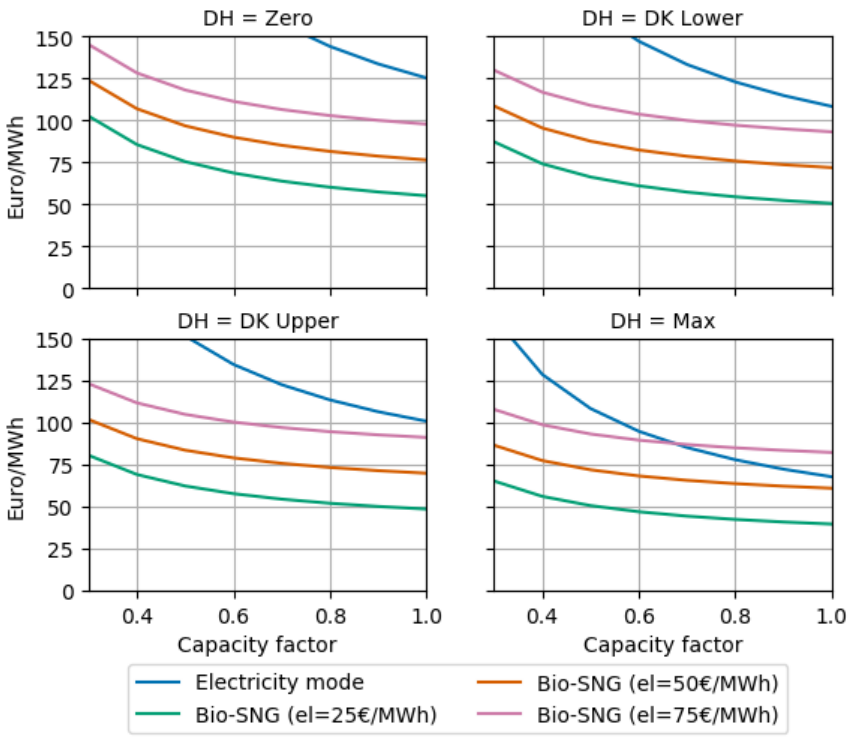

Figure 21 - TRR by system for both electricity and bio-SNG production modes as a function of capacity factor. District heat pricing scenarios are defined in Figure 20.

It can be seen from the figures that there is a significant decrease in TRR when including the district heating sales and an increased capacity factor. To put TRR into perspective, it is worth noting that, according to the Danish Promotion of Renewable Energy Act §44 par. 2 VE-Lov, the premium feed-in tariff for electricity produced from biomass by gasification is ~110 €/MWh, and support for biogas sold for transportation purposes is 36 €/MWh, according to § 43 b par. 2–3 VE-Lov. However, according to a report on energy system integration and economy, the future price of bio-SNG is assumed to be between 44 and 76 €/MWh (12.2 to 21.1 €/GJ) [26], where the lower value is based on the future natural gas price, including saving CO_2, and the upper value is based on the future upgraded biogas price.

Marginal cost and operation mode at provided electricity and bio-SNG prices.

Figure 22 displays the operation mode of the polygeneration system depending on electricity and bio-SNG prices. The modes are 1) shut down (when the fuel and variable O&M costs are greater than the revenues of product sales), 2) bio-SNG mode, and 3) electricity production mode. When operating in bio-SNG mode, the electricity prices are low compared to the bio-SNG prices. When the electricity prices are high, it is more economical to operate in electricity production mode. The figures also display the areas of positive and negative NPV for each operation mode. On the line separating each operation mode, the NPV is the same for each mode.

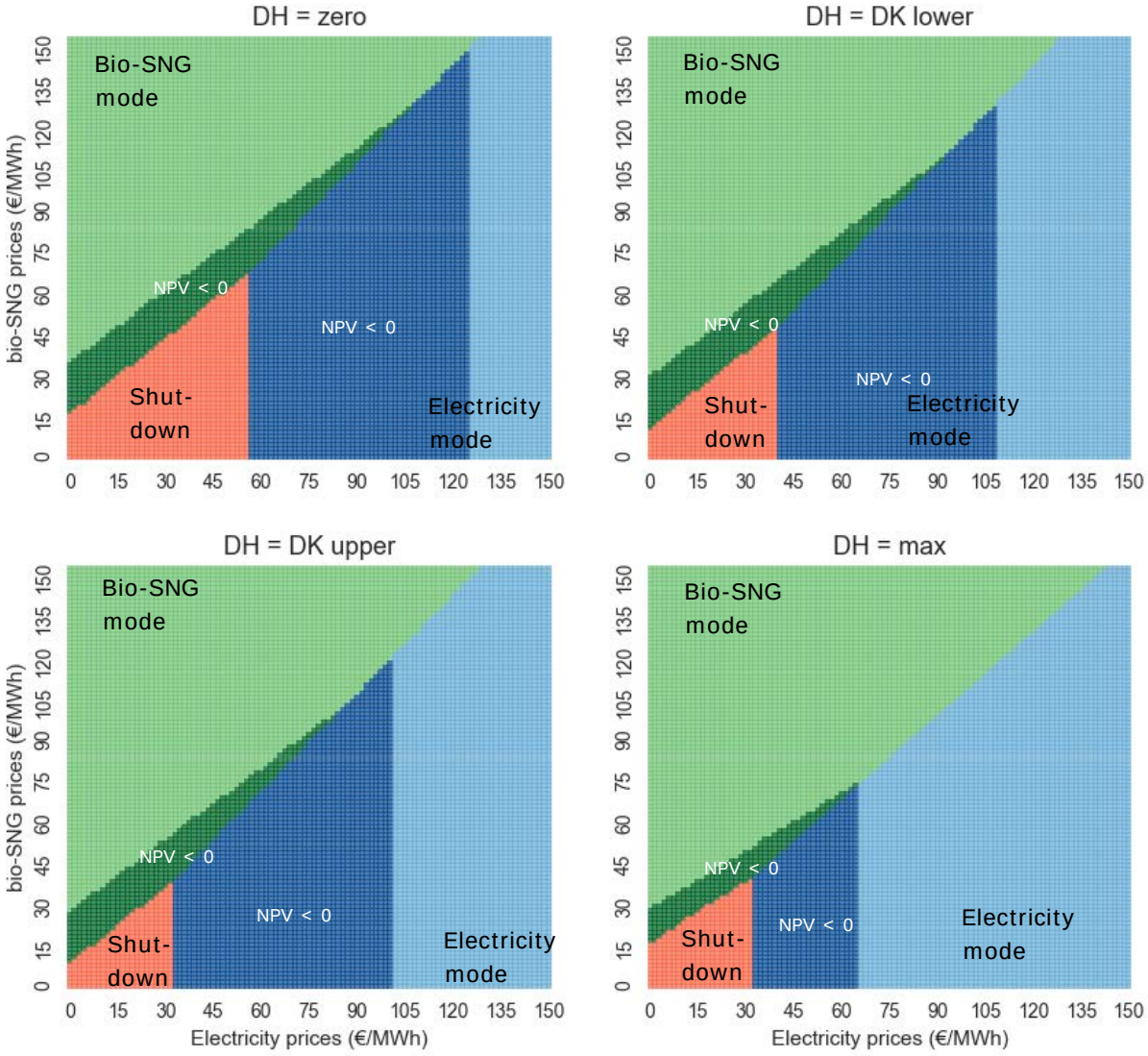

Figure 22 - Graphical display of operation modes at a range of electricity and bio-SNG prices for the four district heat pricing scenarios defined in Figure 20.

If the system could only produce electricity or bio-SNG and not both, depending on the electricity and bio-SNG market prices, the figure above would appear different. If the system could only produce electricity, the bio-SNG area would be removed and the shut-down area would be larger. It would not be possible to operate the system at low electricity prices. If the system could only operate in bio-SNG mode, the blue area would be removed and the shut-down area would be larger. It would then not be possible to operate the system at high electricity prices.

However, constructing this system to be flexible and able to change between different operation modes based on the marginal cost and revenues will increase its capacity factor. The degree to which it will increase depends on the electricity and bio-SNG market prices and the revenues from district heat sales. Figure 23 illustrates how the polygeneration system would operate given the current and predicted electricity and bio-SNG prices.

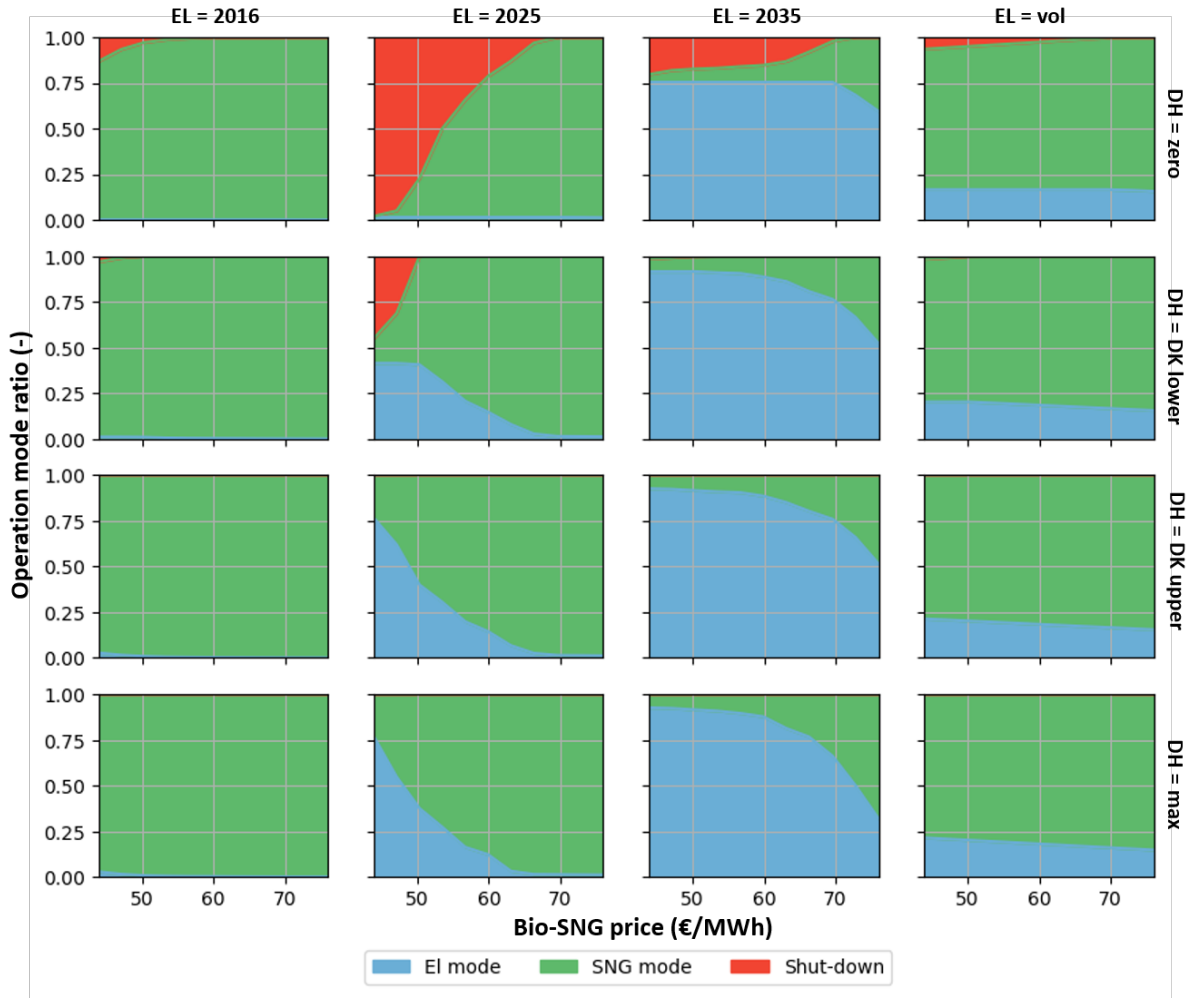

Figure 23 - Annual operation of polygeneration system in electricity, bio-SNG, and shut-down modes for low (44 €/MWh) to high (76 €/MWh) bio-SNG prices. Power price scenarios are defined in Figure 19 and district heat pricing scenarios are defined in Figure 20.

It can be seen from the figure that the time spent in each operating mode differs significantly depending on the assumed power and SNG prices. In the current energy system (2016), the power prices are low, resulting in full bio-SNG mode operation, regardless of the bio-SNG price. The power prices are expected to increase in 2035, and this changes the plant operation. If low bio-SNG prices are assumed together with a low district heating price (DH = DK lower), the plant will operate 92% of the time in electricity mode, 7% in bio-SNG mode, and will be in shut down for the remaining 1.5%. However, if high bio-SNG prices are assumed instead, the plant will operate 52% of the time in electricity mode and 48% in bio-SNG mode. It is worth noting that the system will never shut down if high bio-SNG prices are assumed and at least moderate district heating revenues are achieved.

In Figure 24, the capacity factors for the polygeneration system from Figure 23 are compared with those for the electricity production system and the bio-SNG production system. The figure quantifies the polygeneration effect with respect to the capacity factor.

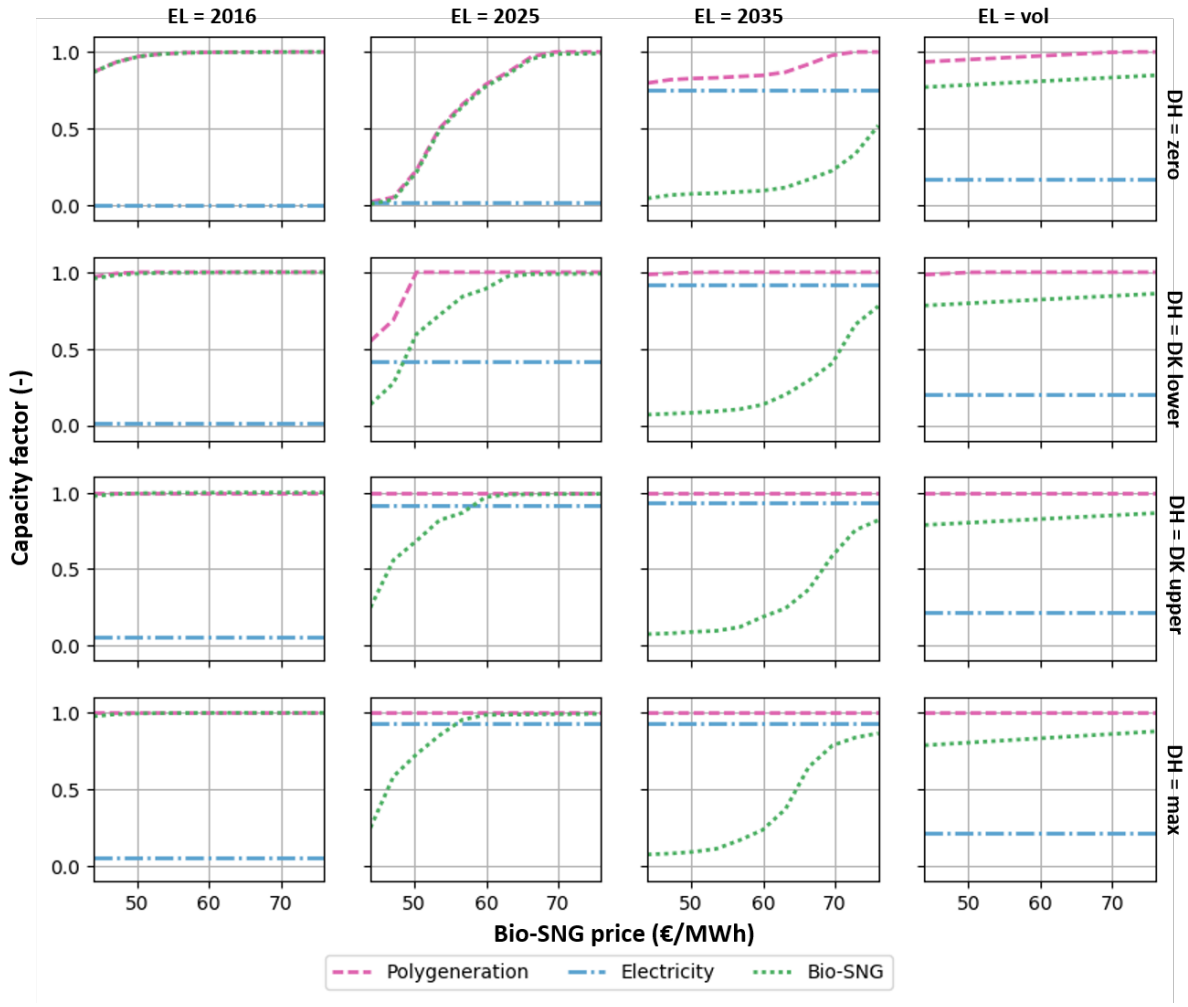

Figure 24 - Capacity factor for the system if running only for bio-SNG or electricity production, compared to combined production of the polygeneration system. Power price scenarios are defined in Figure 19 and district heat pricing scenarios are defined in Figure 20.

As this comparison shows, the capacity factor may increase considerably for the system, but the extent of this increase depends on the pricing scenarios. At low electricity prices (2016), the capacity factor of the polygeneration system will be the same as that of the bio-SNG only system, while the electricity-only system will have a very low capacity factor. At high electricity prices (2035), an opposite trend is observed, namely the capacity factor of the bio-SNG-only system is lower than that of the electricity-only system. However, the capacity factor of the polygeneration system is now higher than that of the electricity-only system, which demonstrates the advantage of polygeneration. This advantage becomes clearer if volatile electricity prices are assumed. A good example is the situation at a moderate district heat price (DH = DK lower) and a bio-SNG price of 70€/MWh: the capacity factor is 100% for the polygeneration system but 50% for the electricity production system and 92% for the bio-SNG production system. A high capacity factor will improve the system economics, as revenue streams can be continued all year. Furthermore, constant, year-round, full-load operation of the biomass gasifier could prove to be important—also from a risk perspective—as gasifier load changes may be challenging.

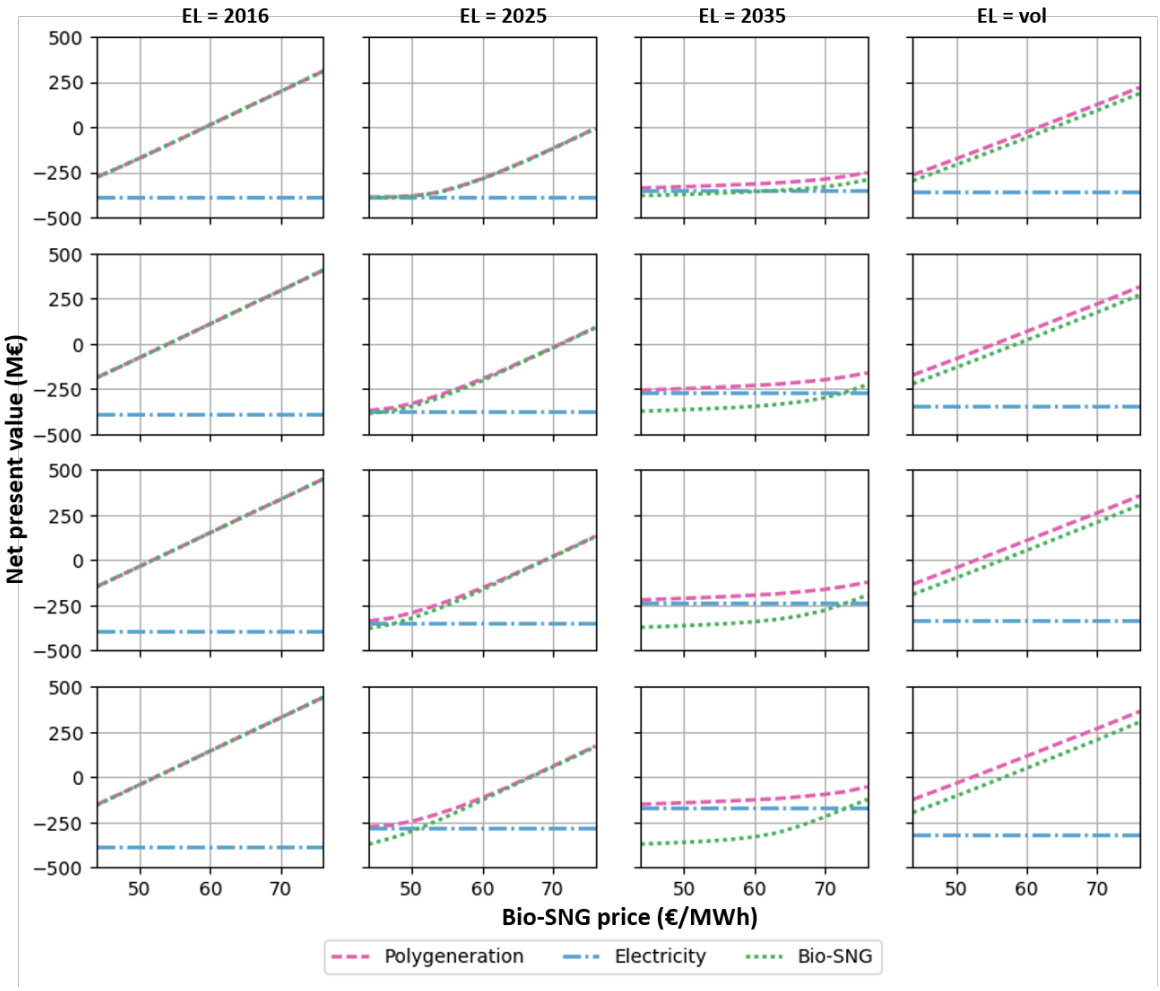

Figure 25 - NPV for system if running only for bio-SNG or electricity production, compared to combined production of polygeneration system. Power price scenarios are defined in Figure 19 and district heat pricing scenarios are defined in Figure 20.

For comparison, the investment cost is recalled to be 216 M€. Figure 25 is similar to Figure 24, but the effect of polygeneration is quantified in terms of NPV instead of capacity factor. When comparing the figures, similar trends can be identified, particularly at low power prices (2016), where the NPV is identical for the polygeneration and bio-SNG-only systems. It should be noted that the investment cost remains constant for all three systems, although, for example, the gas engine could have been removed from the bio-SNG-only system. For all low bio-SNG pricing scenarios, the systems show negative NPVs, but at high bio-SNG prices, the polygeneration and bio-SNG-only systems exhibit a positive NPV, except when operating at high electricity prices (2035). Furthermore, it can be seen that the advantage of polygeneration is greatest when electricity prices are volatile, and the district heating price is high (the sub-figure in the bottom right corner of Figure 25). The reason the district heating price is so important for the polygeneration system is that the income is greatly increased at high district heating prices when operating in electricity mode.

As noted above, in the Danish Promotion of Renewable Energy Act §44 par. 2 VE-Lov, the premium feed-in tariff for electricity produced from biomass by gasification is ~110 €/MWh, while support for biogas sold for transportation purposes is 36 €/MWh, according to § 43 b par. 2-3 VE-Lov. If these subsidies were to be used for the proposed polygeneration system (biogas subsidies added on top of natural gas prices), the optimum operation mode in 2025 would be to run 70% of the time in bio-SNG mode (30% in electricity mode), and in 2035 ~10% of the

time in bio-SNG mode (90% in electricity mode). The vol scenario would result in over 75% operation in bio-SNG mode and 25% in electricity mode. Moreover, all scenarios will result in a positive NPV (using 70€/MWh for bio-SNG). However, these subsides are specific to Denmark and are not guaranteed to exist or remain the same in the future.

Conclusion

This article presented a study on the thermodynamic modeling and simulation of a novel polygeneration plant, along with a techno-economic analysis. The results demonstrated that the hypothesis stands as this system can operate with a high capacity factor in the future Danish electricity market. Furthermore, the results indicated that economic feasibility is greater compared to using stand-alone gasifier and electrolyser plants for electrofuel production.

Based on the results of the study, further conclusions are as follows.

1. The electric efficiency of the plant in electricity production mode is 46%; the total efficiency including heat production is 90%. The fuel efficiency of the plant in bio-SNG mode is 69%; the total efficiency is 85% including heat production.

2. The techno-economic analysis revealed that the investment cost is high, owing to the gasifier and SOC cost. The analysis also indicated that district heating sales are important for economic feasibility of the polygeneration system.

3. Analysis of the marginal cost and mode of operation demonstrated that the operational time in each mode varies significantly depending on future electricity and bio-SNG prices.

4. The ability of a system to choose between producing or consuming electricity depending on the market price can significantly increase its capacity factor compared to a single-mode system, but the increase is greatly dependent on future electricity and bio-SNG prices.

5. The polygeneration system achieves positive net present value when bio-SNG prices are high except when operating at high electricity prices.

6. The polygeneration system achieves a higher NPV than single-mode systems, particularly when electricity prices are volatile and the district heating price is high.

5.4 Upscaling the TwoStage gasifier (WP 4)

5.4.1 Thermodynamic analysis of upscaled TwoStage gasifier concepts

It is desired to design larger gasification plants in order to impact the transition to a green and sustainable energy system via lower specific costs and larger capacities. Several larger gasification plants have shown successful operation, but are associated with relatively complex gas cleaning of tars (if the gas is to be used in a gas engine or fuel synthesis) and/or lower cold gas efficiencies in comparison to efficient small-scale systems such as the TwoStage gasifier concept [27][28][29][10].

The current TwoStage gasification design might not scale well as the currently applied reactor technologies are severely challenged both with regards to scaling and fuel flexibility. The indirect heat transfer in the pyrolysis reactor is relatively inefficient and will either require a very large heat transfer surface in a single reactor or multiple reactors, which is likely not feasible when approaching larger scales – it is estimated that the feasible range is <10MW_{th} with in the

current design constraints [19]. The downdraft char bed has its limitations with regards to operational control and fuel flexibility, as build-up of fines can cause the pressure drop to increase steeply and either cause a low carbon conversion and/or shut down of the gasifier. Thus the downdraft configuration has strict fuel requirements and is dependent on very well-defined fuel such as wood chips if stable and efficient operation is to be maintained.

This study seeks to address these issues and explore alternatives to the current design via implementation of novel concepts and thermodynamic analysis. The framework of the designs is:

- Scalability of ≥10-100MW_{th} as this is the estimated current limit
- Air-blown operation with wet wood chips (50% moisture) for comparison with the current design
- Low tar content of the product gas of ≤1g/Nm^3 in order to limit gas cleaning
- Cold gas efficiency of ≥85% in order to compete with existing gasifier systems and previously upscalings of the system

System designs

A large literature study was carried out long with detailed analysis of subprocesses. The design process is given in detail in the publications in Section 4.1. The key design figure is shown in Figure 19.

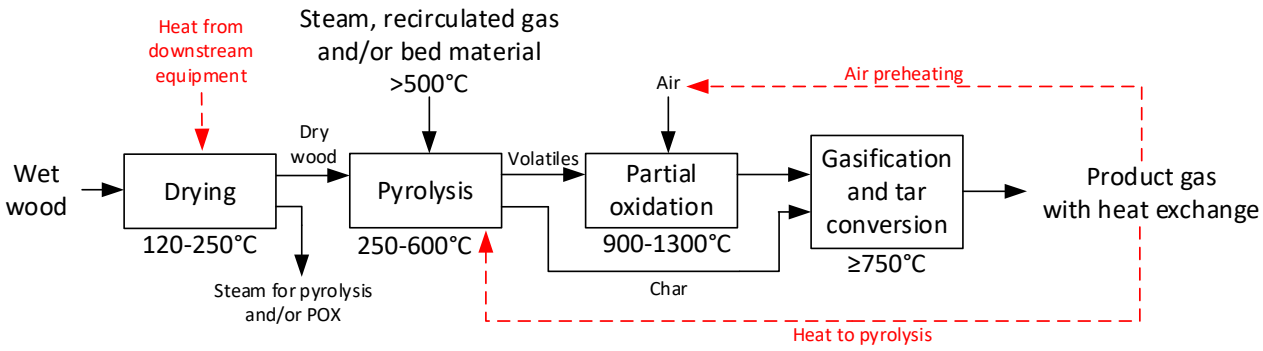

Figure 26 – Design basis for system design, shown as process diagram with process temperature ranges. Tar reduction can also be applied prior to or after the char gasification step.

It was chosen to analyze two fixed and two fluid bed designs to effectively investigate the upscaling possibilities. Initially, the basic designs and constraints are discussed. Note that a steam dryer will be implemented, but are not shown here in the gasifier-centric design phase.
The fixed bed designs are shown in Figure 20. Both concept are based on a novel updraft pyrolysis reactor with gas recirculation that was identified as a promising subproces [30][31]. The countercurrent flow and recirculation of gas enables: 1) an effective heat exchange between gas and fuel; 2) does not cuase dilution of the pyrolysis gas and; 3) enables the use of various heat sources. The fuel is fed at the top of the reactor and is then processed through the reactor to at least 500°C to secure tar release [32]. The produced char is then transported to the gasifier, possibly with a screw conveyer. The Downdraft concept on Figure 20 (left) is primarily generated as a link to compare the current TwoStage gasifier design with the other systems, as it does not address the issue of increased fuel flexibility. The Updraft concept on Figure 20 (right) is interesting as it more tolerant to fines. It does however have its limitations with regards to maximum inlet temperature to the char reactor at the grate. As a solution, a steam ejector is implemented to recirculate product gas to the hot POX gases before the gasifier grate via pressurized steam.

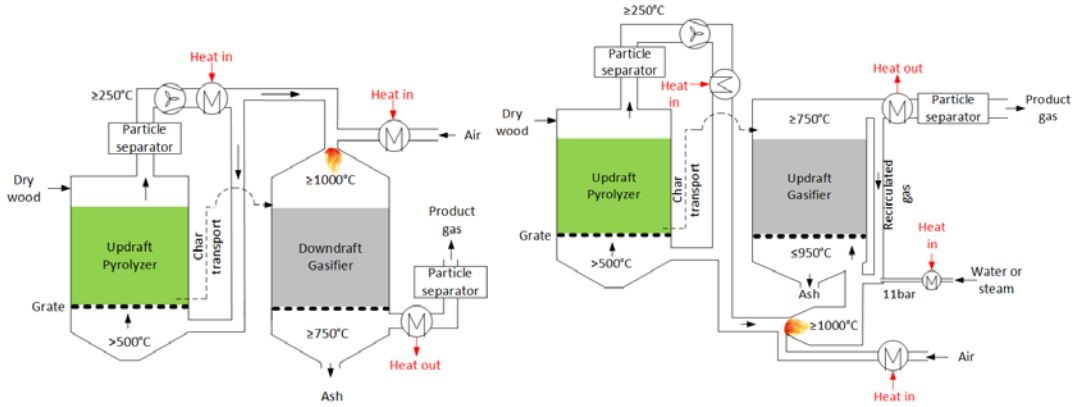

Figure 27 - Fixed bed designs. Left: Downdraft concept. Right: Updraft concept.

The designs for the fluid bed concepts are shown in Figure 21. As fluid bed reactors has significant advantages, it is desired to analyze if the proposed Updraft concept can be designed with fluid bed reactors and still maintain high efficiency and tar conversion – see Figure 21 (left). Fluid beds do however have a much higher pressure drop than fixed beds, which will increase blower consumption, as well as the steam consumption of the ejector. The char transport from the pyrolysis reactor to the gasification reactor will likely be through a loop seal or similar that will transport the top char-rich layer with a minimum of sand as discussed in e.g. [33] – as a simplification this concept will not include bed material/heat transport between the reactors and hence assumes that pure char is transported to the gasifier.

In a more simple fluid bed design (Figure 21, right), the pyrolysis reactor is designed as a steam-blown fluid bed in order to avoid high-temperature blowers. Due to the increased heat capacity/steam content of the pyrolysis gases, the POX will be carried out at 900°C and led through a fixed dolomite bed in order to convert tars effectively and avoid cooling prior to the gasifier. This pyrolysis configuration will however have a relatively high steam consumption due to the smaller temperature difference from 700-500°C (heat exchange assumed limited by a 50°C pinch point between product gas at 750°C) and thus circulation of bed material between gasifier and pyrolyzer might very well be a more effective solution to limit the steam flow.

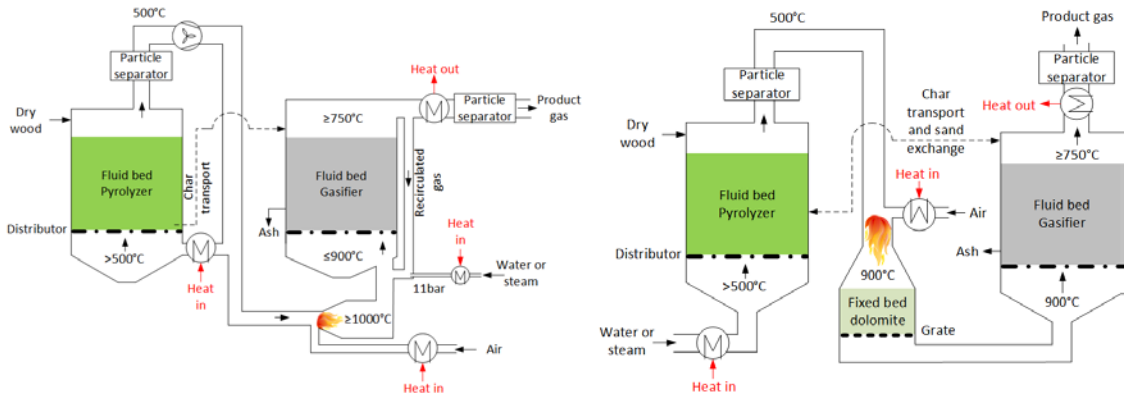

Figure 28 – Fluid bed designs. Left: Fluid bed recirculation concept. Right: Steam-blown fluid bed concept.

Modeling

The systems and all there components were modelled using zero-dimensional components in the DNA software [34][35]. The main assumptions for the systems are listed in Table 13. The modeled systems are evaluated on their cold gas efficiencies, η_{cg}, and total effiencies, η_{total}, as

seen in Equation 4 and Equation 5 – where *PG* denotes product gas and $\dot{W}$ is the electricity consumption of blowers.

Fuel	Wood chips with 50% moisture
Steam dryer	Inlet steam temp. 250°C, outlet steam temp. 120°C, 4wt% of the moisture remains in liquid state in the fuel (corresponding to a fuel moisture of 3.8wt%, pressureloss is 30mbar [31]
Pyrolyzer	Heat loss = 1% fuel input LHV, fixed bed pressure loss = 30mbar [31], fluid bed pressure loss = 146mbar, fixed and fluid bed volatiles are assumed to have a H_2 content of 20v% and 10v% respectively [36][37]
Gasifier	Heat loss = 1% fuel input LHV. Assumes that the water-gas shift reaction is in equilibrium at the outlet temperature. Carbon conversions are 99% and 95% for fixed [38] and fluid bed [39][40] models respectively. The methane content in the gas from the POX is assumed inert through the gasifier. Similar to the pyrolyzer the pressure loss is 146mbar
Bed material recirculation	The flow is modeled as a heat flow from the gasifier to the pyrolyzer assuming that the bed material is sand (c_p=0.83kJ/(kg-°C)) and that the heat flow can be estimated via the temperature difference of the beds (outlet temperature).
Ejector	Assumed efficiency of 20% and 11bar motive pressure [41] and calculated via Equation 3 [42] (States 1 and 2 are the motive and gas fluid respectively and 3 is the resulting)
Heat exchangers	50K pinch point, 10mbar pressure loss, no heat loss
Blowers	40% isentropic efficiency, 95% combined mechanical and electrical efficiency

Table 14 – Main modeling parameters.

$$\eta_{ej} = \frac{\dot{V}_2 P_2 \ln(P_3/P_2)}{\dot{V}_1 (P_1 - P_3)}$$

Equation 3

$$\eta_{cg} = \frac{\dot{m}_{PG} \cdot LHV_{PG}}{\dot{m}_{fuel} \cdot LHV_{fuel}}$$

Equation 4

$$\eta_{total} = \frac{\dot{m}_{PG} \cdot LHV_{PG} - \dot{W}}{\dot{m}_{fuel} \cdot LHV_{fuel}}$$

Equation 5

Results

The 4 systems were modeled and optimized with regards to cold gas efficiency. The resulting flow sheets can be seen in Figure 22-Figure 25. Product gas compositions and efficiencies are given in Table 14 and Table 15, respectively.

The highest performance is achieved by the Downdraft and Updraft concepts, which is namely due to their expected due to their higher carbon conversion, input temperature tolerances and effective updraft pyrolyzer heat exchange. The updraft heat exchange lowers the recircu-

lated flow significantly, which combined with the lower pressure drop and temperature results in 4-7 times lower blower consumption compared to the Fluid bed recirculation concept. The POX temperatures are high for both fixed bed designs and will for the Downdraft concept result in almost complete conversion of tars prior to the gasifier.

The Updraft concept has a penalty with regards to inlet temperatures of the gasification reactor and the cooling driven by the ejector is seen to be very energy intense because of a high steam consumption. The heat required to generate the ejector steam corresponds to approximately a third of the steam dryer heat consumption. The heat needed for ejector steam generation is however assumed to be available in the downstream equipment.

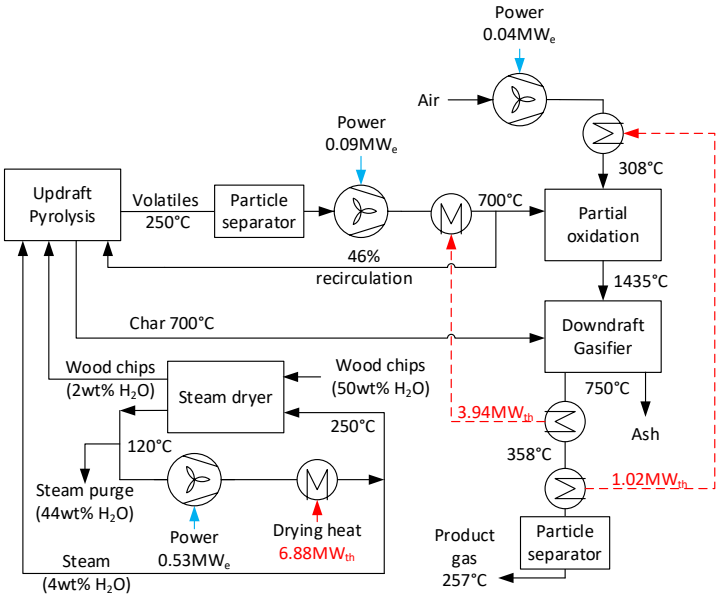

Figure 29 – Model of 50MW$_{th}$ (dry basis) Downdraft concept with relevant state values.

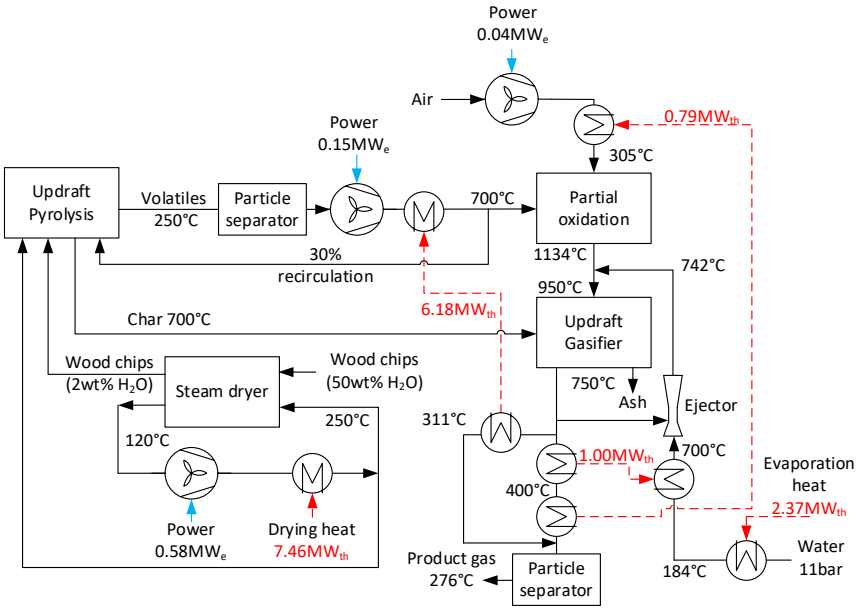

Figure 30 - Model of 50MW$_{th}$ (dry basis) Updraft concept with relevant state values and energy flows

The Fluid bed recirculation concept is seen to achieve a lower cold gas efficiency than the Updraft concept. The system is especially limited by the pyrolysis unit as the applied temperatures here stresses the blower, require a large recirculating flow of gas and causes the product gas temperature to be higher than the 750°C that is applied in the other designs – all of which will lead to lower efficiency. Due to the lower char yield, the POX is significantly cooler than the fixed bed concepts.

The Steam-blown fluid bed concept differs from the other concepts, as no gas recirculation or high-temperature POX is applied. The high steam flow causes significant losses in the heat exchange - especially in the evaporator. In order to minimize the steam flow, the concept is optimized by letting a heat flow run from the gasifier to the pyrolyzer – which is achived by bed material (sand) circulating between the two reactors – where the sand temperature is assumed equal to the product gas temperature. The high steam requirement might be covered entirely by the steam dryer if a fuel with sufficient moisture is used. The Steam-blown concept achieves the lowest cold gas efficiency, but because of the lack of a high-temperature blower, the total efficiency is in range of the Fluid bed recirculation concept.

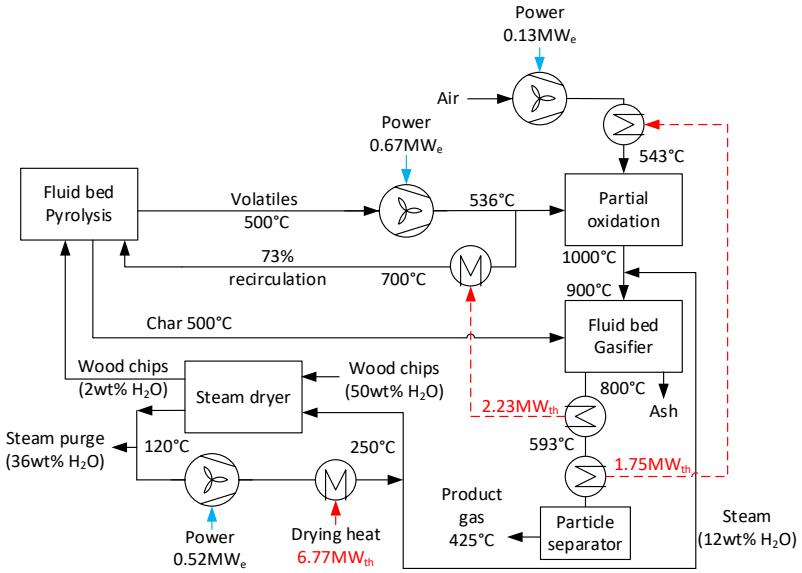

Figure 31 - Model of 50MW$_{th}$ (dry basis) Fluid bed recirculation concept with relevant state values.

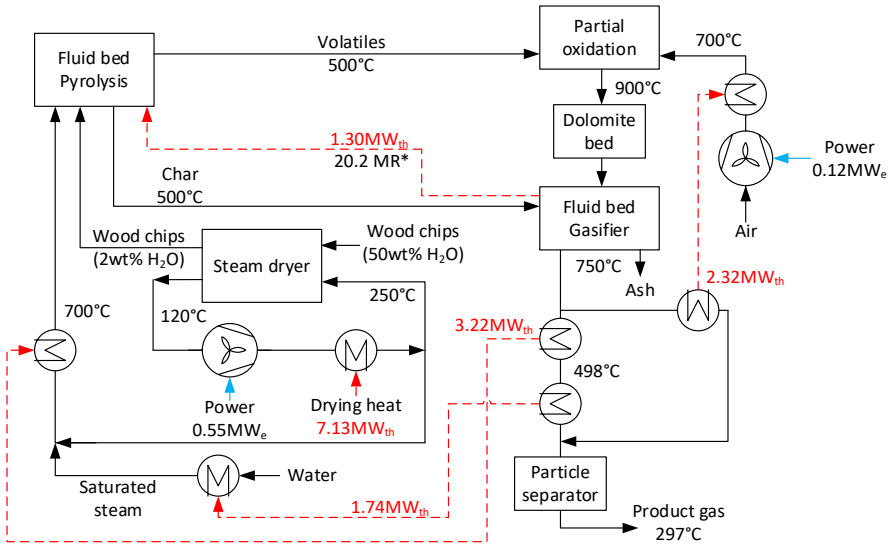

*Figure 32 – Model of 50MW$_{th}$ (dry basis) Steam-blown fluid bed concept with relevant state values. *Mass Ratio of sand-to-char from pyrolysis - bed material mass flow calculated based on the 1.30MW$_{th}$ heat flow from gasifier to pyrolyzer with bed temperatures of 750°C and 500°C respectively and assuming sand as bed material.*

	H_2 [vol%]	CH_4 [vol%]	CO [vol%]	CO_2 [vol%]	N_2 [vol%]	H_2O [vol%]	LHV_{wet} [MJ/kg]	LHV_{dry} [MJ/kg]
Downdraft	29.2	0.0	29.0	6.5	30.0	5.0	7.27	7.61
Updraft	28.2	0.7	9.0	13.5	16.2	32.2	5.07	7.20
Fluid bed recirculation	26.9	0.9	24.6	8.8	29.5	8.9	6.63	7.16
Steam-blown fluid bed	25.5	1.0	8.9	13.9	20.2	30.2	4.65	6.33

Table 15 – Gas compositions and LHV's for the 4 designs.

	η_{cg} [%]	η_{total} [%]
Downdraft	93.4	92.1
Updraft	92.6*	91.1*
Fluid bed recirculation	87.9	85.2
Steam-blown fluid bed	84.7	83.4

*Table 16 – Cold gas and total efficiencies of the concepts (see definitions in section 3). Exergetic efficiencies and analysis is given in the publication 5 in Section 4.1. All concepts assume that low-temperature heat for drying is availbale from downstream gas conversion (to electricity or fuel) *The updraft concept assumes that additional low-temperature heat is availbale from downstream gas conversion to satisfy the steam consumption of the ejector.*

Perspectives

The 4 concepts are designed for medium to large scale (10-100 MW_{th}), for high cold gas efficiency with limited gas cleaning requirements. The concept efficiencies, expected tar concentrations and complexity of gas cleaning are given in Table 16 and compared with the Viking gasifier, LT-BIG and relevant medium- and large-scale state-of-the-art gasifiers. The designed concepts, along with the Viking gasifier, are seen to have a cold gas efficiencies that are 6-22%-points higher, while only applying little gas cleaning. The Steam-blown and the recirculation fluid bed concepts outperform the other direct air-blown fluid bed gasifiers: LT-BIG and Skive – of which the Skive gasifier utilizes extensive gas cleaning, but on the other hand only employs a single reactor for fuel conversion. The indirect gasifiers MILENA and FICFB produces a nitrogen-free product gas, but with the penalty of significantly lower efficiency and more complex gas cleaning. The Carbo-V process is build on some of the same principles as the TwoStage gasifier by using separate pyrolysis and gasification and a POX, but lacks the heat integration by not using the hot product gas for heating the pyrolysis. While the designs does not compare directly to several of the state-of-the-art gasifiers, the developed designs can be technically feasible for the medium-large-scale market.

	η_{cg}	Tar content	Gas cleaning	Reference
Downdraft	93.4%	0.1mg/Nm^3	• Particle filter	This study
Updraft	92.6%	0.1mg/Nm^3	• Particle filter	This study
Fluid bed recirculation	87.9%	1mg/Nm^3	• Active carbon filter • Particle filter	This study
Steam-blown fluid bed	84.7%	4-6mg/Nm^3	• Dolomite reactor • Particle filter	This study
TwoStage Viking gasifier (moving and fixed bed)	87-90%[a]	0.1mg/Nm^3	• Particle filter	[2][43]
LT-BIG (fluid beds)	81%	1mg/Nm^3	• Active carbon filter • Particle filter	[44]
Skive gasifier (fluid bed)	77%[b]	Dew point <30^{o}C	• Dolomite bed material • Tar reformer • Particle filter • Scrubber	[45]
MILENA gasifier (fluid beds)	78%	25-63mg/Nm^3	• Catalytic bed material • Scrubber • Particle filter	[46][47]
FICFB (fluid beds)	55-75%	20mg/Nm^3	• Catalytic bed material • Scrubber • Particle filter	[29][48]
Carbo-V (moving bed and entrained flow)	49[a]-71%	Below detection limit	• Scrubber	[49]

Table 17 – Comparison of cold gas efficiencies and gas cleaning of the TwoStage gasifier concept to relevant medium- and large-scale systems. Tar concentrations and dew points are after gas cleaning. [a]Experimental data (dry basis). [b]Based on 19.5MW$_{th}$ and 6MW$_e$ assuming 40% gas-to-power engine efficiency [50].

While the fixed bed concepts achieve the highest performance parameters and the Updraft concept has some fuel flexibility with regards to particle size, the fluid bed concepts will be much more fuel flexible and are therefore of special interest for further optimization, as especially medium-scale (and possibly large-scale) systems will likely require local and low-value biomass to be competitive [8]. Especially if the ash/char is considered a valued product.
As the gas quality with regards to tars and inorganics is expected to be relatively high when using wood, the gas is most likely suited for processes that require such a quality, such as chemical synthesis, fuel cell and gas turbine/combined cycle plants. In order to gain more insight into the market possibilities and applications it would be ideal to investigate the concepts further. Points of interest are:

- Providing a higher level of detail of the physical design: char transport mechanisms between reactors; dimensioning of reactors etc.
- Converting the concepts to oxygen-blown operation to avoid nitrogen dilution which lowers the cost of liquid fuel synthesis and enables production of synthetic natural gas.

- The technical feasibility of using alternative and cheap fuels with low ash-sintering temperatures such as straw.

Conclusions

Designs of upscaled TwoStage gasifiers with very high tar conversion and efficiencies has been presented, modeled and evaluated on energy and exergy basis. With relatively simple measures and components, the 4 concepts have shown excellent efficiencies including cold gas efficiencies of 84.7-93.4% and low expected tar levels using only limited gas cleaning. Especially interesting is the 1) favourable performance of pyrolysis applied with gas recirculation that allow an effective heat exchange between fuel and product gas, while minimizing dilution of the pyrolysis gas; and 2) the integration of a steam drying unit that can either function as a fluidization medium or partial oxdation quench and allow effective heat integration and high-temperature tar conversion, respectively. The use of partial oxidation is a very effective meaure to reduce tars and the hot gas is effectively used for the endothermic char conversion, which also reduces the tar content even further. Several options for integrating the hot product gas in the pyrolysis and partial oxidation has been presented, with the use of drying steam or recirculated gas proving to be effective. The 4 designs are still in an early development phase, but an overview of large-scale state-of-the-art gasifiers indicates that the high-performing systems can be technically feasible in the medium- and large-scale market.

5.4.2 Analysis of flexible, upscaled TwoStage gasifiers in a polygeneration context

This study investigates the possibilities of improving the TwoStage gasification technology in a polygeneration framewrok in order to improve the feasibility. The study focuses on three key challenges for the system in this context:

- Upscaling capacity: It is considered beneficial to design larger plants to decrease specific investment costs [51]. The TwoStage gasifier has been built up to 1.5MW_{th} input, but is expected to be limited to around 10MW_{th} [19]. This restrain is because of the applied reactors, as the pyrolysis screw conveyer heat exchange area will be either costly and/or inpractical at larger scales and the downdraft char bed might experience difficulty with evenly distributing the char without causing large pressure drops. It is suggested to scale the system to 10-100MW_{th}.

- Air/oxygen flexibility and simple gas cleaning: In recent work [52], it is shown tha the TwoStage gasifier is expected to operate effectively with both air and oxygen as gasification media. And because the downdraft char bed is evaluated as infeasible for this study, it is desired to simplify the tar conversion as tars and coherent complex gas cleaning can represent major costs and complexity [53][54]. It is therefore suggested to design a system that can reduce the tar level sufficiently (depending on application) in a single POX reactor.

- Fuel flexibility: Currently the TwoStage gasifier can only operate on wood chips due to the intolerance to fines and high temperatures, but it is desired to utilize a wide spectre of fuels such as wood and straw pellets. Fuel costs represent around 30-50% of the total cost of the final product when traditional international feedstocks such as wood pellets and chips are used [55][54][51][56]. There is however a significant potential in minimizing fuel costs. Using: 1) local/regional fuels such as agricultural residues and energy crops can reduce fuel costs to 30-60% compared to internationally traded ones; 2) process residues like bagasse, black liquor, waste wood

costs are 15-20%; 3) wastes can have zero or negative, costs [51][8]. This means potential product cost reductions of up to 50% if alternative fuels can be utilized.

This study will investigate these three aspects via thermodynamic modeling and provide preliminary designs of TwoStage gasifier concepts operating within the Polygeneration concept.
Design details and fluid bed experiments can be found in publication 6 in Section 4.1.

Modeling

This study will investigate 3 plant configurations that will each be modeled using air/oxygen and wood/straw – resulting in 12 models. The main difference to the 3 systems is the applied pyrolysis conditions, as the char yield and composition has a significant effect on the POX and gasifier and hence the total system efficiency. Three pyrolysis processes are chosen: updraft fixed bed, slow fluid bed and fast fluid bed. The only modeled difference between the fast and slow fluid bed is the char characteristics, which is an assumption as especially carbon conversion and pressure loss might differ. The design basis for the systems are shown in Figure 26-28 respectively.
The Fixed bed system utilize a fixed bed updraft reactor. The reactor also allows some fuel particle flexibility using chips and pellets. The volatile gas recirculation is done by a blower. It is vital that the outlet temperature of the reactor is sufficiently high to avoid condensation of tars: 250^{o}C is chosen based on previous experiences with the reactor [31]. The produced char will be transported via e.g. a screw conveyer, to a fluid bed char gasifier.
The fluid bed systems similarly utilizes a blower for recirculating volatiles, but it will experience much higher thermal stresses as the gas temperature is projected to be the same as the bed: 500^{o}C is chosen to ensure complete tar release [32]. The Slow fluid bed system will transport the char via a loop seal at the top of the bed that will drain the char-rich layer, while the Fast fluid bed system will apply a cyclone for transporting char and bed material. The systems are initially projected to feature one slow and one fast bed each to simplify the recirculation of bed material, but will not be investigated further here.
The modeling is carried out in the DNA (Dynamic Network Analysis) software that features zero-dimensional components [34][35]. Key main model data are listed in Table 17.

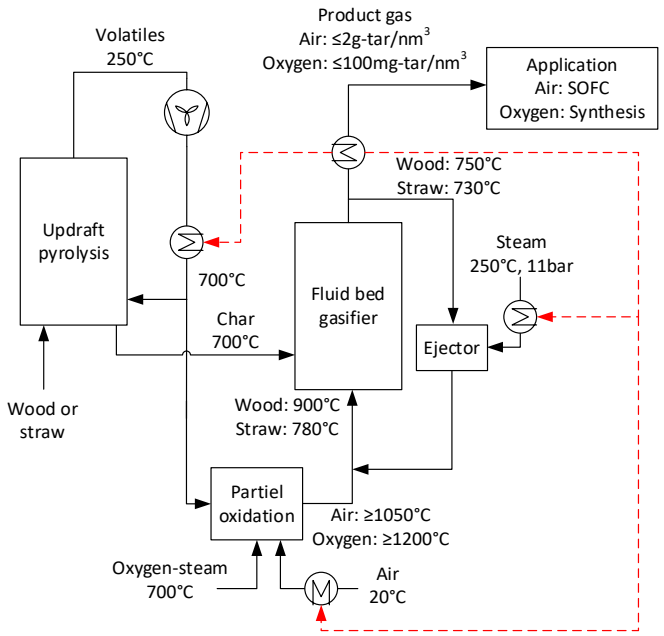

Figure 33 – Design basis for the Fixed bed system. Red dotted lines are heat flows.

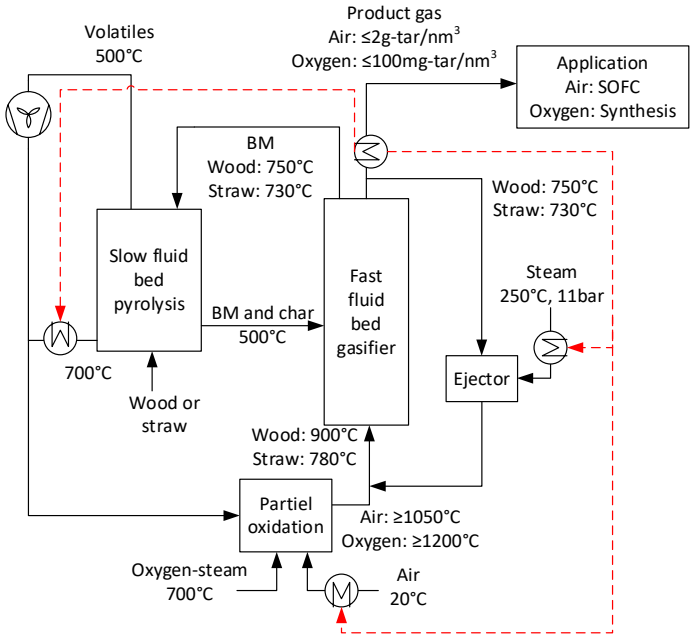

Figure 34 – Design basis for the for the Slow fluid bed system. BM denotes bed material. Red dotted lines are heat flows.

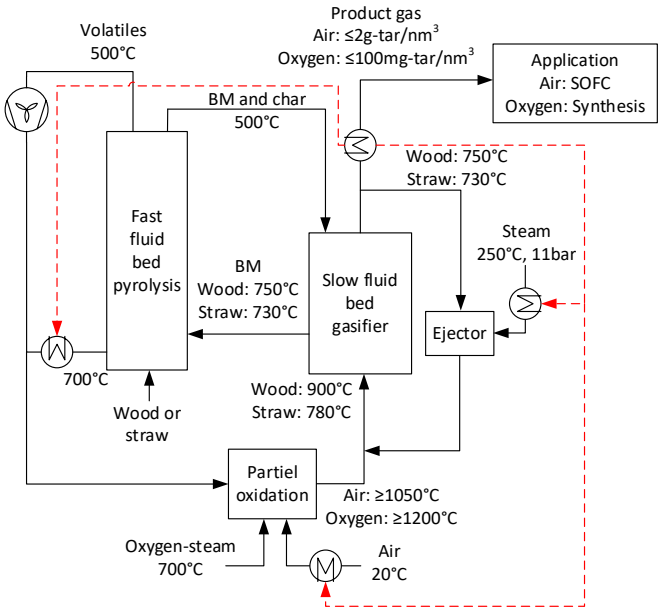

Figure 35 – Design basis for the Fast fluid bed system. BM denotes bed material. Red dotted lines are heat flows.

Fuel	50MWth input, 7% moisture (assuming pellet standard / pre-drying)
Pyrolyzer	Heat loss = 1% fuel input LHV, fixed bed pressure loss = 30mbar, fluid bed pressure loss = 146mbar[a], fixed and fluid bed volatiles are assumed to have a H_2 content of 20v% and 10v% respectively [37][36]
Partial oxidation	Assumes thermal equilibrium (Gibbs minimization) at outlet temperature – method described in [13][57].
Gasifier	Heat loss = 1% fuel input LHV. Assumes that the water-gas shift reaction is in equilibrium at the outlet temperature. Carbon conversions are 95% for all models. The methane content in the gas from the POX is assumed inert through the gasifier. Similar to the pyrolyzer the pressure loss is 146mbar
Bed material recirculation	The flow is modeled as a heat flow from the gasifier to the pyrolyzer assuming that the bed material is sand (c_p=0.83kJ/(kg*°C)) and that the heat flow can be estimated via the temperature difference of the beds (outlet temperature). The mass flow is determined via the recirculation rates in Table 3.
Ejector	Assumed efficiency of 27% and 11bar motive pressure [41] and calculated via Equation 3 [42]
Heat exchangers	50K pinch point, 10mbar pressure loss
Blowers	40% isentropic efficiency, 95% combined mechanical and electrical efficiency

Table 18 – Main modeling parameters.

The cold gas efficiency and total efficiency is calculated on dry basis via Equation 4 and Equation 5.

Results

The main model results are given in Table 18. The cold gas efficiencies are seen to be generally high and rival competing technologies (see Table 19). The efficiencies are within 3% for each concept (Fixed, Slow, Fast) and POX temperatures are varying ≤125°C for wood vs straw and

≤190°C for air vs oxygen for each system, which displays a relative convenient level of process stability. It is also seen that the cold gas efficiencies are within 5%-points for each mode across systems.

The POX temperatures are seen to be high and of all the concepts, only the POX temperature of the Fast fluid bed was set to the minimum design value. The POX temperature of the other concepts was set based on the heat required by the downstream endothermic char gasification. The Fast fluid bed POX temperature causes the gasifier outlet temperature to be 70-90°C above the design value for wood fuels and the ejector steam superheat becomes artificially low (as more heat is available in the exhaust) for straw fuels, both of which in turn decreases the cold gas efficiency. The Slow fluid and Fixed bed system POX temperatures are however very high and are by default (by implementing the design values) 200-250°C higher than needed to accommodate the required reduction of tar. Hence, these systems show some additional flexibility that enables the use of even less gas cleaning and possibly the use of alternative applications that requires cleaner gases e.g. combustion engines.

Using woody fuels with a high ash-sintering temperature significantly reduces the steam consumption as less cooling is needed for the POX – this effect is studied in the following section. These higher flows will lead to system losses as the steam is added at 250°C and removed from the system (in the product gas) at ≈300-500°C. This effect is present in reverse when comparing the oxygen-blown system, as steam is added at 700°C.

		Wood		Straw		
		Air	**Oxygen**	**Air**	**Oxygen**	**Average efficiency**
Fast fluid bed	Cold gas efficiency [%]	86.0	85.0	83.0	83.2	84.3
	Blower consumptions [MW_e]	0.80	0.64	0.78	0.61	
	Total efficiency [%][a]	84.4	83.7	81.4	82.0	82.9
	POX temperature [°C]	1050	1200	1050	1200	
	Steam consumption [kg-steam/kg-fuel(dry)]	0.60	1.00	0.84	0.92	
Slow fluid bed	Cold gas efficiency [%]	86.6	87.2	84.2	84.9	85.7
	Blower consumption [MW_e]	0.81	0.70	1.21	1.10	
	Total efficiency [%]	85.0	85.8	81.8	82.7	83.8
	POX temperature [°C]	1236	1413	1291	1454	
	Steam consumption [kg-steam/kg-fuel(dry)]	1.02	1.22	2.41	2.48	
Fixed bed	Cold gas efficiency [%]	86.8	89.3	86.5	87.7	87.5
	Blower consumption [MW_e]	0.20	0.10	0.20	0.10	
	Total efficiency [%]	86.4	89.1	86.1	87.5	87.3
	POX temperature [°C]	1395	1585	1339	1462	
	Steam consumption [kg-steam/kg-fuel(dry)]	1.34	1.41	2.04	2.05	

Table 19 – Main results from modeling.

Evaluation and perspectives

The choice of which of the three systems are the best will naturally depend on the specific business case. Initially the Fixed bed system looks the most favorable due to its high efficiency and reasonable steam consumption. The fluid bed systems do however have an advantage

with regards to particle sizes, as they will not necessarily require chipped, pelletized or briquetted fuel. This is a distinct advantage when considering the discussed fuel flexibility and corresponding cost reduction. However, as the current market dictates that wood is the primary fuel for gasifiers, the Fixed bed system is likely the currently best performing plant. Preferably, the gasifier residues/biochar can be considered a product, which could justify reducing the carbon conversion and hence a lower steam consumption. While a low pressure loss is beneficial, a better mixed fluid bed reactor might be more relevant, as the increased mixing could limit agglomeration (allow a higher maximum gasifier temperature) and slightly increase carbon conversion. In order to streamline the equipment dimensioning and processes, the carbon conversion could be slightly lowered for straw to match wood operation. These conditions would cause steam consumptions in the range of 1.0-1.4 for wood[1] and straw[2] with efficiencies around 84-88% and 76-80% respectively. At these modified conditions the POX temperature will still be ≥1200^{o}C across air/oxygen and wood/straw.

In order to assess the feasibility of the proposed systems, a comparison of the Fixed bed system, with the modified values discussed in the publication, relevant gasification technologies are presented in Table 19. Compared to the Viking TwoStage gasifier, the performance is similar, but the design allows higher process stability (easier pressure control in gasifier compared to the downdraft reactor) and much higher fuel flexibility.

Other fluid bed gasifier are seen to achieve a roughly 10% lower cold gas efficiency when using wood, while also applying much more complex and expensive gas cleaning. When the Fixed bed system applies straw the cold gas efficiency is similar to the other fluid bed gasifiers.

The LT-CFB gasifier achieves the same efficiency when including the high chemical energy content of the tars. The LT-CFB is originally designed for co-firing in large steam power plants, but is currently limited beyond this application because of the tar content. The designed systems in this study will be able to process straw and utilize them in a variety of applications including combustion engines, gas turbine, boilers and synthesis.

[1] Estimating 925^{o}C, 250mbar pressure loss and 90-95% carbon conversion

[2] Estimating 780^{o}C, 250mbar pressure loss and 80-85% carbon conversion

	Process	Fuels	Gas cleaning[a]	Cold gas efficiency (dry)	Reference
Fixed bed system with modified design values	Two-stage fixed and fluid bed	Wood, straw and more[b] (chips/pellets)	Might need carbon filter in air-straw mode (POX = 1200°C)	Wood: 84-88% Straw: 76-80%	This study
TwoStage Viking gasifier	Two-stage moving/fixed bed	Wood (chips)	-	87%	[2]
LT-BIG	Two-stage coupled fluid beds	Wood	Carbon filter	81%	[44]
Skive gasifier	Turbulent fluid bed	Wood	Catalytic bed material, catalytic reformer, scrubber	77%[c]	[45]
FICFB	Indirect gasification, coupled fluid beds	Wood	Catalytic bed material, scrubber	55-75%	[29][48]
MILENA	Indirect gasification, coupled fluid beds	Wood	Catalytic bed material, scrubber	78%	[46][47]
LT-CFB	Coupled fluid beds	Wood, straw, wastes etc.	-	80%[d]	[58]

Table 20 – Comparison of the Fixed bed system with modified design values and relevant gasification technologies. [a]Particle filter not included. [b]Fuel flexibility depends on agglomeration temperatures. [c]Assuming 40% gas-to-power engine efficiency [50]. [d]The low-temperature gasifier product gas has a very high tar content that constitutes up to 50% of the chemical energy, which is included here.

Conclusions

This study has presented the findings of a product development study of the TwoStage gasifier. It was desired to design a plant based on the TwoStage principles that featured upscaling potential, a high level of fuel flexibility and was compatible with the grid-balancing Polygeneration concept. By investigating multiple plant configurations using wood/straw fuels and air/oxygen the following conclusions can be made:

- Relatively high level of process stability can be obtained in spite of the varying conditions
- Very high partial oxidation temperatures of >1230°C for two of the concepts will ensure a very low level of downstream gas cleaning
- Very high cold gas efficiencies of 83-89% across wood/straw and air/oxygen for the three different systems displays the effectiveness of the overall concept idea

A selected and modified design achieved a slightly lower cold gas efficiency (84-88%) with wood and air compared to the TwoStage Viking gasifier, but outperformed competing gasifiers with roughly 10%-points while having increased flexibility.

6. Utilization of project results

The focus of this research project has been on building up new knowledge on integration of solid oxide cells with biomass gasifier systems and develop future gasifier plants. The project thus provides a steppingstone for further and more specific research applications, whilst also providing commercially attractive solutions for gasification industry.

The project has been a major asset in building up the knowledgebase with regards to other research projects. The study on implementing oxygen-blown gasification will be directly transferred to the SYNFUEL research project (Innovation Fund Denmark nr. 4106-00006B) where another state-of-the-art gasification platform (the LT-CFB - formerly Pyroneer) will be converted into utilizing oxygen and partial oxidation experiments will be made with O_2-CO_2.
As a more direct link, many of the project activities are already being continued in the recently (2017) started EP2GAS research project (EUDP nr. 64017-0011) that is a natural extension of the project. Here the SOFC, oxygen-blown and gasifier design knowledge is being implemented. That project constructs and operates the developed gasifier design in the patent application (Section 4.5) and will provide a proof-of-concept for the design. The solid oxide cell integration will also be done in relation to the studies presented here.
Currently a research application on methanol production via biomass gasification and solid oxide electrolysis is being developed. The project will directly use the oxygen-blown experiences made in this project.

The modeling work in WP3 (Section 5.3) is being further analysed in an upcoming publication(s). The techno economic assessment of the polygeneration plant indicated a benefit of polygeneration compared to separate electricity and bio-SNG production. The study will be followed by a more direct comparison of the polygeneration plant with alternative production by separate electricity and bio-SNG producers focusing on a future fossil-free energy system. In such a scenario, peak demand electricity is often supplied by gas turbines or gas engines operating on bio-SNG. The hypothesis is that the value of the electricity produced by the polygeneration system is even higher in such a scenario because it replaces a part of the in-efficient electricity production from gas turbines operating on expensive bio-SNG. From an energy perspective it also makes sense that as much as possible of the peak demand electricity is provided by conversion of primary energy resources (biomass) instead of a biomass-derived product (bio-SNG). However, a conventional biomass based CHP plant is still thought to be infeasible in the future fossil-free energy system, as the number of operating hours will be too few. A paper on this is currently in the writing phase.

The gasifier patent application (Section 4.5) has generated interest and been pitched to and discussed with companies on several occasions. Following multiple meetings, the contact will be continued during the EP2GAS project, where a prototype of the patent will be constructed and operated. The patented concept has been pitched during open DTU research days and at international conferences and continued promotion of the concept is expected.

The project has also delivered significant dissemination activity that will continue to spread as all the publications are finalized, more presentations are made and time allows scientists to discover the research.

7. Project conclusions and perspectives

The project has dealt with the integration of solid oxide cells with the TwoStage Viking gasifier and the development of upscaled gasifier designs. The project has thus presented how smart grid flexible concepts can be applied to gasification and assessed the performance, which will provide the foundation for future research projects and developments. These analysis' has been coupled with the design basis for future large-scale and flexible gasifier plants that look promising compared to current commercial gasification technologies. Thus the project provides the foundation for the design of future polygeneration plants and concepts.

The main conclusions from the project are:

- It is technically feasible to couple the TwoStage Viking gasifier with an SOFC and achieve high electric efficiencies without extensive additions of equipment or any change in gasifier operation. The system provided state-of-the-art results and showcases the high potential of the gasifier-SOFC coupling. The cells are likely tolerant to smaller concentrations of sulphur, but it is recommended to apply some level of desulphurization (and for other species if needed) to protect the costly component. Gasifier design can however greatly simplify the level of gas cleaning. For power production the system might add a combined cycle power system downstream the stack in order to be competitive as the gains in electrical efficiency is significant.

- The study has shown that the Viking plant has ability to apply alternating operation with air and O_2-CO_2 mixtures as gasification media without major changes in operation. Hence, a proof-of-concept for integrating TwoStage gasification in the polygeneration context has been provided. The system was only slightly modified and provided very high gas quality in-line with air-blown operation. Adjusting the O_2:CO_2 ratio can further optimize operation and provide higher efficiencies, less diluted product gas and enable higher POX temperatures if needed.

- A thermoeconomic analysis of the proposed polygeneration concept found the energy efficiency of each operating mode, and showed the economic benefit of the polygeneration system compared to single mode systems. It was found that higher capacity factors are achieved with polygeneration and the investment in the polygeneration system is lower than the combined investment of two single mode systems. The polygeneration system operated in some scenarios mostly in electricity production mode while in others most in electricity storage mode. This depended mainly on the expected electricity price. The advantage with polygeneration was found to be greatest when electricity prices are volatile.

- From a thermodynamic point-of-view, it is possible to design very effective, large-scale TwoStage gasifier systems within the boundaries of the current technical literature. Designs for polygeneration were also found to be efficient and competitive. All of these designs are technically competitive to current state-of-the-art systems on key areas, which are central to the feasibility of the plants. As a concrete outcome, an updraft gasifier concept has been formulated as a patent application and is currently being constructed for the EP2GAS research project at DTU (EUDP no. 64017-0011).

- This study has provided the academic foundation for thermodynamically developing and/or evaluating gasifier systems going forward. Results across reactor platforms as well as fuel types and gasification media, has provided a multi-dimensional analysis of strengths and weaknesses, as well as discussions, for a given reactor constellation in a two-stage system. Hence, future opportunities and assessments can be engaged from an improved starting point, as these systems will be become increasingly relevant for the entire energy system going forward.

8. References

[1] Gadsbøll R, Thomsen J, Bang-Møller C, Nygaard C, Tomaszewski A, Ahrenfeldt J, et al. Experimental analysis of a solid oxide fuel cell stack coupled with biomass gasification. 23rd Eur. Biomass Conf. Exhib., 2015, p. 555–61.

[2] Ahrenfeldt J, Henriksen UB, Jensen TK, Gøbel B, Wiese L, Kather A, et al. Validation of a continuous combined heat and power (CHP) operation of a Two-Stage biomass gasifier. Energy & Fuels 2006;20:2672–80.

[3] Egsgaard H, Ahrenfeldt J, Ambus P, Schaumburg K, Henriksen UB. Gas cleaning with hot char beds studied by stable isotopes. J Anal Appl Pyrolysis 2014;107:174–82. doi:10.1016/j.jaap.2014.02.019.

[4] Hofmann P, Panopoulos K, Fryda L, Schweiger a, Ouweltjes J, Karl J. Integrating biomass gasification with solid oxide fuel cells: Effect of real product gas tars, fluctuations and particulates on Ni-GDC anode. Int J Hydrogen Energy 2008;33:2834–44. doi:10.1016/j.ijhydene.2008.03.020.

[5] Oudhuis AB., Bos A, Ouweltjes JP, Rietveld G, van der Giesen A. High efficiency electricity and products from biomass and waste, experimental results of proof of principle Presented at the 2nd World Conference and Technology Exhibition. 2nd world Conf. Technol. Exhib. biomass energy, Ind. Clim. Prot., 2004, p. 10–4.

[6] Hofmann P, Schweiger a., Fryda L, Panopoulos KD, Hohenwarter U, Bentzen JD, et al. High temperature electrolyte supported Ni-GDC/YSZ/LSM SOFC operation on two-stage Viking gasifier product gas. J Power Sources 2007;173:357–66. doi:10.1016/j.jpowsour.2007.04.073.

[7] Bang-Moeller C. Design and Optimization of an Integrated Biomass Gasification and solid oxide fuel cell system. Technical University of Denmark, 2010.

[8] International Energy Agency. Technology Roadmap - Bioenergy for Heat and Power. 2012.

[9] Quaak P, Knoef H, Stassen H. Energy from Biomass a review of combustion and gasification technologies. World Bank Tech Pap 1999:1–78. doi:ISBN0 -8213-4335-.

[10] Knoef H, editor. Handbook Biomass Gasification. BTG biomass technology group; 2005.

[11] Ridjan I, Mathiesen BV, Conolly D. A review of biomass gasification technologies in Denmark and Sweden. 2013.

[12] Gadsbøll RØRØ, Thomsen J, Bang-Møller C, Ahrenfeldt J, Henriksen UBUB. Solid oxide fuel cells powered by biomass gasification for high efficiency power generation. Energy 2017;131:198–206. doi:10.1016/j.energy.2017.05.044.

[13] Bang-Moeller C. Design and Optimization of an Integrated Biomass Gasification and solid oxide fuel cell system. Technical University of Denmark, 2010.

[14] Homel M, Gür TM, Koh JH, Virkar A V. Carbon monooxide-fueled solid oxide fuel cell. J Power Sources 2010;195:6367–72.

[15] Jiang Y, Virkar A V. Fuel Composition and Diluent Effect on Gas Transport and Performance of Anode-Supported SOFCs. J Electrochem Soc 2003;150:A942. doi:10.1149/1.1579480.

[16] Yakabe H, Hishinuma M, Uratani M, Matsuzaki Y, Yasuda I. Evaluation and modeling of performance of anode-supported solid oxide fuel cell. J Power Sources 2000;86:423–31. doi:10.1016/S0378-7753(99)00444-9.

[17] Hanaoka T, Hiasa S, Edashige Y. Syngas production by CO 2 / O 2 gasi fi cation of aquatic biomass 2013;116:9–15. doi:10.1016/j.fuproc.2013.03.049.

[18] Campoy M, Gómez-Barea A, Vidal FB, Ollero P. Air-steam gasification of biomass in a fluidised bed: Process optimisation by enriched air. Fuel Process Technol 2009;90:677–85. doi:10.1016/j.fuproc.2008.12.007.

[19] Bentzen JD, Hummelshøj R, Henriksen UB, Gøbel B, Ahrenfeldt J, Elmegaard B. Upscale of the Two-Stage Gasification. Proc. 2nd world Conf. Technol. Exhib. biomass energy Ind., 2004.

[20] Elmegaard B, Houbak N. DNA – A General Energy System Simulation Tool. Proc SIMS 2005 2005:43–52.

[21] Energinet.dk. Energinet.dk's analyseforudsætninger 2012 - 2035, juli 2012. 2012.

[22] Energinet.dk. SIFRE: Simulation of Flexible and Renewable Energy sources. 2015.

[23] Lythcke-Jørgensen C, Clausen LR, Algren L, Hansen AB, Münster M, Gadsbøll RØ, et al. Optimization of a flexible multi-generation system based on wood chip gasification and methanol production. Appl Energy 2017;192:337–59. doi:10.1016/j.apenergy.2016.08.092.

[24] Ahrenfeldt J, Thomsen TP, Henriksen U, Clausen LR. Biomass gasification cogeneration – A review of state of the art technology and near future perspectives. Appl Therm Eng 2013;50:1407–17. doi:10.1016/j.applthermaleng.2011.12.040.

[25] Energitilsynet. Energitilsynets prisstatistik for fjernvarmeområdet, sorteret alfabetisk. 2016.

[26] Biogas - SOEC: Electrochemical upgrading of biogas to pipeline quality by means of SOEC electrolysis - Energy system integration and economy. 2012.

[27] Ahrenfeldt J, Thomsen TP, Henriksen U, Clausen LR. Biomass gasification cogeneration - A review of state of the art technology and near future perspectives. Appl Therm Eng 2013;50:1407–17. doi:10.1016/j.applthermaleng.2011.12.040.

[28] Fjellerup J, Ahrenfeldt J, Henriksen U, Gøbel B. Formation, decomposition and cracking of biomass tars in gasification. 2005.

[29] Hofbauer H, Rauch R. Stoichiometric Water Consumption of Steam Gasification by the FICFB-Gasification Process. Prog Thermochem Biomass Convers 2008:199–208. doi:10.1002/9780470694954.ch14.

[30] Houmøller S, Hansen M, Henriksen UB. Two-Stage Fluid Bed Pyrolysis and Gasification Unit. 9th Eur. Bioenergy Conf., Elsevier; 1996, p. 1347–52.

[31] Jensen TK, Maigaard P, Noes J. Pyrolyse af træflis ved recirkulering af pyrolysegas. 1996.

[32] Ahrenfeldt J, Henriksen UB, Gøbel B, Fjellerup J. Experimental characterisation of residual-tar in wood char. 2005.

[33] Kunii D, Levenspiel O. Fluidization Engineering. 2nd ed. Butterworth-Heinemann; 1991.
[34] Elmegaard B, Houbak N. DNA – A General Energy System Simulation Tool. DNA – A Gen. Energy Syst. Simul. Tool, SIMS 2005 and Tapir Academic Press; 2005, p. 43–52.
[35] Technical University of Denmark. Homepage of the thermodynamic simulation tool DNA. DNA - A Therm Energy Syst Simulator 2009. http://orbit.dtu.dk/en/publications/id(b76040a4-5a29-4b04-a898-12711391c933).html (accessed March 24, 2017).
[36] Iversen HL, Ahrenfeldt J, Egsgaard H, Henriksen UB. Partial oxidation mechanisms of tar destruction [Confidential]. 2006.
[37] Thomsen T, Hauggaard-Nielsen H, Bruun E, Ahrenfeldt J. the potential of pyrolysis technology in climate change mitigation. 2011.
[38] Gøbel B, Henriksen U, Ahrenfeldt J, Jensen TK, Hindsgaul C, Bentzen JB, et al. Status - 2000 Hours of Operation with The Viking Gasifier 2003:3–6.
[39] Thomsen TP, Sárossy Z, Gøbel B, Stoholm P, Ahrenfeldt J, Jappe F, et al. Low temperature circulating fluidized bed gasification and co-gasification of municipal sewage sludge . Part 1 : Process performance and gas product characterization. Waste Manag 2017;66:123–33. doi:10.1016/j.wasman.2017.04.028.
[40] Basu P. Combustion and gasification in fluidized beds. Taylor & Francis; 2006.
[41] GEA Wiegand GmbH. GEA product catalogue. Jet pumps, mixers, heater, vacuum systems. 2017. doi:10.1002/ejoc.201200111.
[42] Wendel CH, Kazempoor P, Braun RJ. Novel electrical energy storage system based on reversible solid oxide cells : System design and operating conditions. J Power Sources 2015;276:133–44. doi:10.1016/j.jpowsour.2014.10.205.
[43] Bentzen JD, Brandt P, Gøbel B, Henriksen UB, Hindsgaul C. Optimering af 100 kW totrinsforgasningsanlæg på DTU: Resultater fra forsøg i uge 37 1998. 1999.
[44] Andersen L, Elmegaard B, Qvale B, Henriksen U. Modeling the low-tar BIG gasification concept. Proc. 16. Int. Conf. Effic. Cost, Optim. Simulation, Environ. Impact Energy Syst., 2003, p. 7.
[45] Andritz, Carbona. Carbona Gasification Technologies - Biomass Gasification Plant in Skive. October 2010:28–9.
[46] Meijden CM van der, Veringa HJ, Vreugdenhil BJ, Drift B van der. Bioenergy II: Scale-Up of the Milena Biomass Gasification Process. Int J Chem React Eng 2009;7. doi:10.2202/1542-6580.1898.
[47] Rhyner U, Kienberger T, Zuber C, Schildhauer TJ, Rabou LPLM, Van der Drift B, et al. Synthetic Natural Gas from Coal, Dry Biomass, and Power-to-Gas Applications. First edit. John Wiley & sons Ltd; 2016. doi:10.1002/9781119191339.
[48] Hofbauer H, Rauch R, Loeffler G, Kaiser S, Fercher E, Tremmel H. Six years experience with the FICFB-gasification process. 12th Eur Conf Technol Exhib Biomass Energy, Ind Clim Prot 2002:982–985.
[49] Bundesministerium für Ehrnärung Landwirtschaft und Verbraucherschutz. Schriftenreihe “Nachwachsende Rohstoffe”. Band 29. Analyse und Evaluierung der thermo-chemischen Vergasung von Biomass. 2006.
[50] Jenbacher type 6 gas engines n.d. https://powergen.gepower.com/products/reciprocating-engines/jenbacher-type-6.html (accessed March 29, 2017).
[51] International Renewable Energy Agency. Renewable energy technologies: cost analysis series. Biomass for Power Generation. 2012.
[52] Gadsbøll RØ, Sarossy Z, Jørgensen L, Ahrenfeldt J, Henriksen UB. Oxygen-blown operation of the TwoStage gasifier. Energy 2018;158:495–503. doi:10.1016/j.energy.2018.06.071.
[53] Devi L, Ptasinski KJ, Berends RH, Padban N, Beesteheerde J, Veringa HJ. Primary measures to reduce tar formation in fluidised-bed biomass gasifiers. 2004.
[54] Hannula I. Hydrogen enhancement potential of synthetic biofuels manufacture in the European context: A techno-economic assessment. Energy 2016;104:199–212. doi:10.1016/B978-0-08-022703-0.50014-8.
[55] Sigurjonsson HÆ, Clausen LR. Solution for the future smart energy system: A polygeneration plant based on reversible solid oxide cells and biomass gasification producing either electrofuel or power. Appl Energy 2018;216:323–37. doi:10.1016/j.apenergy.2018.02.124.
[56] Henrich E, Dahmen N, Dinjus E. Cost estimate for biosynfuel production via biosyncrude gasification. Biofuels, Bioprod Biorefining 2009;3:28–41. doi:10.1002/bbb.
[57] Elmegaard B. Simulation of boiler dynamics - Development, evaluation and application of a general energy system simulation tool. Technical University of Denmark, 1999.
[58] Nielsen RG. Optimering af Lav Temperatur Cirkulerende Fluid Bed forgasningsprocessen til biomasse med højt askeindhold. Phd thesis. Lyngby, Denmark: Technical University of Denmark; 2007.

9. Annex (NOT TO BE PUBLISHED)

The 6 publications listed in Section 4.1 are presented here.

Energy 131 (2017) 198–206

Contents lists available at ScienceDirect

Energy

journal homepage: www.elsevier.com/locate/energy

Solid oxide fuel cells powered by biomass gasification for high efficiency power generation

Rasmus Østergaard Gadsbøll [a, *], Jesper Thomsen [a], Christian Bang-Møller [b], Jesper Ahrenfeldt [a], Ulrik Birk Henriksen [a]

[a] Technical University of Denmark, Department of Chemical and Biochemical Engineering, Frederiksborgvej 399, 4000 Roskilde, Denmark
[b] Haldor Topsoe A/S, Haldor Topsøes allé 1, 2800 Kgs. Lyngby, Denmark

ARTICLE INFO

Article history:
Received 2 February 2017
Received in revised form
5 May 2017
Accepted 7 May 2017
Available online 8 May 2017

Keywords:
Bioenergy
Biomass
Gasification
Fuel cell
SOFC
Power generation

ABSTRACT

Increased use of bioenergy is a very cost-effective and flexible measure to limit changes in the climate and the infrastructure. One of the key technologies toward a higher implementation of biomass is thermal gasification, which enables a wide span of downstream applications. In order to improve efficiencies, flexibility and possibly costs of current biomass power generating systems, a power plant concept combining solid oxide fuel cells (SOFC) and gasification is investigated experimentally. The aim of the study is to examine the commercial operation system potential of these two technologies. Investigations are done by combining the commercial TwoStage Viking gasifier developed at the Technical University of Denmark and a state-of-the-art SOFC stack from Topsoe Fuel Cell for high efficiency power generation. A total of 5 tests were performed including polarization tests at various gas flows to study part-load operation; and a longer test to investigate stability. The study shows experimentally the potential and feasibility of a SOFC-gasification system with a commercial gasifier and a SOFC stack by measuring the highest reported values of such a system, with biomass-to-electricity efficiencies up to 43%. Results from related modeling studies are also presented, showcasing the intriguing potential of the system with modeled cycle electric efficiencies up to 62%.

1. Introduction

The most cost-effective path to reduce climate change is through increasing the share of bioenergy significantly, because biomass to a large extent can directly substitute fossil fuels in the present infrastructure [1–3]. Currently, biomass is mainly utilized as a substitute to fossil fuels in large (>50 MW_{th}), efficient, and modern steam power plants that reach electric efficiencies up to about 40–50% [1]. However, such plants are limited to high capacities, if high efficiencies are to be maintained. In smaller typical biomass power plants (10–50 MW_{th}) electrical efficiencies drop to 18–33% and will require flexible operation on cheap, local feedstock to be competitive in the future [1]. So, the future energy system will require advanced biomass conversion and power generating technologies to ensure environmental as well as economic sustainability.

Solid oxide fuel cell (SOFC) technology is an interesting option for high-efficient power generation in future energy systems. SOFC technology is currently under extensive research as one of the most promising near-future power technologies. Fuel cells convert gaseous chemical energy directly into electric energy through electrochemical reactions and are thus subject to less loss than traditional power generation technologies. The SOFC's are especially interesting for smaller scale power systems, as they offer high fuel flexibility (CO, H_2, CH_4), compared to other fuel cell types and can maintain their very high electric efficiency at smaller scales and part load operation. The high operating temperatures of 700–900 °C in the SOFC allows internal reforming of e.g. hydrocarbons in the stack, which increases its fuel flexibility greatly. SOFC operation is however limited by its nickel containing anode, which requires a reducing atmosphere to stay active and forces the fuel cell to exhaust excess fuel. The fraction of fuel used is called the *fuel utilisation* (FU).

In order to utilize biomass as a fuel for fuel cells, a conversion from solid to gaseous fuel is required, this can be achieved via gasification. At high temperatures, thermal gasification offers a very

* Corresponding author.
E-mail address: rgad@kt.dtu.dk (R.Ø. Gadsbøll).

http://dx.doi.org/10.1016/j.energy.2017.05.044
0360-5442/

flexible and highly efficient platform to convert solid carbonaceous matter into a combustible *product gas*. This gas typically consists of lower hydrocarbons, CO, CO_2, H_2, N_2, inorganic impurities and tars. State-of-the-art gasification plants reach cold gas efficiencies of 80–93% (biomass to product gas [LHV]) [4]. The produced gas can afterwards be processed for a variety of applications including power, heat, chemical and fuel production applications.

As a joint technology platform, SOFC-gasification systems that combine the fuel flexibility and conversion efficiency of gasification and the high electric efficiency of fuel cell technology have very high potential. Recent modeling studies from the Bio-SOFC project have shown that SOFC-gasification systems can reach electric efficiencies of 42–62% with proper design – see e.g. Refs. [5–7]. However, product gas quality and capital costs pose a challenge to further development and commercialization [8]. Product gas quality relates specifically to tars, inorganics, and particulates that can terminate fuel cell operation and thus strict gas conditioning is typically required.

SOFC-gasification systems are still on the laboratory scale and limited tests have been performed on real product gas from a gasifier [9–14]. In addition, most of these tests have only been on single cells, at low loads and/or for short time periods. The focus of these studies has mostly been on gas quality. Hofmann et al. [9–11] and Jewulski et al. [12] discussed and tested internal reforming of tars and lower hydrocarbons in the SOFC, and concluded that these compounds can be utilized as a component in the fuel if sufficient steam is added to the gas stream to avoid carbon deposition. Tests with product gas above 10 g/nm^3 of tars from a circulating fluid bed were found to be feasible at low loads [11] and tests with product gas from an updraft gasifier showed tolerance to tars up to 85 g/nm^3 at low loads [14]. While product gas with no tars, low levels of steam and light hydrocarbon levels above 9 vol% caused carbon deposition and mechanical fracture as a result of internal endothermic reforming reactions [12]. Caution should be taken when evaluating tar concentrations, as both composition and concentration will depend on the gasifier design and applied conditions.

SOFC operating on product gas at high load (fuel utilisation of >70%) have shown high electric efficiencies of up to 38% [10,13]. Hofmann et al. [10] operated a downdraft gasifier with low tar levels (<0.2 g/nm^3), but found that the high load caused anode oxidation. Oudhuis et al. [13] employed a pyrolyzer with extensive gas cleaning and thus obtained a clean gas that proved stable operation with the SOFC.

As mentioned, studies of SOFC-gasification systems are mainly focus on gas quality investigations and do therefore not represent a commercially operating system. Such a system will be operated at high loads, at various gas flow rates, and with limited gas cleaning to lower costs. Also, the gasifier will have to be very efficient in retaining as much of the chemical energy in the solid fuel into gas with a high cold gas efficiency, as the chemical energy is a main bottleneck for electrochemical combustion.

The TwoStage biomass gasifier at the Technical University of Denmark are a proven and commercial gasification system that can achieve a very high cold gas efficiency of 93%, while producing only an insignificant amount of tars and around 1 vol% light hydrocarbons (methane) with only a bag filter for gas cleaning [15] [16] [17]. Given the challenges of the previous cited works within SOFC's with product gas, it is expected that the proposed system will provide a clean gas that will minimize risk of carbon deposition and be technically feasible on commercial terms, including a relatively low level of complexity. Therefore it is expected that the coupling of the TwoStage gasifier and a state-of-the-art fuel cell stack will provide a system that will move the joint technology platform closer to commercialization and feature: 1) very high electric efficiency; 2) low levels of gas cleaning; 3) stable operation.

In 2007, the TwoStage gasifier was operated with a single-cell SOFC continuously for 150 h at low load and showed potential for stable operation [9]. This project continues the investigations previously started in Ref. [9] and will investigate commercial terms of operation. The current study operates an 800 W_e state-of-the-art SOFC stack at high load on real product gas from the TwoStage gasifier. Specifically, this study examines the full- and part-load performance of the stack when varying flow rates and load and performs long-term tests of the stack at high load. The study shows experimentally the potential and feasibility of a SOFC-gasification system with a commercial gasifier and a SOFC stack, coupled using only a bag filter, activated carbon filter, a humidifier, and a desulphuriser.

2. Materials and methods

The study was carried out at the facilities at the Technical University of Denmark (DTU), Risø Campus. The experimental equipment included the TwoStage 'Viking' gasifier, necessary fuel cell gas conditioning and the SOFC stack.

2.1. TwoStage gasifier

The TwoStage gasification concept has been developed at DTU over several decades and it has been upscaled several times and commercially up to 1.5MW_{th} [15]. The gasifier is a staged downdraft concept, where the pyrolysis and gasification are carried out in separate reactors with a partial combustion zone in between. The gasifier is unique in its ability to produce gas with virtually no tars (<1 mg/nm^3), using only a simple bag house filter and while still obtaining a high cold gas efficiency of 93% [16]. The applied TwoStage gasifier plant is a 80 kW_{th} Viking plant, which is fully automated, have been operated for more than 3000 h and have shown very stable operating characteristics with regards to continuous operation, gas composition and engine operation [17].

A flow diagram of the Viking gasifier is shown in Fig. 1. The gasifier is operated at atmospheric pressure levels. Pine wood chips of ≈40% humidity are fed into an externally heated screw conveyor that dries and pyrolyzes the fuel up to 600 °C. No fuel analysis was made, but the fuel is very similar to the fuel used in previous tests, which is shown is Table 1. The screw conveyor is heated using superheated engine exhaust. The pyrolysis products are led to the second reactor and are partially oxidized by air, raising the temperature above 1100 °C. Hereby, the tar content is reduced by 99%. The gas and char then pass through a hot fixed char bed, where the

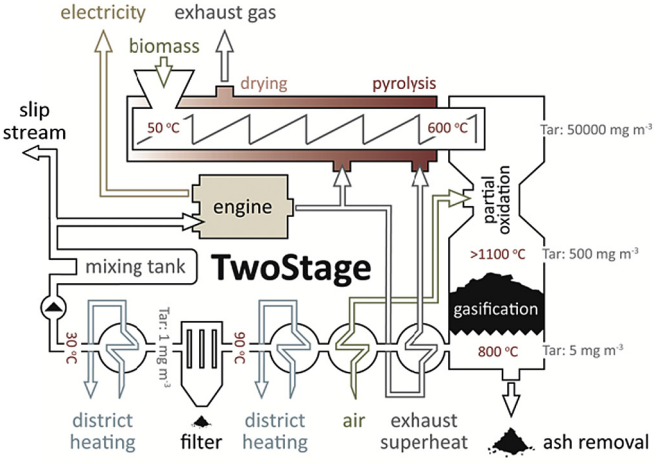

Fig. 1. Flow diagram of TwoStage gasification with an engine.

Table 1
Fuel measurements of wood chips from previous tests with the Viking gasifier [17].

Component	Method	Measure 1	Measure 2
Ash [wt%, dry]	550 °C, app. 20 h	–	–
HHV [MJ/kg, dry]	ISO 1928	19.60	–
LHV [MJ/kg, dry]	ISO 1928	18.28	–
C (wt%, dry)	ASTM 5373	48.90	49.00
H (wt%, dry)	ASTM 5373	6.20	6.00
N (wt%, dry)	ASTM 5373	0.17	0.40
S (wt%, dry)	ASTM 4239C	0.022	0.07
Cl (wt%, dry)	ASTM 4208, IC	0.063	–
O (wt%, dry)	–	–	44.00
Moisture (wt%)	–	–	32.20

char is gasified and the temperature is subsequently lowered to 800 °C at the bed outlet. The hot char bed acts as a tar cleaning unit, removing 99% of the remaining tars [17,18], yielding a near tar-free gas. The obtained product gas then flows through a series of heat exchangers and a bag house filter that removes small amounts of particles, tars and water. Afterwards, the gas enters a mixing tank, where a slipstream of about 2 kW_{th} was directed to the fuel cell setup.

2.2. Fuel cell gas conditioning

Gas conditioning is essential when using fuel cells, as this technology is highly sensitive to several gas components. Levels of hydrocarbons have to be monitored, as they will be reformed internally in the anode and cause thermal stresses by cooling and can cause carbon deposition. The reforming of hydrocarbons needs a sufficient water vapor pressure in order to avoid carbon deposition and thus the gas needs to be humidified. Inorganic compounds, including sulphur, need to be completely removed to avoid anode deactivation.

The product gas initially flowed through two active carbon filters at room temperature with a retention time of 53 s. These filters act as guard beds, removing inorganic compounds and tars.

Afterwards, the gas passed through an electrically heated water spray tower, where it was humidified to reach an oxygen-carbon molar ratio of 2. The humidification temperature was 60 °C, which correspond to a water molar fraction of about 19.5% in the humidified product gas.

The humid product gas was electrically heated to 245 °C and led through a fixed guard bed with ZnO pellets that removed remaining sulphur compounds up to 10 ppm. Afterwards the gas was heated electrically to 670 °C before being fed to the SOFC. An overview of the gas conditioning is shown in Fig. 2.

The gas composition was measured at dry and tar-free conditions with an Advance Optima 2020 Modular continuous process gas analyzer system, with an Caldos 15 cell for H_2 analysis and an Uras 14 cell for CO, CO_2 and CH_4 (ABB, Switzerland). The O_2 content was measured with an PMA 10 O_2-analyzer. The uncertainty of the gas analyzer is ±1% of the measured value. The continuous gas flow for the analyzer system was taken via a twist filter following the carbon filters.

Tars and sulphur compounds were measured at the inlet and outlet of the carbon filters. For tar analysis, solid phase adsorption (SPA) samples were taken during the experimental work with tubes from Supelco with an aminopropyl adsorbent. Three samples were taken before and after the carbon filter. The samples were analysed by gas chromatography/mass spectrometry (GC/MS) with acetone as the solvent with the modification of using stable isotopes of polycyclic aromatic hydrocarbon standards as the internal standards – see further details in Ref. [17]. Sulphur was measured using 250 mL gas probes and GC/MS with three measurements before and after the carbon filter.

2.3. SOFC stack

The SOFC stack is produced by Topsoe Fuel Cell. The stack is made of 50 planar, anode supported cells. The anode is made of yttrium-stabilized zirconia (YSZ), nickel catalysts and a mechanical support structure. The electrolyte is made of YSZ and the cathode of lanthanum strontium manganite. The stack is an 'S 1–02' type, with a footprint of 12 × 12 cm and a nominal capacity of 800 W_e. It was operated at near atmospheric pressure and the operation was designed for 700 °C fuel exhaust. The stack was fed with air as oxidizer at 670 °C. The SOFC stack was placed in an electrically heated oven at 700 °C, as the stack was not insulated. The SOFC was heated at 200 K/h to minimize thermal stresses. The start-up was carried out at open-circuit conditions with Formier10 gas (10v% H_2, 90v% N_2) and as 700 °C was reached, the stack was stabilized for 30min before switching to product gas. After switching to product gas the SOFC was similarly left for 30min before drawing power from the stack. A picture of the mounted SOFC stack is shown in Fig. 3.

2.4. Experimental procedure

The experimental work was carried out over 3 campaigns for a total operating time of 145 h with real product gas as described in Ref. [19]. An overview of reported tests is shown in Table 2. Tests started when the SOFC voltage was stabilized after the warm-up (usually after 6 h). Measurements of voltage, power and gas composition were taken as averages over 3–10 min, except values at maximum current that were taken as an average over 60 min of operation. National Instruments' LabView 2015 software via a Siemens Step 7 PLC system was used for the data acquisition.

Flow rates were measured using manual measurements with a flow meter during the tests and are therefore a calculated average value. The SOFC stack load was controlled by increasing the current to specified values on an electric load box. The current was held to a maximum of 25 A, as specified by Topsoe Fuell Cell. During all tests, air was fed non-pressurised at 90 l/min (measured at 20 °C).

3. Results and discussion

3.1. Product gas and SOFC stack temperature

The product gas was examined three times for tars and sulphur.

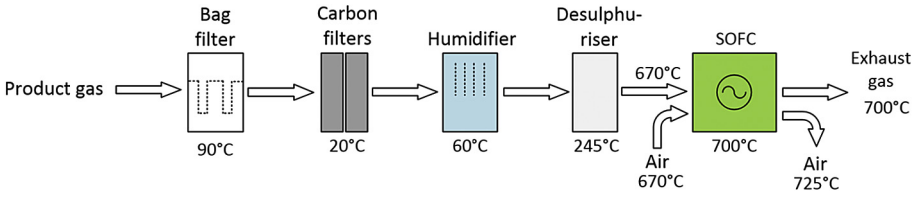

Fig. 2. Overview of fuel cell gas conditioning with approximate operating temperatures. Electric heaters are not shown.

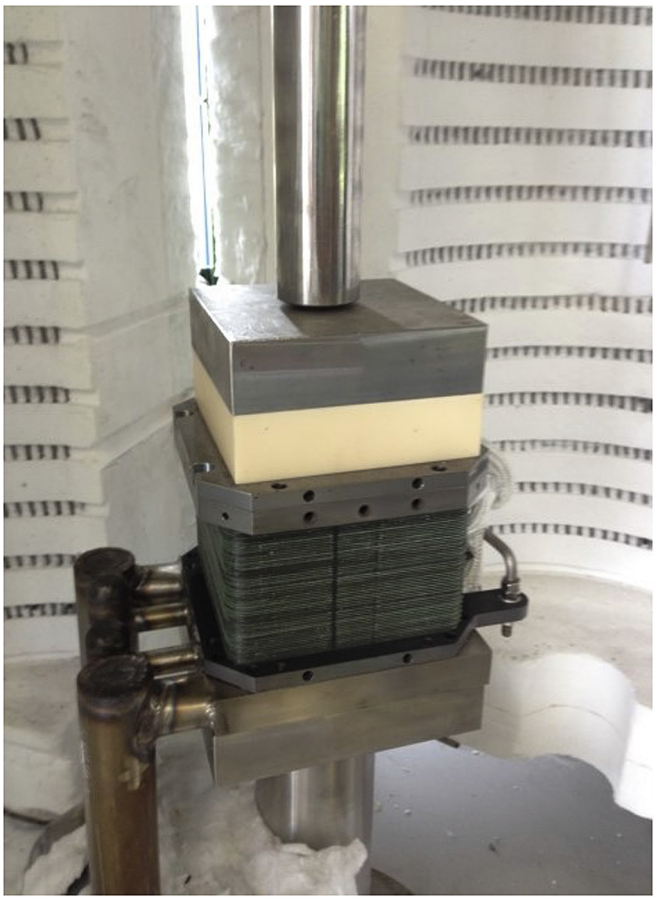

Fig. 3. SOFC stack mounted in oven.

No tars could be detected using the SPA tar analysis, which is expected as shown in previous campaigns with the gasifier [17]. The SOFC's tolerance towards tars are discussed several places and as mentioned, several tests has been made e.g. Refs. [9–11]. As rough estimate, Aravind and de Jong [19] gave a threshold value of 2 g/Nm^3 tars in order to avoid carbon deposition, but states that it naturally depends on the tar species, temperature and gas composition. These findings indicate that the TwoStage gasifier design could be altered to reduce the tar conversion, in order to obtain other benefits (e.g. using a smaller char bed/reactor or increasing fuel flexibility by using a fluid bed for char conversion) as a slightly higher tar concentration will not affect the SOFC performance.

Sulphur was analysed for the COS and H_2S compounds, but only COS could be detected with an average value before the carbon filter of 3.7 ppm and <0.1 ppm after the carbon filters [20], displaying the relatively simple carbon filters effectiveness. The SOFC's tolerance towards sulphur species is extremely depending on gas composition and temperature, but Rostrup-Nielsen et al. [21] found that a SOFC stack at 800°C using partially oxidized jet fuel (gas composition similar to TwoStage product gas) was not affected by 10 ppm H_2S, and while 50 ppm decreased performance 10%, the SOFC could easily be regenerated to original performance levels. These findings indicate that the already simple gas condition applied in Fig. 2 might be further reduced, so that only the integrated gasifier bag filter (and possibly humidifier depending on the hydrocarbon/tar level) remains upstream of the SOFC, while also allowing the gasifier to increase its tar production if needed.

Table 2
Overview of tests performed. *Flow measured at 20 °C and atmospheric pressure. **Test 5 were stopped for 2.5 h due to a 1-h gasfier failure during the test.

Test #	Gas flow* [l/min]	Duration [h]	Range of current values for tests [A]
1	15.9	1.5	0–15.1
2	22.5	3.5	0–23.1
3	23.0	7	0–24.1
4	28.8	2	10.0–25.1
5	22.4	62**	20.1

During the campaigns, only small fluctuations in the product gas composition from the TwoStage gasifier were seen. Average gas compositions during the tests are shown in Table 3. Fig. 4 shows as reference, the gas composition fluctuations during Test 5.

Some gas fluctuations were observed during the tests: the bag filter was cleansed and back flushed with nitrogen to reduce pressure drop; and pressure spikes occurred regularly. The pressure spikes occured probably because of water droplet evaporation from the humidifier. Voltages were affected by the pressure increases, resulting in negative spikes until the pressure was reset shortly after – see Fig. 8.

The temperature of the stack increased as the current increased, due to generated waste heat. During Test 5, temperatures were constant as the current was not varied. Results from the measurements of product gas, exhaust gas and air temperatures are shown in Table 4.

3.2. Performance of SOFC stack

The performance of the SOFC stack is evaluated based on power output, voltage and electric efficiency (power to fuel input [LHV]). The FU is an appropriate dimensionless base of comparison value across fuel flows and gas compositions. As the FU increases, so does the internal losses in the SOFC, due to mass transfer and concentration losses as the load increases. The FU can be defined using the current, I, as the ampere value is a measure of conducted electrons (and thus proportional to the number of conducted oxygen-ions). As the steam reforming and water-gas-shift (WGS) reactions by the nickel catalysts at the anode of CO and CH4 are faster than the electrochemical reactions [22,23], a molar hydrogen equivalent, $n_{H2\text{-}eq}$, is calculated based on complete steam reforming and WGS of CO and CH_4, shown in Equation (1). The FU is defined in Equation (2) on a molar basis. N_c is the number of cells in the stack and F is Faradays constant.

$$n_{H2-eq} = n_{H2} + n_{CO} + 4 \cdot n_{CH4} \tag{1}$$

$$FU = \frac{\frac{I}{2 \cdot F} N_c}{n_{H2-eq}} \tag{2}$$

The SOFC performance was tested in a large operating area in order to simulate part- and full-load conditions. Voltage, power density and voltage standard deviation as a function of current density for Test 2 is shown in Fig. 5 and the power outputs of the SOFC stack for Test 1–4 are shown in Fig. 6. The corresponding electric efficiencies for Test 1–4 are shown in Fig. 7. During testing, it was seen that one of the 50 SOFC's in the stack was not producing any power.

Even though the FU was up to 90.2%, there was no significant decline in power in following tests due to internal losses in the stack (see Fig. 7) and tests at different flows yielded nearly equal electrical efficiencies across FU. This means that part-load operation down to 55% flow (Test 1 compared to Test 4) does not reduce the efficiency of the stack, which is an important factor in an energy system with large fluctuations from e.g. wind and solar power.

Table 3
Overview of average dry product gas compositions during the different tests. Compositions are calculated as average values over 3–10 min. Nitrogen content is calculated by difference. *Gas energy calculated based on average LHV of gas and flow during the experiment.

Test #	CH_4 [vol%]	CO [vol%]	CO_2 [vol%]	H_2 [vol%]	N_2 (rest) [vol%]	Sum [vol%]	Gas energy flow (LHV)*[W]
1	0.6	15.2	15.4	27.2	41.6	100.0	1245
2	0.7	14.1	15.1	26.3	43.8	100.0	1723
3	0.7	15.6	14.1	26.7	42.8	99.9	1826
4	0.5	14.9	15.3	26.0	43.3	100.0	2200
5	0.6	13.3	16.0	24.8	45.3	100.0	1588

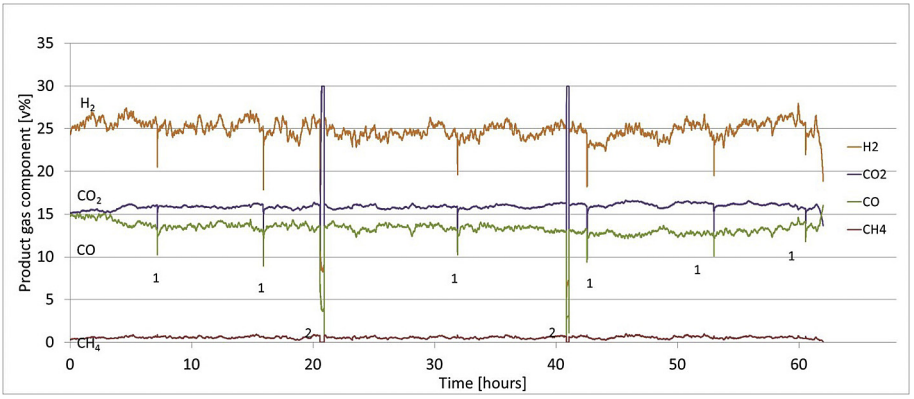

Fig. 4. Gas composition during Test 5 for 62 h. Incidents marked '1' are during flushing of the bag filter and '2' are measurements of SOFC exhaust.

Table 4
Gas temperature measurement ranges during tests in and out of the SOFC stack caused by changes in load and gas compositions.

Test #	Product gas [°C]	Exhaust gas [°C]	Air in [°C]	Air out [°C]
1	658–666	676–688	657–668	684–711
2	649–670	672–698	654–671	680–732
3	650–670	675–700	655–675	680–730
4	651–682	687–706	663–675	700–733
5	661–683	691–705	663–677	719–731

and a current density of 260 mA/cm^2 – compared to 700°C and ≈50–100 mA/cm^2 (depending on test and gas flow). An evaluation of the increased temperature with higher efficiency versus shorter SOFC lifetime should be made when designing such a system.

Considering the gasifier-SOFC system, a plant efficiency η_{plant} can be estimated based on the present results. Using Equation (3), the combinations of SOFC efficiency at maximum FU and gasification efficiency gives TwoStage-SOFC electrical efficiencies of

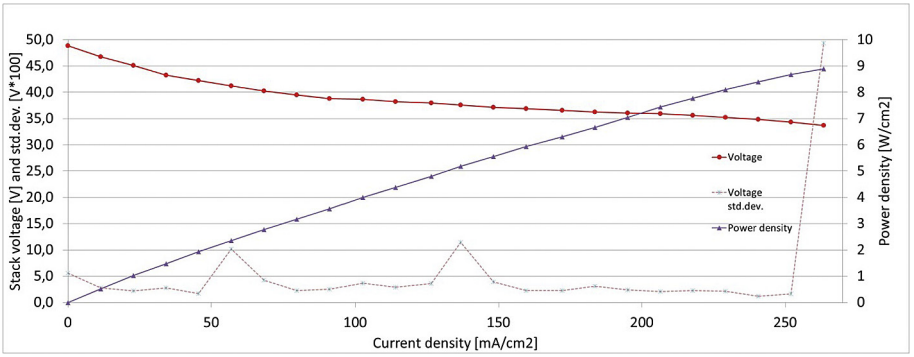

Fig. 5. SOFC stack voltage with standard deviation and power density shown as a function of current density for Test 2.

The peak values for Test 1–4 are shown in Table 5, showing the data for the measurements at max FU. The maximum efficiency value (46.4%), power (875 W) and FU (90.2%) achieved are, to the authors knowledge, the highest values found in literature for product gas operation. These efficiencies are markedly higher than previous tests in which 38% was reached [10,13]. Previous tests with the TwoStage gasifier and a single-cell SOFC showed electric efficiency of 24% at a fuel utilisation of 30% [9], which is higher than the roughly 18% obtained here at the same FU. Even though the gas was similar it should be noted that the previous test operated at 850°C

38–43%. TwoStage cold gas efficiency is denoted with η_{cg} and the SOFC stack efficiency with η_{SOFC}. The range of this approximation is confirmed through mathematical modeling of system [24].

$$\eta_{\text{plant}} = \eta_{cg} \cdot \eta_{SOFC} \tag{3}$$

The TwoStage-SOFC system is thought as a decentralised constellation in the <20MW$_{th}$ range, as downdraft gasifiers have limitations with regards to scaling [25,26]. The efficiencies of this system are significantly higher than typical competing

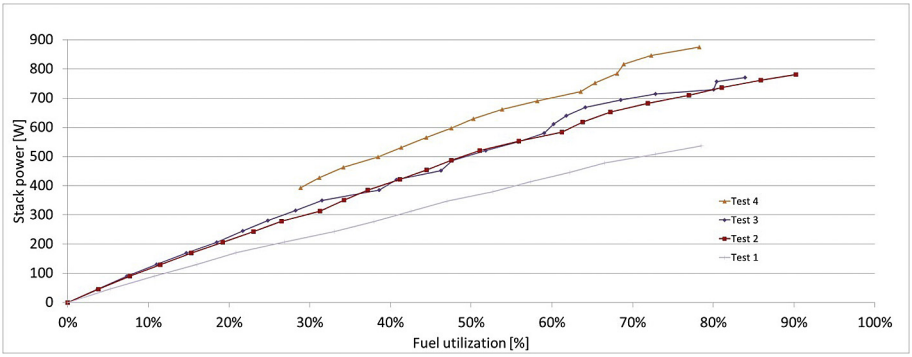

Fig. 6. SOFC stack power output shown as a function of fuel utilisation for Test 1–4.

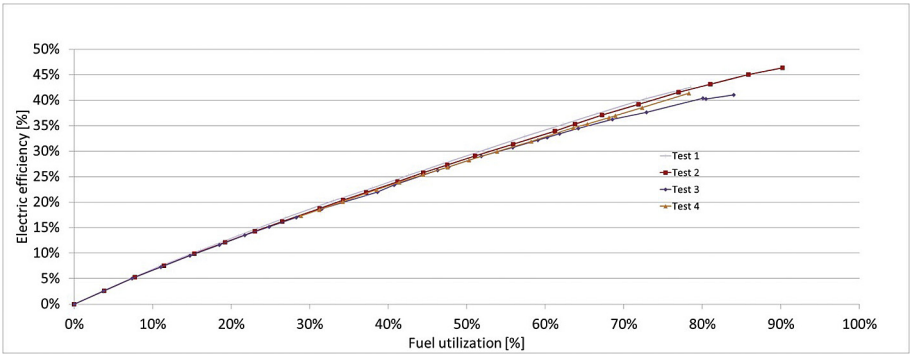

Fig. 7. SOFC stack electric efficiencies shown as a function of fuel utilisation for Test 1–4.

Table 5
Data for max fuel utilisation (FU) measurements. Data are taken as averages over 60 min.

Test #	Flow compared to Test 4 [%]	Power [W]	Electric efficiency [%]	FU [%]
1	55.2	537	42.6	78.5
2	78.1	780	46.4	90.2
3	79.9	771	41.0	84.0
4	100	875	41.4	78.3

decentralised biomass power plants at 18–33% [1]. The obtained efficiencies are comparable with those of biomass power plants with capacities above 100 MW_{th} [1]. Gasification systems typically have electrical efficiencies of 18–33% [26], similar to those of decentralised power plants, with the typically engine operated TwoStage gasifier of 29% (gross) [17]. Two of the most efficient demonstrated biomass gasification systems, not using fuel cells, are the Värnamo combined cycle and Skive engine plants. These plants reach electrical efficiencies of 33% and 30% respectively [27,28] and are significantly outperformed in comparison to these tests.

3.3. Long-term performance of SOFC stack

In order to investigate any decline in the performance of the SOFC stack when continuously using product gas, the results of the 62 h-test (Test 5) have been used. During the test, the gasifier stopped for 1 h due to a fuel feeding fault and the SOFC stack was consequently stopped. The SOFC stack did however assume full-load operation at 20.1 A again after 2.5 h after the stop. The performance of the stack is shown as stack voltage on Fig. 8 and key data are presented in Table 6.

The SOFC operation during the 62 h was generally stable throughout the test, with power fluctuating within ±10 W, which is to be expected with slightly varying gas flow and composition (see Fig. 4). As seen in Fig. 8 and as mentioned earlier, the voltage did however experience some spikes during operation, which is likely caused by droplets that are carried over from the humidifier and in turn evaporates when reaching the heat exchangers. The sudden evaporation will cause the local steam concentration to increase and lower the heating value of the gas locally, which decreases the stack voltage. The drop in voltage was very short and voltage was stabilized quickly after.

In order to assess the SOFC performance, the voltage is calculated independently of product gas fluctuations as these will affect the voltage. By evaluating the stacks overpotential using the Nernst equation, the internal losses can be assessed. The data for Test 5 is divided into sections of 30 min that are averaged. The overpotential V_{OP} can then be calculated as in Equation (4) from the measured voltage, V_{exp}, using the Nernst equation [22], assuming complete steam reforming of CO and CH_4. E^0 is the electrode potential at standard conditions for hydrogen and P is the average partial pressure of the product gas in the stack. $P_{H2\text{-}eq}$ is the accumulated partial pressures of H_2, CO and four times CH_4 as in Equation (1).

It can be challenging to model a precise SOFC performance using a zero-dimensional model as chosen here. Multiple factors as varying temperature, gas composition, and pressure across the

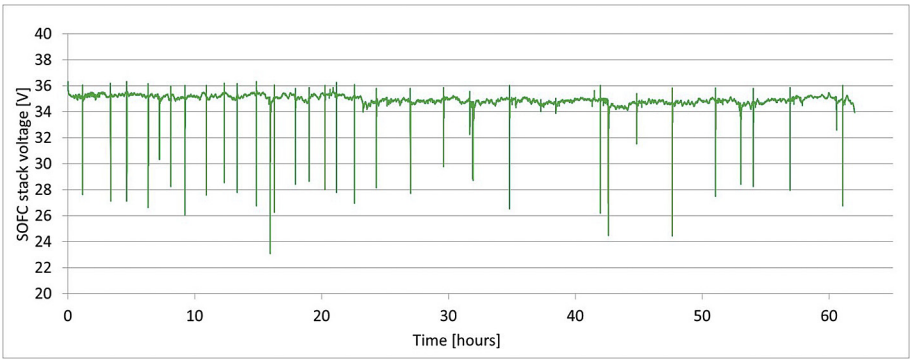

Fig. 8. SOFC stack voltage during Test 5 for 62 h. Spikes are caused by sudden pressure increases upstream of the SOFC. A stop of 2.5 h is marked, but not shown.

Table 6
Key data for Test 5 taken as an average over 62 h with standard deviation for power as primary measurement. *Gas flows are measured at 20 °C and atmospheric pressure.

Gas flow* [l/min]	Current [A]	Power [W]	Electric efficiency [%]	FU [%]
22.4	20.1	704 ± 9.8	44.3	83.0

electrode structure causes relatively simple models to rely on estimates. This is discussed by Bang-Møller [24], where the approach taken here with Equation (4) is evaluated against a more precise form, which caused the Nernst and cell voltage to be 4% and 19% lower respectively at similar conditions. However, as the calculations of this project focuses on a trend in voltage and because the gas composition is very stable (see Fig. 4), the error in modeling will only affect the trend to a minor degree.

$$V_{\exp} = \left(E^0 - \frac{R \cdot T}{2 \cdot F} \ln \left[\frac{P_{H2O}}{P_{H2-eq} \cdot P_{O2}} \right] - V_{OP} \right) N_c \quad (4)$$

The calculated overpotential for the SOFC stack is shown in Fig. 9. The value fluctuates slightly, which is due the discussed modeling assumptions above and to minor disturbances in the system, namely the gas pump was found to fluctuate. The overpotential of the stack is split into two sections: before and after the 2.5 h fall-out. Before, the overpotential is increasing at a low rate, indicating that the stack performance is declining. After the stop, however, the overpotential is stable, but with a higher value, indicating that the stack has been damaged by the sudden stop in operation. This effect is likely due to the thermal cycling that the SOFC experiences during the sudden stop in operation - the SOFC control was designed to shut off power when the gasifier stopped, meaning that the current went from 20.1 A to 0 A in an instance. This immediate shut-down, can decrease the contacting between electrodes and electrolyte/interconnect and hence increase losses as the remaining contact sites are forced to increase load, resulting in increased overpotential – this phenomenon is discussed in e.g. Ref. [29]. Hence, future tests should implement a revised control strategy that gradually lowers the drawn current from the stack in order to limit degradation. Following the stop, the continuous operation with product gas did not affect the stack after the stop. As the test showed some increase in overpotential before the stop and constant operation after, there is not enough data to conclude whether long-term operation is feasible and longer tests are recommended.

In all, a total of 145 h of operation was however carried out on product gas, without significant decline in SOFC performance that indicates loss of performance when combining these two technologies. However, two aspects should be kept in mind when evaluating these results: 1) the stack performance has not been tested before and after the tests with a reference gas, so specifics on a possible performance decline has not been investigated – for instance could the high fuel utilisation have caused a decline in performance that cannot be assessed over the operating time of this project; 2) the stacks initial condition is unknown by Topsoe Fuell Cell and the stack might have decreased performance compared to an unused stack. Following the test campaigns, the gas separation of the stack was tested at room temperature with gas tracing and it was found that there was a leak between anode and cathode, which will lead to either anode oxidation and/or loss of fuel, but in all cases a loss of performance.

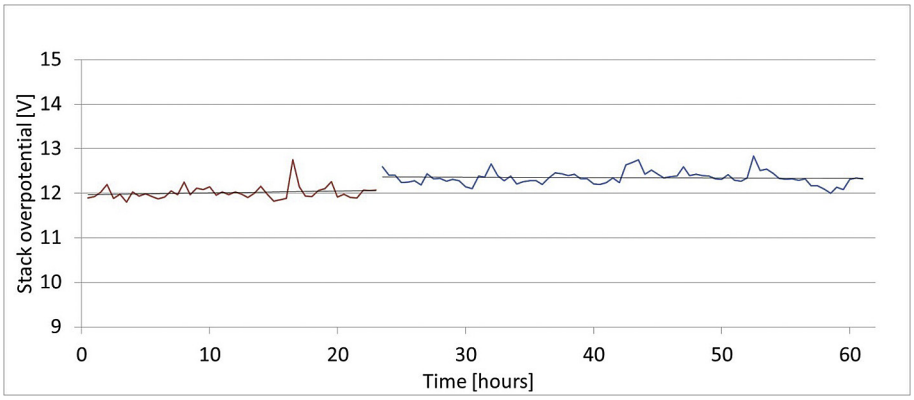

Fig. 9. Overpotential, V_{OP} during Test 5 for 62 h, as described by Equation (4). The curve is split where there was a 2.5 h stop in operation. Trendlines are added for each curve.

3.4. Comparison with modeling studies

Within the BioSOFC project, the coupling of the TwoStage gasifier and SOFC's has been studied by mathematical modeling in other publications [5–8,24,30,31]. The main results from these publications are discussed here in relation to the experimental data and the system potential. The TwoStage-SOFC system is projected as a decentralised plant with capacities below 10MW$_e$. The system were modeled to have an electrical efficiency of 44.9% with a FU of 85% [5], which is within range of the results presented here. The modeled results for the SOFC fit well with the obtained experimental results in e.g. Ref. [5].

However, as the SOFC is subject to a certain FU, there are high quality heat and excess fuel available downstream that can heighten the system efficiency. Therefore, combined cycle (CC) concepts that enhance the electrical efficiency have been modeled. The efficiencies for various CC configurations are shown in Table 7, showcasing the very high potential of decentralised power based on biomass gasification and SOFC technologies. The results stress the need to utilize the SOFC off-gases in order to be as competitive on efficiency as possible and design some of the most efficient systems available. Downstream power generation could also be implemented as a cost reduction measure as lower FU also leads to lower maintenance costs of the SOFC.

Thermoeconomic studies were also included in Refs. [8,30]. Both studies concluded that the main expense of the system is the investment cost. Specifically the SOFC capital cost was found to be the main bottleneck for commercialization. Electricity prices were found to be close to competitive with other biomass power generation, but not sufficiently high to justify the high investment. Thus continued technology maturation and SOFC cost reduction will be needed if the plant will be competitive without incentives.

4. Conclusions

Experimental studies were performed on an 800 W$_e$ SOFC stack, operated on real product gas from the TwoStage gasifier. The test setup featured the TwoStage biomass gasifier, the SOFC stack and simple gas cleaning consisting of only a bag filter, two carbon filters, a humidifier and a desulphuriser. No tar could be detected. Only small amounts of sulphur compounds were found, enabling both the carbon filters and desulphuriser to remove them, which can reduce complexity even further. Thus the TwoStage gasifier is very well suited for operating SOFC with only a minimum of gas conditioning.

The SOFC was operated at 700 °C and was subject to 4 tests with different flows from 15 to 28 l/min and currents from 0 to 24.1 A for up to 62 h. The 4 tests displayed the SOFC stacks excellent part-load performance down to 55% flow, without loss of efficiency. The tests achieved the highest reported values of such a system globally, with a SOFC stack electric efficiency of 46.4% at 90% fuel utilisation. A gasifier-SOFC system electric efficiency was estimated to be around 40%, which is considerably higher than those from traditional decentralised biomass power plants and showcases the systems intriguing potential.

A total of 145 h of operation was achieved without significant losses in SOFC performance.

Table 7
Main results of modeling studies with TwoStage gasifier, SOFC and further downstream power generation.

Power system configuration	Scale [MW$_e$]	Electric efficiency [%]
SOFC [5]	1.4	44.9
SOFC-Stirling engine [8]	0.12	42.4
SOFC-Organic rankine cycle [6]	0.1	54–62
SOFC-Gas turbine [24]	0.3	55–58
SOFC-Kalina cycle [31]	8	49–58
SOFC-Steam cycle [7]	10	48–56
SOFC-Steam injected gas turbine [30]	10	48–50

Acknowledgements

The authors would like to thank the ForskEL- and ForskVE-programmes of Energinet.dk for financial support through the BioSOFC (ForskEL-10456) and Biomass Gasification Polygeneration (ForskVE-12205) projects. The authors would like to thank Topsoe Fuel Cell for delivering the SOFC stack and the DTU Energy department for technical assistance.

References

[1] Technology roadmap - bioenergy for heat and power. International Energy Agency; 2012.
[2] IPCC. Renewable energy sources and climate change mitigation: special report of the intergovernmental panel on climate change. Choice Rev Online 2012;49. http://dx.doi.org/10.5860/CHOICE.49-6309.
[3] Energiscenarier frem mod 2020. Danish Energy Agency; 2014. 2035 og 2050.
[4] Ahrenfeldt J, Thomsen TP, Henriksen U, Clausen LR. Biomass gasification cogeneration - a review of state of the art technology and near future perspectives. Appl Therm Eng 2013;50(2):1407–17. http://dx.doi.org/10.1016/j.applthermaleng.2011.12.040.
[5] Bang-Møller C, Rokni M, Elmegaard B, Ahrenfeldt J, Henriksen UB. Decentralized combined heat and power production by two-stage biomass gasification and solid oxide fuel cells. Energy 2013;58:527–37. http://dx.doi.org/10.1016/j.energy.2013.06.046.
[6] Pierobon L, Rokni M, Larsen U, Haglind F. Thermodynamic analysis of an integrated gasification solid oxide fuel cell plant combined with an organic Rankine cycle. Renew Energy 2013;60:226–34. http://dx.doi.org/10.1016/j.renene.2013.05.021.
[7] Rokni M. Thermodynamic investigation of an integrated gasification plant with solid oxide fuel cell and steam cycles. Green 2012;2(2–3):71–86. http://dx.doi.org/10.1515/green-2011-0022.
[8] Rokni M. Thermodynamic and thermoeconomic analysis of a system with biomass gasification, solid oxide fuel cell (SOFC) and stirling engine. Energy 2014;76:19–31. http://dx.doi.org/10.1016/j.energy.2014.01.106.
[9] Hofmann P, Schweiger a, Fryda L, Panopoulos KD, Hohenwarter U, Bentzen JD, et al. High temperature electrolyte supported Ni-GDC/YSZ/LSM SOFC operation on two-stage Viking gasifier product gas. J Power Sources 2007;173(1):357–66. http://dx.doi.org/10.1016/j.jpowsour.2007.04.073.
[10] Hofmann P, Panopoulos K, Fryda L, Schweiger a, Ouweltjes J, Karl J. Integrating biomass gasification with solid oxide fuel cells: effect of real product gas tars, fluctuations and particulates on Ni-GDC anode. Int J Hydrogen Energy 2008;33(11):2834–44. http://dx.doi.org/10.1016/j.ijhydene.2008.03.020.
[11] Hofmann P, Panopoulos KD, Aravind PV, Siedlecki M, Schweiger A, Karl J, et al. Operation of solid oxide fuel cell on biomass product gas with tar levels >10 g Nm-3. Int J Hydrogen Energy 2009;34(22):9203–12. http://dx.doi.org/10.1016/j.ijhydene.2009.07.040.
[12] Jewulski J, Stepien M, Blesznowski M, Nanna F. Slip stream testing with a SOFC unit at Güssing and Trisaia plants. 2010.
[13] Oudhuis AB, Bos A, Ouweltjes JP, Rietveld G, van der Giesen A. High efficiency electricity and products from biomass and waste, experimental results of proof of principle presented at the 2nd world conference and technology exhibition. In: The 2nd world conference and technology exhibition on biomass for energy, industry and climate protection; 2004. p. 10–4.
[14] Nagel F. Electricity from wood through the combination of gasification and solid oxide fuel cells systems analysis and proof-of-concept. 2008. p. 17856. http://dx.doi.org/10.3929/ethz-a-005773119.
[15] Henriksen U, Ahrenfeldt J, Jensen TK, Gøbel B, Bentzen JD, Hindsgaul C, et al. The design, construction and operation of a 75 kW two-stage gasifier. Energy 2006;31(10–11):1542–53. http://dx.doi.org/10.1016/j.energy.2005.05.031.
[16] Gøbel B, Henriksen U, Ahrenfeldt J, Jensen TK, Hindsgaul C, Bentzen JB, et al. Status - 200 hours of operation with the viking gasifier. 2003. p. 3–6. Retrieved from http://medcontent.metapress.com/index/A65RM03P4874243N.pdf.
[17] Ahrenfeldt J, Henriksen UB, Jensen TK, Gøbel B, Wiese L, Kather A, et al. Validation of a continuous combined heat and power (CHP) operation of a two-stage biomass gasifier. Energy Fuels 2006;20:2672–80.
[18] Egsgaard H, Ahrenfeldt J, Ambus P, Schaumburg K, Henriksen UB. Gas cleaning with hot char beds studied by stable isotopes. J Anal Appl Pyrolysis 2014;107:174–82. http://dx.doi.org/10.1016/j.jaap.2014.02.019.
[19] Aravind PV, de Jong W. Evaluation of high temperature gas cleaning options for biomass gasification product gas for solid oxide fuel cells. Prog Energy Combust Sci 2012;38(6):737–64. http://dx.doi.org/10.1016/j.pecs.2012.03.006.
[20] Gadsbøll R, Thomsen J, Bang-Møller C, Ahrenfeldt J, Henriksen U. Experimental analysis of solid oxide fuel cell coupled with biomass gasification. In:

Proceedings of the conference. 2015 European biomass conference and exhibition; 2015. p. 555–61.
[21] Rostrup-Nielsen JR, Hansen JB, Helveg S, Christiansen N, Jannasch a-K. Sites for catalysis and electrochemistry in solid oxide fuel cell (SOFC) anode. Appl Phys A 2006;85(4):427–30. http://dx.doi.org/10.1007/s00339-006-3702-1.
[22] Braun RJ. Optimal design and operation of solid oxide fuel cell systems for small-scale stationary applications. PhD thesis. University of Wisconsin-Madison; 2002.
[23] Larminie J, Dicks A. Fuel cell systems explained. second ed. John Wiley & sons Ltd; 2003.
[24] Bang-Moeller C. Design and optimization of an integrated biomass gasification and solid oxide fuel cell system. PhD thesis. Technical university of Denmark; 2010.
[25] Basu. Biomass gasification, pyrolysis and torrefraction. second ed. Dalhouse University; 2013.
[26] Quaak P, Knoef H, Stassen H. Energy from biomass a review of combustion and gasification technologies, vol. 422; 1999. p. 1–78. World Bank Technical Paper, ISBN0 -8213-4335-.
[27] Knoef H. Handbook biomass gasification. first ed. BTG biomass technology group; 2005.
[28] Ridjan I, Mathiesen BV, Conolly D. A review of biomass gasification technologies in Denmark and Sweden. 2013.
[29] Greco F, Nakajo A, Wuillemin Z, Van herle J. Thermo-mechanical reliability of SOFC stacks during combined long-term operation and thermal cycling. ECS Trans 2015;68(1):1921–31. http://dx.doi.org/10.1149/06801.1921ecst.
[30] Mazzucco A, Rokni M. Thermo-economic analysis of a solid oxide fuel cell and steam injected gas turbine plant integrated with woodchips gasification. Energy 2014;76:114–29. http://dx.doi.org/10.1016/j.energy.2014.04.035.
[31] Pierobon L, Rokni M. Thermodynamic analysis of an integrated gasification solid oxide fuel cell plant with a kalina cycle. Int J Green Energy 2014;12(6):610–9. http://dx.doi.org/10.1080/15435075.2013.867267.

Solid oxide fuel cell stack coupled with an oxygen-blown TwoStage gasifier using minimal gas cleaning

Rasmus Østergaard Gadsbøll*, Adrian Vivar Garcia, Jesper Ahrenfeldt, Ulrik Birk Henriksen
[1]Technical university of Denmark, Department of chemical and biochemical engineering, Frederiksborgvej 399, 4000 Roskilde, Denmark
*Corresponding author, Tel: +4560668815, E-mail: rgad@kt.dtu.dk

Abstract
The coupling of biomass gasification and solid oxide cell technologies is very intriguing due to its high efficiency and flexibility potential. One of the key challenges in order to realize such a system design is a clean quality gas that can meet the strict requirements of the SOFC. This study presents the result of an experimental campaign with the TwoStage Viking biomass gasifier and a Topsoe Fuel Cell SOFC stack connected via a carbon filter and a desulphurizer. The stack is operated with both air- and O_2-CO_2-blown product gas, at 700°C and 800°C, and tests without any gas cleaning was conducted. The study found electric efficiencies up to 40% at 69% fuel utilization and an 8-11% increase in power when raising the SOFC temperature to 800°C. The O_2-CO_2-blown product gas showed lower efficiencies due to lower CO performance in the SOFC. A short-term test with no gas cleaning between the gasifier and SOFC, and a 1.5-2.8ppm sulphur concentration showed no change in operational voltage. Hence the study finds that gasifier design can greatly simplify the demand for gas cleaning equipment.

Keywords: Biomass Gasification, Two-stage gasifier, SOFC, Gas cleaning

1 Introduction
The potential for coupling thermal biomass gasification with solid oxide fuel cells (SOFC) is very intriguing. This joint technology platform features very high conversion efficiencies and flexibility, which in turn can manifest itself in improved resource management and economics for future renewable energy plants. Gasification is very versatile and efficient technology that can process a wide variety of biomasses at high temperatures into an energy rich product gas containing up to >90% of the fuel energy (LHV basis) [1]. It can therefore unlock a series of resources that other biotechnologies cannot utilize, whilst doing it extreme efficient. The product gas can then be further processed into heat, power or gaseous/liquid fuels in highly efficient applications such as combined cycles, bio-refineries and SOFC's. The latter is an intensely investigated platform, but has not been widely applied, namely due to costs [2]. The SOFC technology offers good fuel flexibility and very high efficiency, which makes them an ideal fit with gasification. By harnessing all of these characteristics in a single system, gasification-SOFC systems can prove to be an integral part of increasing efficiency and potentially reducing costs in future energy systems [3].

Biomass gasification product gas has been tested with SOFC in laboratory-scale on several occasions e.g. [4][5][6][7][8][9][10]. Till this point, most tests have featured single cells, at low loads and/or for short time periods with their focus mostly on gas quality. A few studies have however tested SOFC stacks with product gas, showing electric efficiencies of the stacks between 38-46% and modeled gasification-SOFC-combined cycle efficiencies up to 62% [4][6][9]. Similar for these 3 studies is that they all applied a significant level of

gas conditioning between the gasifier and SOFC including tar removal, inorganic removal and scrubbing, which in turn increases the complexity and cost of the plant. It is therefore important do discover alternative systems that require significantly less and/or simpler cleaning equipment.

While the potential is high, there are still considerable technical challenges of the gasifier-SOFC system that needs to be addressed. One of the key challenges is the SOFC's low tolerance for gas impurities, which for most product gases mainly include sulphur and tar. Chlorine and other components can also be a serious concern, but is not relevant for this study because the gasifier does not produce any of these and it will therefore not be discussed further – the reader is referred to e.g. [11][12][13]. The impact of sulphur and tar is affected by several factors including temperatures, materials and gas composition and therefore this study will shortly review Ni-YSZ-based cells (as this study applies) mostly in the 700-850°C temperature range with varying gas compositions.

Sulphur

The influence of sulphur on catalytic and chemical activity has been studied intensively. The main subject to sulphur poisoning is that the nickel catalysts in the cell are subject to deactivation and it is generally accepted that sulphur poisoning causes lower SOFC performance via lower hydrogen oxidation, water-gas shift reactions and steam reforming of hydrocarbons [14][15][16][17].

Sulphur poisoning experiments with pure H_2-fuel have shown high SOFC performance losses at even a few ppm. Rasmussen and Hagen [18] studied the impact of H_2S and experienced at voltage drop of 10% at 850°C for 2 ppm. Similar results were found at 2ppm by Blesznowski et al. [13]. Sasaki et al. [19] also studied H_2-operation, finding that 5ppm H_2S caused a 20% performance drop at 1000°C and >50% at 850°C.

Tests with product gases or comparable gases have however showed higher tolerances to sulphur. Rostrup-Nielsen et al. [15] investigated the effect of H_2S addition to a catalytic partially oxidized jet fuel with a 11% CO, 13v% CO_2, 12v% H_2, 2v% CH_4, 60% N_2 composition in a SOFC stack. The tests showed that at temperatures of 800°C the performance was not impacted at 10 ppm H_2S, but the power production dropped roughly 10% at 50ppm at 700°C and 800°C. Similarly Schubert et al. [20] studied reformate gas (27v% H_2, 11v% CO, 3v% CO_2, 2v% CH_4, 51 v% N_2) to which 8, 10, 15 and 20 ppm H_2S was added. At 850°C performance losses were <4% when the sulphur was added. In a more extreme case Trembly et al. [21] found that coal syngas with similar composition and 200-240ppm H_2S only caused reductions in power production of 6-13%, which in line with the other studies point to a saturation/equilibrium condition at the anode. Li et al. [22] studied an 800°C SOFC with a synthetic syngas (4v% CH_4, 5v% CO, 13v% CO_2, 48v% H_2, 30v% H_2O) an with an introduction of 2ppm H_2S, no decline in performance were observed besides a reduced methane conversion. Bao et al. [23] found that 1ppm H_2S caused a performance drop of 2-4% at 750^{o}C (30v% CO, 12v% CO_2, 31v% H_2, 28v% H_2O). Li et al. [24] found that especially steam and CO_2 had an effect on the sulphur tolerance of an SOFC at 800°C, as they benefitted the recovery of the cell after 12.5ppm H_2S exposure. The authors suggest that the presence of these components can suppress the formation of elemental sulphur at the anode and hence increase the recovery rate. Hofmann et al. [7] operated a SOFC with product gas at 850°C and experienced an unintentional slip of up to 1.5ppm, which did not affect the performance.

Hence only very few ppm, if any, of sulphur should be allowed to enter the SOFC if stable short-term operation and very low performance losses are to be maintained. Dependent on fuel, in the range of 10ppm at 800°C, and lower yet for reduced temperatures, might be applicable. This also suggested in [12].

Tar

Unlike sulphur and chlorine, tars and lighter hydrocarbons are not necessarily poisonous to the catalysts inside the fuel cell and can be considered fuel components to some extent. However, as with hydrocarbons carbon deposition should be evaluated at the given circumstances. Tars are a diverse group of hydrocarbons, that ranges from relatively simple aliphatic organics to highly polymerized aromatic hydrocarbons and their structure vary depending on the current design of the process, which should be kept in mind when evaluating experimental studies [25].

While the literature about tars is not as deep as for sulphur, several studies have shown that a high concentration of tar can be processed effectively inside the SOFC. Baldinelli et al. [26] operated an 800°C SOFC up to 10g/nm^3 with Toluene as model tar and Hofmann et al. [7] operated an 850°C SOFC with a >10g/nm^3 real tar load, with neither experiencing performance degradation, but increases of performance. Both studies did however operate under very low loads, with fuel utilizations only up to around 24%. Tests at lower temperature of 735°C by Mermelstein et al. [27] with a tar load of 15g/nm^3 benzene using simulated product gas did however find that carbon formation was significant. The carbon deposition was found to be significantly different for other anode materials.

Aim of this study

As an extension of previous tests with a SOFC single-cell for 150 hours [5] and stack for 145 hours [4], this study will investigate the use of product gas from the commercialized TwoStage Viking gasifier in a commercial SOFC stack. Specifically, it will investigate the performance using only minimal gas cleaning – incuding a test with no gas cleaning prior to the stack. Also, differences in air- and O_2-CO_2-blown product gas and the effect of SOFC temperature is investigated.

2 Methods and materials

2.1 Test overview

Tests was carried out over 3 days in which the SOFC stack was coupled to the TwoStage Viking gasifier plant (see Section 2.2 for details). The first day featured air-blown operation of the gasifier and the last to featured 21v% O_2 in CO_2 as gasification medium – gasification tests are described in detail here [28]. On Day 1 and 2, the operation conditions were changed by varying the SOFC operation temperature and gas composition, whilst using an active carbon filter and a desulphurizer at the SOFC setup. On Day 3, the gas cleaning equipment at the SOFC setup was removed and product gas was fed directly to the stack. An overview of the tests is shown in Table 1.

Test #	Time	Gasification media	SOFC operating temperature [°C]	SOFC current range [A]	Gas cleaning
1	Day 1 12:25-15:53	Air	≈700	0-20	Yes
2	Day 1 16:42-18:54	Air	≈800	0-20	Yes
3	Day 2 12:22-15:20	21v% O_2 in CO_2	≈700	0-20	Yes
4	Day 3 13:33-17:02	21v% O_2 in CO_2	≈700	0-20	No

Table 1 – Overview of experimental tests

2.2 The TwoStage Viking gasifier and fuel analysis

The TwoStage gasification concept has been developed for many years at the Technical University of Denmark. It is staged system that relies on separate pyrolysis and char gasification with a partial oxidation zone in between to process wood chips – see Figure 1. This reactor design allows both high heat integration and internal tar conversion that manifests itself in a negligibly low tar concentration in the product gas. The hot product gas from the char reactor is cooled to ≈90°C and then led through a simple bag filter and a condenser before being led to a buffertank that serves the SOFC setup. Data from the 80kW$_{th}$ TwoStage Viking gasifier plant has previously shown tar levels of <15mg/nm^3 and a very high cold gas efficiency of 93%$_{wet}$ [29][30].

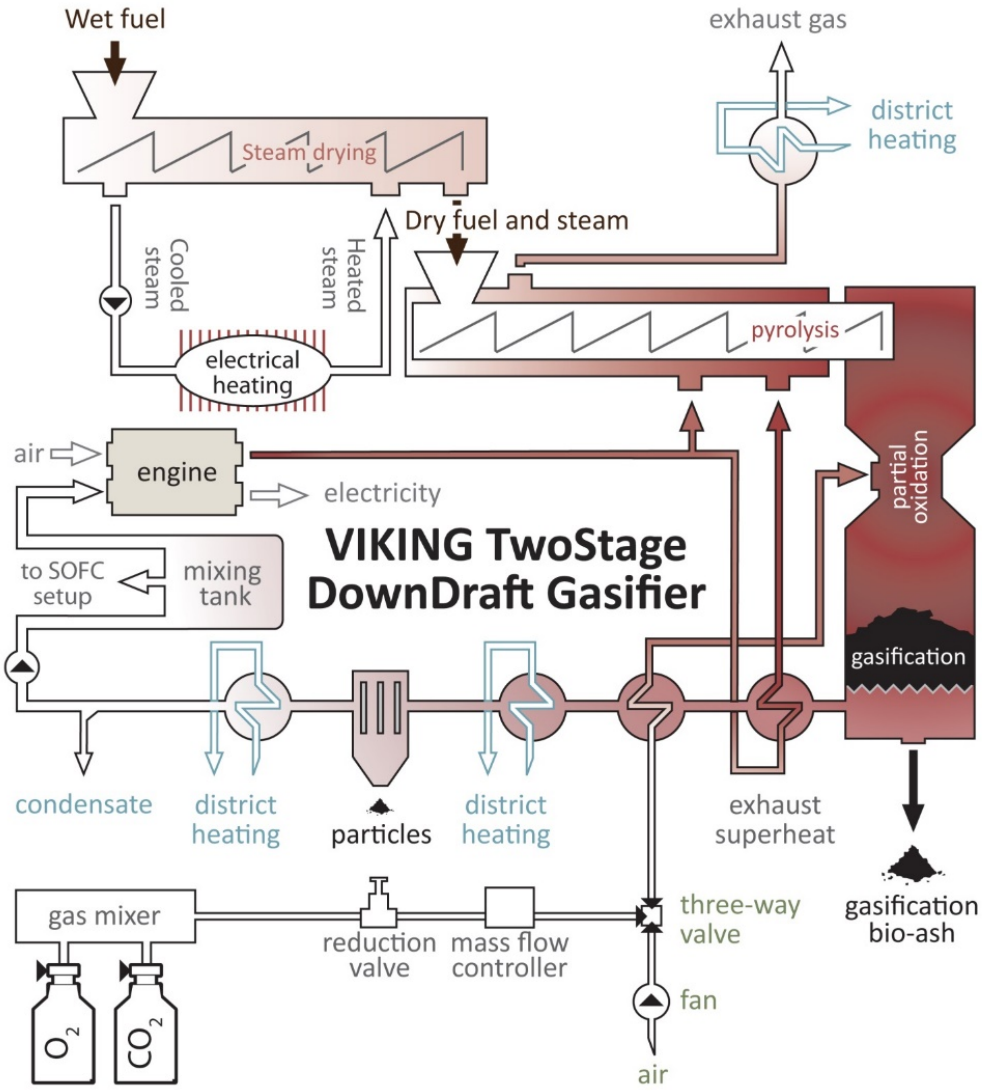

Figure 1 – Schematic overview of the Viking gasifier with an installed steam dryer and O_2-CO_2 mixing setup [28].

This article does only concern itself with the product gas flow into the SOFC setup and the reader is therefore reffered to [28] for detailed details and data for the O_2-CO_2 gasification.

Fuel

Danish spruce wood chips were applied as gasification fuel – the C, H, N, O content are given in [28]. An

inorganic analysis was carried out via ICP-OES analysis as shown in Table 1. The primary elements, C, H, O and N were not measured, but figures to be very close to previously measured values [30]. The moisture content was measured to 16-17% on 4 occasions.

Element	Al	B	Ca	Cu	Fe	K	Mg	Mn	Na	P	S	Zn
Sample #1	38.6	1.6	1063.0	1.2	38.4	295.0	116.5	8.2	112.2	76.2	130.3	8.7
Sample #2	36.9	1.3	1061.9	1.5	36.2	262.1	113.8	8.0	109.3	77.2	125.5	8.5

Table 2 – Inorganic elements detected in the applied wood chips [µg/g]$_{dry,biomass}$

2.3 SOFC setup gas cleaning

Gas from the buffertank is led via an underground pipe (with a simple gas-water separator) to the workshop where the SOFC setup is located. Fed by a gas pump, the setup includes an active carbon filter at room temperature and a desulphurizer – see Figure 2. The carbon filter contains a blend of Norit RB 3 and Norit ROZ 3 active carbons. The filters can be by-passed. The gas retention time in the carbon filter is in the range of 53s based on previous tests [4]. The desulphurizer applies ZnO pellets from Haldor Topsoe A/S at 245°C in a fixed bed reactor.

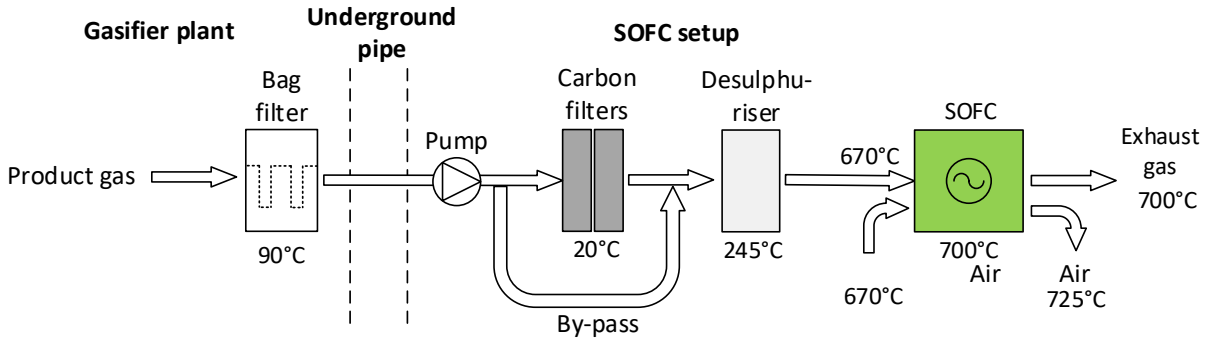

Figure 2 – Overview of gas cleaning from the char gasification reactor to the SOFC. The underground pipe includes a water separator. The by-pass around the carbon filter is controlled by a valve and the filters are only by-passed in Test 5. In Test 5, the gas was led through the empty, vacuum cleaned desulphurizer reactor. Heat exchangers on the setup are not shown.

2.4 Gas analysis

The gas composition of the product gas was measured at the gasifier plant with online gas measurement equipment on a dry and tar-free basis. An Advance Optima 2020 Modular continuous process gas analyzer system were applied, with a Caldos 15 cell H_2-analyzer, an Uras 14 cell CO-, CO_2 and CH_4 analyzer, and a PMA 10 O_2-analyzer. N_2 was calculated by the system as the difference. All analyzer has a ±1% measurement uncertainty.

As the online equipments CO_2-range are limited to 30v%, gas pipette samples were taken to measure the composition in a GC-MS. The tar concentration of the product gas was measured during the air- and O_2-CO_2-blown operation with solid phase adsorption (SPA). Sulphur measurements were carried out via GC-MS. Specific handling methods and measurements of gas pipettes, SPA and sulphur can be seen elsewhere [28]. While the samples were not taken directly at the SOFC inlet, previous tests [4] showed that the sulphur content into the SOFC setup was typical for previous measurements at the gasifier [5][31].

2.5 Solid oxide fuel cell

Topsoe has produced and delivered the 'S 1-02' SOFC stack. It is a 50-cell planar and anode-supported type with an yttrium-stabilized zirconia- (YSZ) and nickel catalyst-based anode structure. The electrolyte is based

on YSZ and the cathode lanthanum strontium manganite (LSM). The nominal capacity is 800W_e. The stack was installed without manifold in an electrically heated oven as shown in Figure 3. The stack was operated near atmospheric pressure.

Figure 3 – SOFC stack mounted in oven.

Concrete operating temperatures and gas flows during the tests are given in Table 2.

Test #	Product gas [°C]	Exhaust gas [°C]	Air in [°C]	Air out [°C]	Gas flow[a] [l/min]
1	650-674	669-694	653-671	677-735	25.0
2	756-778	765-788	732-754	787-823	25.0
3	650-673	672-692	653-667	686-734	24.8
4	648-673	668-696	654-670	673-736	24.0

Table 3 – Gas temperature measurement ranges and average gas pump flow. [a]Average flow measured over ≥14min via manual flowmeter readings.

The stack is started up by adding a small flow of Fomier10 gas (10v% H_2 in N_2), whilst being heated at a rate of 200K/h. As the operating temperature is reached, the setup is fed for 15min with Formier10gas and thermally stabilized to a point where only insignificant changes in temperature occur. Then product gas is added for ≥28min at open-circuit voltage (OCV) for near-complete thermal stability. SOFC data points has been logged by the second and they will be utilized as averages over ≥3min at the given current. The averaged data is taken after approximately 1min of stabilization time at the new current. At 20A the average is taken over ≥15min.

3 Results and discussion

3.1 Gas composition and SOFC temperatures

The product gas composition was similarly stable in all tests. As an example of this, the online composition from Test 1 and 2 is shown in Figure 4. The average gas compositions for Test 1-3 are shown in Table 4. It was not possible to take a sample for gas composition during Test 4, but operating conditions were almost

identical to Test 3 at the reactor outlet (714-692°C in Test 3 and 708°C in Test 4 [28]) and the moisture content were within 1% on 4 occasions, hence the gas composition is therefore expected to very similar.

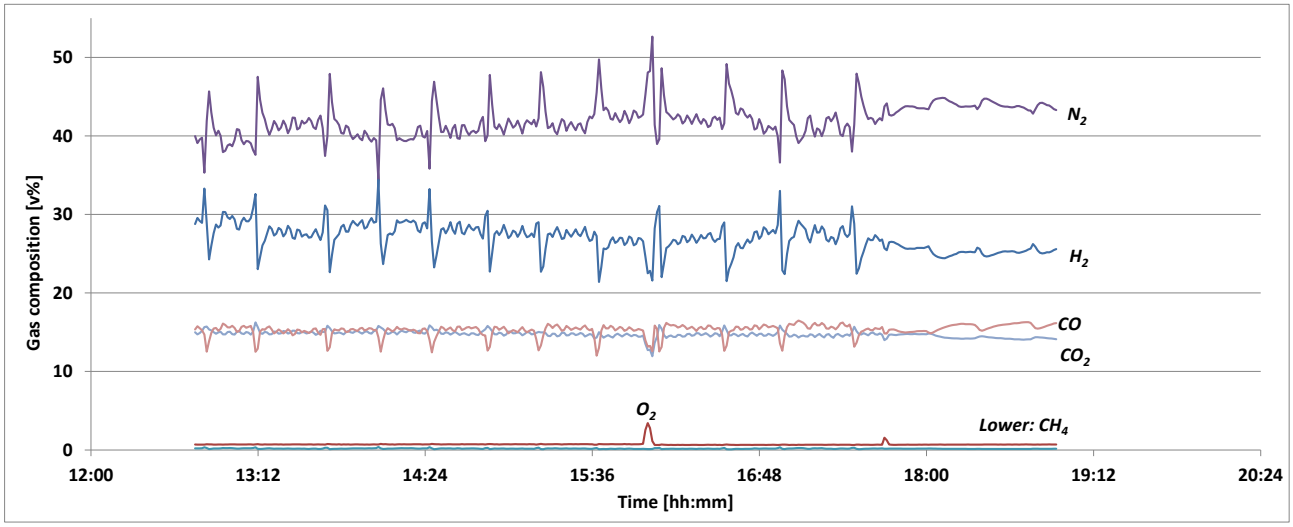

Figure 4 – Gas composition for air-blown operation during Day 1. The spikes of N_2 are caused by filter flushing and these are minimized around 17:30 where the gas analysis is taken after the product gas buffer tank instead of before.

	Day - time	Test #	H_2 [v%]	CO_2 [v%]	CO [v%]	CH_4 [v%]	N_2 [v%]	SUM
Air	1 – 12:45-15:53	1	27.8	14.9	15.1	0.2	41.3	99.3
	1 - 16:42-18:45	2	26.1	14.5	15.6	0.2	42.9	99.3
21v% O_2-CO_2	2 – 13:20	3	21.2	43.2	24.9	0.16	4.7	94.2
	2 – 13:22	3	20.6	44.3	25.8	0.22	4.6	95.5

Table 4 – Average online gas analysis for air and single-sample gas chromatography data from gas pipette samples for O_2-CO_2-blown product gas.

Four SPA samples from the air-blown operation only showed 0-3mg/nm^3 of pyrene before and after the bag filter, while three SPA samples during O_2-CO_2 operation showed only 0-1mg/nm^3 of pyrene. No other tar components were found.

Sulphur results sampled at the gasifier are shown in Table 5. The low levels of up to 3ppm is very similar to previous tests with the system [4][5][31].

Samplingtime	Location	Gasification media	H_2S [ppm]	COS [ppm]	Total S [ppm]
Day 1, 12:23	After filter	Air	0.1	0.5	0.6
Day 1, 12:36	After filter	Air	0.4	1.0	1.4
Day 3, 10:57	After filter	21v% O_2-CO_2	0.4	2.4	2.8

Day 3, 11:41	After filter	21v% O_2-CO_2	0.2	1.3	1.5
Day 3, 12:12	After filter	21v% O_2-CO_2	0.2	1.3	1.5

Table 5 – Measurements for sulphur in the product gas for Tests 1 and 4.

3.2 Air-blown product gas operation: 700°C vs 800°C

SOFC data for the air-blown Tests 1 and 2 are given in Figure 6. Stack voltage and power density were increased up to +11% and are at +8% at 20A when comparing 800°C to 700°C. Only minimal changes in gas composition is seen between the tests (Table 4). The results for 700°C are in line with previous tests [4].

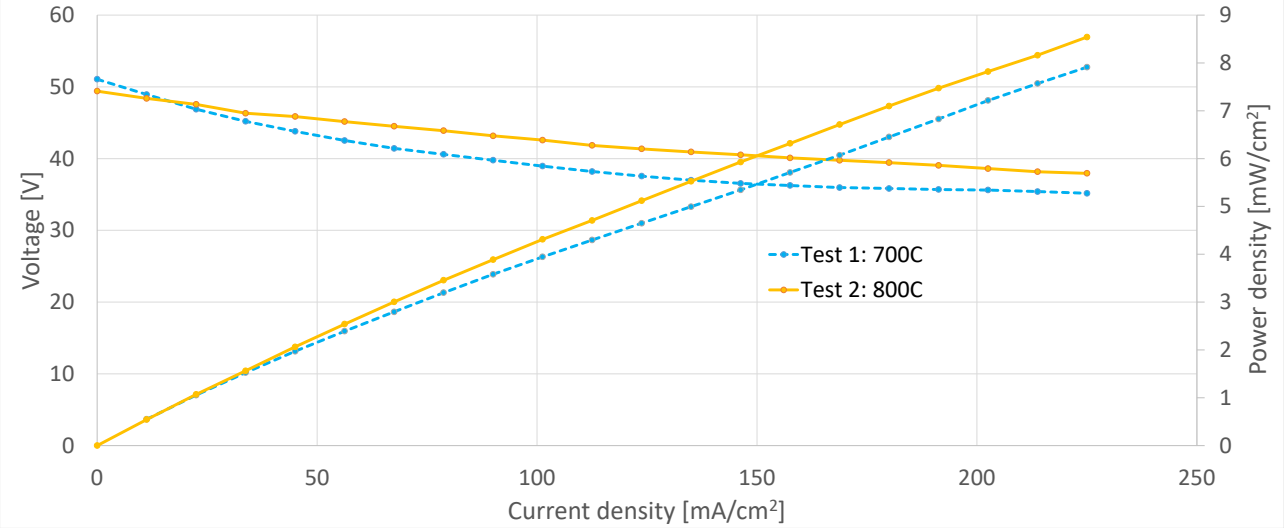

Figure 5 – Stack voltage and power density as a function of applied current at 700°C and 800°C using air-blown product gas.

3.3 O_2-CO_2 product gas operation: with and without gas cleaning

SOFC data for the 700°C Tests 1 and 3 are given in Figure 7. Differences in stack voltage and power density were fluctuating between -2.0% and +2.5%. Small differences in operation between the tests are seen, the key being the difference in gas composition as the CO content is significantly higher in Test 3 (25.4v% vs 15.1v% in Test 1). While the molar hydrogen equivalent (Equation 1) is 7.5% higher in Test 3, CO causes a higher overpotential/loss during conversion due to its lower diffusion rate [32][33][34], which lowers the voltage.

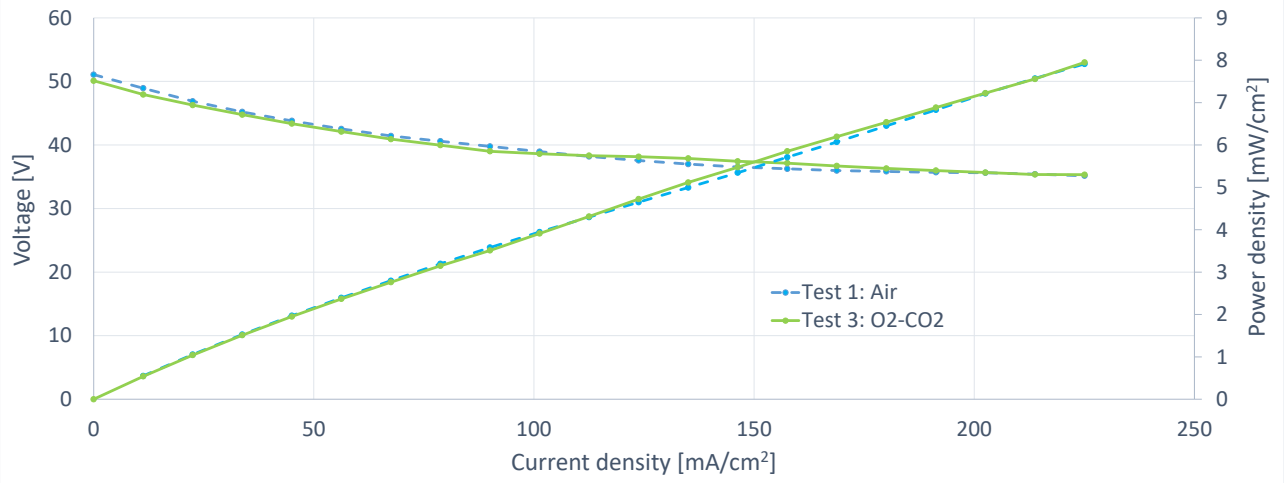

Figure 6 – Stack voltage and power density as a function of applied current at 700°C using air- and O_2-CO_2-blown product gas.

In Test 4, the ZnO pellets were removed from the desulphurizer and the reactor was vacuum cleaned thoroughly – see Figure 7. The setup was then started up as usual (see Section 2.5) with Formier10gas. While no gas composition measurements were taken during Test 4, the operating temperatures of the gasifier were very stable – see Figure 9. Product gas was added through the carbon filters to the setup at OCV, and after 30min of stable operation the carbon filters were by-passed. Following 30min of operation without gas cleaning, it can be seen on Figure 7 that the impact was negligible. The sulphur content into the system was 1.5-2.8ppm sulphur (Table 5). Therefore it was decided to ramp up the current to investigate any possible effects at higher current densities.

Figure 7 – Emptied and vacuum cleaned desulphurizer reactor

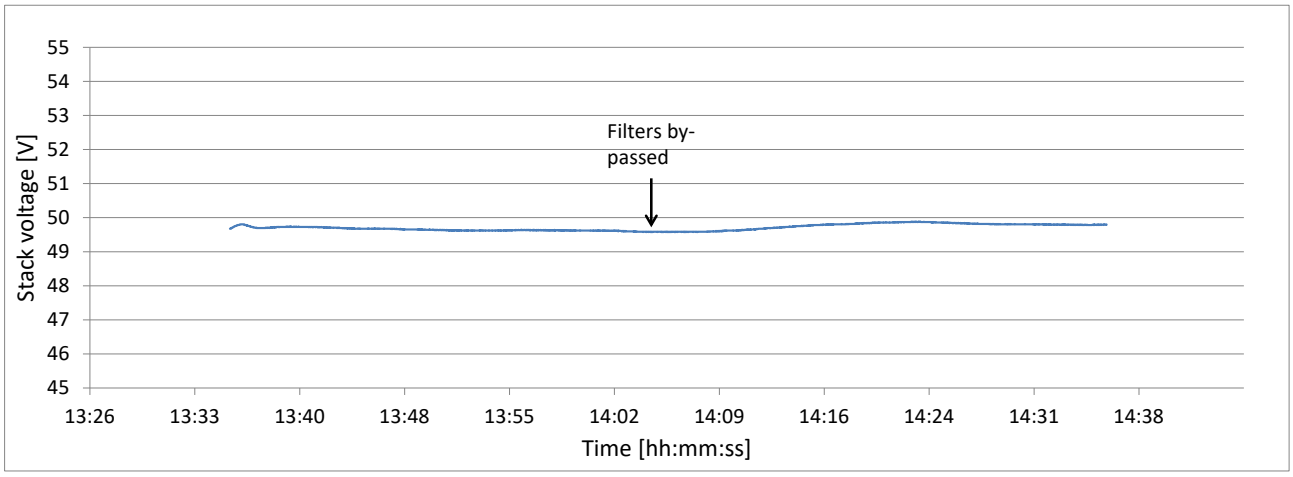

Figure 8 – SOFC open-circuit voltage with carbon filters and by-passed filters

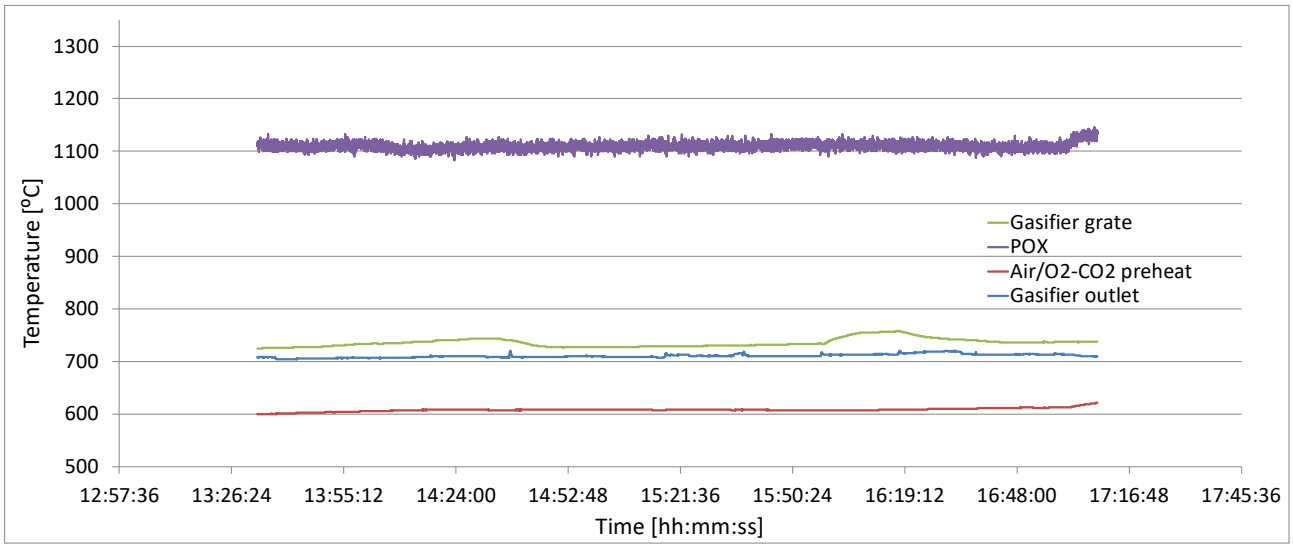

Figure 9 – Operating temperatures of the gasifier during Test 4

SOFC data for the O_2-CO_2-blown Tests 3 and 4 (with and without gas cleaning respectively) are given in Figure 8. Differences in stack voltage and power density are down to -5.2% and are at -2.5% at 20 A. One difference in operation between the tests were that the pump flow was 3.2% lower in Test 4, which indicates the change in performance with and without gas cleaning is negligible.

Following Test 4, the current was ramped down to 0A and the system was stabilized for 5min. The average voltage over the following 15min was 50.3V. For comparison, the average voltage in Figure 8 was 49.7V, which indicates no significant damage to the stack. This is however somewhat inconclusive as no hard data for situational gas composition and only a short evaluation period were given.

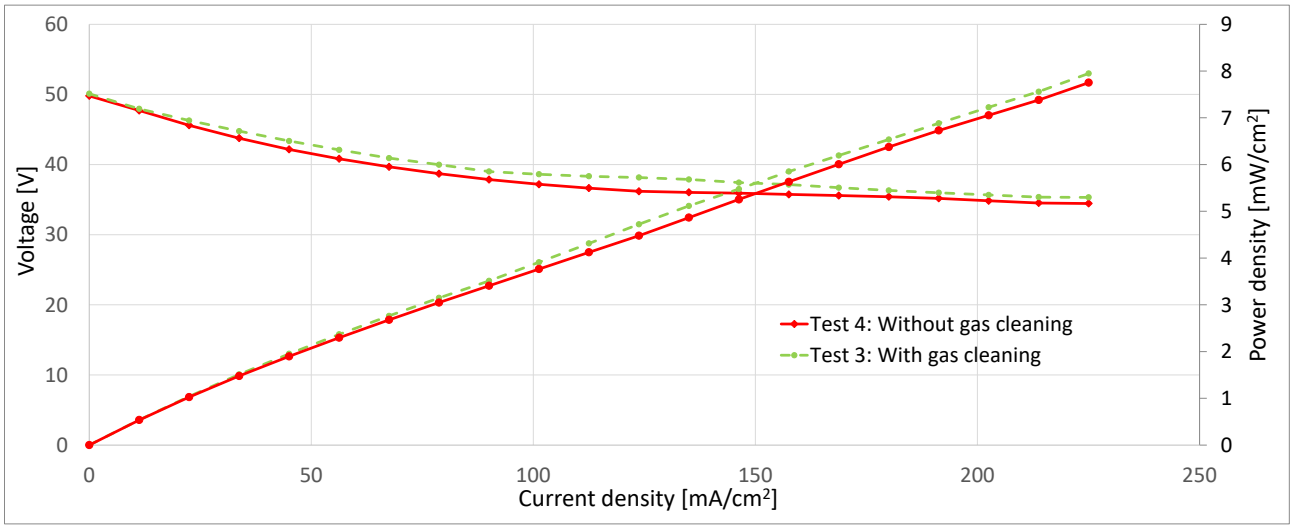

Figure 10 - Stack voltage and power density as a function of applied current at 700°C with and without gas cleaning using O_2-CO_2-blown product gas.

3.4 Stack efficiencies

The fuel utilization (FU) is a dimensionless base of comparison for fuel cell load between tests that operate different fuel flows and/or gas compositions. A molar hydrogen equivalent, $n_{H2\text{-}eq}$, is calculated based on complete conversion of CO and CH_4 with steam - shown in Equation 1. While there is only a negligible steam content at the conditions of these tests, the equivalent is only used to determine the traditionally used utilization parameter. The FU is defined in Equation 2 on a molar basis. N_c is the number of cells in the stack, I is the current and F is Faradays constant. The average gas compositions from Table 4 are used for the calculation – Test 3 as an average of the latter two compositions. The gas temperature at the gas pump is assumed to be 15°C. The values at peak performance for Test 1-3 are given in Table 6 along with the corresponding electric (gas-to-power) efficiencies and should be seen as a supplement to the discussions in Sections 3.2 and 3.3.

$$n_{H2-eq} = n_{H2} + n_{CO} + 4 \cdot n_{CH4}$$

Equation 1

$$FU = \frac{\frac{I}{2 \cdot F} N_c}{n_{H2-eq}}$$

Equation 2

	Test 1	Test 2	Test 3
FU [%]	67.3	69.2	63.0
η_{SOFC}[a] [%]	35.8	39.6	32.6

Table 6 – Fuel utilization and electric efficiencies for Test 1-3 at 20A. [a]Calculated electric gas-to-power efficiency via Equation 3, where *W* is the produced power and *V* is the volume flow of product gas to the stack.

$$\eta_{SOFC} = \frac{W_{SOFC}}{V_{gas} \cdot LHV_{gas}}$$

Equation 3

4 Conclusions and further work

The study presented successful operation of a relatively simple TwoStage gasifier-SOFC system. Only minimal gas cleaning was applied with a 90°C bag filter, room-temperature carbon filter and a desulphurizer separating the gasifier and the SOFC. Gas-to-power efficiencies reached up to 39.6% at fuel utilizations up to 69.2%. An 8-11% increase in power and 3.8% increase in efficiency was seen when increasing the SOFC operating temperature from 700°C to 800°C. Changing air- to O_2-CO_2-blown product gas was seen to effect the performance, as the SOFC efficiency was seen to decrease due to the lower performance of CO compared to H_2. As the carbon filter and desulphurizer were bypassed, no short-term changes in operational voltage was seen with 1.5-2.8ppm sulphur in the feed gas. This indicates that the gasifier design can be a key feature when constructing gas cleaning trains for gasifier-SOFC systems, as in-situ gas cleaning can reduce the downstream cleaning significantly.

Further work in gasification-SOFC systems will be carried out in the 'Efficient Power 2 Gas' research project in the ForskEL-programme, which will feature pyrolysis gas operation and studies of SOFC/SOEC flexibility.

5 Acknowledgements

The authors would like to thank the ForskVE-programme of Energinet.dk for financial support through the Biomass Gasification Polygeneration project (ForskVE-12205).

6 References

[1] Ahrenfeldt J, Thomsen TP, Henriksen U, Clausen LR. Biomass gasification cogeneration - A review of state of the art technology and near future perspectives. Appl Therm Eng 2013;50:1407–17. doi:10.1016/j.applthermaleng.2011.12.040.

[2] International Energy Agency. Technology Roadmap: Hydrogen and fuel cells. 2015. doi:10.1007/SpringerReference_7300.

[3] International Energy Agency. Technology Roadmap - Bioenergy for Heat and Power. 2012.

[4] Gadsbøll RØRØ, Thomsen J, Bang-Møller C, Ahrenfeldt J, Henriksen UBUB. Solid oxide fuel cells powered by biomass gasification for high efficiency power generation. Energy 2017;131:198–206. doi:10.1016/j.energy.2017.05.044.

[5] Hofmann P, Schweiger a., Fryda L, Panopoulos KD, Hohenwarter U, Bentzen JD, et al. High temperature electrolyte supported Ni-GDC/YSZ/LSM SOFC operation on two-stage Viking gasifier product gas. J Power Sources 2007;173:357–66. doi:10.1016/j.jpowsour.2007.04.073.

[6] Hofmann P, Panopoulos K, Fryda L, Schweiger a, Ouweltjes J, Karl J. Integrating biomass gasification with solid oxide fuel cells: Effect of real product gas tars, fluctuations and particulates on Ni-GDC anode. Int J Hydrogen Energy 2008;33:2834–44. doi:10.1016/j.ijhydene.2008.03.020.

[7] Hofmann P, Panopoulos KD, Aravind PV, Siedlecki M, Schweiger A, Karl J, et al. Operation of solid oxide fuel cell on biomass product gas with tar levels >10 g Nm^-3. Int J Hydrogen Energy 2009;34:9203–12. doi:10.1016/j.ijhydene.2009.07.040.

[8] Jewulski J, Stepien M, Blesznowski M, Nanna F. Slip stream testing with a SOFC unit at Güssing and

Trisaia plants. 2010.

[9] Oudhuis AB., Bos A, Ouweltjes JP, Rietveld G, van der Giesen A. High efficiency electricity and products from biomass and waste, experimental results of proof of principle Presented at the 2nd World Conference and Technology Exhibition. 2nd world Conf. Technol. Exhib. biomass energy, Ind. Clim. Prot., 2004, p. 10–4.

[10] Nagel F. Electricity from wood through the combination of gasification and solid oxide fuel cells Systems analysis and Proof-of-concept 2008. doi:10.3929/ethz-a-005773119.

[11] Ud Din Z, Zainal ZA. The fate of SOFC anodes under biomass producer gas contaminants. Renew Sustain Energy Rev 2017;72:1050–66. doi:10.1016/j.rser.2016.10.012.

[12] Aravind PV, de Jong W. Evaluation of high temperature gas cleaning options for biomass gasification product gas for Solid Oxide Fuel Cells. Prog Energy Combust Sci 2012;38:737–64. doi:10.1016/j.pecs.2012.03.006.

[13] Blesznowski M, Jewulski J, Zieleniak A. Determination of H2S and HCl concentration limits in the fuel for anode supported SOFC operation. Cent Eur J Chem 2013;11:960–7. doi:10.2478/s11532-013-0228-1.

[14] Hofmann P, Panopoulos KD, Aravind PV, Siedlecki M, Schweiger a., Karl J, et al. Operation of solid oxide fuel cell on biomass product gas with tar levels >10 g Nm−3. Int J Hydrogen Energy 2009;34:9203–12. doi:10.1016/j.ijhydene.2009.07.040.

[15] Rostrup-Nielsen JR, Hansen JB, Helveg S, Christiansen N, Jannasch a.-K. Sites for catalysis and electrochemistry in solid oxide fuel cell (SOFC) anode. Appl Phys A 2006;85:427–30. doi:10.1007/s00339-006-3702-1.

[16] Birss V, Deleebeeck L, Paulson S, Smith T. Understanding Performance Losses at Ni-Based Anodes due to Sulphur Exposure 2011;35:1445–54.

[17] Kromp A, Dierickx S, Leonide A, Weber A, Ivers-Tifée E. Electrochemical Analysis of Sulphur-Poisoning in Anode-Supported SOFCs under Reformate Operation 2012;41:161–9.

[18] Rasmussen JFB, Hagen A. The effect of H2S on the performance of Ni–YSZ anodes in solid oxide fuel cells. J Power Sources 2009;191:534–41. doi:10.1016/j.jpowsour.2009.02.001.

[19] Sasaki K, Susuki K, Iyoshi A, Uchimura M, Imamura N, Kusaba H, et al. H[sub 2]S Poisoning of Solid Oxide Fuel Cells. J Electrochem Soc 2006;153:A2023. doi:10.1149/1.2336075.

[20] Schubert SK, Kusnezoff M, Wunderlich C. Characterisation of Sulphur Poisoning of Anodes in Single-Cell SOFC Stacks Using Impedance Spectroscopy. FuelconDe 2008:1–12.

[21] Trembly JP, Marquez AI, Ohrn TR, Bayless DJ. Effects of coal syngas and H2S on the performance of solid oxide fuel cells: Single-cell tests. J Power Sources 2006;158:263–73. doi:10.1016/j.jpowsour.2005.09.055.

[22] Li TS, Xu M, Gao C, Wang B, Liu X, Li B, et al. Investigation into the effects of sulfur on syngas reforming inside a solid oxide fuel cell. J Power Sources 2014;258:1–4. doi:10.1016/j.jpowsour.2014.02.041 Short communication.

[23] Bao JE, Krishnan GN, Jayaweera P, Lau KH, Sanjurjo A. Effect of various coal contaminants on the

performance of solid oxide fuel cells: Part II. ppm and sub-ppm level testing. J Power Sources 2009;193:617–24. doi:10.1016/j.jpowsour.2009.04.035.

[24] Li TS, Miao H, Chen T, Wang WG, Xu C. Effect of Simulated Coal-Derived Gas Composition on H[sub 2]S Poisoning Behavior Evaluated Using a Disaggregation Scheme. J Electrochem Soc 2009;156:B1383. doi:10.1149/1.3232006.

[25] Milne TA, Evans RJ. Biomass Gasifier Tars: Their Nature , Formation , and Conversion Biomass Gasifier. 1998.

[26] Baldinelli A, Cinti G, Desideri U, Fantozzi F. Biomass integrated gasifier-fuel cells: Experimental investigation on wood syngas tars impact on NiYSZ-anode Solid Oxide Fuel Cells. Energy Convers Manag 2016;128:361–70. doi:10.1016/j.enconman.2016.09.048.

[27] Mermelstein J, Millan M, Brandon N. The impact of steam and current density on carbon formation from biomass gasification tar on Ni/YSZ, and Ni/CGO solid oxide fuel cell anodes. J Power Sources 2010;195:1657–66. doi:10.1016/j.jpowsour.2009.09.046.

[28] Gadsbøll RØ, Sarossy Z, Jørgensen L, Ahrenfeldt J, Henriksen UB. Oxygen-blown operation of the TwoStage gasifier. Energy 2018. doi:10.1016/j.energy.2018.06.071.

[29] Henriksen U, Ahrenfeldt J, Jensen TK, Gøbel B, Bentzen JD, Hindsgaul C, et al. The design, construction and operation of a 75kW two-stage gasifier. Energy 2006;31:1542–53. doi:10.1016/j.energy.2005.05.031.

[30] Ahrenfeldt J, Henriksen UB, Jensen TK, Gøbel B, Wiese L, Kather A, et al. Validation of a continuous combined heat and power (CHP) operation of a Two-Stage biomass gasifier. Energy & Fuels 2006;20:2672–80.

[31] Bang-Moeller C. Design and Optimization of an Integrated Biomass Gasification and solid oxide fuel cell system. Technical University of Denmark, 2010.

[32] Homel M, Gür TM, Koh JH, Virkar A V. Carbon monooxide-fueled solid oxide fuel cell. J Power Sources 2010;195:6367–72.

[33] Jiang Y, Virkar A V. Fuel Composition and Diluent Effect on Gas Transport and Performance of Anode-Supported SOFCs. J Electrochem Soc 2003;150:A942. doi:10.1149/1.1579480.

[34] Yakabe H, Hishinuma M, Uratani M, Matsuzaki Y, Yasuda I. Evaluation and modeling of performance of anode-supported solid oxide fuel cell. J Power Sources 2000;86:423–31. doi:10.1016/S0378-7753(99)00444-9.

Energy 158 (2018) 495–503

Contents lists available at ScienceDirect

Energy

journal homepage: www.elsevier.com/locate/energy

Oxygen-blown operation of the TwoStage Viking gasifier

Rasmus Østergaard Gadsbøll [a, *], Zsuzsa Sárossy [a], Lars Jørgensen [b], Jesper Ahrenfeldt [a], Ulrik Birk Henriksen [a]

[a] Technical University of Denmark, Department of Chemical and Biochemical Engineering, Frederiksborgvej 399, 4000 Roskilde, Denmark
[b] Danish Gas Technology Centre, Dr Neergaards vej 5, 2970 Hørsholm, Denmark

ARTICLE INFO

Article history:
Received 6 April 2018
Received in revised form
24 May 2018
Accepted 11 June 2018
Available online 12 June 2018

Keywords:
Biomass gasification
Two-stage gasifier
Thermodynamic analysis
Experimental
Gas quality

ABSTRACT

The TwoStage Viking gasifier from the Technical University of Denmark is being further developed for biofuel synthesis applications. In order to optimize the gasification process, it is suggested to apply an O_2-CO_2 gas mixture as gasification medium, instead of air, to limit N_2-dilution of the product gas. It is found through a modeling study that the system is expected to achieve operating conditions in the range of air-blown operation, when 21v% O_2 in CO_2 is applied, and nearly identical parameters as the concentration is increased to 30v%. An experimental campaign with the 80kW$_{th}$ Viking pilot plant using 21v% oxygen confirms this, as operation temperatures are seen to slightly decrease the partial oxidation (POX) temperature by 52–69 °C and grate temperature by 31–36 °C. Tests with 25v% oxygen were also carried out with slightly higher temperatures. Detailed gas analysis showed that N_2 had effectively been reduced to a few percent and that tar and sulphur levels were similar to the very high standards of the air-blown operation: only a few mg/Nm^3 of tar and <3 ppm sulphur were detected. The lone gas cleaning, a bag filter, was found to be virtually inactive for capturing these impurities. Hence, the gasifier had been successfully demonstrated with O_2-CO_2 mixtures and is expected to be able to maintain its simple design, whilst enabling very high system efficiency.

1. Introduction

It is very cost-effective to use biomass-based energy to reduce the impact on climate change, because it to a large extent can be directly utilized into the current fossil infrastructure. Biomass as a flexible resource can be used for heat and power production, but is especially relevant as a carbon source for transport fuels. The fuels can be produced in a number of ways, but the thermal gasification platform offers maximum fuel and product flexibility along with very high conversion efficiency.

The production of biofuels via biomass gasification is a well-studied area and there are a number of limitations and challenges in this coupling of technologies which are namely associated with gas quality. Synthesis reactors are very sensitive to harmful gas impurities such as tars and inorganics and while no hard conclusions can be made on tolerances[1] some overall considerations can be made. These reactors utilize catalytic material at elevated temperatures of ≈200–700 °C for synthesis [1,2,3], which are typically in the range of the dew points of tar species in the product gas at ≈200–500 °C, which can cause fouling of equipment via condensation [4,5,6] and deactivate catalysts via carbon deposition [1,7]. Hence tar concentrations should be kept very low, in range of <100mg/Nm^3, depending especially on the dew point at the given conditions when applying catalytic reactors [1,8]. Sulphur and chlorine are both poisons to catalyst reactors and should be removed to <0.1–1.0ppmv and preferably completely removed to ensure years of catalyst lifetime [9,10].

Another critical gas component, nitrogen (N_2) is of special interest when coupling gasification and biofuel synthesis. It is especially central when synthesizing gaseous fuels such as synthetic natural gas (SNG), as nitrogen separation is expensive and dilution of the gas product might bring the Wobbe index and relative density out of the limits of the local natural gas grid.[2] This typically limits the nitrogen content to a few percent of the final product. As

* Corresponding author.
E-mail address: rgad@kt.dtu.dk (R.Ø. Gadsbøll).

[1] Tolerances for gas impurities are set based on catalyst, operating conditions and economic analysis and will vary.

[2] According to Danish law, the Wobbe Index must be higher than 50.76 MJ/Nm^3 (HHV) and the relative density must be higher than 0.555 [34].

https://doi.org/10.1016/j.energy.2018.06.071
0360-5442/

an inert gas, nitrogen is also problematic as it will increase the size of the costly synthesis reactors and is recommended around <2v% [10].

1.1. Modifying the TwoStage Viking gasifier

The TwoStage Viking gasifier has been developed for many years at the Technical University of Denmark [11]. The air-blown downdraft system is designed with separate pyrolysis and gasification, with a partial oxidation (POX) in between and is namely characterized by its ability to process biomass into product gas at a very high cold gas efficiency of 87–90% (dry) and a very low tar content of <0.1mg/Nm^3 [12,13]. The plant is presented in detail in Section 3.1. In order to develop the fuel synthesis application platform of the system, oxygen-blown operation is desired to avoid nitrogen dilution of the product gas - which coupled with the high efficiency and low tar content would make the system ideal for biofuel production. This study will therefore investigate an oxygen-blown configuration of the gasifier system.

The oxygen is initially projected to be used with a carrier gas such as CO_2 or steam in order to ease the implementation, obtain operating parameters similar to air and protect equipment, as it acts as a thermal buffer during oxidation and reduces potential erosion from the hot oxygen flow in the heat exchanger and piping. CO_2 is initially preferred over steam as carrier gas, as it: 1) can be easily implemented from gas bottles; 2) is much less energy intense (no need for vaporization) to implement; 3) and can possibly be recycled from a downstream product upgrader (CO_2 separator) and led back to the POX.

Replacing N_2 with CO_2 is expected to affect the POX zone, as the gases have significantly different properties - see Table 1. While no studies have been found on O_2-CO_2 partial oxidation of pyrolysis gas, several references [14,15,16,17,18] have dealt with flame studies of O_2-CO_2 burners in oxy-fuel combustion of coal. The main differences between these burners and typical air burners are related to the gas properties that can cause (21v% O_2 and similar flow rates as reference):

- Higher flame instability and flame retarding via a lower flame propagation speed [14,15,17].
- Generally lower gas temperatures of ≈100–200 °C [15,16].
- Increased diffusion resistance of CO_2 that can cause a more compact flame [16].
- Similar operational parameters for air and O_2-CO_2 are reached at O_2 concentrations of 28–35v% [14,15,16,17].

Thus it will be important for the POX zone to optimize the mixing/contact between reactants to obtain a stable flame and maximize the tar exposure to high-temperatures in the potentially smaller flame zone, which will be even more important as the temperature is expected to decrease.

Gasification with O_2-CO_2 mixtures has been studied on several occasions and compared to air-blown operation. Pohorely et al. [19] studied air and O_2-CO_2 (21v% O_2) gasification in a limestone-fed bubbling fluid bed at 850 °C and found that replacing N_2 with CO_2 generally heightens both carbon conversion and cold gas efficiency compared to air. This could partially be due to an increased inlet energy content, as the CO_2-mix has a higher heat capacity and same inlet temperature as the air. Higher CO and lower H_2 yields were also found, likely due to a shift in the water-gas shift equilibrium. Tar and light hydrocarbon concentrations were found to be significantly higher for O_2-CO_2 operation, which the authors explain by increased CO and CO_2 partial pressures that could shift the reforming reaction equilibrium away from conversion. Similar findings of carbon conversion, effciency and CO_2 and H_2 yields were found by Hanaoka et al. [20]. The study gasifies aquatic biomass at 900 °C in a downdraft fixed bed reactor with O_2-CO_2 and O_2-He operation and also found that an increased CO_2 flow caused larger concentrations of sulphur species (H_2S, COS), which could be related to increased carbon conversion, as the sulphur content of the char were found to be relatively high.

This study will present the use of O_2-CO_2 in the TwoStage Viking gasifier and compare it to its typical air-blown operation - both via mathemcatical modeling and experimentally. An experimental campaign will show the effects on the operating conditions of the partial oxidation and the char bedm, and also assess the impact on gas quality including gas composition, tars and sulphur compounds. These aspects are not well-studied and will be investigated further here as a link in the development of the TwoStage gasifier and further development towards fuel synthesis applications.

2. Modeling O_2-CO_2-blown TwoStage gasification

In order to project and plan out experimental work, the TwoStage Viking gasifier is modeled and projected with air and O_2-CO_2 mixtures. The core process is modeled via three main components: pyrolyzer, POX and gasifier. The thermodynamic modeling is carried out in DNA (Dynamic Network Analysis) that is a zero-dimensional modeling tool for simulating energy systems [21,22].

Initially a model using air is constructed and calibrated to match current gasifier data. The main assumptions are given in Table 2 and are mainly based on the very detailed experimental campaign report by Bentzen et al. [13]. Note that this report deals with a previously constructed, but very similar, TwoStage gasifier plant. The pyrolysis features a reactor that based on atomic balances and input calculates a char and volatile fraction at the specified temperature. The POX and gasifier utilizes Gibbs minimization for calculating the gas composition and process parameters.

The model calibration included adjusting gasifier equilibrium temperature and allocating the total heat loss of 4% on to the pyrolyzer and gasifier. The air-blown model is pictured in Fig. 1 with resulting key data. Main model results including gas composition are compared to operational data for the TwoStage gasifier in Table 3 showing an overall satisfying fit. One of the key differences is the CH_4 content that is negligible in the model, but in practice typically 1–2% methane is formed in and/or slips by the partial oxidation zone, which converts most of it and other hydrocarbons. This difference will namely cause a slightly higher hydrogen content in the model as well as a slight difference in partial oxidation temperature due to endothermic reforming reactions. The POX (maximum) temperature is seen to be within range of the measured temperature, but this value will in practice fluctuate

Table 1
Properties of N_2 and CO_2 at 850 °C and 1 bar [18].

	Density [kg/m^3]	Heat capacity [J/mol-K]	Mass diffusion coefficient of O_2 in N_2/CO_2 [m^2/s]
N_2	0.244	34.18	$1.7 \cdot 10^4$
CO_2	0.383	57.83	$1.3 \cdot 10^4$
Ratio N_2/CO_2	0.640	0.59	1.31

Table 2
Modeling parameters.

Fuel[a]	49% moisture, 20 °C, composition: C = 49% H = 6% O = 44% N = 0.2% Ash = 0.8% (balance) LHV = 18.28 MJ/kg (dry)
Pyrolyzer	Volatiles are assumed to have a H_2 and CH_4 content of 5v% and 13v% [13], tars are represented by *n*-hexane (C_6H_{14}), char yield of 25% [23], 1% heat loss of fuel input, $LHV_{in} = LHV_{out}$, outlet temperature of volatiles and char = 600 °C Char composition: C = 93%.0 H = 2.2% N = 0.2% HHV = 33.6 MJ/kg (dry) [23]
Gasification media	Air: O_2 = 21% N_2 = 77% H_2O = 1% Ar = 1%, O_2-CO_2: O_2 = 21% CO_2 = 79%, 20 °C input, 450 °C after heat exchanger
Partial oxidation	Assumes thermal equilibrium at outlet temperature via Gibbs minimization of volatiles-air mixture – method described in Ref. [24,25].
Gasifier	3% fuel input heat loss [13], gas outlet thermal equilibrium = 800 °C, gas composition calculated via chemical equilibrium (water-gas shift), carbon conversion = 99% when using air [12], pressure loss is 30 mbar, outlet temperature = 750 °C

[a] Composition from Ref. [12] and moisture from Ref. [13].

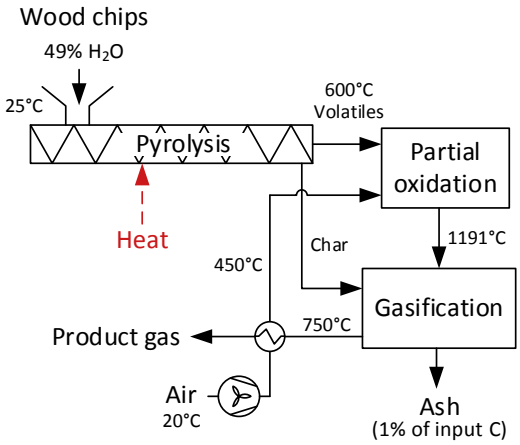

Fig. 1. Model of TwoStage gasifier.

Table 3
Comparison of TwoStage gasifier [13] and model. All flows and fractions are dry.

	Unit	TwoStage Viking gasifier	Model
Air/fuel flow	[kg/kg]	1.36	1.33
POX temperature	[°C]	1150 ± 100	1191
Cold gas efficiency	[%] (LHV)	90	89.1
H_2	[v%]	34	36
CO	[v%]	17	17
CO_2	[v%]	17	17
CH_4	[v%]	2	0
N_2	[v%]	31	30
LHV	[MJ/kg]	6.6	6.4

between ≈1100 and 1300 °C.

The calibrated model is used to project various O_2-CO_2 mixtures, which are compared to the air-blown mode by implementing similar parameters. Two main weaknesses by using this direct comparison are namely that the CH_4 concentration can be affected by a change in operation and that the product gas and air/O_2-CO_2 temperatures are assumed constant across gasification media.

As seen in Table 4 the direct substitution of CO_2 for N_2 with 21v% O_2 will cause a decline in gasifier performance with lower temperatures and subsequent carbon conversion and efficiency. Namely the higher heat capacity is responsible for this decline, as the gasifier exhaust will have a higher content of sensible heat. In order to keep the efficiency and POX temperature at similar levels, a ≈12% larger volume flow is required. Generally it is seen that the efficiency and POX temperature are in the same range as for the air-blown mode.

In line with the literature review, it is seen that an O_2-concentration of 30v% obtain very similar parameters to those of the air-blown mode. As an extreme case, pure oxygen might be added to the process, which is seen to obtain higher performance across parameters, as the otherwise large amounts of N_2/CO_2 does not need to be heated and carried through the system. Increasing the O_2 concentration for higher cold gas efficiency is in line with experimental studies e.g. Ref. [20,26]. The use of pure oxygen on the plant might however be challenging with regards to the present plant design (temperatures, materials, gas flows etc.) and highly dependent on the fuel moisture levels in order to avoid hot spots. Therefore it is seen as reasonable to blend the oxygen with a carrier gas in order to make the system more robust and allow dryer fuels and potential other fuels with a lower volatile fraction that both will increase the POX temperature.

Based on the literature and modeling studies presented, the TwoStage Viking gasifier plant was modified and experimental campaigns were carried out over 3 days. The campaign details are presented in the following sections.

3. Experimental methods and materials

3.1. The gasifier plant

The TwoStage Viking gasifier has been developed for many years at the Biomass Gasification Group at the Technical University of Denmark. The 80kW_{th} gasifier pilot plant processes wood chips in two stages: moving bed pyrolysis and downdraft fixed bed char gasification with a POX zone in between – see Fig. 2. The pyrolyzer employs an externally heated screw conveyer that processes the fuel up to 600 °C by utilizing engine exhaust for heat supply. The released volatiles and char are led to the second reactor where they are exposed to a POX zone where 99% of the residual tar is converted [27]. The hot gases and char are then led to the char bed where the char is gasified and the remaining tars are reduced to a minimum by a 95–99% [27], resulting in a reported tar content of ≤0.1 mg/nm^3 [12]. Coupled with a high carbon conversion of 99%, the cold gas efficiency reaches 87% on dry basis and 93% on wet basis (34 wt% moisture) [12]. The gasifier applies only a simple bag filter for gas cleaning in order to capture particles and a condenser to dry the product gas.

As part of the development of the system, a steam dryer has been installed on the Viking plant. This will enable the use of fuel with high moisture contents up to ≈60–70% and also enable separation of the high-temperature pyrolysis heat exchanger area as shown in scaled up designs [28]. The steam dryer utilizes a steam loop, where it is moved and heated by a blower and an electrical heater. As seen on Fig. 2, the steam is then passed through a screw conveyer where the fuel moisture evaporates. The main fraction of the steam is then recirculated via a blower and reheated, while the produced moisture-steam is carried with the dry fuel to the pyrolyzer. The inlet steam temperature to the steam dryer was 173 °C.

The standard gasification medium is atmospheric air that is delivered to the system via a blower. Replacing the air injection

Table 4
Model comparison using air or O_2-CO_2.

	Unit	Air	O_2-CO_2	O_2-CO_2	O_2-CO_2	O_2
Oxygen fraction	[v%]	**21**	**21**	**21**	30	100
Gas/fuel flow	[m3[a]/kg (dry)]	**1.13**	**1.13**	1.26	0.80	0.22
Gas preheat to 450 °C	[kW_{th}[b]]	2.6	3.6	4.0	2.6	0.5
POX temperature	[°C]	1191	1085	1144	1197	1307
Carbon conversion	[%]	**99.0**	90.2	**99.0**	**99.0**	**99.0**
Cold gas efficiency	[%](dry,LHV)	89.1	80.9	87.8	89.2	91.0
H_2	[v% (dry)]	36	30	28	36	52
CO	[v% (dry)]	17	25	26	27	25
CO_2	[v% (dry)]	17	46	46	37	23
CH_4	[v% (dry)]	0	0	0	0	0
N_2	[v% (dry)]	30	0	0	0	0
LHV_{mass}	[MJ/kg]	6.4	5.1	5.1	6.6	10.8
LHV_{vol}	[MJ/Nm^3]	5.8	6.1	6.1	7.0	8.5

[a] At 20 °C, 1 bar.
[b] Based on 80kW_{th} fuel input (LHV).

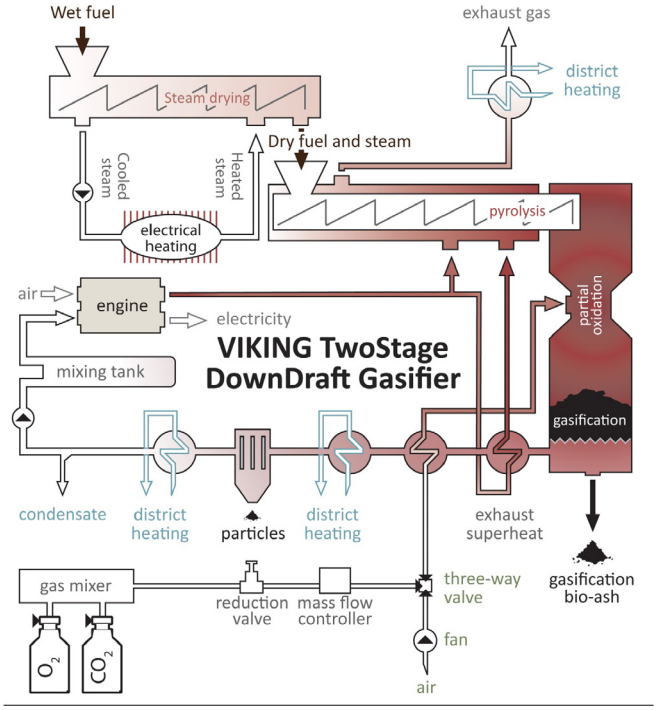

Fig. 2. Schematic overview of the Viking gasifier with an installed steam dryer and O_2-CO_2 mixing setup.

Fig. 3. Experimental setup for converting the air-blown gasifier to O_2-CO_2-blown. Left: Gas bottles. Upper right: gas mixer. Lower right: mass flow controller.

with an O_2-CO_2 mixture is done via the following setup. The O_2 and CO_2 are supplied via gas bottles, reduced to 10 bar via reduction valves and led to a gas mixer (Dansensor MAP Mix Provectus.) The gas mixer is based on two mass flow controllers, which secure the correct composition within 1%. The mixer feeds a 100 L buffer tank with a reduction valve, that secures a stable outlet pressure at 3 bar. The system feeds a thermal mass flow controller (Aalborg Model GFC) that uses the original air blower signal from the PLC (Siemens Step7) to dose the mixture near atmospheric pressure levels. The flow controller has an accuracy of ±1%. The mixture composition is manually set at the mixer and has been thoroughly tested beforehand. The equipment is shown in Fig. 3.

The gasifier can be operated via various strategies, but a constant air/O_2-CO_2 flow into the POX zone is chosen as the primary setpoint. The fuel feed is automatically set to maintain a bed height within a specified interval. The ash is discharged by the grate as the pressure difference builds up. When switching to the 21v% oxygen-mix, the volume flow is maintained similar to air. The 25v% oxygen-mix volume flow is set to match the absolute oxygen flow, meaning a smaller total gas flow is applied.

3.2. Fuel analysis

Standard Danish spruce wood chips were used as fuel for the gasifier. The main fuel elements (C, H, N, S, O) was analyzed with the VarioEL III (Elementar Analysensysteme GmbH, Germany) and results are shown in Table 5. The inorganic elements were measured by inductively coupled plasma optical emission spectrometry (ICP-OES) analysis and are shown in Table 6. The analysis showed a high amount of Ca (1063.0 and 1061.9 μg/g), whereas the presence of K, Mg and Na were also significant in the fuel.

The moisture content was relatively low compared to previous tests and was measured to 16-17 wt% on 4 occasions during testing, by weighing samples before and after at least 24 h residence in a 105 °C oven.

Table 5
Composition of dry spruce wood chips used in the experiments based on 4 samples.

	C [%]	H [%]	N [%]	S [%]	O (rest) [%]
Average	53.8	4.9	0.1	0.1	41.2

Table 6
Inorganic elements detected in the wood chips $[\mu g/g]_{dry}$.

Element	Al	B	Ca	Cu	Fe	K	Mg	Mn	Na	P	S	Zn
Sample #1	38.6	1.6	1063.0	1.2	38.4	295.0	116.5	8.2	112.2	76.2	130.3	8.7
Sample #2	36.9	1.3	1061.9	1.5	36.2	262.1	113.8	8.0	109.3	77.2	125.5	8.5

3.3. Gas analysis

Several types of analyses were performed on the collected product gas. For tar measurements, solid phase adsorption (SPA) was used. Sulphur was measured via gas samples and gas chromatography. For gas composition measurements, both gas chromatography from pipettes and online measurements were used, because the gas composition were out of the online equipment measurement range when applying O_2-CO_2.

3.3.1. Solid phase adsorption (SPA)

The tar measurements were taken at two locations: before the bag filter and after the condenser. Sampling was done through a needle connected to the filter and subsequently a 100 ml syringe – see Fig. 4. The needle was placed in the middle of the hot gas flow as the samples were taken. Sample was done over approximately 30 s.

The received SPA filters were removed, extracted and resulting samples were analyzed by gas chromatography – mass spectrometry (GC-MS). The cartridges were removed from the SPE tubes and were stored overnight after addition of 10 ml acetone, 1 ml phenol D5 and 1 ml polycyclic aromatic hydrocarbon (PAH) standard mixture. (The PAH standard mixture included: naphthalene D8, acenaphthene D10, anthracene D10, phenanthrene D10, fluorene D10, pyrene D10). Theacetone was then evaporated and the samples were redissolved in 1 ml acetone. The samples were analyzed by GC-MS using a Hewlett Packard HP 6890 gas chromatograph interfaced to a HP5973 Mass Selective Detector (Agilent, Denmark). Samples (1 μl) were injected in split mode (1:20) using an HP 7683 autosampler (Agilent, Denmark). The source and rod temperatures were 230 °C and 150 °C, respectively. The products were separated using a 0.32-mm i.d. × 30 m WCOT-fused silica column coated with VF-23 ms at a thickness of 0.25 μm (Analytical Instruments as, Denmark). The carrier gas was He at a flow rate of 1.2 ml/min. Separation of products was achieved using a temperature program from 70 to 250 °C at 10 °C/min. The applied ionization energy was 70 eV. Full mass spectra were recorded every 0.3s (mass range m/z 40–450). Products were identified using NIST search engine version 2.0 f. (Agilent, Denmark). The deuterated stable isotopes were used as internal standards and used for quantification, as they were added to the system in a known amount.

3.3.2. Sulphur measurements

Gas sampling for analysing the sulphur components H_2S and COS were performed Day 1 (air blown gasifier operation) and Day 3 (25v% oxygen blown gasifier operation). Both days sampling were performed upstream (before particle filter) and downstream (after the condenser) of the gasifier gas cleaning equipment. Three samples were taken at each location comprising a total number of six samples each of the two days. The gas samples were extracted into dedicated 5 L Supel™ Inert Foil gas sampling bags with screw cap valves from SUPELCO. Upstream gas cleaning the product gas pressure was negative and an EX gas pump was used to extract the gas into the SUPELCO bags. Downstream gas cleaning the product gas pressure was positive and large enough to fill the sampling bags by just opening the sampling port valve. Prior to the sampling the sampling connection tubes were flushed to get rid of air and accumulated condensed water in the sampling ports.

The sampling on Day 1 was performed as described above, but the subsequently analysis revealed sensitivity issues using the Agilent GCMS due the high water content in the gas samples. Therefore it was decided to add an amount of helium (He) to the gas sampling bags before performing the actual measurements at October 12. The result was diluted gas samples with water dew point lower than 100% (unsaturated gas samples) which caused lesser issues during analysis.

Analysis was done with an Agilent 7890A gas chromatograph combined with 5975C mass selective detector. Pre-concentration of the sample was done with a Markes Unity 2 thermal desorber with air sampler. Pre-concentration conditions: Markes T6SUL-2S cold trap at −30 °C; gas flow 50 ml/min during 5 min. Injection: trap heating at maximum rate to 300 °C; total split ratio 29.4. Analysis: separation of H_2S and COS was done at an Agilent DB-5ms column (20 m × 180 mm x 0,14 mm) at 35 °C with He as carrier gas. Other components were removed from the column by heating to 200 °C at 25 °C/min.

3.3.3. Gas analysis from gas pipettes

The gas sampling was done after the product gas condenser, where the pipettes were connected to the sampling port with a rubber tube – see Fig. 5. The vessel was flushed thoroughly for roughly 1 min by opening both ends and afterwards filled. Gas analysis was carried out within 1–2 h to avoid leakage of H_2.

The samples were analyzed by an Agilent Technologies 7890A gas chromatograph (Agilent, Denmark). Samples (volumes 100–1000 μl) were injected in split mode (1:25) using Pressure-Lok® Syringes (Vici, Baton Rouge, USA). For measurements of H_2, CO and CH_4, the gas components were separated using a 0.32-mm i.d. × 25 m PLOT-fused silica column coated with Molsieve 5A

Fig. 4. SPA sampling: needle with cartridge fastened to syringe via rubber band.

Fig. 5. Gas pipette sampling with rubber tube connection to sampling port.

(Analytical Instruments as, Denmark). The carrier gas was Ar at a flow rate of 1 ml/min. For CO measurements, He carrier gas was used. Separation of products was achieved using a temperature program from 50 to 235 °C at 10 °C/min. For measurements of CO_2, the gas components were separated using a 0.32-mm i.d. × 25 m PLOT-fused silica column coated with Poraplot U (Analytical Instruments as, Denmark). The carrier gas was He at a flow rate of 1 ml/min. Separation of products was achieved using a temperature program from 75 to 235 °C at 16 °C/min. Gas components were detected with a thermal conductivity detector (TCD).

3.3.4. Online gas measurements

On dry and tar-free basis, the gas composition were measured by an Advance Optima 2020 Modular continuous process gas analyzer system. The system was equipped with a Caldos 15 cell for analysis of H_2 and an Uras 14 cell for CO, CO_2 and CH_4 (ABB). The only issue with the Uras 14 cell was that the CO_2 measurement range is 30%, which makes the gas composition data unprecise above this limit. An PMA 10 O_2-analzer were also applied. N_2 was calculated as difference. All of the equipment has a ±1% unvertainty range.

4. Experimental results

The gasifier was heated up to stable operating conditions over roughly 24 h using initially gas burners and afterwards air-blown operation from afternoon till next morning. The reported tests were carried out over 3 following days: Day 1 - air-blown, Day 2–21 and 25v% O_2-CO_2-blown, Day 3–21v% O_2-CO_2-blown. While tests were run during work hours, the system was kept thermally stable by operating it fully automated and unmanned overnight with air.

4.1. Operating temperatures and gas composition

Time dependent temperature data for air and O_2-CO_2 operation is shown in Fig. 6 and Fig. 7 respectively, while the corresponding online gas measurements are given in Fig. 8 and Fig. 9. Temperature measurements were taken after the air preheater, at the POX zone, just above the gasifier grate and at the reactor outlet and all parameters showed satisfying process stability. In- and decreasing trends can be due to changes in fuel moisture and/or thermal stability. The operating data is within range of previous tests with the gasifier [12,13,25].

The operating temperatures and gas compositions are summarized as averages in Table 7 and gas pipette gas compositions are given in Table 8. As discussed in the modeling study (Section 2), it is seen that the general trend is that the temperatures are decreasing in the gasifier as the process is switched from air to 21v% O_2-CO_2: a POX temperature reduction of 52–69 °C with grate temperatures decreasing with 31–36 °C. The preheating temperature is generally somewhat lower, which is expected as the heat capacity is significantly higher compared to air. At 25v% oxygen, both preheat, POX and grate temperatures are increased and are more similar to air-blown data.

The N_2 content is drastically reduced, but a couple of percentages remain, which is mainly due to fuel feed ash silo N_2 purging. The level is expected to be reduced to a negligible content if e.g. CO_2-purge is applied instead. As expected from the modeling, the H_2 content is slightly lower, which is likely a result of a displacement in the water-gas shift reaction as the CO_2 concentration is much higher. The CO_2 and CO concentrations are in line with the predictions of the model, but slightly lower though. This small difference can – amongst several minor differences – be partly attributed to a lower steam content (model fuel moisture 49%, while 16–17% experimentally) content that will promote CO_2 conversion in the char bed. As mentioned, the oxygen flow is constant across tests, meaning that the CO_2 will be lower at 25v% O_2, which is the main cause of the lower CO_2 concentration at this condition. The lower CO level at 25v% O_2-CO_2 is likely due to reduced char-CO_2 gasification reactions. Methane contents are low and similar for both tests as the POX temperature remains high.

The samples during the 25v% O_2-CO_2 operation is seen to be somewhat inaccurate, as the sum of gas components did not close in on 100% and it is still unknown why this is the case.

4.2. Tars and inorganics

Tar measurements are shown in Table 9. For air-blown operation, the results show expected low results in the low mg/m^3-range with only PAH compounds present. The particle filter is seen to not cause any significant reduction in tar concentration, however on day 1 no tars could be measured after the filter. While the relative difference between tar concentrations in the air and O_2-CO_2 samples is high, the absolute difference is seen to be very small. Hence no significant difference is seen between the two states. It is however interesting to provide a brief overview of the parameters

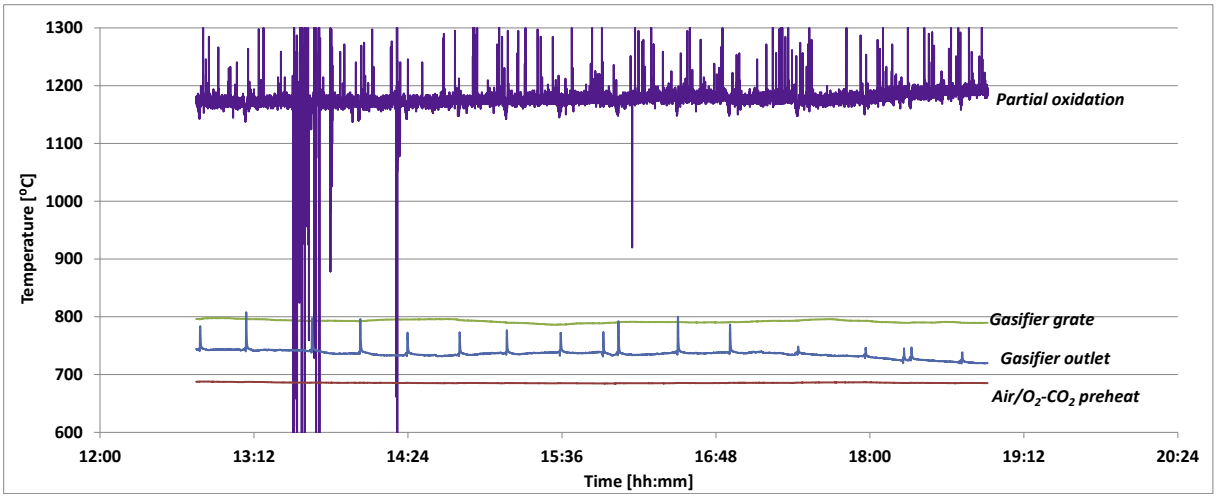

Fig. 6. Operating temperatures for air-blown operation during Day 1.

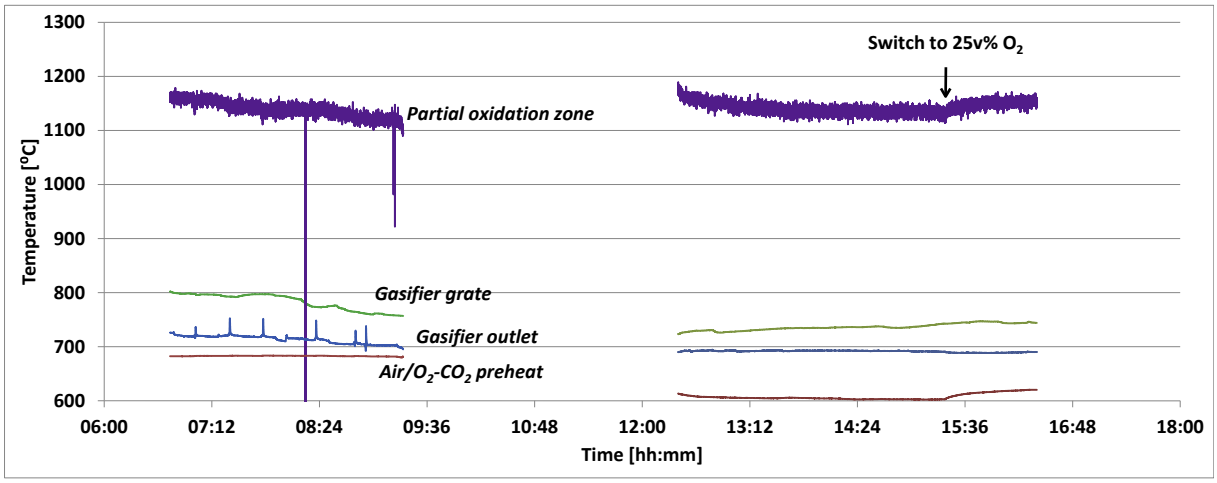

Fig. 7. Operating temperatures for 21v% and 25v% O_2-CO_2-blown operation during the time of testing. The two periods before the switch to 25v% O_2-CO_2 is 21v% O_2-CO_2. Day 2.

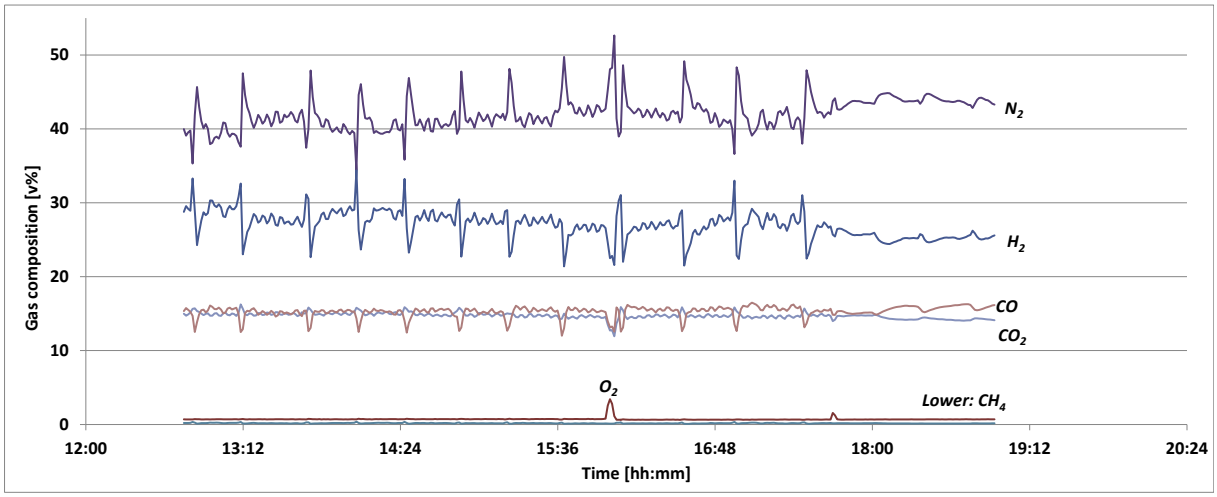

Fig. 8. Gas composition for air-blown operation during Day 1. The spikes of N_2 are caused by filter flushing and these are minimized around 17:30 where the gas analysis is taken after the product gas buffer tank instead of before.

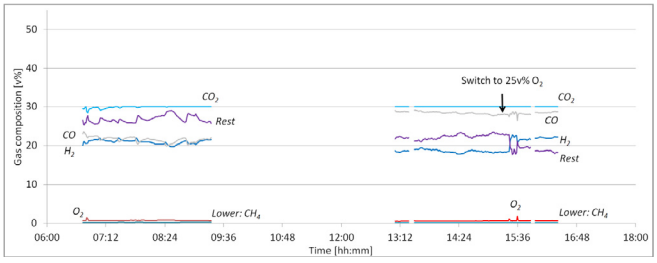

Fig. 9. Gas composition for 21v% and 25v% O_2-CO_2-blown operation during Day 2. Test were interrupted by a power outage around 9:20.Note that the measurements are out the measurement range and therefore not precise.

that could cause a difference (char bed height and product gas flows were seen to be similar across the samples and are not expected to impact the tar):

- Reduced grate and POX temperature with O_2-CO_2 of ≈60 °C and ≈40 °C respectively will decrease tar conversion, as the conversion by thermal and chemical (char) means will be reduced.

Table 7
Day-by-day Averaged temperature and online gas data for the test campaigns.

Test Time period	Day	$T_{preheat}$ [°C]	T_{POX} [°C]	T_{grate} [°C]	T_{outlet} [°C]
Air 12:45–18:45	1	686	1177	792	736
Air #2[a] 0:00–6:13	2	680	1188	766	719
21v% O_2-CO_2 6:44–9:20	2	683	1137	730	714
21v% O_2-CO_2 13:05–15:24	2	604	1136	735	692
25v% O_2-CO_2 15:24–16:24	2	616	1149	745	689
Air #3[a] 0:00–6:23	3	640	1183	766	695
21v% O_2-CO_2 10:42–17:00	3	595	1114	731	708

[a] Test data for overnight operation without gas analysis.

- Applying a CO_2-rich gasification medium will affect the char structure, as it has shown to produce char with a larger microstructure, specifically increase micro- and mesopore area e.g. Ref. [29], which will likely increase tar conversion [29,30].

Table 8
Data from online gas analysis (air) and gas chromatography data from gas pipette samples (21v% and 25v% O_2-in-CO_2).

	Day - time	H_2 [v%]	CO_2 [v%]	CO [v%]	CH_4 [v%]	N_2 [v%]	SUM
Air	1–12:45–18:45	27.0	14.7	15.3	0.4	42.1	99.5
21v% O_2-CO_2	2–11:15	24.0	42.6	26.9	0.05	4.6	98.2
	2–13:20	21.2	43.2	24.9	0.16	4.7	94.2
	2–13:22	20.6	44.3	25.8	0.22	4.6	95.5
25v% O_2-CO_2	2–15:50	21.2	39.3	18.6	0.04	3.8	82.9
	2–16:50	22.8	39.4	20.6	0.09	4.6	87.5

Table 9
Tar measurements [mg/Nm^3] before and after the bag filter of the gasifier. Preliminary samples were taken during the initial tests of system 2 months prior to the main experimental work that is reported here – operation conditions were very similar.

Time	Location	Gasifier medium	Pyrene	Naphthalene	Sum [mg/Nm^3]	Sum [ppm]
Pre-liminary	Before filter	Air	4.9 ± 0.2	0	**4.9**	**N/A**
Pre-liminary	After filter	Air	4.2 ± 0.5	0	**4.2**	**N/A**
10:29 Day 1	Before filter	Air	2.8	0	**2.8**	**0.003**
11:00 Day 1	Before filter	Air	3	0	**3**	**0.003**
10:05 Day 1	After filter	Air	0	0	**0**	**0**
10:17 Day 1	After filter	Air	0	0	**0**	**0**
Preliminary	Before filter	21v% O_2-CO_2	5.7 ± 0.8	3.5 ± 2.5	**9.2**	**N/A**
Preliminary	After filter	21v% O_2-CO_2	3.8 ± 0.2	6.5 ± 0.4	**10.3**	**N/A**
13:53 Day 2	Before filter	21v% O_2-CO_2	0	0	**0**	**0**
13:42 Day 2	After filter	21v% O_2-CO_2	1	0	**1**	**0.001**
13:47 Day 2	After filter	21v% O_2-CO_2	0	0	**0**	**0**

- By increasing the CO_2 partial pressure, it is likely that an increase in dry reforming of tar over the char will be present and hence decrease the tar concentration.

Gas samples were taken during Day 1 and 3 to assess the sulphur load and results are shown in Table 10. The range of 0.6–2.8 ppm total sulphur is within previous measurements of the gasifier of 3.7 ppm of COS (no H_2S) [25], 0.17–0.28 ppm of COS (no H_2S) [32] and <2 ppm H_2S + COS [33], which is also in line with the sulphur content of the applied wood fuels (Table 6) and is similar to previous analysis of wood fuel for the Viking [12]. It was expected that the bag filter might capture some of the sulphur species, as it will be partially coated with char from the gasifier and hence act as a carbon filter. It is however seen that this is not the case, as the

Table 10
Measurements for sulphur in the product gas.

Samplingtime	Location	Gasification media	H_2S [ppm]	COS [ppm]	Total S [ppm]
Day 1 12:20	Before filter	Air	0.1	0.6	0.7
Day 1 12:23	After filter	Air	0.1	0.5	0.6
Day 1 12:27	Before filter	Air	0.1	1.0	1.1
Day 1 12:32	Before filter	Air	0.4	1.1	1.5
Day 1 12:36	After filter	Air	0.4	1.0	1.4
Day 3 10:52	Before filter	21v% O_2-CO_2	0.3	1.8	2.1
Day 3 10:57	After filter	21v% O_2-CO_2	0.4	2.4	2.8
Day 3 11:36	Before filter	21v% O_2-CO_2	0.2	1.6	1.8
Day 3 11:41	After filter	21v% O_2-CO_2	0.2	1.3	1.5
Day 3 12:07	Before filter	21v% O_2-CO_2	0.2	1.8	2.0
Day 3 12:12	After filter	21v% O_2-CO_2	0.2	1.3	1.5

filters' capture, if any, is negligible. The sampling and analysis were carried out by Danish Gas Technology Center and the relative uncertainty was estimated based on experiences to 40% for the first three samples in Table 10 and 25% for the remaining samples.

Between the media, the difference in sulphur species is negligible, with an additional 1 ppm extra on average for the O_2-CO_2 blend. This is due to additional COS, that could be slightly promoted with the given gas composition. As mentioned, previous tests have shown higher COS levels when air was applied, and hence the difference might also be due to small variations in operation from Day 1–3.

5. Conclusions

The Viking gasifier has been successfully converted from its original air-blown configuration to using O_2-CO_2 as gasification medium. Literature, modeling and experimental studies showed that operating conditions were expected to be in the range of air-blown values at 21-30v% O_2-in-CO_2, with partial oxidation and grate temperatures reduced by 52–69 °C and 31–36 °C respectively at 21v% O_2. Detailed gas analysis for tar and sulphur species showed that the gas qualities during O_2-CO_2 operation were comparable to the very high standards of the typical air-blown mode at <11mg/Nm^3 and <3 ppm respectively – without any downstream gas cleaning equipment.

Hence the system can be successfully converted to operate with an O_2-CO_2 blend without major additions to existing design. Compared to the more typically applied O_2-H_2O medium in the literature, applying CO_2 might be better suited for some applications, as the media can be: 1) conveniently recirculated back to the oxygen source without need for high evaporation heat; 2) be completely converted into biofuels by addition of electrolytic hydrogen downstream of the system.

Acknowledgements

The authors would like to thank the ForskVE-programme of Energinet.dk for financial support through the Biomass Gasification Polygeneration project (ForskVE-12205).

References

[1] Basu P. Biomass gasification, pyrolysis and torrefraction. second ed. Dalhouse University: Elsevier Inc.; 2013.
[2] Held J. Gasification - status and technology. 2012. doi:1102-7371.
[3] Topsøe Haldor. From solid fuels to substitute natural gas (SNG) using TREMP. 2009.
[4] Rabou LPLM, Van der Drift B, Van Dijk EHAJ, Meijden CM, Van der, Vreugdenhil BJ. Synthetic natural gas from coal, dry biomass, and power-to-gas applications. first ed. John Wiley & sons Ltd; 2016.
[5] Devi L, Ptasinski KJ, Berends RH, Padban N, Beesteheerde J, Veringa HJ. Primary measures to reduce tar formation in fluidised-bed biomass gasifiers. 2004.
[6] Zwart RWR. Gas cleaning downstream biomass gasification Status Report 2009. 2009.
[7] Aravind PV, de Jong W. Evaluation of high temperature gas cleaning options for biomass gasification product gas for Solid Oxide Fuel Cells. Prog Energy Combust Sci 2012;38:737–64. https://doi.org/10.1016/j.pecs.2012.03.006.
[8] Kienberger T, Zuber C. Synthetic natural gas from coal, dry biomass, and power-to-gas applications. first ed. John Wiley & sons inc; 2016. https://doi.org/10.1002/9781119191339.
[9] Schildhauer TJ. Synthetic natural gas from coal, dry biomass, and power-to-gas applications. John Wiley & sons inc.; 2016. https://doi.org/10.1002/9781119191339.
[10] Hofbauer H, Rauch R, Ripfel-Nitsche K. Report on gas cleaning for synthesis Applications: Gas treatment. 2007. p. 75.
[11] Henriksen U, Ahrenfeldt J, Jensen TK, Gøbel B, Bentzen JD, Hindsgaul C, et al. The design, construction and operation of a 75 kW two-stage gasifier. Energy 2006;31:1542–53. https://doi.org/10.1016/j.energy.2005.05.031.
[12] Ahrenfeldt J, Henriksen UB, Jensen TK, Gøbel B, Wiese L, Kather A, et al. Validation of a continuous combined heat and power (CHP) operation of a Two-Stage biomass gasifier. Energy Fuels 2006;20:2672–80.
[13] Bentzen JD, Brandt P, Gøbel B, Henriksen UB, Hindsgaul C. Optimering af 100 kW totrinsforgasningsanlæg på DTU: Resultater fra forsøg i uge 37 1998. 1999.
[14] Kiga T, Takano S, Kimura N, Omata K, Okawa M, Mori T, et al. Characteristics of pulverized-coal combustion in the system of oxygen/recycled flue gas combustion. Energy Convers Manag 1997;38:S129–34. https://doi.org/10.1016/S0196-8904(96)00258-0.
[15] Liu H, Zailani R, Gibbs BM. Comparisons of pulverized coal combustion in air and in mixtures of O 2/CO 2. Fuel 2005;84:833–40. https://doi.org/10.1016/j.fuel.2004.11.018.
[16] Tan Y, Croiset E, Douglas MA, Thambimuthu KV. Combustion characteristics of coal in a mixture of oxygen and recycled flue gas. Fuel 2006;85:507–12. https://doi.org/10.1016/j.fuel.2005.08.010.
[17] Suda T, Masuko K, Sato J, Yamamoto A, Okazaki K. Effect of carbon dioxide on flame propagation of pulverized coal clouds in CO2/O2 combustion. Fuel 2007;86:2008–15. https://doi.org/10.1016/j.fuel.2006.11.038.
[18] Brix J. Oxy-fuel combustion of coal. Technical University of Denmark; 2011.
[19] Pohorely M, Jeremias M, Svoboda K, Kamenikova P, Skoblia S, Beno Z. CO2 as moderator for biomass gasification. Fuel 2014;117:198–205. https://doi.org/10.1016/j.fuel.2013.09.068.
[20] Hanaoka T, Hiasa S, Edashige Y. Syngas production by CO 2/O 2 gasi fi cation of aquatic biomass 2013;116:9–15. https://doi.org/10.1016/j.fuproc.2013.03.049.
[21] Technical University of Denmark. Homepage of the thermodynamic simulation tool DNA. DNA - A Therm Energy Syst Simulator. 2009. http://orbit.dtu.dk/en/publications/id(b76040a4-5a29-4b04-a898-12711391c933).html. [Accessed 24 March 2017].
[22] Elmegaard B, Houbak N. DNA – a general energy system simulation tool. DNA – a gen. Energy syst. Simul. Tool. SIMS 2005 and Tapir Academic Press; 2005. p. 43–52.
[23] Gøbel B. Dynamisk modellering af forgasning i fixed koksbed. Technical University of Denmark; 1999.
[24] Elmegaard B. Simulation of boiler dynamics - development, evaluation and application of a general energy system simulation tool. Technical University of Denmark; 1999.
[25] Gadsbøll RØ, Thomsen J, Bang-Møller C, Ahrenfeldt J, Henriksen UB. Solid oxide fuel cells powered by biomass gasification for high efficiency power generation. Energy 2017;131:198–206. https://doi.org/10.1016/j.energy.2017.05.044.
[26] Campoy M, Gómez-Barea A, Vidal FB, Ollero P. Air-steam gasification of biomass in a fluidised bed: process optimisation by enriched air. Fuel Process Technol 2009;90:677–85. https://doi.org/10.1016/j.fuproc.2008.12.007.
[27] Brandt P, Larsen E, Henriksen U. High tar reduction in a two-stage gasifier. Energy Fuels 2000;14:816–9. https://doi.org/10.1021/ef990182m.
[28] Bentzen JD, Hummelshøj R, Henriksen UB, Gøbel B, Ahrenfeldt J, Elmegaard B. Upscale of the two-stage gasification. In: Proc. 2nd world Conf. Technol. Exhib. biomass energy Ind.; 2004.
[29] Klinghoffer N, Castaldi MJ, Nzihou A. Catalyst properties and catalytic performance of char from biomass gasification. I&Ec; 2012. p. 13113–22. https://doi.org/10.1021/ie3014082.
[30] Mastral A, García T, Callén M, Navarro M, Galbán J. Assessement of phenanthrene removal from hot gas by porous carbons. Energy Fuels 2001;15:1–7. https://doi.org/10.1021/ef000116g.
[32] Hofmann P, Schweiger a, Fryda L, Panopoulos KD, Hohenwarter U, Bentzen JD, et al. High temperature electrolyte supported Ni-GDC/YSZ/LSM SOFC operation on two-stage Viking gasifier product gas. J Power Sources 2007;173:357–66. https://doi.org/10.1016/j.jpowsour.2007.04.073.
[33] Bang-Moeller C. Design and Optimization of an Integrated Biomass Gasification and solid oxide fuel cell system. Technical University of Denmark; 2010.
[34] The Danish Gas Legislation. Bekendtgørelse Om Gasreglementets Afsnit C-12, Bestem Om Gaskvaliteter. n.d. https://www.retsinformation.dk/Forms/R0710.aspx?id=144715. [Accessed 31 July 2017].

Applied Energy 216 (2018) 323–337

Contents lists available at ScienceDirect

Applied Energy

journal homepage: www.elsevier.com/locate/apenergy

Solution for the future smart energy system: A polygeneration plant based on reversible solid oxide cells and biomass gasification producing either electrofuel or power

Hafthor Ægir Sigurjonsson*, Lasse R. Clausen

Section of Thermal Energy, Department of Mechanical Engineering, The Technical University of Denmark (DTU), Nils Koppels Allé Bld. 403, DK-2800 Kgs. Lyngby, Denmark

HIGHLIGHTS

- Solution suggested in future smart energy systems built on fluctuating sources.
- Polygeneration system operating in either electricity or bio-SNG production modes.
- The system used reversible solid oxide cells to either use or produce electricity.
- This flexible system increases the capacity factor of the thermal power plant.
- Which will also increase the net present value of such an investment.

GRAPHICAL ABSTRACT

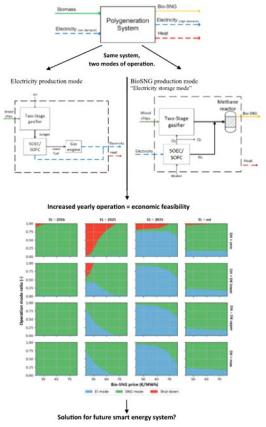

ARTICLE INFO

Keywords:
Polygeneration
Electrolysis
Fuel cell
Gasification
Techno-economic analysis

ABSTRACT

The Danish energy system will continue to evolve in the years ahead as the goal is to be independent of fossil fuels by 2050. This introduces several challenges in dealing with intermittent energy sources, such as wind and solar. A novel biomass-based polygeneration system concept is proposed, which can offer certain solutions to these challenges. The main concept is storing electricity by producing bio-SNG from syngas generated by biomass gasification and electrolytic hydrogen when electricity prices are low, and producing electricity when prices are high. The analytical framework is built on thermodynamic modeling, and techno-economic analysis is applied to determine the total revenues required and net present value, given a range of bio-SNG and electricity prices. The marginal cost of operation is then used to estimate the average operation time in each production mode. The results demonstrate that both electricity (46%) and bio-SNG (69%) production efficiencies are high. If district heating is coproduced, the total efficiencies increase to 85% and 90%, respectively. Furthermore, it was found that the annual operation time in each mode varies significantly depending on the future electricity price scenario and bio-SNG price. A system that can select the production or consumption of electricity depending on the market price enables constant operation all year round. This results in a higher net present value for the system and may lead to a positive return on investment, given the appropriate market price of electricity and bio-SNG. However, the techno-economic analysis revealed that the district heating product may be important for the

* Corresponding author.
E-mail address: hafsig@mek.dtu.dk (H.Æ. Sigurjonsson).

https://doi.org/10.1016/j.apenergy.2018.02.124
Received 11 August 2017; Received in revised form 16 February 2018; Accepted 17 February 2018
Available online 22 February 2018

economic feasibility of the polygeneration plant. This system may offer solutions in a smart energy system connecting electrofuel, heat, and power production, toward a 100% renewable system.

1. Introduction

The Danish energy system is continuing to develop to be independent of fossil fuels by 2050 [1]. Moreover, the goal is to decrease greenhouse gas emissions significantly in future decades [2]. This is a challenge for the energy system, as transformation from fossil to a more sustainable energy system is likely to increase the utilization of intermittent energy sources such as wind. The energy system needs to be flexible and adaptive for the effective use of intermittent energy sources [3,4]. The increased penetration of wind has and will continue to change the operation time and hourly profile loads of thermal power plants significantly, which will severely impact their economic feasibility [4]. However, the role of thermal power plants can still be important in balancing demand and supply; to phase out fossil fuels cost effectively using intermittent resources, a smart system must be coupled with a flexible thermal plant that can produce additional electricity when required or store electricity when production is high but demand is low. Mathiesen et al. [5] stated that electricity storage technologies such as batteries serve a function in the future energy system for managing short-term fluctuations, but do not play a large-scale role in handling annual fluctuations in a system with electricity produced by intermittent resources. In a review article on energy storage technologies by Luo et al. [6], hydrogen production and fuel cells are regarded as an option for dealing with fluctuating production from renewables, as electricity can be used in a water electrolyser to generate hydrogen when electricity demand is low (low market price), and hydrogen can be used in a fuel cell to produce electricity when demand is high (high market price). Another method could be the use of a reversible operation of solid oxide cells (SOCs) under electrolysis and fuel cell modes [7], which will decrease the number of components required, thereby increasing economic feasibility. Another means could be the use of hydrogen to create synthetic natural gas (SNG), which can be stored in existing natural gas grids, where the carbon source for SNG could be syngas from gasified biomass. An important advantage of generating SNG compared to hydrogen is that SNG has a higher energy density per volume, which makes it easier to store and use in the transportation sector.

Lund and Mathiesen [8] provided a 100% renewable energy system case analysis for Denmark in the years 2030 and 2050, which demonstrated its feasibility. However, the biomass demand is potentially high for its sustainable utilization. Mathiesen et al. [5] further illustrated that a 100% renewable energy system can be achieved with sustainable biomass consumption by creating a smart energy system. In this model, the electricity, heating, and transportation sectors are merged by producing electrofuels using electrolysis based on electricity from intermittent resources and biomass gasification, supplying electricity and additional heat through combined heat and power plants. Connolly et al. [9] introduced transition steps toward a 2050 smart energy system for Europe, where the final steps involve producing renewable electrofuels to provide new transport fuels, replace coal and oil, and finally, replace natural gas. Thermochemical and biochemical conversions are the two important bioenergy technologies for converting biomass, whereas combustion, pyrolysis, and gasification are the main options for thermochemical conversion [10]. The integration of gasification and electrolysis for fuel synthesis is not a novel approach, and has recently been researched in detail [11–15]. However, this research did not include a reversible system that can choose between electricity production and consumption for bio-SNG production. The purpose of this study is to introduce a system that can provide a solution for electricity markets with intermittent production in a future energy system by demonstrating the relevance of the ability to change operation between producing and using electricity based on market price. The proposed system is analyzed using the predicted hourly price duration curve in the Danish electricity market for the years 2025 and 2035. The hypothesis is that such a system can operate with a high capacity factor by enabling full operation all year round. This will increase the economic feasibility of future energy systems compared to using stand-alone gasifier and electrolyser plants.

1.1. System description

A biomass-based polygeneration system concept is proposed, which includes storage of electricity from fluctuating sources. The system produces heat, electricity, and SNG (bio-SNG), and stores electricity by producing bio-SNG when electricity market prices are low and producing electricity when market prices are high. Fig. 1 illustrates the main inputs and outputs of the proposed system.

This system is divided into two operation modes, namely the electricity production and bio-SNG production (electricity storage) modes. The main components of the system are depicted in Figs. 2 and 3 for the electricity and bio-SNG production modes, respectively. This model is designed to operate in an energy system with highly fluctuating renewable energy input (for example, wind) by taking advantage of the varying electricity prices, providing electricity and heat when required, and producing renewable electrofuel (bio-SNG) when electricity prices are low. This system can serve as a crucial component of a future smart energy system, as suggested by Mathiesen et al. [5] and Connolly et al. [9].

1.2. Analytical framework

The analytical framework is constructed based on thermodynamic modeling using DNA software, which is a component-based thermodynamic modeling and simulation tool [16]. DNA is open-source

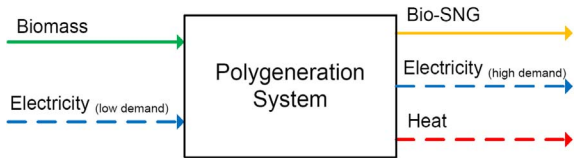

Fig. 1. Simplified diagram of proposed polygeneration system.

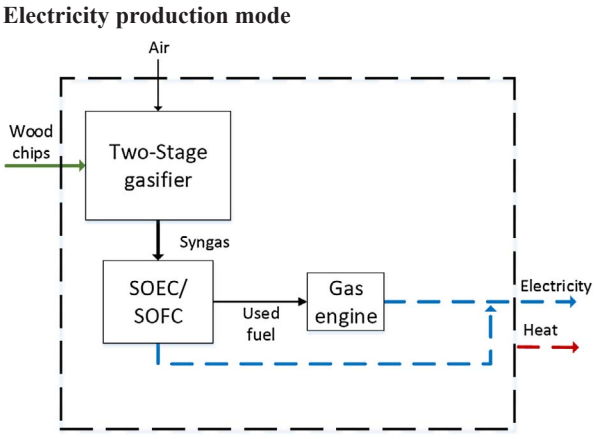

Fig. 2. Simplified diagram of polygeneration plant in electricity production mode.

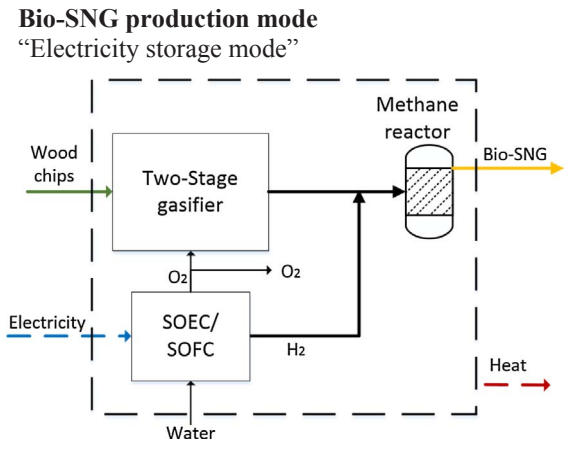

Fig. 3. Simplified diagram of polygeneration plant in electricity storage/bio-SNG mode.

software developed in the Thermal Energy Section of the Mechanical Engineering Department at DTU (an in-depth description is provided by Brian Elmegaard [17]). Mass and energy conservation is automatically included in DNA, providing the foundation for electricity and bio-SNG production energy analysis by the system. The techno-economic analysis was modeled in Python using process data from DNA, and the analysis was used to determine the total revenues required and net present value, given a range of bio-SNG and electricity prices. The marginal cost of operation for both production modes is calculated by fuel and other running costs, along with the electricity market spot price, which determines the yearly running time of the system (capacity factor). To determine the yearly running time, the current (2016) and predicted power price cumulative curves are used, along with district heat price scenarios over a range of possible bio-SNG prices.

2. Methods

2.1. Design of energy system

As shown in Fig. 2, the system uses wood chips in an air-blown gasifier, and the produced syngas is supplied to a reversible solid oxide cell operating as a fuel cell (SOFC) to produce electricity. The unconverted fuel from the SOFC is subsequently used in a gas engine to increase electricity production further. Moreover, a significant amount of heat is generated by the system, which is used to produce district heating. The system is thus fueled by wood chips, producing electricity as its primary product and district heat as its secondary product (in electricity mode).

The bio-SNG production mode, illustrated in Fig. 3, utilizes the same gasifier, but in this case, it is oxygen blown. Oxygen is produced along with hydrogen in the reversible SOC, operating as an electrolyser cell (SOEC). Hydrogen is mixed with syngas from the gasifier and converted into SNG in a methane reactor. Significant heat is also generated in this operation mode and used to produce district heat as in the electricity production mode. Therefore, the system is effectively fueled with wood chips and electricity, and its primary product is bio-SNG, while the secondary product (in bio-SNG mode) is district heat. The main components of the polygeneration system are described below, and the process design parameters are illustrated in Table 1.

2.1.1. Gasification block

In both the electricity production and bio-SNG production modes, the gasifier is preceded by a steam dryer that dries the wood chips to a very low moisture content. The evaporated steam is used as an input to the gasifier along with dried wood chips and either air or oxygen, depending on the operation mode. The function and operation of the specific gasifier used on this process is detailed in Refs. [18–21]. Thermochemical conversion is achieved in the two-stage downdraft gasifier, a maturing technology developed at DTU [18,19], which can be operated at a high cold gas efficiency. The produced syngas has a very low tar content [19], which is achieved by splitting pyrolysis, partial oxidation and gasification into three separated reactors. After the wood chips have been pyrolysed, the pyrolysis gas is partially oxidized at a temperature above 1100C, and then the partially oxidized gas is passed through a downdraft bed where the gasification reaction occurs. That bed consists of coke from the pyrolysis stage [18], resulting in less than 15 mg/N m^3 tar in the produced syngas [20]. The very low tar content also makes the required gas cleaning simple, only comprising a bag house filter for particle removal and a sulfur guard to remove traces of sulfur. It has been demonstrated that gas from the two-

Table 1
Process design parameters used in modeling.

Feedstock	Wood chips, where the dry and ash free composition (daf) is assumed to be (wt.%): LHV = 18.28 MJ/kg_{daf}. c_p = 1.35 kJ/(kg_{dry} * K). The biomass input is 100 MW[a] to the gasifier (LHV dry), moisture content = 45.0%. Ultimate analysis (daf): 49.6% C, 6.1% H, 44.1% O, 0.1% N, 0.06% S [24] Proximate analysis (db): 84.1% VM, 15.7% FC, 0.2% Ash [24]
Steam dryer	T_{exit} = 115 °C. $T_{superheat}$ = 200 °C. Dry biomass moisture content = 2 wt%. Pressure loss = 0.03 bar
Gasifier air blown[b]	P = 1.0 bar. Carbon conversion = 99% [19] (partial oxidation temperature > 1100 °C [18]). Heat loss = 3% of wood chips thermal input (LHV dry). T_{exit} = 730 °C [19]. The gas (excl. CH_4) is assumed to be in chemical equilibrium at 750 °C. $CH_4/(CO + CO_2 + CH_4)$ = 2.55%. Pyrolysis is modeled by assuming a c_p = 1.85 kJ/ (kg * K) for completely dry and ash free biomass. c_p of ash = 1 kJ/(kg * K). Pressure loss = 0.03 bar. Steam to wood chip (dry) input mass flow ratio is 0.82 at 630 °C
Gasifier O_2 blown[c]	P = 1.0 bar. Carbon conversion = 99%. Heat loss = 3% of wood chips thermal input (LHV dry). T_{exit} = 730 °C. The gas (excl. CH_4) is assumed to be in chemical equilibrium at 750 °C. $CH_4/(CO + CO_2 + CH_4)$ = 2.13%. Pyrolysis is modeled by assuming a c_p = 1.85 kJ/ (kg * K) for completely dry and ash free biomass [25]. c_p of ash = 1 kJ/(kg * K). Pressure loss = 0.03 bar. O_2 is blown in with steam (15 mol% O_2 and 85 mol% H_2O) in a 1.07 mass flow ratio to wood chips (dry) at 700 °C
SOEC[c]	Operates at ambient pressure. Exit temperature = 800 °C [26]. Losses = 5% of input electricity. 10% H_2 in feed steam. 10% steam in outlet H_2. Current density is set at 1 A/cm^2. These data result in inlet temperature = 710 °C, total energy efficiency from electricity to hydrogen of 91% and cell area of 4912 m^2.
SOFC[b]	Operates at ambient pressure. The cell area is set by the SOEC operation at 4912 m^2. Inlet temperature = 650 °C. Exit temperature = 850 °C. Current density is set to 0.5 A/cm^2. These data result in fuel utilization of 70%. Electric efficiency based on converted fuel = 56%
Compressor[c]	$\eta_{isentropic}$ = 90%, $\eta_{mechanical}$ = 98%. $\eta_{electrical}$ = 98%, compressed to 7 bar
SNG synthesis[c]	Boiling water reactor followed by adiabatic reactor. Chemical equilibrium at reactor outlet temperature and pressure. Reactor outlet temperature of boiling water reactor: 300 °C [15]. Reactor pressure: 7 bar
Gas engine[b]	The cooled used fuel (20 °C) at ambient pressure from the SOFC is mixed with air and turbocharged to 2 bar before combustion. Electrical efficiency is 38%. Flue gas composition is calculated based on flow and composition of oxidant and fuel. λ = 2
Heat production	All surplus heat in both operation modes is used to produce district heat with a forward temperature of 80 °C and return temperature of 40 °C

[a] The two-stage gasifier is being upscaled to 100 MW, and this paper is part of research to demonstrate its relevance.
[b] Only refers to electricity mode.
[c] Only refers to bio-SNG mode (electricity storage).

Table 2
Components for which investment is calculated using capacity factored methods.

Unit	Reference cost C_{ref} [M€]	Reference capacity CAP_{ref}	Scale exp.	Installation factor, I_f	Lifetime	Reference
Pre-processing[b]	0.054	33.5 tonnes/hour	0.75	2.0	20	[28]
Drying	0.017	10 m^3/hour	0.74	1.5	20	[29]
Two-stage gasifier	2.50	1.0 MW input	0.6[a]	1.355[a]	20	[30]
SOEC/SOFC	0.59	5.0 MWel input	0.90	1.355[a]	20	[30]
Gas engine	0.950	5.0 MWel output	0.70	1.355[a]	20	[30]
Methane reactor	0.0230	859.0 Nm^3/h gas output	0.60	2.0	20	[31]
HEX	9.45	138.1 MWth exchanged	0.60	2.0	20	[28]
Gas cooling	35.8	74.1 m^3/s syngas	1.0	1.86	20	[28]
Gas filter[c]	1.90	12.1 m^3/s syngas	0.65	2.0	20	[28]

[a] Estimated value (not in reference).
[b] Storage and feeding systems.
[c] Gas cleaning with metal oxides is accounted for.

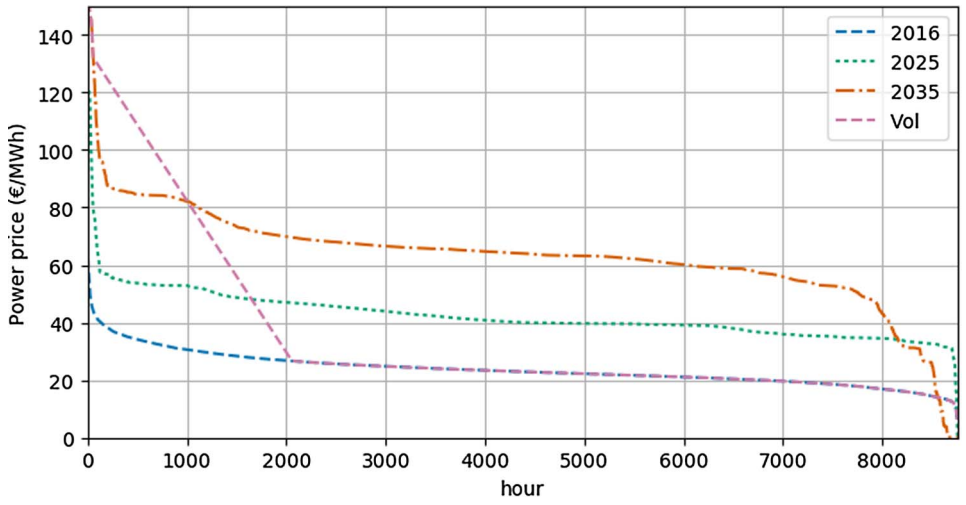

Fig. 4. Cumulative curves for current and predicted power prices.

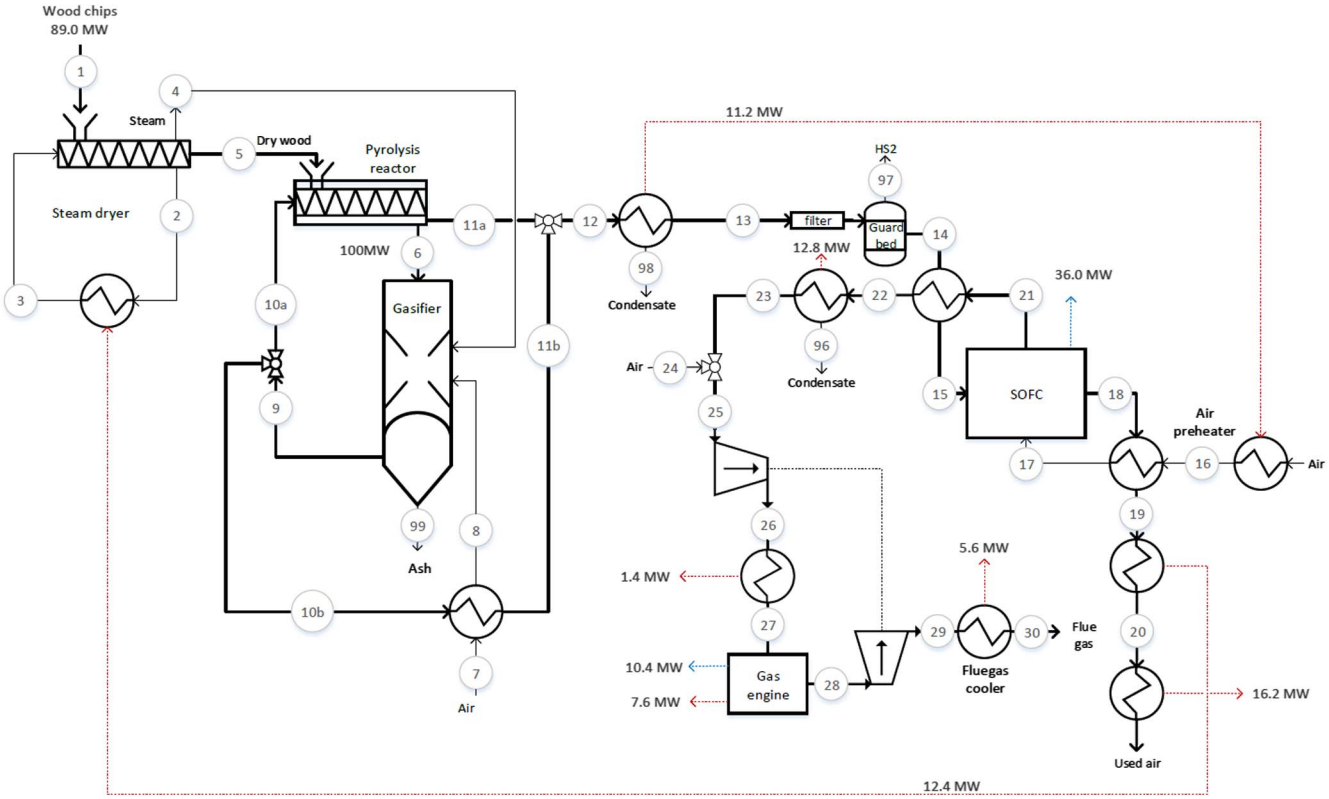

Fig. 5. Flow sheet of polygeneration plant in electricity storage mode. Note: red lines denote heat flows and blue lines denote electricity production. (For interpretation of the references to colour in this figure legend, the reader is referred to the web version of this article.)

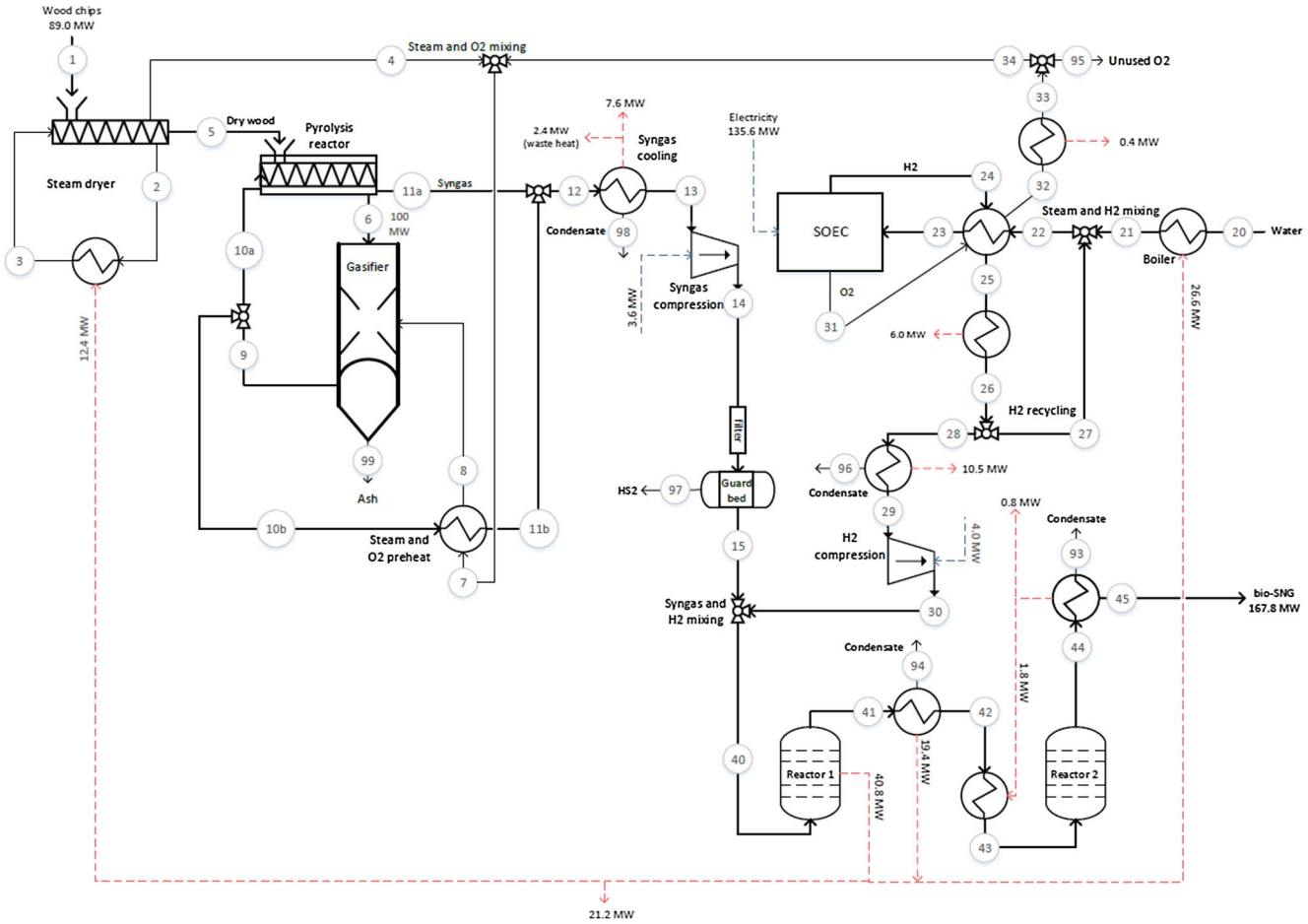

Fig. 6. Flow sheet of polygeneration plant in electricity storage mode. Note: red lines denote heat flows and blue lines denote electricity consumption. (For interpretation of the references to colour in this figure legend, the reader is referred to the web version of this article.)

stage gasifier can be efficiently converted in an SOFC [21].

When the gasifier is air blown, the hot syngas is used to preheat the air input. When the gasifier is oxygen blown, oxygen is mixed with steam from the steam dryer and this mixture is fed to the gasifier. The syngas gas composition and energy content were calculated by DNA, assuming chemical equilibrium at 750 °C. The methane content was adjusted according to the measurements.

2.1.2. Reversible SOC

SOCs are inherently reversible, and reversible SOC operation has been demonstrated at scales of up to 120 kWe input/50 kWe output [22]. When the SOC is operated as an SOFC, gas from the gasifier is sent to the SOFC in which most combustible gases are converted to CO_2 and H_2O through the generation of electricity and heat. The unconverted gas is then combusted in a gas engine, which increases the total heat and power production.

In the bio-SNG mode, the SOC is operated as an SOEC, and generates oxygen for the gasifier and hydrogen for the methanation. The operation mode defines the SOC unit size. The current density is set to $-1.0\ A/cm^2$ when it is operated as an SOEC, and $+0.5\ A/cm^2$ when it is operated as an SOFC.

The SOC is set to operate at an ambient pressure because this matches the gasifier pressure and gas engine. It could also operate at the methanation reactor pressure (7 bar) to avoid the energy consumption and cost of a hydrogen compressor. Pressurized SOEC operation of up to 25 bar has been demonstrated at the stack level in a laboratory [23]. It is considered infeasible to change the SOC operating pressure when changing the operating mode (from SOFC to SOEC).

2.1.3. Gas engine

The gas engine uses unconverted fuel from the SOFC and combusts it with air to increase electricity production, with the additional benefit of improved heat production, as the waste heat is used to provide district heating. The turbocharged gas engine is modeled in DNA as a simple gas engine, where the chamber gas is burned under perfect combustion and the electric and “cooling” efficiencies are predefined along with pressure and heat loss. The air input is defined by the air-to-fuel ratio, which is also set. The heat loss was assumed to be 5% of the inlet LHV flow, and the pressure drop, 2%.

2.1.4. Synthesis reactor block

Syngas and hydrogen are synthesized in a cooled methane reactor at a 7 bar pressure. The released heat is used for biomass steam drying and for raising steam to SOEC. The methane reactor gas is then cooled, and water is condensed out at an ambient temperature before being sent to an adiabatic methane reactor to increase the methane content. Water is completely removed from bio-SNG before it is sent to the grid.

2.2. Techno-economic analysis

The economic analysis of the polygeneration system was based on determining the total revenue requirement (TRR) for every unit of electricity and bio-SNG produced, and the net present value (NPV) of the investment. The cost of each system component was estimated using data found in the literature and adjusted to represent the capacity of the system components with the desired biomass input [27].

Table 3
Mass flow, temperature, and pressure for all state points in Fig. 5.

Node	M (kg/s)	T (°C)	P (bar)
1	9.95	15	–
2	73.6	115	1.018
3	73.6	200	1.018
4	4.42	115	1.018
5	5.53	115	–
6	5.47	115	–
7	6.23	15	1.018
8	6.23	700	1.018
9	16.10	730	1.013
10a	11.97	730	1.013
10b	4.13	730	1.013
11a	11.97	244	1.013
11b	4.13	80	1.013
12	16.10	203	1.013
13	13.37	25	1.013
14	13.37	25	1.013
15	13.37	650	1.013
16	107.36	118	1.013
17	107.36	650	1.013
18	103.29	850	1.013
19	103.29	320	1.013
20	103.29	204	1.013
21	17.44	850	1.013
22	17.44	333	1.013
23	14.78	50	1.013
24	9.10	15	1.013
25	23.88	38	1.013
26	23.88	105	2
27	23.88	20	2
28	23.88	400	2
29	23.88	336	1.13
30	23.88	125	1.13
96	2.66	50	1.013
97	0.00	25	1.013
98	2.73	25	1.013
99	0.08	730	–

$$C_{inv} = C_{ref} \cdot \left(\frac{CAP_{inv}}{CAP_{ref}} \right)^{exp} \cdot I_F \quad (1)$$

In the above, C, CAP, exp, and I_F represent the capital cost, capacity, scale exponent, and an installation factor, respectively, while the $_{inv}$ and $_{ref}$ subscripts refer to the component invested in and the reference component. Table 2 displays the capital cost of each component, together with the reference capacity, scale exponent, installation factor, and its lifetime.

It is assumed that the discount rate is 7%, income tax is 23.5% of revenues, and insurance and other tax are estimated to be 2% of the capital cost annuity. The yearly operation and maintenance costs are assumed to be 3% of the capital cost [28] of all components, except for the gasifier and SOFC/SOEC unit, while the biomass fuel cost is assumed to be 7.1 €/GJ as wood chips [32]. The fixed O&M cost of the gasifier is assumed to be 57,000 €/MW/year, while the variable O&M cost is 17 €/MWh syngas produced [30]. The O&M cost of the SOFC/SOEC unit is assumed to be 15,000 €/MW electricity input [30]. The O&M cost of the gasifier and SOFC/SOEC are subject to economies of scale, as is the case for their investment cost, using Eq. (1).

The TRR to achieve a positive NPV based on the specified 20-year lifetime of the system at a 7% rate of return was determined by calculating the sum of the present value of the 20 annual values and then

Table 5
Mass flow, temperature, and pressure for all state points in Fig. 6.

Node	M (kg/s)	T (°C)	P (bar)
1	9.95	15	–
2	72.94	115	1.043
3	72.94	200	1.043
4	4.36	115	1.013
5	5.58	115	–
6	5.47	115	–
7	5.87	102	1.013
8	5.87	700	1.008
9	11.26	730	1.008
10a	5.69	730	1.008
10b	5.57	730	1.008
11a	5.69	253	1.008
11b	5.57	150	1.008
12	11.26	203	1.008
13	8.61	30	1.008
14	8.61	254	7
15	8.61	254	7
20	10.19	15	1.013
21	10.19	100	1.013
22	10.45	95	1.013
23	10.45	709	1.013
24	2.30	800	1.013
25	2.30	369	1.013
26	2.30	50	1.013
27	0.26	50	1.013
28	2.05	50	1.013
29	1.43	30	1.013
30	1.43	276	7
31	8.15	800	1.013
32	8.15	105	1.013
33	8.15	50	1.013
34	1.39	50	1.013
40	10.04	265	7
41	10.04	300	7
42	3.75	40	7
43	3.75	220	7
44	4.75	283	7
45	3.56	50	7
93	0.19	50	7
94	6.29	99	7
95	6.75	50	1.013
96	0.62	30	1.013
97	0.00	254	7
98	2.65	30	1.008
99	0.08	730	–

Table 4
Gas compositions in electricity production mode.

Mole frac.	Gasifier outlet	Gas input SOFC	Gas outlet SOFC	Air outlet SOFC	Engine flue gas
Node number	9	15	21	18	27
H_2	0.296	0.366	0.089		0.056
O_2				0.179	0.106
N_2	0.210	0.259	0.255	0.800	0.555
CO	0.138	0.170	0.078		0.049
CO_2	0.131	0.162	0.258		0.164
H_2O	0.215	0.031	0.320	0.122	0.065
CH_4	0.007	0.009			
Ar	0.003	0.003		0.010	0.005
Mean mole mass	20.20	20.71	26.64	28.74	29.00
LHV (MJ/kg)	5.76	6.93	1.63	–	0.95

Table 6
Gas compositions in bio-SNG production mode in mole fractions.

	Syngas gasifier outlet	Syngas before mixing	Hydrogen from SOEC	Mixed syngas and hydrogen	Bio-SNG after first reactor	Bio-SNG after second reactor	Bio-SNG after drying
Node number	9	15	24	40	42	44	45
H_2	0.382	0.499	0.900	0.740	0.059	0.011	0.011
O_2							
N_2		0.001			0.001	0.001	0.001
CO	0.179	0.234		0.111			
CO_2	0.164	0.214		0.102	0.015	0.027	0.027
H_2O	0.267	0.042	0.100	0.043	0.220	0.017	
CH_4	0.007	0.010		0.005	0.704	0.967	0.985
Mean mole mass	17.95	17.92	3.62	9.93	16.07	16.02	16.00
LHV (MJ/kg)	8.31	10.86	60.02	21.57	36.05	48.61	49.60

Table 7
System production efficiencies and energy ratios in both electricity and bio-SNG operation modes. LHV on a dry basis is used.

Electricity mode	
Electrical efficiency [MW electricity/MW biomass]	46%
District heat efficiency [MW heat/MW biomass]	44%
Total efficiency [(MW electricity + MW heat)/MW input]	90%
Bio-SNG mode	
Bio-SNG efficiency [MW bio-SNG/MW input]	69%
District heat efficiency [MW heat/MW input]	16%
Total efficiency [(MW bio-SNG + MW heat)/MW input]	85%
Electricity input fraction [MW electricity/MW input]	59%
Biomass input fraction [MW biomass/MW input]	41%

using the capital recovery factor (CRF) to transform this value into an equivalent annuity, as in Bejan et al. [27].

$$P_n = F_n \cdot \frac{1}{(1 + i_{eff})^n} \quad (2)$$

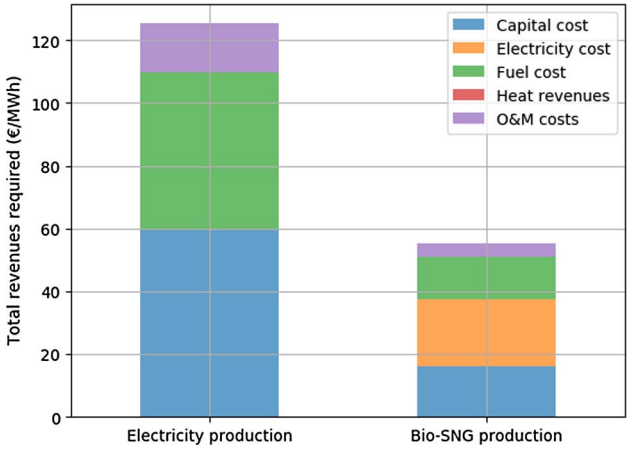

Fig. 8. TRR (€) per MWh of product for both electricity and bio-SNG operation modes when assuming constant operation and electricity cost of 25 €/MWh (bio-SNG production). Note that, in this figure, heat is not seen as a product.

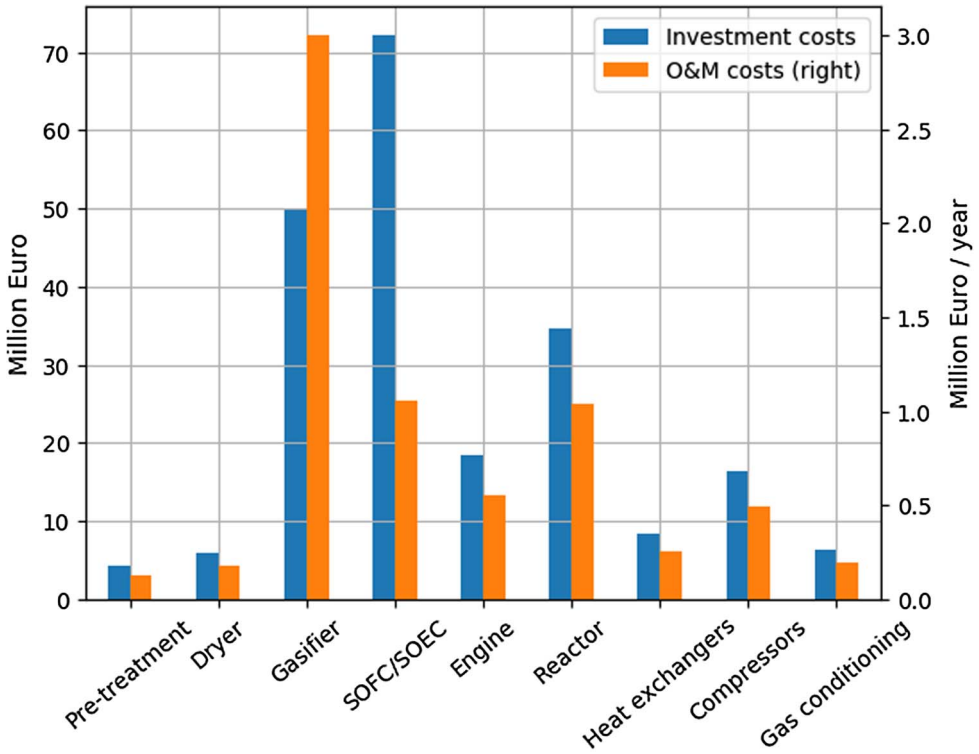

Fig. 7. Investment and O&M costs of system components for both electricity and bio-SNG modes (100 MW biomass input). The total investment cost is 216 M€ and the total yearly O&M cost is 6.9 M€.

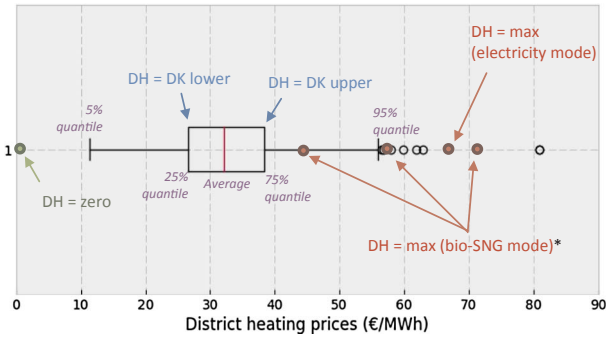

Fig. 9. Price of district heating produced by polygeneration system based on energy content allocation between produced products and true district heating production cost in Denmark by statistical distribution [35]. *Price is determined based on average electricity price in 2016, 2025, and 2035, i.e., 23.6 €/MWh, 42.5 €/MWh, and 63.0 €/MWh.

$$CRF = \frac{A}{P} = \frac{i_{eff} \cdot (1 + i_{eff})^n}{(1 + i_{eff})^n - 1} \quad (3)$$

$$NPV = \sum P_n; \quad n = 1\text{–}20 \quad (4)$$

Here, F, P, and A are the future value, present value, and annuity, respectively, and i_{eff} and n are the rate of return and years (1–20).

2.3. Marginal cost and operation mode at provided electricity and bio-SNG prices

The marginal cost is calculated to represent the cut-off price for operation; that is, below this price the plant is shut down, for both the electricity and bio-SNG production modes. The marginal operation cost is based on the short-run marginal cost definition: "the change in short run total cost for an extremely small change in output" [33], which is given as the price of fuel and variable O&M at a given time. The fuel price is represented by the fuel cost, which consists of (1) the biomass fuel cost and (2) the electricity input cost when operating in bio-SNG (electricity storage) mode.

However, the marginal operation cost is also allocated to the district heat coproduct. The allocation method is energy based and district heat is always sold at production cost, as required in Denmark [34]. The cost allocation to the district heat product applies to both the operation modes because both produce district heat, but the ratio between the main output (electricity or bio-SNG) to coproduct district heat differs. In order to be conservative, the impact of district heat sales is determined by scenario analysis in which the cost allocation scenario represents the maximum cost allocation to the heat product. The other three heat scenarios include one with no heat sales and two with moderate heat revenues based on the district heating price in all major municipalities in Denmark [35]. The official data are presented in prices to the consumer with VAT. In order to account for this, 25% VAT is excluded, 30% of the consumer price is assumed to be due to distribution, and an average of 10% heat losses on the network is assumed. Furthermore, it is assumed that the yearly district heat capacity factor is 75%. The cash flow for both the electricity (CF_e) and bio-SNG (CF_s) production modes can be described by the following equation.

$$Cf_e = el_o \times el_{price} + dh_o \times dh_{price} - bio_i \times bio_{price} \quad (5)$$

$$CF_s = sng_o \times sng_{price} + dh_o \times dh_{price} - bio_i \times bio_{price} - el_i \times el_{price} \quad (6)$$

In the above equations, the subscripts o and i represent the system output and input, respectively, while *bio*, *el*, *dh*, and *sng* represent the biomass, electricity, district heat, and bio-SNG, respectively. By including the marginal operation cost, electricity market price, and bio-SNG price, the optimal operation mode can be determined, namely shut-down, electricity production, or bio-SNG production mode. Three reference years were used to describe the electricity system

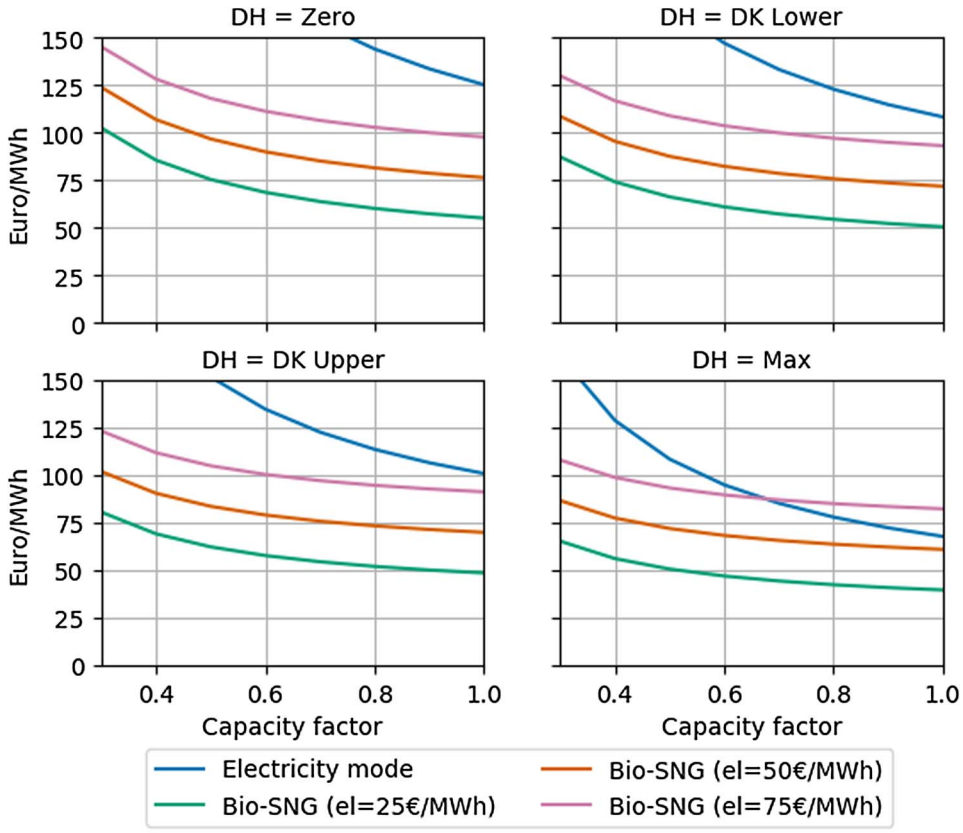

Fig. 10. TRR by system for both electricity and bio-SNG production modes as a function of capacity factor. District heat pricing scenarios are defined in Fig. 9.

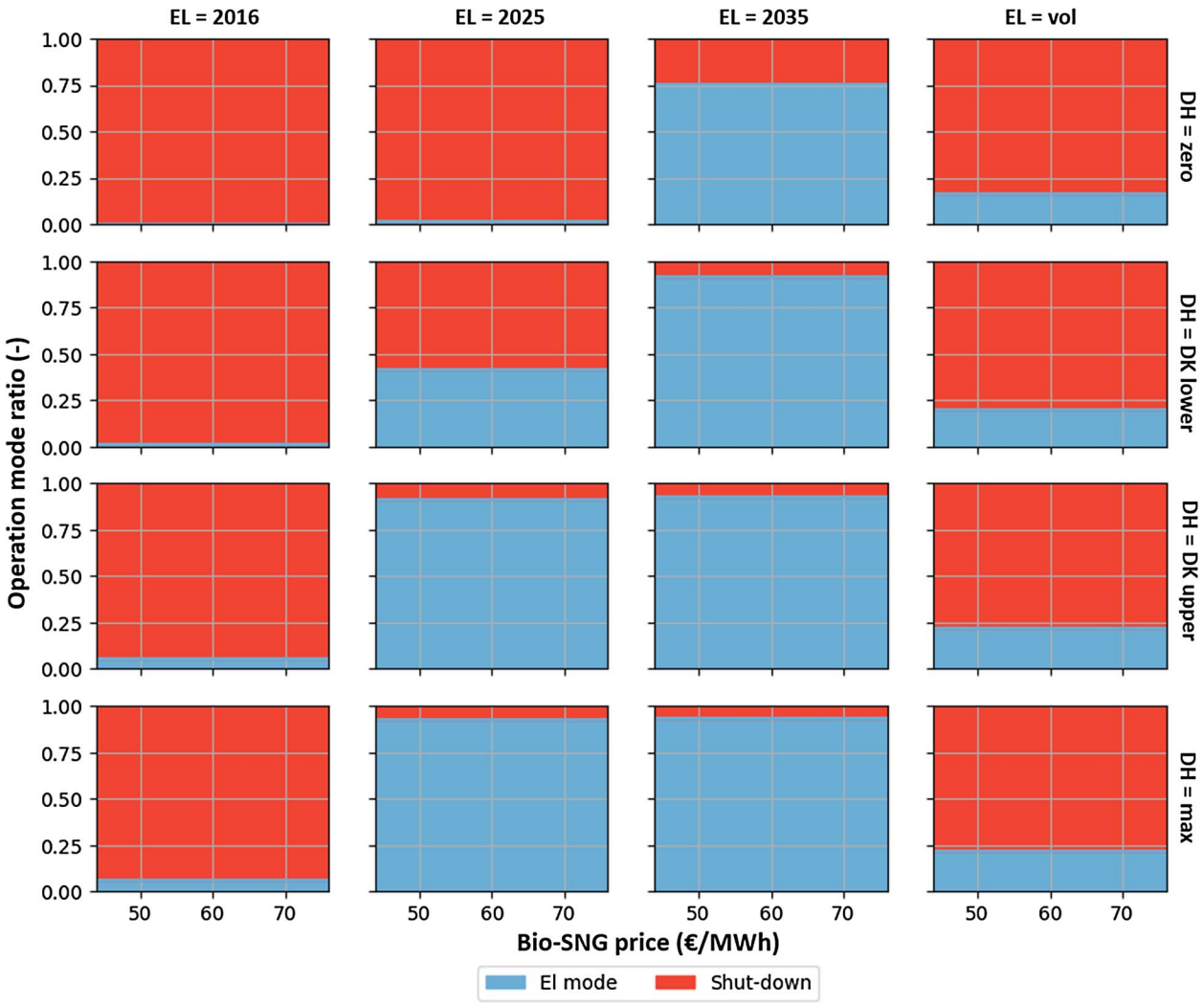

Fig. 11. Annual operation of electricity production system in electricity and shut-down modes. Power price scenarios are defined in Fig. 4 and district heat pricing scenarios are defined in Fig. 9. Note that the capacity factor is shown as a function of the bio-SNG price for ease of comparison with the following figures.

development in Denmark. Fig. 4 displays the current (2016) and projected (2025 and 2035) power price (€/MWh) cumulative curves in the Nordpool electricity market, based on analysis work by the Danish transmission system operator (TSO) Energinet.dk [36] using the energy system model SIFRE [37], as reported by Lythcke-Jørgensen et al. [38]. An alternative scenario is provided ("vol"), representing the increased volatility of power prices over the years. This scenario is constructed based on the 2016 curve, but has 2000 h of higher prices.

As shown in the figure, the price per MWh of electricity is expected to increase significantly in the next 10–20 years; however, the cumulative curve shape is expected to change less. The mean power price changes from 23.8 €/MWh in 2016 to 42.5 €/MWh in 2025 and 63 €/MWh in 2035 (43.5 €/MWh in vol). The standard deviation of the power price also changes, from 5.8 €/MWh in 2016 to 8.5 €/MWh in 2025 and 17.2 €/MWh in 2035 (37.0 €/MWh in vol).

3. Results

The results of the thermodynamic modeling of the two operation modes are presented below. First, the energy system simulation results are presented, followed by the techno-economic analysis. Then, the marginal cost and mode of operation are presented for the given electricity and bio-SNG prices, along with the operation time in each mode. Finally, the capacity factor and NPV of the polygeneration system are provided, based on scenario analysis and in reference to a single operation mode.

3.1. Energy system simulation

Fig. 5 illustrates the flow sheet of the electricity production mode, while Fig. 6 depicts the same for the bio-SNG production mode. The flow sheets are accompanied by Table 3 and Table 5, which provide the mass flow, temperature, and pressure at the main production states with reference to Figs. 5 and 6, respectively. Table 4 and Table 6 display the gas compositions for selected mass flows.

From the results, it can be observed that the electrical efficiency is ~46%, while the district heat production efficiency is ~44%, resulting in an overall efficiency of 90% on a dry biomass basis. This can be compared with electricity production from biomass gasification cogeneration. In a review article by Ahrenfeldt et al. [21] regarding state-of-the-art and future perspectives, the overall efficiencies ranged from 80 to 97%, with electrical efficiency ranging from 6 to 50%. Part of the reason for the high efficiency of the system is the utilization of unconverted fuel from the SOFC by the gas engine, which increases the electrical efficiency from 36 to 46%. Gas with a similar chemical composition to that of the unconverted fuel was tested in a gas engine

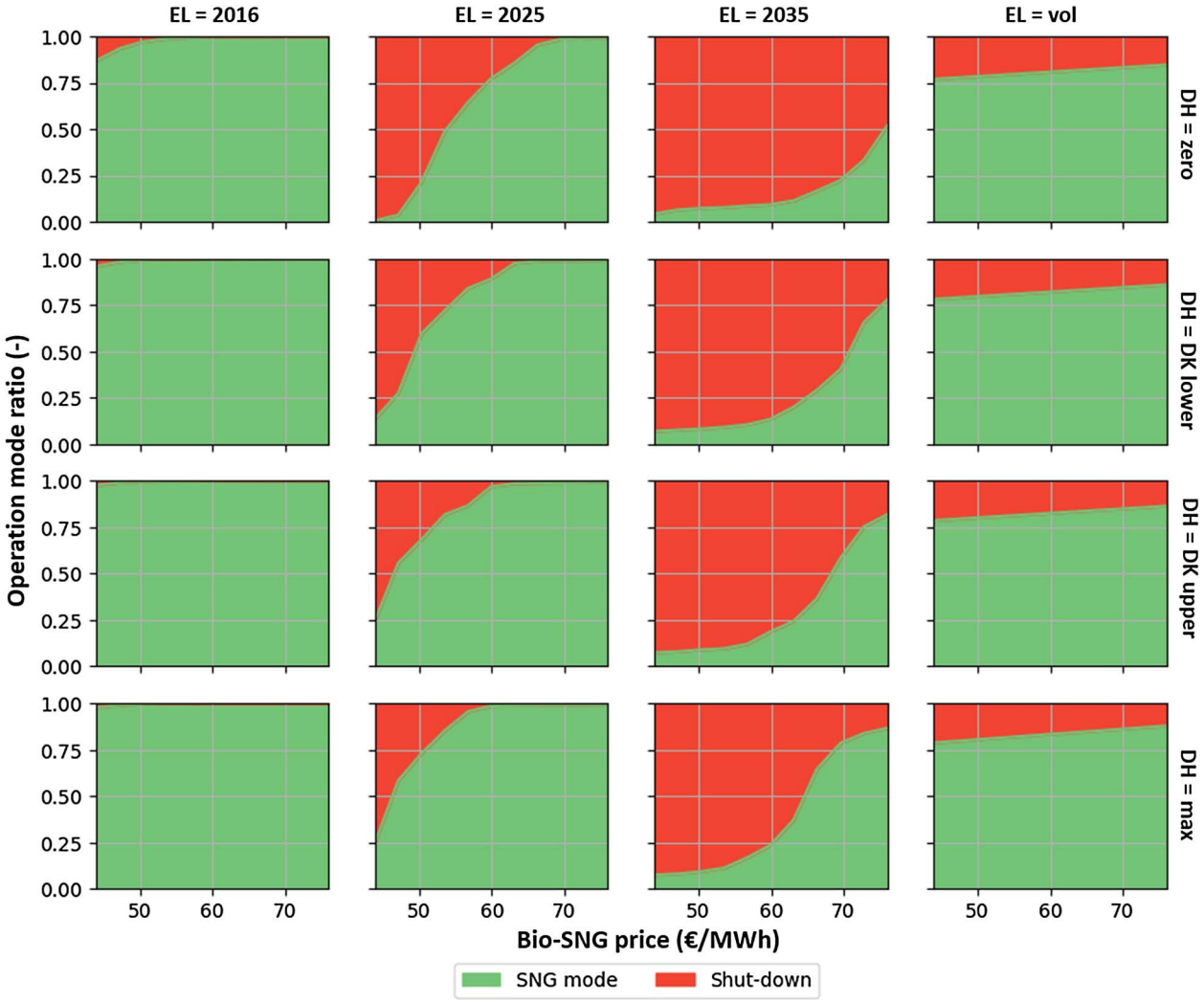

Fig. 12. Annual operation of bio-SNG production system in bio-SNG and shut-down modes for low (44 €/MWh) to high (76 €/MWh) bio-SNG prices. Power price scenarios are defined in Fig. 4 and district heat pricing scenarios are defined in Fig. 9.

for proof of concept, and the engine was run successfully.

The electricity storage mode results indicate that the conversion efficiency from biomass and electricity to bio-SNG is 69%, while the heat production efficiency is 16%, resulting in an overall efficiency of 85%. Furthermore, it can be seen that bio-SNG methane content is 98.5%, which is more than required to supply it to the grid. Table 7 provides a summary of the production efficiencies in both the operation modes.

3.2. Techno-economic analysis

Fig. 7 displays the investment and O&M costs in M€ for every component of the polygeneration system. The cost is calculated by Eq. (1), using data from Table 2 and the provided O&M costs, based on a 100 MW biomass input capacity.

It can be seen in the figure that the highest investment cost is for the reversible SOC (SOFC/SOEC), followed by the gasifier and methane reactor, while the highest component O&M cost is for the gasifier, followed by the SOC and reactor. As seen in Table 2, the reference investment cost is higher for the gasifier than for the SOC unit, but the capacity is lower, as shown in Fig. 6. Furthermore, the economies of scale exponent are assumed to be higher for SOC, because current designs are based on relatively small stacks; therefore, SOC relies on the economy of numbers rather than economy of scale.

Fig. 8 illustrates TRR in €/MWh when operating the system in the electricity and bio-SNG modes, levelized to the main output of each mode, namely electricity and bio-SNG. The figure also illustrates the contribution of each cost category to the product cost. The levelized capital and O&M costs were determined using data from Fig. 7 and Eqs. (2) and (3).

It can be seen in the figure that the required income per unit of energy produced is considerably higher for the electricity mode than the bio-SNG mode. This is because the bio-SNG output (168 MW) is significantly higher than that of electricity (46 MW) in the respective modes. These results do not include the secondary heat product produced in both the modes of operation. Table 7 provides the district heat production efficiencies for both operation modes.

Fig. 9 provides a comparison of the price of district heat production using the polygeneration plant and that in all major municipalities in Denmark [35]. As noted in Section 2.3, cost allocation for the primary and secondary products is based on energy contents. Consequently, 49% of the capital, O&M, and fuel costs are allocated to the district heat production in electricity mode, and 19% in bio-SNG mode. The price of district heat production from the system, calculated by energy content allocation, is represented by DH = max in the figure below.

The figure indicates that the price of district heating produced by the polygeneration plant is high compared to district heating prices in Denmark, and the district heating price would be among the highest in Denmark. It was therefore decided to include four pricing scenarios for the district heat product by using the lower and upper quantile of

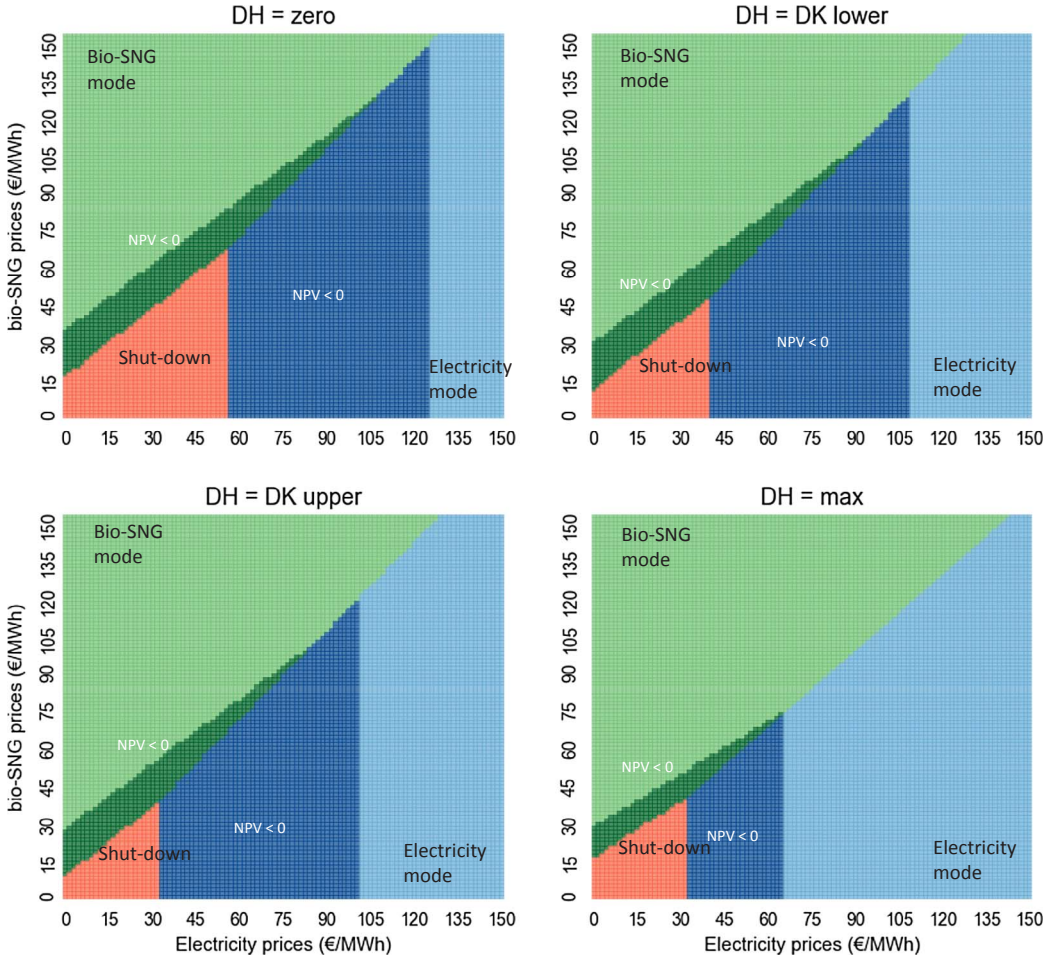

Fig. 13. Graphical display of operation modes at a range of electricity and bio-SNG prices for the four district heat pricing scenarios defined in Fig. 9.

district heating prices in Denmark, as shown in the figure. The remainder of the analysis considers heat price scenarios and includes the following cases: (1) no heat sales (DH = zero), (2) moderately low heat price for lower quantile 26.6 €/MWh (DH = DK lower), moderately high heat price for upper quantile 38.4 €/MWh (DH = DK upper), and (3) high heat price using cost allocation based on energy output (65 €/MWh for electricity mode and 87 €/MWh for bio-SNG mode).

Fig. 10 illustrates TRR in €/MWh as a function of the primary production capacity factor, where the revenues from district heating sales using the pricing scenarios introduced above are included. The bio-SNG mode results are provided for three electricity prices in order to highlight the importance of this parameter. Through comparison with the electricity price scenarios in Fig. 4, it can be seen that the assumed electricity prices are relevant. It should be noted that TRR shown in Fig. 8 (such as 125 €/MWh for electricity production) can be seen in Fig. 10 at a capacity factor of 1 and DH = zero.

It can be seen from the figures that there is a significant decrease in TRR when including the district heating sales and an increased capacity factor. To put TRR into perspective, it is worth noting that, according to the Danish Promotion of Renewable Energy Act §44 par. 2 VE-Lov, the premium feed-in tariff for electricity produced from biomass by gasification is ~ 110 €/MWh, and support for biogas sold for transportation purposes is 36 €/MWh, according to § 43b par. 2–3 VE-Lov. However, according to a report on energy system integration and economy, the future price of bio-SNG is assumed to be between 44 and 76 €/MWh (12.2–21.1 €/GJ) [31], where the lower value is based on the future natural gas price, including saving CO_2, and the upper value is based on the future upgraded biogas price.

3.2.1. Marginal cost and operation mode at provided electricity and bio-SNG prices

Fig. 11 shows the system capacity factor of the system if the electricity mode is the only possible operation mode. This is determined by using the marginal cost of producing electricity and the predicted power price cumulative curves depicted in Fig. 4.

It can be seen that the capacity factor, determined by the marginal operation cost, differs significantly depending on both the district heat pricing and predicted power price scenarios. As an example, in 2016, the capacity factor ranges from 0.7 to 5.7%, in 2025 it ranges from 1.4 to 92.9%, and in 2035 it ranges from 75.4 to 93.2% (and 16.6–21.9% for vol), depending on the district heat pricing scenario.

Fig. 12 illustrates the system capacity factor if the bio-SNG mode is the only possible operation mode. This is determined by using the marginal cost of producing bio-SNG and the predicted power price scenarios from Fig. 4, along with the predicted bio-SNG price of 44 €/MWh (low bio-SNG) to 76 €/MWh (high bio-SNG).

Similar to the capacity factors shown for the electricity mode in Fig. 11, the capacity factor using only the bio-SNG mode varies for different district heat pricing and power price scenarios. However, here it can be seen that the predicted bio-SNG price contributes significantly as well. As an example, the capacity factor in 2035 ranges from 4.2 to 7.4% depending on the district heat pricing scenario at a low bio-SNG price, but from 51.9 to 86.6% at a high bio-SNG price.

Fig. 13 displays the operation mode of the polygeneration system depending on electricity and bio-SNG prices. The modes are 1) shut down (when the fuel and variable O&M costs are greater than the revenues of product sales), 2) bio-SNG mode, and 3) electricity production mode. When operating in bio-SNG mode, the electricity prices

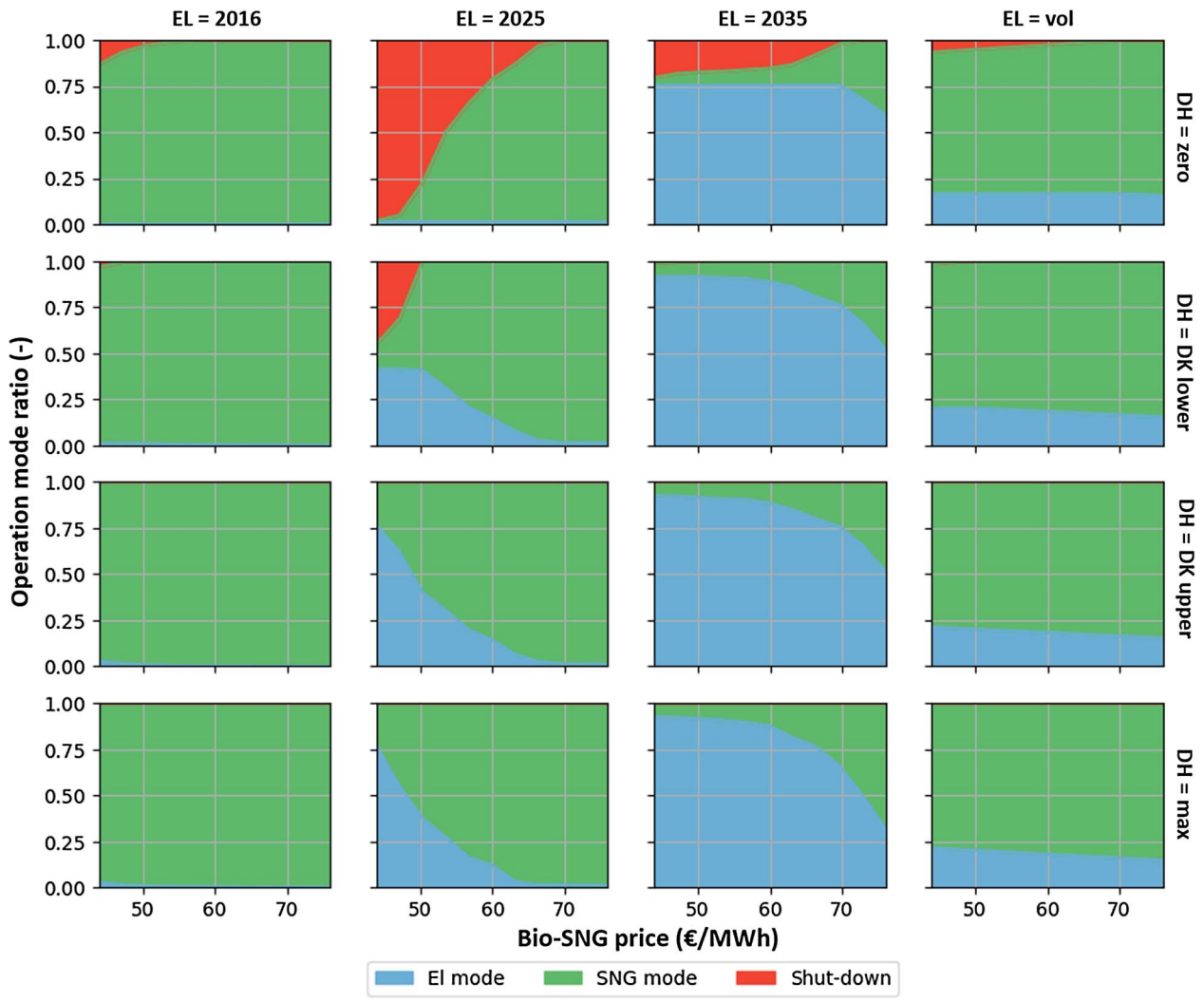

Fig. 14. Annual operation of polygeneration system in electricity, bio-SNG, and shut-down modes for low (44 €/MWh) to high (76 €/MWh) bio-SNG prices. Power price scenarios are defined in Fig. 4 and district heat pricing scenarios are defined in Fig. 9.

are low compared to the bio-SNG prices. When the electricity prices are high, it is more economical to operate in electricity production mode. The figures also display the areas of positive and negative NPV for each operation mode. On the line separating each operation mode, the NPV is the same for each mode.

If the system could only produce electricity or bio-SNG and not both, depending on the electricity and bio-SNG market prices, the figure above would appear different. If the system could only produce electricity, the bio-SNG area would be removed and the shut-down area would be larger. It would not be possible to operate the system at low electricity prices. If the system could only operate in bio-SNG mode, the blue area would be removed and the shut-down area would be larger. It would then not be possible to operate the system at high electricity prices. However, constructing this system to be flexible and able to change between different operation modes based on the marginal cost and revenues will increase its capacity factor. The degree to which it will increase depends on the electricity and bio-SNG market prices and the revenues from district heat sales.

Fig. 14 illustrates how the polygeneration system would operate given the current and predicted electricity and bio-SNG prices. The results are shown for the same bio-SNG price ranges as those used in Figs. 11 and 12.

It can be seen from the figure that the time spent in each operating mode differs significantly depending on the assumed power and SNG prices. In the current energy system (2016), the power prices are low, resulting in full bio-SNG mode operation, regardless of the bio-SNG price. The power prices are expected to increase in 2035, and this changes the plant operation. If low bio-SNG prices are assumed together with a low district heating price (DH = DK lower), the plant will operate 92% of the time in electricity mode, 7% in bio-SNG mode, and will be in shut down for the remaining 1.5%. However, if high bio-SNG prices are assumed instead, the plant will operate 52% of the time in electricity mode and 48% in bio-SNG mode. It is worth noting that the system will never shut down if high bio-SNG prices are assumed and at least moderate district heating revenues are achieved.

In Fig. 15, the capacity factors for the polygeneration system from Fig. 14 are compared with those for the electricity production system from Fig. 11 and the bio-SNG production system from Fig. 12. The figure quantifies the polygeneration effect with respect to the capacity factor.

As this comparison shows, the capacity factor may increase considerably for the system, but the extent of this increase depends on the pricing scenarios. At low electricity prices (2016), the capacity factor of the polygeneration system will be the same as that of the bio-SNG only system, while the electricity-only system will have a very low capacity factor. At high electricity prices (2035), an opposite trend is observed, namely the capacity factor of the bio-SNG-only system is lower than that of the electricity-only system. However, the capacity factor of the polygeneration system is now higher than that of the electricity-only system, which demonstrates the advantage of polygeneration. This

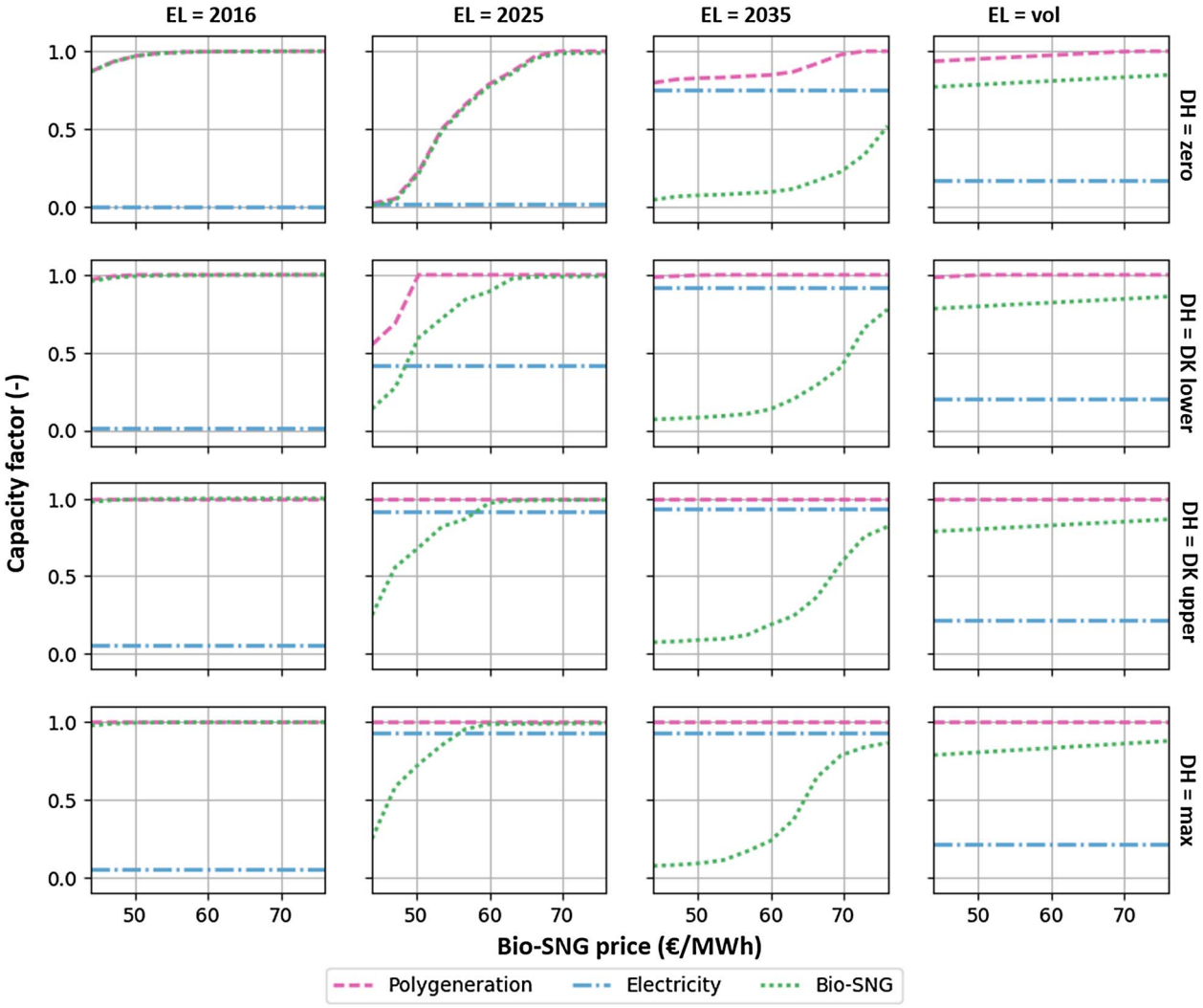

Fig. 15. Capacity factor for the system if running only for bio-SNG or electricity production, compared to combined production of the polygeneration system. Power price scenarios are defined in Fig. 4 and district heat pricing scenarios are defined in Fig. 9.

advantage becomes clearer if volatile electricity prices are assumed. A good example is the situation at a moderate district heat price (DH = DK lower) and a bio-SNG price of 70€/MWh: the capacity factor is 100% for the polygeneration system but 50% for the electricity production system and 92% for the bio-SNG production system. A high capacity factor will improve the system economics, as revenue streams can be continued all year. Furthermore, constant, year-round, full-load operation of the biomass gasifier could prove to be important—also from a risk perspective—as gasifier load changes may be challenging.

Fig. 16 is similar to Fig. 15, but the effect of polygeneration is quantified in terms of NPV instead of capacity factor. When comparing the figures, similar trends can be identified, particularly at low power prices (2016), where the NPV is identical for the polygeneration and bio-SNG-only systems. It should be noted that the investment cost remains constant for all three systems, although, for example, the gas engine could have been removed from the bio-SNG-only system. For all low bio-SNG pricing scenarios, the systems show negative NPVs, but at high bio-SNG prices, the polygeneration and bio-SNG-only systems exhibit a positive NPV, except when operating at high electricity prices (2035). Furthermore, it can be seen that the advantage of polygeneration is greatest when electricity prices are volatile, and the district heating price is high (the sub-figure in the bottom right corner of Fig. 16). The reason the district heating price is so important for the polygeneration system is that the income is greatly increased at high district heating prices when operating in electricity mode.

As noted above, in the Danish Promotion of Renewable Energy Act §44 par. 2 VE-Lov, the premium feed-in tariff for electricity produced from biomass by gasification is ~ 110 €/MWh, while support for biogas sold for transportation purposes is 36 €/MWh, according to § 43 b par. 2–3 VE-Lov. If these subsidies were to be used for the proposed polygeneration system (biogas subsidies added on top of natural gas prices), the optimum operation mode in 2025 would be to run 70% of the time in bio-SNG mode (30% in electricity mode), and in 2035 ~10% of the time in bio-SNG mode (90% in electricity mode). The vol scenario would result in over 75% operation in bio-SNG mode and 25% in electricity mode. Moreover, all scenarios will result in a positive NPV (using 70€/MWh for bio-SNG). However, these subsides are specific to Denmark and are not guaranteed to exist or remain the same in the future.

4. Conclusion

This article presented a study on the thermodynamic modeling and simulation of a novel polygeneration plant, along with a techno-economic analysis. The results demonstrated that the hypothesis stands as this system can operate with a high capacity factor in the future Danish

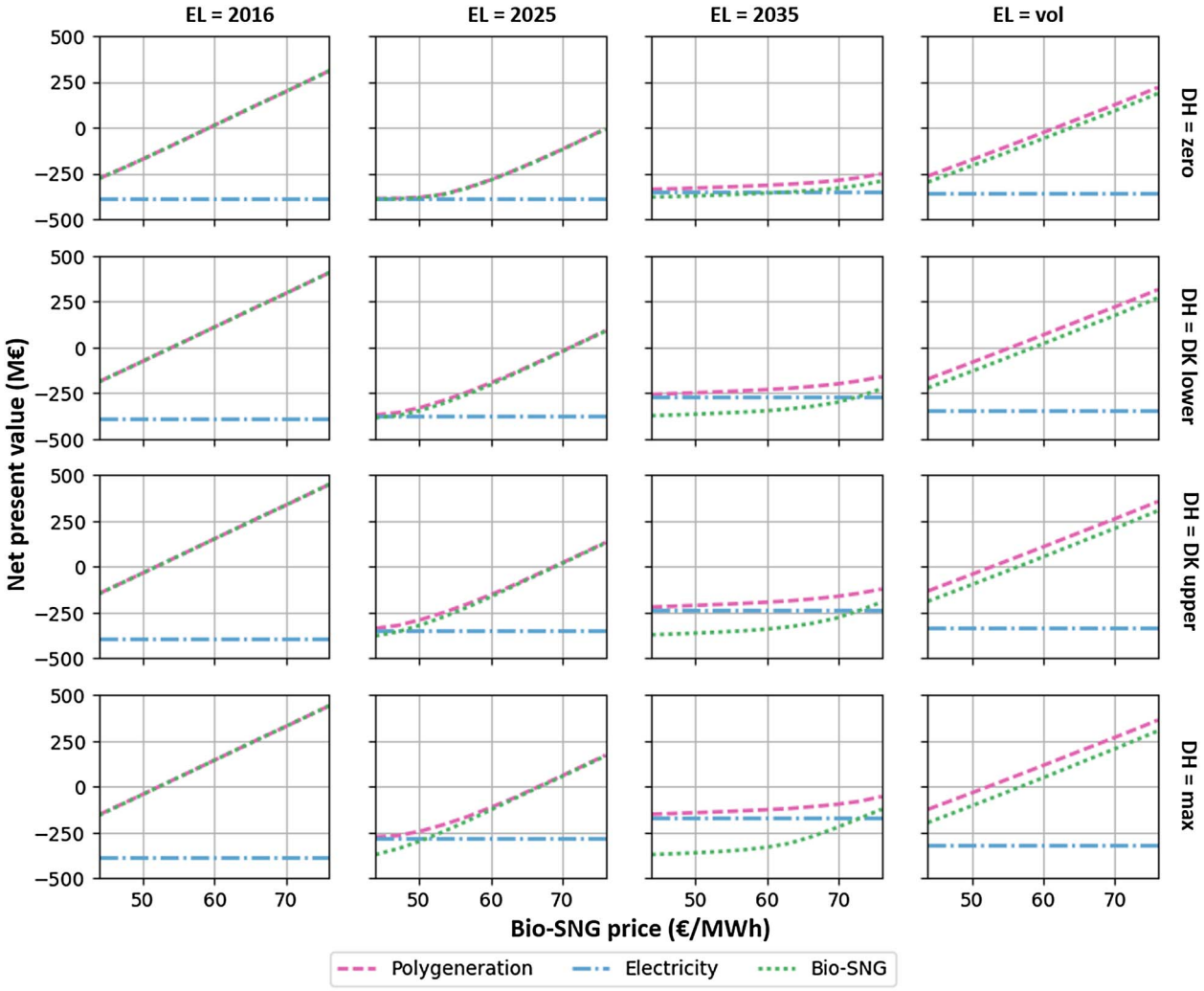

Fig. 16. NPV for system if running only for bio-SNG or electricity production, compared to combined production of polygeneration system. Power price scenarios are defined in Fig. 4 and district heat pricing scenarios are defined in Fig. 9. For comparison, the investment cost is recalled to be 216 M€.

electricity market. Furthermore, the results indicated that economic feasibility is greater compared to using stand-alone gasifier and electrolyser plants for electrofuel production.

Based on the results of the study, further conclusions are as follows.

1. The electric efficiency of the plant in electricity production mode is 46%; the total efficiency including heat production is 90%. The fuel efficiency of the plant in bio-SNG mode is 69%; the total efficiency is 85% including heat production.
2. The techno-economic analysis revealed that the investment cost is high, owing to the gasifier and SOC cost. The analysis also indicated that district heating sales are important for economic feasibility of the polygeneration system.
3. Analysis of the marginal cost and mode of operation demonstrated that the operational time in each mode varies significantly depending on future electricity and bio-SNG prices.
4. The ability of a system to choose between producing or consuming electricity depending on the market price can significantly increase its capacity factor compared to a single-mode system, but the increase is greatly dependent on future electricity and bio-SNG prices.
5. The polygeneration system achieves positive net present value when bio-SNG prices are high except when operating at high electricity prices.
6. The polygeneration system achieves a higher NPV than single-mode systems, particularly when electricity prices are volatile and the district heating price is high.

Acknowledgements

The authors would like to thank the ForskEL programme for funding this research.

References

[1] Danish Ministry of Climate. Energy and Buildings. OUR FUTURE ENERGY. Copenhagen; n.d.
[2] Working G. The Danish Climate Policy Plan Towards a low carbon society. Copenhagen; 2013.
[3] Lund H, Hvelplund F, Østergaard PA, Möller B, Mathiesen BV, Karnøe P, et al. System and market integration of wind power in Denmark. Energy Strateg Rev 2013;1:143–56.
[4] Puga JN. The importance of combined cycle generating plants in integrating large levels of wind power generation. Electr J 2010;23:33–44.
[5] Mathiesen BV, Lund H, Connolly D, Wenzel H, Østergaard PA, Möller B, et al. Smart Energy Systems for coherent 100% renewable energy and transport solutions. Appl Energy 2015;145:139–54.
[6] Luo X, Wang J, Dooner M, Clarke J. Overview of current development in electrical energy storage technologies and the application potential in power system operation. Appl Energy 2015;137:511–36.
[7] Ferrero D, Lanzini A, Leone P, Santarelli M. Reversible operation of solid oxide cells under electrolysis and fuel cell modes: experimental study and model validation. Chem Eng J 2015;274:143–55.

[8] Lund H, Mathiesen BV. Energy system analysis of 100% renewable energy systems—the case of Denmark in years 2030 and 2050. Energy 2009;34:524–31.
[9] Connolly D, Lund H, Mathiesen BV. Smart Energy Europe: The technical and economic impact of one potential 100% renewable energy scenario for the European Union. Renew Sustain Energy Rev 2016;60:1634–53.
[10] McKendry P. Energy production from biomass (part 2): conversion technologies. Bioresour Technol 2002;83:47–54.
[11] Bernical Q, Joulia X, Noirot-Le Borgne I, Floquet P, Baurens P, Boissonnet G. Sustainability assessment of an integrated high temperature steam electrolysis-enhanced biomass to liquid fuel process. Ind Eng Chem Res 2013;52:7189–95.
[12] Clausen LR, Houbak N, Elmegaard B. Technoeconomic analysis of a methanol plant based on gasification of biomass and electrolysis of water. Energy 2010;35:2338–47.
[13] Clausen LR. Maximizing biofuel production in a thermochemical biorefinery by adding electrolytic hydrogen and by integrating torrefaction with entrained flow gasification. Energy 2015;85:94–104.
[14] Pozzo M, Lanzini A, Santarelli M. Enhanced biomass-to-liquid (BTL) conversion process through high temperature co-electrolysis in a solid oxide electrolysis cell (SOEC). Fuel 2015;145:39–49.
[15] Clausen LR. Energy efficient thermochemical conversion of very wet biomass to biofuels by integration of steam drying, steam electrolysis and gasification. Energy 2017;125:327–36.
[16] Elmegaard B, Houbak N. DNA – a general energy system simulation tool. Proc SIMS 2005;2005:43–52.
[17] Elmegaard B. The Engineer's "DNA by Example." Tech Univ Denmark; 2003.
[18] Henriksen U, Ahrenfeldt J, Jensen TK, Gøbel B, Bentzen JD, Hindsgaul C, et al. The design, construction and operation of a 75kW two-stage gasifier. Energy 2006;31:1542–53.
[19] Ahrenfeldt Jesper, Henriksen Ulrik, Jensen Torben K, Gøbel Benny, Wiese Lars, Kather Alphons, et al. Validation of a continuous combined heat and power (CHP) operation of a two-stage biomass gasifier; 2006.
[20] Brandt P, Larsen E, Henriksen U. High tar reduction in a two-stage gasifier. Energy Fuels 2000;14:816–9.
[21] Ahrenfeldt J, Thomsen TP, Henriksen U, Clausen LR. Biomass gasification cogeneration – a review of state of the art technology and near future perspectives. Appl Therm Eng 2013;50:1407–17.
[22] Sunfire supplies Boeing with largest reversible solid oxide electrolyser/fuel cell system. Fuel Cells Bull 2016;2016. 10.1016/S1464-2859(16)70002-2.
[23] Jensen SH, Sun X, Ebbesen SD, Chen M. Pressurized operation of a planar solid oxide cell stack. Fuel Cells 2016;16:205–18.
[24] Vassilev SV, Baxter D, Andersen LK, Vassileva CG. An overview of the chemical composition of biomass. Fuel 2010;89:913–33.
[25] Clausen LR, Elmegaard B, Ahrenfeldt J, Henriksen U. Thermodynamic analysis of small-scale dimethyl ether (DME) and methanol plants based on the efficient two-stage gasifier. Energy 2011;36:5805–14.
[26] Hauch A, Brodersen K, Chen M, Mogensen MB. Ni/YSZ electrodes structures optimized for increased electrolysis performance and durability. Solid State Ion 2016;293:27–36.
[27] Bejan A, Tsatsaronis G, Moran MJ. Thermal design and optimization. John Wiley & Sons; 1996.
[28] Hamelinck C, Faaij A, Denuil H, Boerrigter H. Production of FT transportation fuels from biomass; technical options, process analysis and optimisation, and development potential. Energy 2004;29:1743–71.
[29] Peduzzi E. Biomass to liquids: thermo-economic analysis and multi-objective optimisation. EPFL 2015. http://dx.doi.org/10.5075/EPFL-THESIS-6529.
[30] Technology data for energy plants – generation of Electricity and District Heating, Energy Storage and Energy Carrier Generation and Conversion; n.d.
[31] Biogas - SOEC: electrochemical upgrading of biogas to pipeline quality by means of SOEC electrolysis – energy system integration and economy; 2012.
[32] Bang C, Vitina A, Gregg JS, Lindboe HH. Analysis of biomass prices – future danish prices for straw, wood chips and wood pellets; 2013.
[33] Mchugh A. Short run marginal cost – discussion paper. Perth, Western Australia; 2008.
[34] Bæk M. Regulation and planning of district heating in Denmark; 2015.
[35] Energitilsynet. Energitilsynets prisstatistik for fjernvarmeområdet, sorteret alfabetisk; 2016.
[36] Energinet.dk. Energinet.dk's analyseforudsætninger 2012–2035, juli 2012; 2012.
[37] Energinet.dk. SIFRE: simulation of Flexible and Renewable Energy sources; 2015.
[38] Lythcke-Jørgensen C, Clausen LR, Algren L, Hansen AB, Münster M, Gadsbøll RØ, et al. Optimization of a flexible multi-generation system based on wood chip gasification and methanol production. Appl Energy 2017;192:337–59.

Flexible TwoStage biomass gasifier designs for polygeneration operation

Rasmus Østergaard Gadsbøll*[,1], Lasse Røngaard Clausen[2], Tobias Pape Thomsen[1], Jesper Ahrenfeldt[1], Ulrik Birk Henriksen[1]

[1]Technical university of Denmark, Department of chemical and biochemical engineering, Frederiksborgvej 399, 4000 Roskilde, Denmark

[2]Technical university of Denmark, Department of mechanical engineering, Nils Koppels Allé 403, 2800 Kgs. Lyngby, Denmark

*Corresponding author, Tel: +4560668815, E-mail: rgad@kt.dtu.dk

Abstract

As increasing amounts of wind and solar are integrated into the energy system, there is a growing need for the development of flexible and efficient biomass-based energy plants. Currently, a Polygeneration concept is being investigated: a system based on thermal biomass gasification and solid oxide cells that can either produce power or biofuels depended on the electricity prices. This study investigates gasifier design opportunities for a large-scale and fuel flexible TwoStage concepts that only applies partial oxidation for tar conversion. Thermodynamic modeling is carried out for a total of 12 gasifier cases, featuring 3 main systems that each can process wood/straw and use air/oxygen. It was found that despite the varying operation conditions, process parameters reamined relatively stable and that partial oxidation could be effectively applied as the only tar reducing measure. The systems all achieved high cold gas efficiencies of 84-88% and was found to be significantly more effective than competing technologies, while also obtaining higher fuel flexibility.

Keywords: Biomass gasification, Polygeneration, Thermodynamic analysis, Two-stage gasifier

1 Introduction

A joint technology platform of gasification and flexible solid oxide cells is the foundation of the Polygeneration concept that has been proposed by Biomass Gasification Group at the Technical University of Denmark. The basic flow sheet of the concept is shown in Figure 1, where a gasifier fed with biomass is used to either: 1) produce power by converting the product gas in SOFC-mode; 2) produce synthetic natural gas (SNG) in SOEC-mode by using the oxygen in gasifier and mixing with the product gas to form a optimal synthesis gas. This concept enables grid balancing as well as an effective storage solution in the form of SNG that can be injected into the natural gas grid [1]. The respective energy efficiencies of the concept for power and SNG production have been modeled to around 43-63% and 69-70% (LHV), which all are state-of-the-art results [2][3][4][5]. Besides being advantageous to the grid, the plant operator is also expected to see increased economic feasibility, as the alternating operation will result in a higher net present value and an increased number of yearly operating hours (capacity factor) compared to the equivalent stand-alone systems (producing only power or SNG) [2].

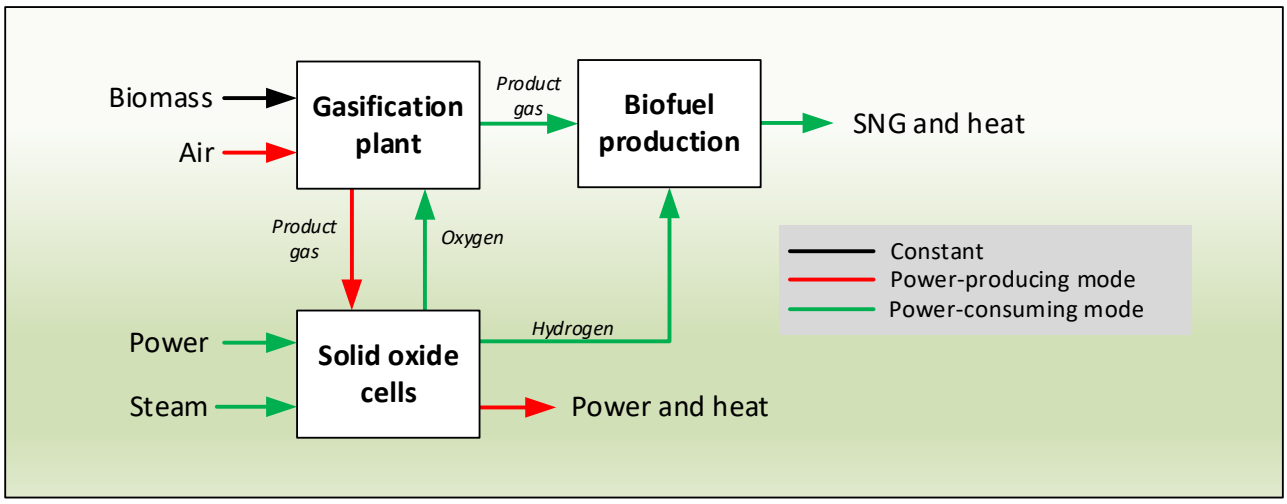

Figure 1 – The proposed Polygeneration concept.

The Polygeneration concept is based on the TwoStage Viking gasifier at the Technical University of Denmark [6]. The gasifier is shown in Figure 2 and processes wet wood chips via staged pyrolysis and gasification with an intermediate partial oxidation (POX) zone. The system applies an indirectly heated screw conveyer that use either engine exhaust or product gas heat as source, and a downdraft fixed bed char gasifier. The gasifier is mainly characterized by a very high cold gas efficiency of 93% (wet basis) and a very low tar content of <15mg/Nm^3 using only a bag filter as gas cleaning [6][7][8].

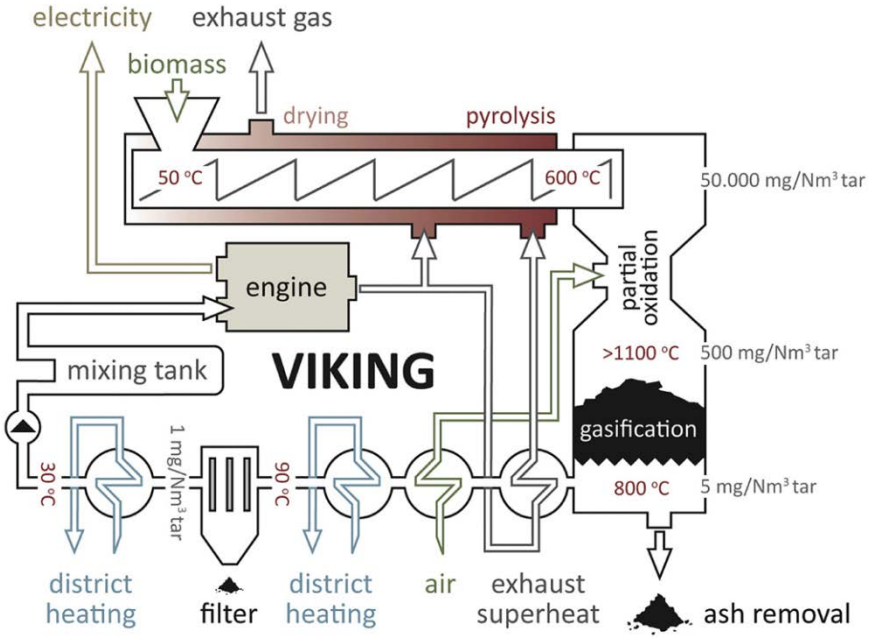

Figure 2 - Flow diagram of the TwoStage Viking gasifier with approximate temperatures and tar concentrations [9].

1.1 Aim of this study

This study investigates the possibilities of improving the TwoStage gasification technology in a polygeneration framewrok in order to improve the feasibility. The study focuses on three key challenges for the system in this context:

- Upscaling capacity: It is considered beneficial to design larger plants to decrease specific investment costs [10]. The TwoStage gasifier has been built up to 1.5MW_{th} input, but is expected to be limited to around 10MW_{th} [11]. This restrain is because of the applied reactors, as the pyrolysis screw conveyer heat exchange area will be either costly and/or inpractical at larger scales and the downdraft char bed might experience difficulty with evenly distributing the char without causing large pressure drops. It is suggested to scale the system to 10-100MW_{th}.

- Air/oxygen flexibility and simple gas cleaning: In recent work [8], it is shown tha the TwoStage gasifier is expected to operate effectively with both air and oxygen as gasification media. And because the downdraft char bed is evaluated as infeasible for this study, it is desired to simplify the tar conversion as tars and coherent complex gas cleaning can represent major costs and complexity [12][13]. It is therefore suggested to design a system that can reduce the tar level sufficiently (depending on application) in a single POX reactor.

- Fuel flexibility: Currently the TwoStage gasifier can only operate on wood chips due to the intolerance to fines and high temperatures, but it is desired to utilize a wide spectre of fuels such as wood and straw pellets. Fuel costs represent around 30-50% of the total cost of the final product when traditional international feedstocks such as wood pellets and chips are used [2][13][10][14]. There is however a significant potential in minimizing fuel costs. Using: 1) local/regional fuels such as agricultural residues and energy crops can reduce fuel costs to 30-60% compared to internationally traded ones; 2) process residues like bagasse, black liquor, waste wood costs are 15-20%; 3) wastes can have zero or negative, costs [10][15]. This means potential product cost reductions of up to 50% if alternative fuels can be utilized.

This study will investigate these three aspects via thermodynamic modeling and provide preliminary designs of TwoStage gasifier concepts operating within the Polygeneration concept.

2 Considerations and system designs

The gasifier concepts presented here are characterized by staging the fuel conversion and applying recirculating gases around both pyrolysis and gasifier. Figure 3 provides an overview of the overall design. The loop around the pyrolysis serves two main purposes: avoid dilution of the volatiles; and use of the sensible heat of the product gas to drive the process. The recirculation is carried out with a high-temperature blower. The loop around the gasifier is used to quench the POX gases to avoid agglomeration/sintering of fuel ashes and are done with a steam ejector due to the high temperatures. The ejector steam consumption is substantial and is assumed to be provided via downstream waste heat from biofuel synthesis or engine/SOFC exhaust – this is modeled in similar studies up to amounts of 2.3 kg-steam/kg-fuel(dry) (70% fuel moisture) [2][4][16]. The oxygen is produced via a SOEC, where steam is applied as sweep gas resulting in an assumed 50-50v% oxygen-steam mixture at 700^{o}C [17]. The SOEC steam consumptions is unaccounted for in this gasifier study. Design gasifier outlet temperatures depend on the application, as the air-blown system will have a significant tar concentration the temperature should not be below 400^{o}C to avoid condensation - unless the POX temperature is higher than 1200^{o}C. A more detailed design basis is given in Figures 5, 6 and 7.

The use of alternative fuels, fluid bed reactors and POX along with the design parameters in Figure 3 will be discussed in the next section.

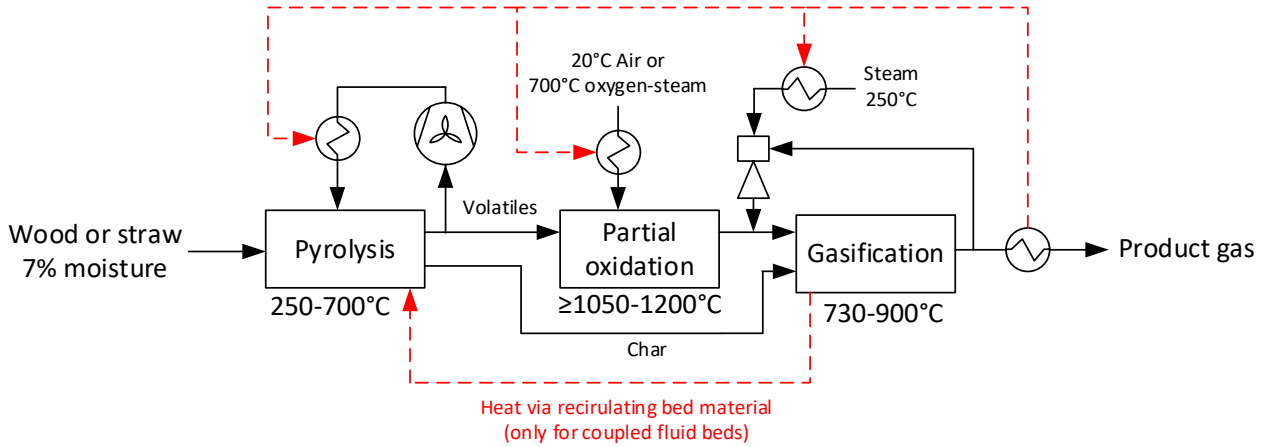

Figure 3 – Overall basis for the system designs. The diagram shows components, design temperatures and flows of heat, fuel, steam and oxidizer.

2.1 Fuels: wood and straw

The total primary use of energy in the world in 2016 was around 573 EJ while the end use consumption was around 395 EJ [18]. Wood is currently the primary global bioenergy carrier and forests supplied approximately 85% of the total biomass used for energy purposes in 2012 [19]. Recent estimates of use and potential of forestry products for energy purposes found the use in 2012 to be around 49 EJ and the near future potential (2035) to be between 72 and 84 EJ [19]. However, several other options exist which can be made available for more fuel flexible energy platforms - potentially at a much lower price than fuel wood. Development of the global energy sector towards such new resources may very well reduce the share of forestry products in the global bioenergy mix to around 50% in 2030 [19]. A short overview of selected alternative organic resources is included in Table 1.

Resource	Geographical scope	Global Potential	Reference
Sewage sludge	Global	1-5 EJ HHV[1,2]	[20–22]
Municipal organic waste	Global	23 EJ HHV[1]	[23–26]
Manure fibers	Global	18 EJ HHV[1]	[27–29]
Cereal straw[3]	Global	15-19 EJ LHV[4]	[30,31]
Sugarcane residues	Global	9-17 EJ LHV[4]	[30,31]
Rice husks and straw	Mainly Asia	18-28 EJ LHV[4]	[30,31]
Maize residues	Global	17-40 EJ LHV[4]	[30,31]
Soy bean straw	South America and Asia	6-10 EJ LHV[4]	[30,31]

1: Scaled from the resource potential in EU 27+China and re-calculated from biogas potentials reported in [32]

2: The conservative range estimate is based on estimated global production of dry mass and an average heating value of undigested sludge from [33,34]

3: Wheat, oat, barley and rye included

4: Based on FAO statistics on global production of main crops in 2010-2014 combined with residue-to-crop ratios and lower heating value (LHV) values as received from FAO report on residues

Table 1: Global energy potential in selected waste and crop residue resources. HHV: Higher Heating Value. LHV: Lower Heating Value. EJ: ExaJoule (=10^{18} Joule)

The majority of the non-wood biomass avaliable for energy purposes is herbaceous, and the global potential of many different straw types are substantial (Table 1). Straw is applied to some extent in various energy systems encompassing combustion, pyrolysis as well as gasification. However, traditionally straw is regarded as a highly problematic resource for thermal processes as the very low ash melting temperature of most straw types usually lead to operational issues with ash sintering, agglomeration and defliúidisation of fluid bed systems. An overview of selected ash-related experiences from various thermal systems is collected in Table 2.

Fuel	Thermal platform	Critical temperature	Problematic elements	Key parameters	Reference
Danish wheat straw	LT-CFB gasifier (lab test)	780°C, defluidization	Alkali (potassium), chloride and silicium	Fluidisation velocity, K/Si ratio and particle diameter	[35]
Danish wheat straw	LT-CFB gasifier	825°C, defluidization	Potassium and chloride	Mixing and anti-agglomerating influence of residual char	[36]
Wood bark	Fluid bed gasification	930°C, defluidization			[37][38]
Wood	Fluid bed gasification	940-950°C, defluidization			[38]
Oil palm bunch and rice straw	Bubbling fluidized bed combustion (lab test)	Defluidization at all temperatures from 750-900°C	Potassium content was the main cause through silicate melts	Ash composition (main parameter), fluidization velocity, bed temperature and particle sizes	[39]
American straw	mullite BFB gasifier	750°C, initial agglomeration		Bed material and reactor/process design	[40]
Straw	sand-BFB gasifier	800°C, initial agglomeration			[41]
Wheat straw	Fluid bed gasification	680-780°C, initial agglomeration			[42]
Cardoon (thistle)	BFB gasification w. sand or sepiolite	870-930°C, defluidization		Bed density and mixing of fuel, ash and bed material	[43]
25 different biomass fuels	BFB combustion (lab test)	From <800 °C (DDGS, corn cub) to >1000 °C (different wood types)		Ash compositions, particle size and fluidization velocity	[44]

Table 2: Overview of selected ash-related operational experiences from thermal systems converting biomass and biomass fuel mixtures.

Despite the limited number of studies published on critical ash behaviour in fluidized bed gasification of biogenic fuels, it seems that the safe zone for thermal conversion of straw with regard to ash-induced bed agglomeration and potential defluidization constitutes the lower end of the allowable temperature range (Table 2). Depending on other operation parameters (particle size, bed density, fluidization velocity and mixing) the maximum operation temperature for straw gasification will most likely be somewhere in the range from below 750^{o}C to around 800^{o}C. Maximum gasification temperatures of 780^{o}C (from experiences in [35]) and 900^{o}C for straw and wood respectively are chosen as design temperatures for this study.

2.2 Fluid bed reactors and bed material recirculation

As seen in Section 3, this study will examine three concepts that all apply fluid bed gasifiers and two of them fluid bed pyrolyzer. The fluid bed reactor is chosen because of its high-level operational control and tolerance towards smaller particle sizes. These criteria fit very well with the desired fuel and the upscaling potential is hundreds of MW_{th}.

Staged fluid bed systems are typically applied with a relatively fixed recirculation rate of bed material that serves two main purposes: transfer of char from the pyrolyzer to the gasifier and transport of heat from the gasifier to the pyrolyzer. The recirculation rate will therefore have a significant impact on system performance with regards to residence times, temperature levels and cold gas efficiency. Char transport is closely linked to the applied fluidization regimes, as the degree of mixing should be direct consequence of the fluidization velocity: slower regimes (stationary, bubbling) experiences less mixing that fast ones (turbulent, circulating). As a consequence, bubbling beds will have a char-rich top layer because of the lower density of char. Faster regimes will naturally experience some difference in concentration, but will be closer to perfectly mixed. This phenomenon is discussed below in Section 2.2.1.
Recirculation of bed material allows large transfer of heat between reactors, which can be very beneficial in some systems e.g. indirect gasifiers. The transfer is however typically associated with a significant loss of efficiency because of the relatively high temperature difference between reactors that can be several hundred degrees [46][47][48]. Recirculation is however a relatively simple tool to transport char between reactors, as it can be complex to separate char and bed material continuously, and is therefore, as a whole, typically beneficial. But overall the circulation should be minimized in order to obtain the highest cold gas efficiency.

2.2.1 Experimental investigation and overview of bed material/char ratio

To validate expectations about the distribution of char, ash and bed material an experiment has been conducted in April 2016 on a 100kW_{th} low-temperature circulating fluid bed (LT-CFB) gasifier – see [48] for system overview. 20 hours of operation on a wheat straw fuel was succeeded by 12 hours of operation on a fuel mixture of 85 wt% straw and 15wt% sewage sludge. After termination of the operation, the system was cooled and emptied. The content of the char reactor was extracted as 7 fractions of approximately 15 kg each and numbered 1 to 7 from bottom to top in the reactor. Top fractions 1 and 3 and bottom fractions 6 and 7 were sieved across a 0.6 mm sieve. There were no sintering or bed agglomeration and as such, the large particle fractions were completely free of the original bed material and consisted only of unconverted fuel, char and ash particles. The shares of large particles in the 4 sieved fractions are shown in Figure 4. From the results it is evident that there is almost 3 times as much large particle mass in the top of the reactor compare to the bottom.

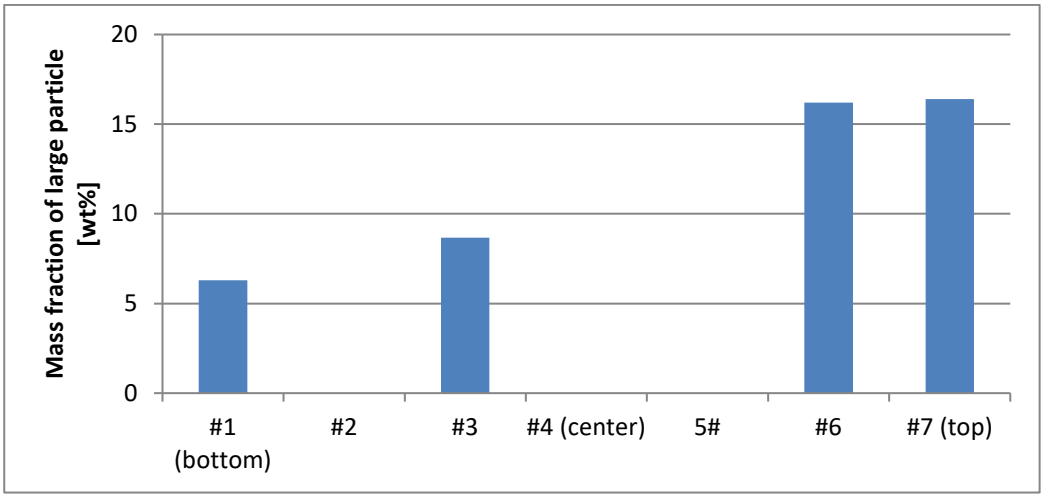

Figure 4: Share of large particles (>0.6 mm) in char reactor bed mass after 32 hours of LT-CFB gasification of straw and a straw/sewage sludge mixture

The experimental results are listed in Table 3 with literature findings of coupled fluid beds and the applied values for this study. It is seen that there indeed is a char-rich top layer in the bubbling fluid bed reactor and that it is nearly twice the amount of the average concentration. The top layer concentration is in the range of the LT-BIG value (see "sand recirculation" in Table 3), but significantly less than the FICFB, which is likely because the indirect gasifier circulates and increased amount of bed material due to necessary heat transport. The average concentration is on the high end compared to the MILENA and LT-CFB, which is expected as the turbulent beds are not perfectly mixed throughout their length and hence will have a higher concentration of low-density char at the top. The experimental values of 6 and 10 kg-BM/kg-char are seen as reasonable and will be applied in this study for slow and fast fluid beds respectively.

	Pyrolysis –gasifier coupling	Sand recirculation kg-BM/kg-char	Fuel (assumed char yield)[a]	Reference
LT-CFB[b]	Turbulent –bubbling fluid bed	Top: 6 Bottom: 16 Average: 10.0	Straw (25%) & Straw-sludge (30%)	This study, Figure 1
MILENA	Turbulent-bubbling fluid bed	5-8	Wood, 20%	[47]
LT-CFB	Turbulent –bubbling fluid bed	4-7	Straw-sludge, 25%	[49]
LT-BIG	Bubbling-turbulent fluid bed	3-6	Wood, 20%	[46]
FICFB	Bubbling-circulating fluid bed	10	Wood, 20%	[50]
Slow fluid bed	Bubbling-turbulent fluid bed	6	Wood, 20% Straw, 30%	Used for this study
Fast fluid bed	Turbulent-bubbling fluid bed	10	Wood, 12% Straw, 20%	Used for this study

Table 3 – Bed material (BM) recirculation rates for various fluid bed systems. [a]Defined as char/input fuel wt%. [b]Results show fraction of particles >0.6 mm. As some char and ash particles are smaller than this, these values should be considered maximum values.

2.3 Tar tolerances and partial oxidation

The alternating Polygeneration system utilizes the product gas in either a SOFC for power production or a synthesis reactor for SNG production. These applications have very different tolerances towards tar concentrations and hence the operation modes and design should reflect this. It is important to recall that the gasifier is air-blown when is sent to the SOFC, while the gasifier is oxygen-blown when the gas is used for synthesis.

SOFC's have been tested with tar-loaded product gas in several studies. Hoffman et al. [51][52] has in multiple studies investigated the conversion of gasifier tars in SOFC's. The studies operated both fluid bed and fixed bed gasifiers that were coupled to an operating SOFC at 850°C. Tar concentrations of 3g/nm^3 and >10g/nm^3 respectively were found to not cause carbon deposition/operational problems. As tars are a very complex compound group and fuel cells differ from study to study, the tolerance will be very dependent on the applied system. Aravind & de Jong [53] did however suggest a feasible and rough 2g/nm^3 concentration tolerance based on literature analysis, which will be used as a general guideline here.
When using synthesis reactors, tars should be removed to very low levels in order to avoid tar condensation. Especially as the gas is to be pressurized to the synthesis reactor pressure, which lowers the tar dew point. While the tolerance is very dependent on the process conditions, a rough estimate of the concentration after the POX is set to 0.1g/nm^3 [54][55].

POX is a powerful tool to reduce tar concentrations by more than 99% and can be applied with a subsequent very high cold gas efficiency, as with the current TwoStage gasifier. Tars are converted via two mechanisms in the POX: thermal decomposition and oxidation – an overview of POX and thermal treatment studies are collected in Table 4. The TwoStage gasifier concept has shown in several instances that applying temperatures at 1100-1200°C in the POX zone reduce the tar concentration to 1.0-1.5g/nm^3 [46][56][57]. In order to meet tar requirements of the SOFC and synthesis reactor it is estimated that the POX temperature should be around 1050 and 1200°C respectively.

Temperature [°C]	Stoichiometric air ratio	Tar content [mg/nm^3,dry][a]	Note	Reference
900	0.5	115	POX	[58]
900	0.34	960	POX	[59]
900	-	2844	POX	[60]
1050	0.4	≈846[b]	POX	[61]
1100	0.34	1000	POX	[62]
1100	-	1150	POX	[46]
1100	0.5	1200	POX	[56]
1100-1200	-	1220	POX	[57]
1200-1300	-	≈100	POX	[46]
1000	0	5000	Thermal treatment	[58]
1100	0	8000	Thermal treatment	[62]
1200	0	385	Thermal treatment	[63]
1250	0	50	Thermal treatment	[63]

Table 4 – Overview of partial oxidation and thermal treatment studies. [a]Based on 2.6nm3/kg gas production from biomass, as for the TwoStage gasifier [56]**. [b]Estimate.**

3 Modeling

This study will investigate 3 plant configurations that will each be modeled using air/oxygen and wood/straw – resulting in 12 models. The main difference to the 3 systems is the applied pyrolysis conditions, as the char yield and composition has a significant effect on the POX and gasifier and hence the total system efficiency. Three pyrolysis processes are chosen: updraft fixed bed, slow fluid bed and fast fluid bed. The only modeled difference between the fast and slow fluid bed is the char characteristics, which is an assumption as especially carbon conversion and pressure loss might differ (these are however discussed in Section 4.1). The design basis for the systems are shown in Figures 5, 6 and 7 respectively.

The Fixed bed system utilize a fixed bed updraft reactor. The reactor also allows some fuel particle flexibility using chips and pellets. The volatile gas recirculation is done by a blower. It is vital that the outlet temperature of the reactor is sufficiently high to avoid condensation of tars: 250^{o}C is chosen based on previous experiences with the reactor [64]. The produced char will be transported via e.g. a screw conveyer, to a fluid bed char gasifier.

The fluid bed systems similarly utilizes a blower for recirculating volatiles, but it will experience much higher thermal stresses as the gas temperature is projected to be the same as the bed: 500^{o}C is chosen to ensure complete tar release [65]. This will likely cause the blower to be water-cooled and more complex/expensive - and might be applied with preccoling of the gas or even replaced by an ejector if necessary. The Slow fluid bed system will transport the char via a loop seal at the top of the bed that will drain the char-rich layer, while the Fast fluid bed system will apply a cyclone for transporting char and bed material. The systems are initially projected to feature one slow and one fast bed each to simplify the recirculation of bed material, but will not be investigated further here.

The modeling is carried out in the DNA (Dynamic Network Analysis) software that features zero-dimensional components [66][67]. Key model data are listed in Table 5.

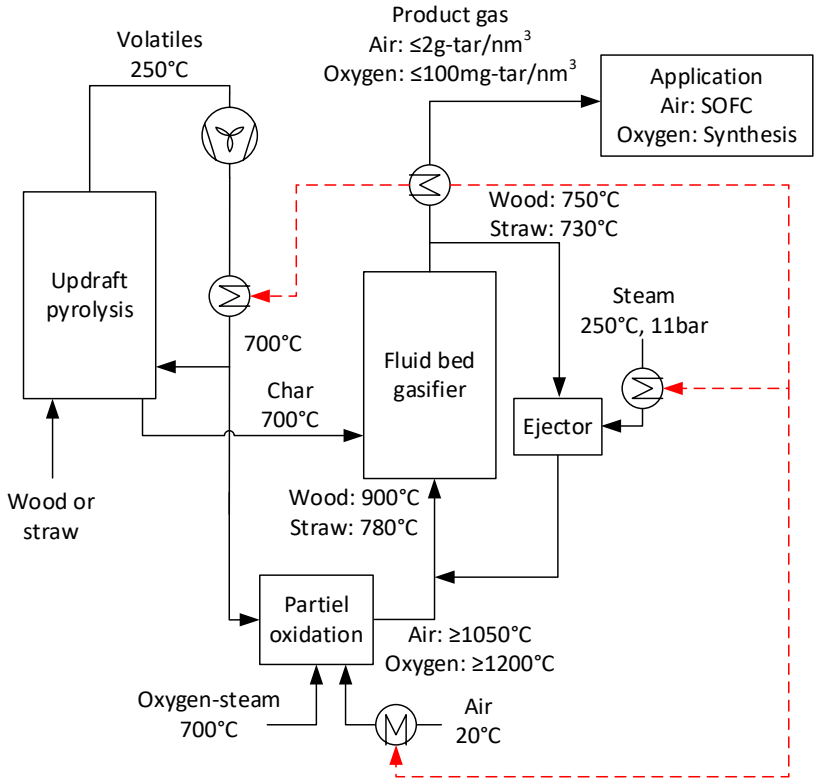

Figure 5 – Design basis for the Fixed bed system. Red dotted lines are heat flows.

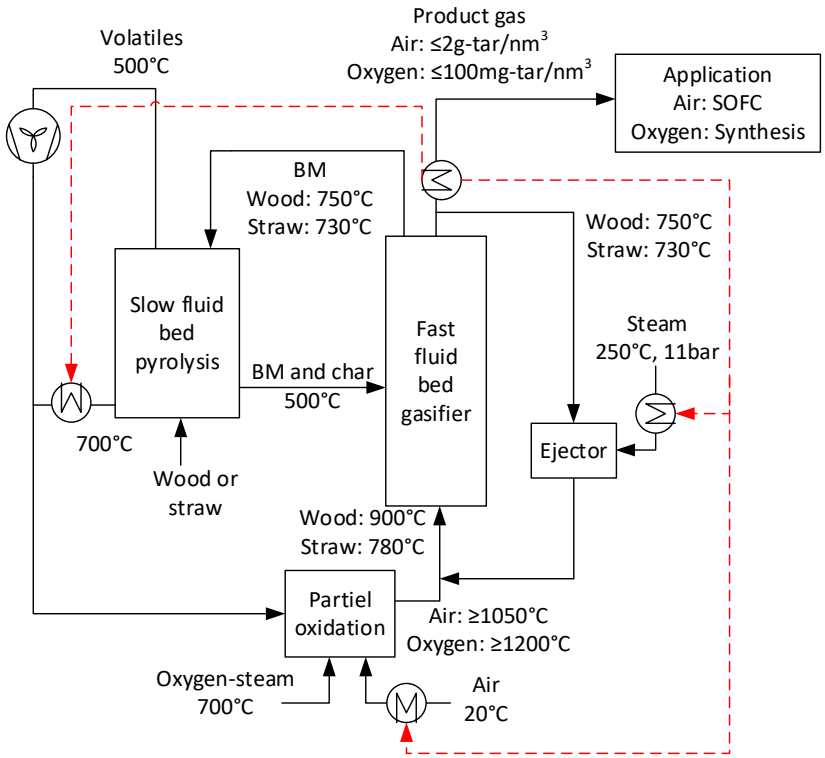

Figure 6 – Design basis for the for the Slow fluid bed system. BM denotes bed material. Red dotted lines are heat flows.

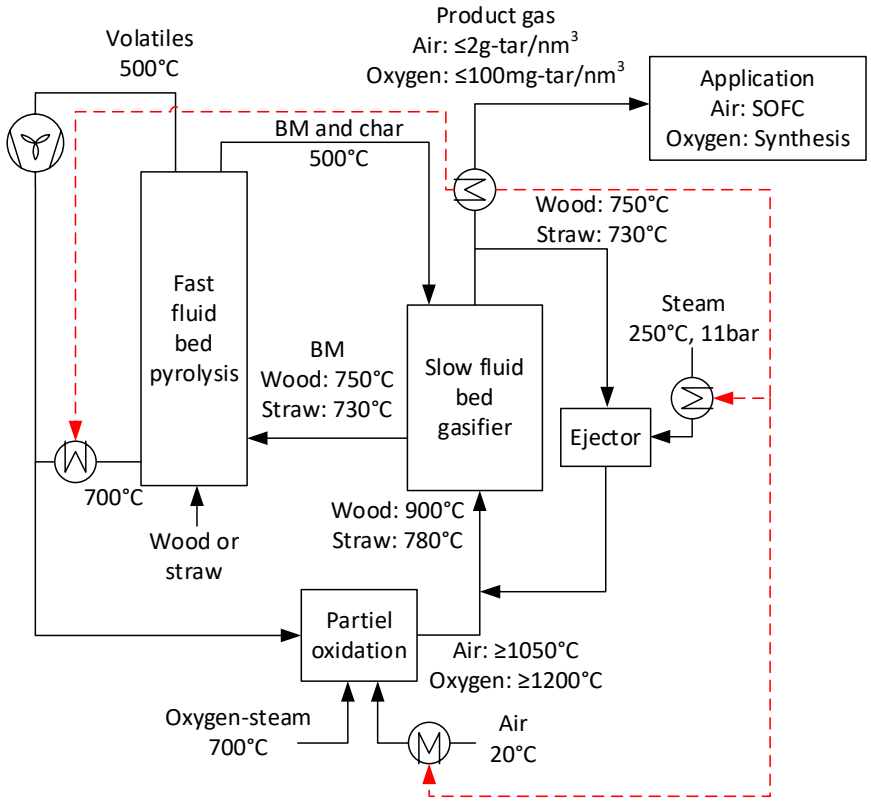

Figure 7 – Design basis for the Fast fluid bed system. BM denotes bed material. Red dotted lines are heat flows.

Fuel	50MWth input, 7% moisture (assuming pellet standard / pre-drying)
Pyrolyzer	Heat loss = 1% fuel input LHV, fixed bed pressure loss = 30mbar, fluid bed pressure loss = 146mbar[a], fixed and fluid bed volatiles are assumed to have a H_2 content of 20v% and 10v% respectively [68][69]
Partial oxidation	Assumes thermal equilibrium (Gibbs minimization) at outlet temperature – method described in [5][70].
Gasifier	Heat loss = 1% fuel input LHV. Assumes that the water-gas shift reaction is in equilibrium at the outlet temperature. Carbon conversions are 95% for all models. The methane content in the gas from the POX is assumed inert through the gasifier. Similar to the pyrolyzer the pressure loss is 146mbar
Bed material recirculation	The flow is modeled as a heat flow from the gasifier to the pyrolyzer assuming that the bed material is sand (c_p=0.83kJ/(kg*°C)) and that the heat flow can be estimated via the temperature difference of the beds (outlet temperature). The mass flow is determined via the recirculation rates in Table 3.
Ejector	Assumed efficiency of 27% and 11bar motive pressure [71] and calculated via Equation 1 [17]
Heat exchangers	50K pinch point, 10mbar pressure loss
Blowers	40% isentropic efficiency, 95% combined mechanical and electrical efficiency

Table 5 – Main modeling parameters. [a]Calculated for a minimum fluidization conditions for a sand (density = 2600kg/m3) bed height of 0.95m with a distributor loss of 20%[45], voidage fraction of 50% [72] and a temperature of 700°C.

$$\eta_{ej} = \frac{\dot{V}_2 P_2 \ln(P_3/P_2)}{\dot{V}_1 (P_1 - P_3)}$$

Equation 1

The cold gas efficiency and total efficiency is calculated on dry basis via Equation 2 and 3 respectively. Product gas is denoted *PG* and electricity consumption $\dot{W}_e$.

$$\eta_{cg} = \frac{\dot{m}_{PG} \cdot LHV_{PG}}{\dot{m}_{fuel} \cdot LHV_{fuel}}$$

Equation 2

$$\eta_{tot} = \frac{\dot{m}_{PG} \cdot LHV_{PG} - \dot{W}_e}{\dot{m}_{fuel} \cdot LHV_{fuel}}$$

Equation 3

3.1 Pyrolysis

The pyrolysis is modeled via the fuel parameters shown in Table 6. Based on the fuel data, atomic balances and heating value balance of inlet and outlet flows as well as a general mass and energy balance, an outlet gas composition can be estimated for a given temperature. The released tars are not modeled in specifics, but are estimated by methane and n-hexane (C_6H_{14}) that will satisfy the beforehand mentioned criteria and ensure a correct heating value of the gas.

	C [wt%]	H [wt%]	O [wt%]	N [wt%]	Ash [wt%]	Char yield [wt%]	HHV [MJ/kg]	Reference
Fast fluid bed pyrolysis								
Wood	51.3	5.7	40.5	0.2	2.3	12	19.0	[73]
Wood char	57.0	3.3	20.3	0.4	19.0	-	20.9[a]	
Straw	45.7	6.0	40.9	1.4	6.0	20	18.4	
Straw char	67.2	4.5	27.0	1.4	30.0[b]	-	20.1[a]	
Slow fluid bed pyrolysis								
Wood	50.8	6.6	41.3	0	1.3	20	21.2[a]	Composition: [74] Ash: [75]
Wood char	85.1	2.8	5.6	0	6.5	-	33.7[a]	
Straw	42.1	5.4	46.2[c]	0	6.3	25	16.1[a]	Composition: [76] Char yield: [77]
Straw char[d]	58.7	3.0	16.7	0	21.6	-	21.8	[68]
Fixed bed pyrolysis								
Wood	48.1	6.4	44.8	0.1	0.6	25	18.3	

								[78]
Wood char	90.7	2.1	4.5	0.2	2.5	-	33.6	
Straw	40.8	5.8	47.5[c]	0.2	5.7	31	16.09	[79]
Straw char	71.2	3.0	7.0[b]	0.3	18.5[b]	-	30.5[b]	

Table 6 – Applied pyrolysis data for the modeling. Note that all straw data are for wheat. [a]Calculated based on chemical composition via Equation 4 [80]. [b]Calculated in DNA via composition and heating value. [c]Calculated by difference. [d]Data estimated via reference.

$$HHV = 0.3491C + 1.1783H + 0.1005S - 0.1034O - 0.0151N - 0.0211A\ [MJ/kg]$$

Equation 4

3.2 Partial oxidation adjustment

While the basic Gibbs reactor model will only produce a negligible methane content, experiences from POX tests proves that there typically is a significant methane content remaining under 1300°C due to slip and tar decomposition reactions [69]. The outlet methane contents are therefore calculated as linear functions from concentrations of 1/4 of the pyrolysis methane concentrations of 13.97v% and 5.85v% for fixed and fluid beds respectively at 900°C to a 0v% concentration at 1300°C – see Equation 5. As an example, a partial oxidation of volatiles from a fixed pyrolysis will yield 3.49v% CH_4.

$$\boldsymbol{vol\%_{CH4} = y \cdot 0.25 \frac{1300^0C - T}{1300^0C - 900^0C}}$$

Equation 5

4 Results and discussion

The main model results are given in Table 7 and detailed flow sheets are given in the Appendix. The cold gas efficiencies are seen to be generally high and rival competing technologies (see Section 4.2). The efficiencies are within 3% for each concept (Fixed, Slow, Fast) and POX temperatures are varying ≤125°C for wood vs straw and ≤190°C for air vs oxygen for each system, which displays a relative convenient level of process stability. It is also seen that the cold gas efficiencies are within 5%-points for each mode across systems.

The POX temperatures are seen to be high and of all the concepts, only the POX temperature of the Fast fluid bed was set to the minimum design value. The POX temperature of the other concepts was set based on the heat required by the downstream endothermic char gasification. As seen in Table A6 (appendix), the Fast fluid bed POX temperature causes the gasifier outlet temperature to be 70-90°C above the design value for wood fuels and the ejector steam superheat becomes artificially low (as more heat is available in the exhaust) for straw fuels, both of which in turn decreases the cold gas efficiency. The Slow fluid and Fixed bed system POX temperatures are however very high and are by default (by implementing the design values) 200-250°C higher than needed to accommodate the required reduction of tar. Hence, these systems show some additional flexibility that enables the use of even less gas cleaning and possibly the use of alternative applications that requires cleaner gases e.g. combustion engines.
It is also seen that the POX temperature difference between air and oxygen modes of ≈150-200°C matches very well with the difference in tar requirements for SOFC and synthesis reactors (1050°C vs 1200°C).

Some general tendencies regarding the efficiencies can be seen. As a relatively simple measure, the exhaust temperatures can be evaluated. The temperatures averaged across the systems are 502°C, 404°C and 303°C for the Fast fluid, Slow fluid and Fixed bed system respectively and these are easily coupled to the average efficiencies. The difference is namely found in the pyrolysis process and the POX temperatures. While the Fixed bed pyrolysis consumes 4.60MW_{th} compared to 2.93W_{th} and 2.12W_{th} for the Slow and Fast fluid bed pyrolysis' respectively, the efficient heat exchange that cools the volatiles to 250°C (compared to 500°C for the fluid beds) enables splitting of the product gas and hence higher superheat of the ejector steam. The difference between the Fast and Slow fluid bed exhausts is namely related to the constraint that the POX should reach 1050°C and 1200°C. While the Slow fluid bed achieves these by default, the Fast fluid bed system needs additional air/oxygen to reach these temperatures and hence it experiences a drop in cold gas efficiency.

Using woody fuels with a high ash-sintering temperature significantly reduces the steam consumption as less cooling is needed for the POX – this effect is studied in Section 4.1. These higher flows will lead to system losses as the steam is added at 250°C and removed from the system (in the product gas) at ≈300-500°C. This effect is present in reverse when comparing the oxygen-blown system, as steam is added at 700°C.

		Wood		Straw		
		Air	**Oxygen**	**Air**	**Oxygen**	**Average efficiency**
Fast fluid bed	Cold gas efficiency [%]	86.0	85.0	83.0	83.2	84.3
	Blower consumptions [MW_e]	0.80	0.64	0.78	0.61	
	Total efficiency [%][a]	84.4	83.7	81.4	82.0	82.9
	POX temperature [°C]	1050	1200	1050	1200	
	Steam consumption [kg-steam/kg-fuel(dry)]	0.60	1.00	0.84	0.92	
Slow fluid bed	Cold gas efficiency [%]	86.6	87.2	84.2	84.9	85.7
	Blower consumption [MW_e]	0.81	0.70	1.21	1.10	
	Total efficiency [%]	85.0	85.8	81.8	82.7	83.8
	POX temperature [°C]	1236	1413	1291	1454	
	Steam consumption [kg-steam/kg-fuel(dry)]	1.02	1.22	2.41	2.48	
Fixed bed	Cold gas efficiency [%]	86.8	89.3	86.5	87.7	87.5
	Blower consumption [MW_e]	0.20	0.10	0.20	0.10	
	Total efficiency [%]	86.4	89.1	86.1	87.5	87.3
	POX temperature [°C]	1395	1585	1339	1462	
	Steam consumption [kg-steam/kg-fuel(dry)]	1.34	1.41	2.04	2.05	

Table 7 – Main results from modeling.

4.1 Parameter studies

This section will investigate some key parameters from the modeling. The main focus will be on values related to the significant ejector steam consumption. The investigations will deal with the Fixed bed system as it is the system with the highest efficiency, but similar variations for the other concepts should yield similar results.

As the system is projected to use a variety of fuels that features a variety of ash composition, the maximum allowable temperature in the gasifier might vary – depend on the degree of agglomeration. Other aspects such as the use of anti-slagging additives or detailed fuel mixing might also raise the critical temperature. This has been observed in two recent studies on fluid bed combustion straw versus co-combustion of straw and sewage sludge. Fuel mixing of sludge (10-30wt%) and straw increased the initial deformation temperature of the fuel ash from 750 °C in the straw fired system to 960-970 °C in the co-fired system, while the agglomeration tendency was decreased and the defluidization time prolonged [81,82]. This temperature is of interest as it will result on limited cooling demand from the ejector outlet gas – and hence reduce the ejector steam consumption. The design gasifier inlet temperature is compared to a +50°C scenario in Table 8. It is seen that by increasing the temperature, the steam consumptions significantly decrease by 28% and 45% for wood and straw respectively. This indicates that straw could preferably be co-fired with other fuels or additives which would increase ash melting and bed agglomeration temperatures. Recent co-firing studies with straw have indicated that this may be achieved by mixing with fuels rich in especially sulfur and phosphorus [81,82].

The pressure loss of the fluid bed gasifier is somewhat unknown as the system design has not been finally specified. The loss is related to several aspects including bed height and gas velocity (fluidization regime) [72] and both of these should be reduced if a lower pressure loss is desired. A varying pressure loss is given in Table 8 and is seen to be less important than the maximum inlet temperature. For all cases shown in Table 8, the efficiencies stays within ±1% and POX temperatures within 30°C.

Gasifier max temperature [°C]	Gasifier pressure loss [mbar]	Steam consumption [kg-steam/kg-fuel(dry)]
Wood fuel, air		
900	146	1.34
900	250	1.51
900	350	1.74
950	146	0.97
950	350	1.33
Straw fuel, air		
780	146	2.04
780	250	3.06
780	350	3.47
830	146	1.13
830	350	1.72

Table 8 – Parameter study of the gasifier max temperature and pressure loss for the Fixed bed system using air and wood/straw

The carbon conversion is set to 95% as a design value and is typically a value that can be changed and based on the system design. This value can however be significantly lower and are in the range of 80-95% for most traditional fluid bed gasifiers [45]. While a higher conversion than the design value seems unrealistic for a fluid bed system, lower rates might be feasible if it can simplify the system and/or provide a valuable biochar product. Optimizing thermal conversion systems towards co-production of high quality and high value biochar products may increase the product portfolio and economical robustness of the plant [83]. Straw scenarios for the Fixed bed system are examined for varying carbon conversions because: 1)

straw contains significantly more inorganics compared to wood and hence are more interesting from a inorganic/nutrient perspective; and 2) has higher steam consumptions. From an agricultural perspective, carbon conversion should be restricted to maximum 80–86% and the carbon rich ash/biochar returned to the straw production site if the natural balance is to be maintained [84]. This will remedy some of the negative effects of removing straw from the agricultural system, and such a compromise between energy efficiency and biochar production can be beneficial in terms of long term soil productivity and the overall climate change impact of an integrated wheat production and bioenergy system [84].

The carbon conversion has a significant effect on the process parameters as shown in Table 9. Every 5% of decrease results in a cold gas efficiency loss of 3.5-4.0%, which will either increase the fuel consumption or reduce the gas product, but possibly increase any profit from biochar sales.
The influence on the POX temperatures and subsequent ejector steam consumption are significant. The POX is still able to maintain its high tar conversion at 80% carbon conversion and the steam consumption is reduced by roughly 20-25% for every 5% decrease from the design value.

Carbon conversion [%]	POX temperature [^{o}C]	Steam consumption [kg-steam/kg-fuel(dry)]	Cold gas efficiency [%]
Straw fuel, **air**			
95	1339	2.04	86.5
90	1279	1.55	82.9
85	1221	1.11	79.2
80	1166	0.70	75.4
Straw fuel, **oxygen**			
95	1462	2.05	87.7
90	1382	1.57	83.9
85	1307	1.12	80.1
80	1237	0.71	76.3

Table 9 – Parameter study of the carbon conversions influence on process parameters for the Fixed bed system using straw and air/oxygen

As subjects for further modeling studies, two more design alternations could be made.

- Utilizing cooled product gas as the ejector motive fluid would drastically minimize the impact of dilution and eliminate the steam consumption completely. This could be implemented by e.g. a water quench and subsequent compression to a few bars. Alternately, wet fuels could be steam dried and the steam could afterwards be used in the ejector.
- Pneumatically transport of char from the pyrolyzer to the gasifier could be implemented for the fixed bed design. Using high velocity POX gas to transport the char would reduce the steam consumption significantly, as the hot gases would cool via endothermic char gasification reactions and hence reduce the ejector flow. Ashes are not expected to sinter, as they would be encapsulated in the initial char matrix and hence limit sintering [85,86].

4.2 Evaluation and perspectives

The choice of which of the three systems are the best will naturally depend on the specific business case. Initially the Fixed bed system looks the most favorable due to its high efficiency and reasonable steam

consumption. The fluid bed systems do however have an advantage with regards to particle sizes, as they will not necessarily require chipped, pelletized or briquetted fuel. This is a distinct advantage when considering the discussed fuel flexibility and corresponding cost reduction. However, as the current market dictates that wood is the primary fuel for gasifiers, the Fixed bed system is likely the currently best performing plant. Preferably, the gasifier residues/biochar can be considered a product, which could justify reducing the carbon conversion and hence a lower steam consumption. While a low pressure loss is beneficial, a better mixed fluid bed reactor[1] might be more relevant, as the increased mixing could limit agglomeration (allow a higher maximum gasifier temperature) and slightly increase carbon conversion. In order to streamline the equipment dimensioning and processes, the carbon conversion could be slightly lowered for straw to match wood operation. These conditions would cause steam consumptions in the range of 1.0-1.4 for wood[2] and straw[3] with efficiencies around 84-88% and 76-80% respectively. At these modified conditions the POX temperature will still be ≥1200^{o}C across air/oxygen and wood/straw.

In order to assess the feasibility of the proposed systems, a comparison of the Fixed bed system, with the modified values discussed above to current, relevant gasification technologies are presented in Table 10. Compared to the Viking TwoStage gasifier, the performance is similar, but the design allows higher process stability (easier pressure control in gasifier compared to the downdraft reactor) and much higher fuel flexibility – that can result in reductions of costs up to 50% (Section 1).
Other fluid bed gasifier are seen to achieve a roughly 10% lower cold gas efficiency when using wood, while also applying much more complex and expensive gas cleaning. When the Fixed bed system applies straw the cold gas efficiency is similar to the other fluid bed gasifiers.
The LT-CFB gasifier achieves the same efficiency when including the high chemical energy content of the tars. The LT-CFB is originally designed for co-firing in large steam power plants, but is currently limited beyond this application because of the tar content. The designed systems in this study will be able to process straw and utilize them in a variety of applications including combustion engines, gas turbine, boilers and synthesis.

	Process	Fuels	Gas cleaning[a]	Cold gas efficiency (dry)	Reference
Fixed bed system with modified design values	Two-stage fixed and fluid bed	Wood, straw and more[b] (chips/pellets)	Might need carbon filter in air-straw mode (POX = 1200^{o}C)	Wood: 84-88% Straw: 76-80%	This study
TwoStage Viking gasifier	Two-stage moving/fixed bed	Wood (chips)	-	87%	[7]
LT-BIG	Two-stage coupled fluid beds	Wood	Carbon filter	81%	[16]
Skive gasifier	Turbulent fluid bed	Wood	Catalytic bed material, catalytic reformer, scrubber	77%[c]	[87]
FICFB	Indirect gasification,	Wood	Catalytic bed	55-75%	[88][89]

[1] As stated in Table 5, the design pressure drop of 146mbar is for minimum fluidization
[2] Estimating 925^{o}C, 250mbar pressure loss and 90-95% carbon conversion
[3] Estimating 780^{o}C, 250mbar pressure loss and 80-85% carbon conversion

	coupled fluid beds		material, scrubber		
MILENA	Indirect gasification, coupled fluid beds	Wood	Catalytic bed material, scrubber	78%	[47][90]
LT-CFB	Coupled fluid beds	Wood, straw, wastes etc.	-	80%[d]	[49]

Table 10 – Comparison of the Fixed bed system with modified design values and relevant gasification technologies. [a]Particle filter not included. [b]Fuel flexibility depends on agglomeration temperatures. [c]Assuming 40% gas-to-power engine efficiency [91]. [d]The low-temperature gasifier product gas has a very high tar content that constitutes up to 50% of the chemical energy, which is included here.

5 Conclusions

This study has presented the findings of a product development study of the TwoStage gasifier. It was desired to design a plant based on the TwoStage principles that featured upscaling potential, a high level of fuel flexibility and was compatible with the grid-balancing Polygeneration concept. By investigating multiple plant configurations using wood/straw fuels and air/oxygen the following conclusions can be made:

- Relatively high level of process stability can be obtained in spite of the varying conditions
- Very high partial oxidation temperatures of >1230^{o}C for two of the concepts will ensure a very low level of downstream gas cleaning
- Very high cold gas efficiencies of 83-89% across wood/straw and air/oxygen for the three different systems displays the effectiveness of the overall concept idea
- A selected and modified design achieved a slightly lower cold gas efficiency (84-88%) with wood and air compared to the TwoStage Viking gasifier, but outperformed competing gasifiers with roughly 10%-points while having increased flexibility

6 Acknowledgements

The authors would like to thank the ForskVE-programme of Energinet.dk for financial support through the Biomass Gasification Polygeneration project (ForskVE-12205).

7 References

[1] International Energy Agency. Technology Roadmap: Hydrogen and fuel cells. 2015. doi:10.1007/SpringerReference_7300.

[2] Sigurjonsson HÆ, Clausen LR. Solution for the future smart energy system: A polygeneration plant based on reversible solid oxide cells and biomass gasification producing either electrofuel or power. Appl Energy 2018;216:323–37. doi:10.1016/j.apenergy.2018.02.124.

[3] Gadsbøll RØRØ, Thomsen J, Bang-Møller C, Ahrenfeldt J, Henriksen UBUB. Solid oxide fuel cells powered by biomass gasification for high efficiency power generation. Energy 2017;131:198–206. doi:10.1016/j.energy.2017.05.044.

[4] Clausen LR. Energy efficient thermochemical conversion of very wet biomass to biofuels by integration of steam drying, steam electrolysis and gasification. Energy 2017;125:327–36. doi:10.1016/j.energy.2017.02.132.

[5] Bang-Moeller C. Design and Optimization of an Integrated Biomass Gasification and solid oxide fuel cell system. Technical University of Denmark, 2010.

[6] Henriksen U, Ahrenfeldt J, Jensen TK, Gøbel B, Bentzen JD, Hindsgaul C, et al. The design,

construction and operation of a 75 kW two-stage gasifier. Energy 2006;31:1542–53. doi:10.1016/j.energy.2005.05.031.

[7] Ahrenfeldt J, Henriksen UB, Jensen TK, Gøbel B, Wiese L, Kather A, et al. Validation of a continuous combined heat and power (CHP) operation of a Two-Stage biomass gasifier. Energy & Fuels 2006;20:2672–80.

[8] Gadsbøll RØ, Sarossy Z, Jørgensen L, Ahrenfeldt J, Henriksen UB. Oxygen-blown operation of the TwoStage gasifier. Energy 2018. doi:10.1016/j.energy.2018.06.071.

[9] Ahrenfeldt J, Thomsen TP, Henriksen U, Clausen LR. Biomass gasification cogeneration – A review of state of the art technology and near future perspectives. Appl Therm Eng 2013;50:1407–17. doi:10.1016/j.applthermaleng.2011.12.040.

[10] International Renewable Energy Agency. Renewable energy technologies: cost analysis series. Biomass for Power Generation. 2012.

[11] Bentzen JD, Hummelshøj R, Henriksen UB, Gøbel B, Ahrenfeldt J, Elmegaard B. Upscale of the Two-Stage Gasification. Proc. 2nd world Conf. Technol. Exhib. biomass energy Ind., 2004.

[12] Devi L, Ptasinski KJ, Berends RH, Padban N, Beesteheerde J, Veringa HJ. Primary measures to reduce tar formation in fluidised-bed biomass gasifiers. 2004.

[13] Hannula I. Hydrogen enhancement potential of synthetic biofuels manufacture in the European context: A techno-economic assessment. Energy 2016;104:199–212. doi:10.1016/B978-0-08-022703-0.50014-8.

[14] Henrich E, Dahmen N, Dinjus E. Cost estimate for biosynfuel production via biosyncrude gasification. Biofuels, Bioprod Biorefining 2009;3:28–41. doi:10.1002/bbb.

[15] International Energy Agency. Technology Roadmap - Bioenergy for Heat and Power. 2012.

[16] Andersen L, Elmegaard B, Qvale B, Henriksen U. Modeling the low-tar BIG gasification concept. Proc. 16. Int. Conf. Effic. Cost, Optim. Simulation, Environ. Impact Energy Syst., 2003, p. 7.

[17] Wendel CH, Kazempoor P, Braun RJ. Novel electrical energy storage system based on reversible solid oxide cells : System design and operating conditions. J Power Sources 2015;276:133–44. doi:10.1016/j.jpowsour.2014.10.205.

[18] IEA. Key World Energy Statistics 2016. Paris, France: 2016. doi:10.1787/9789264039537-en.

[19] WBA. Global Biomass Potential Towards 2035 2016:6.

[20] Fytili D, Zabaniotou A. Utilization of sewage sludge in EU application of old and new methods-A review. Renew Sustain Energy Rev 2008;12:116–40. doi:10.1016/j.rser.2006.05.014.

[21] LeBlanc RJ, Matthews P, Richard RP. Global Atlas of Excreta, Wastewater Sludge, and Biosolids Management: Moving Forward the Sustainable and Welcome Uses of a Global Resource. Nairobi, Kenya: UN-HABITAT; 2008. doi:10.2175/193864709793846402.

[22] Kang SW, Dong JI, Kim JM, Lee WC, Hwang WG. Gasification and its emission characteristics for dried sewage sludge utilizing a fluidized bed gasifier. J Mater Cycles Waste Manag 2011;13:180–5. doi:10.1007/s10163-011-0016-y.

[23] Chen Y-C. Potential for energy recovery and greenhouse gas mitigation from municipal solid waste using a waste-to-material approach. Waste Manag 2016;In Press:1–7. doi:10.1016/j.wasman.2016.09.007.

[24] Han Z, Ma H, Shi G, He L, Wei L, Shi Q. A review of groundwater contamination near municipal solid waste landfill sites in China. Sci Total Environ 2016;569:1255–64. doi:10.1016/j.scitotenv.2016.06.201.

[25] Havukainen J, Zhan M, Dong J, Liikanen M, Deviatkin I, Li X, et al. Environmental impact assessment of Municipal solid waste management incorporating mechanical treatment of waste and incineration in Hangzhou, China. J Clean Prod 2016;141:453–61. doi:10.1016/j.jclepro.2016.09.146.

[26] Zaman AU, Swapan MSH. Performance evaluation and benchmarking of global waste management systems. Resour Conserv Recycl 2016;114:32–41. doi:10.1016/j.resconrec.2016.06.020.

[27] World Bioenergy Association. WBA fact sheet: BIOGAS – An important renewable energy source. Stockholm, Sweden: WBA; 2013.

[28] Teenstra E, Vellinga T, Aektasaeng N, Amatayakul W, Ndambi A, Pelster D, et al. Global Assessment of Manure Management Policies and Practices. AH Wageningen, The Netherlands: 2014.

[29] van Dijk KC, Lesschen JP, Oenema O. Phosphorus flows and balances of the European Union Member States. Sci Total Environ 2016;542:1078–93. doi:10.1016/j.scitotenv.2015.08.048.

[30] Koopmans A, Koppejan J. Agricultural and forest residues -generation, utilization and availability. Proc. Reg. Expert Consult. Mod. Appl. Biomass Energy, FAO Reg. Wood Energy Dev. Program. Asia, Rep. No. 36, Bangkok., FAO; 1998, p. 23.

[31] Food and Agriculture Organization of the United Nations. FAOSTAT - Crops. Online Stat Database 2017.

[32] Thomsen TP, Ahrenfeldt J. Scenario based assessment of domestic biomass potential and technical application for energy production in Denmark – now and near future. 2013.

[33] Zsirai I. Sewage Sludge as Renewable Energy. J Residuals Sci Technol 2011;8:165–79.

[34] Spliethoff H. Power Generation from Solid Fuels. Berlin, Heidelberg: Springer Berlin Heidelberg; 2010. doi:10.1007/978-3-642-02856-4.

[35] Narayan V, Jensen PA, Henriksen UB, Glarborg P, Lin W, Nielsen RG. Defluidization in fluidized bed gasifiers using high-alkali content fuels. Biomass and Bioenergy 2016;91:160–74. doi:10.1016/j.biombioe.2016.05.009.

[36] Stoholm P, Nielsen RG, Sarbæk L, Tobiasen L, Fock MW, Richardt K, et al. The Low Temperature CFB gasifier - Further test results and possible applications. Proc. 12. Eur. Biomass Conf., 2002, p. 706–9.

[37] Ohman M, Pommer L, Nordin A. Bed Agglomeration Characteristics and Mechanisms during Gasification and Combustion of Biomass Fuels. Energy & Fuels 2005;19:1742–8.

[38] Zevenhoven-onderwater M, Marcus O, Skrifvars B-J, Backman R, Nordin A, Hupa M. Bed Agglomeration Characteristics of Wood-Derived Fuels in FBC. Energy & Fuels 2006;20:818–24.

[39] Chaivatamaset P, Sricharoon P, Tia S, Bilitewski B. The characteristics of bed agglomeration/defluidization in fluidized bed firing palm fruit bunch and rice straw. Appl Therm Eng

2014;70:737–47. doi:10.1016/j.applthermaleng.2014.05.061.

[40] Mac an Bhaird ST, Walsh E, Hemmingway P, Maglinao AL, Capareda SC, McDonnell KP. Analysis of bed agglomeration during gasification of wheat straw in a bubbling fluidised bed gasifier using mullite as bed material. Powder Technol 2014;254:448–59. doi:10.1016/j.powtec.2014.01.049.

[41] Ergudenler A, Ghaly AE. AGGLOMERATION OF SILICA SAND IN A FLUIDIZED BED GASIFIER OPERATING ON WHEAT STRAW. Biomass and Bioenergy 1993;4:135–47.

[42] van der Drift A, Olsen A. Conversion of biomass, Prediction and Solution Methods for Ash Agglomeration and Related Problems. Final Report, Non-Nuclear Energy Program Joule 3 1999.

[43] Serrano D, Sánchez-Delgado S, Sobrino C, Marugán-Cruz C. Defluidization and agglomeration of a fluidized bed reactor during Cynara cardunculus L. gasification using sepiolite as a bed material. Fuel Process Technol 2015;131:338–47. doi:10.1016/j.fuproc.2014.11.036.

[44] Gatternig B, Karl J. The influence of particle size, fluidization velocity and fuel type on ash-induced agglomeration in biomass combustion. Front Energy Res 2014;2:1–12. doi:10.3389/fenrg.2014.00051.

[45] Basu P. Combustion and gasification in fluidized beds. Taylor & Francis; 2006.

[46] Bentzen JD, Hummelshøj R, Henriksen U, Ahrenfeldt J. Storskala trinopdelt forgasning. 2004.

[47] Meijden CM van der, Veringa HJ, Vreugdenhil BJ, Drift B van der. Bioenergy II: Scale-Up of the Milena Biomass Gasification Process. Int J Chem React Eng 2009;7. doi:10.2202/1542-6580.1898.

[48] Thomsen TP, Sárossy Z, Gøbel B, Stoholm P, Ahrenfeldt J, Jappe F, et al. Low temperature circulating fluidized bed gasification and co-gasification of municipal sewage sludge . Part 1 : Process performance and gas product characterization. Waste Manag 2017;66:123–33. doi:10.1016/j.wasman.2017.04.028.

[49] Nielsen RG. Optimering af Lav Temperatur Cirkulerende Fluid Bed forgasningsprocessen til biomasse med højt askeindhold. Phd thesis. Lyngby, Denmark: Technical University of Denmark; 2007.

[50] Hofbauer H, Fercher E, Fleck T, Rauch R, Veronik G. Two years experience with the FICFB-gasification process. 10th Eur Conf Technol Exhib Wurzbg 1998:3–6.

[51] Hofmann P, Panopoulos KD, Aravind PV, Siedlecki M, Schweiger A, Karl J, et al. Operation of solid oxide fuel cell on biomass product gas with tar levels >10 g Nm^-3. Int J Hydrogen Energy 2009;34:9203–12. doi:10.1016/j.ijhydene.2009.07.040.

[52] Hofmann P, Panopoulos K, Fryda L, Schweiger a, Ouweltjes J, Karl J. Integrating biomass gasification with solid oxide fuel cells: Effect of real product gas tars, fluctuations and particulates on Ni-GDC anode. Int J Hydrogen Energy 2008;33:2834–44. doi:10.1016/j.ijhydene.2008.03.020.

[53] Aravind PV, de Jong W. Evaluation of high temperature gas cleaning options for biomass gasification product gas for Solid Oxide Fuel Cells. Prog Energy Combust Sci 2012;38:737–64. doi:10.1016/j.pecs.2012.03.006.

[54] Basu. Biomass Gasification, Pyrolysis and Torrefraction. Second Edi. Dalhouse University: Elsevier Inc.; 2013.

[55] Kienberger T, Zuber C. Synthetic Natural Gas from Coal, Dry Biomass, and Power-to-Gas

Applications. 1st ed. John Wiley & sons inc.; 2016. doi:10.1002/9781119191339.

[56] Brandt P, Larsen E, Henriksen U. High tar reduction in a two-stage gasifier. Energy and Fuels 2000;14:816–9. doi:10.1021/ef990182m.

[57] Gerun L, Paraschiv M, Vîjeu R, Bellettre J, Tazerout M, Gøbel B, et al. Numerical investigation of the partial oxidation in a two-stage downdraft gasifier. Fuel 2008;87:1383–93. doi:10.1016/j.fuel.2007.07.009.

[58] Brandt P, Henriksen U. Decomposition of tar in pyrolysis gas by partial oxidation and thermal cracking. Part 2. Proc Conf 10th Eur Conf Technol Exhib Biomass Energy Ind 1998:1616–9.

[59] Su Y, Luo Y, Chen Y, Wu W, Zhang Y. Experimental and numerical investigation of tar destruction under partial oxidation environment. Fuel Process Technol 2011;92:1513–24. doi:10.1016/j.fuproc.2011.03.013.

[60] Zhao S, Luo Y, Zhang Y, Long Y. Experimental investigation of the synergy effect of partial oxidation and bio-char on biomass tar reduction. J Anal Appl Pyrolysis 2015;112:262–9. doi:10.1016/j.jaap.2015.01.016.

[61] Ahrenfeldt J, Egsgaard H, Stelte W, Thomsen T, Henriksen UB. The influence of partial oxidation mechanisms on tar destruction in TwoStage biomass gasification. Fuel 2013;112:662–80. doi:10.1016/j.fuel.2012.09.048.

[62] Wu WG, Luo YH, Chen Y, Su Y, Chen L, Wang Y. Experimental Investigation of Tar Destruction Under Partial Oxidative Condition in a Continuous Reactor 2011:900.

[63] Brandt P, Henriksen U. Decomposition of tar in gas from updraft gasifier by thermal cracking. 1st World Conf Biomass Energy Ind 2000:3.

[64] Jensen TK, Maigaard P, Noes J. Pyrolyse af træflis ved recirkulering af pyrolysegas. 1996.

[65] Ahrenfeldt J, Henriksen UB, Gøbel B, Fjellerup J. Experimental characterisation of residual-tar in wood char. 2005.

[66] Elmegaard B, Houbak N. DNA – A General Energy System Simulation Tool. DNA – A Gen. Energy Syst. Simul. Tool, SIMS 2005 and Tapir Academic Press; 2005, p. 43–52.

[67] Technical University of Denmark. Homepage of the thermodynamic simulation tool DNA. DNA - A Therm Energy Syst Simulator 2009. http://orbit.dtu.dk/en/publications/id(b76040a4-5a29-4b04-a898-12711391c933).html (accessed March 24, 2017).

[68] Thomsen T, Hauggaard-Nielsen H, Bruun E, Ahrenfeldt J. the potential of pyrolysis technology in climate change mitigation. 2011.

[69] Iversen HL, Ahrenfeldt J, Egsgaard H, Henriksen UB. Partial oxidation mechanisms of tar destruction [Confidential]. 2006.

[70] Elmegaard B. Simulation of boiler dynamics - Development, evaluation and application of a general energy system simulation tool. Technical University of Denmark, 1999.

[71] GEA Wiegand GmbH. GEA product catalogue. Jet pumps, mixers, heater, vacuum systems. 2017. doi:10.1002/ejoc.201200111.

[72] Kunii D, Levenspiel O. Fluidization Engineering. 2nd ed. Butterworth-Heinemann; 1991.

[73] Trinh TN, Jensen PA, Kim DJ, Knudsen NO, Sørensen HR, Hvilsted S. Comparison of lignin, macroalgae, wood, and straw fast pyrolysis. Energy and Fuels 2013;27:1399–409. doi:10.1021/ef301927y.

[74] Pedersen ST, Andersen SM. Pyrolyse af træflis. 2001.

[75] Vassilev S V., Baxter D, Andersen LK, Vassileva CG. An overview of the chemical composition of biomass. Fuel 2010;89:913–33. doi:10.1016/j.fuel.2009.10.022.

[76] Fahmi R, Bridgwater A V., Donnison I, Yates N, Jones JM. The effect of lignin and inorganic species in biomass on pyrolysis oil yields, quality and stability. Fuel 2008;87:1230–40. doi:10.1016/j.fuel.2007.07.026.

[77] Scott DS, Majerski P, Piskorz J, Radlein D. A second look at fast pyrolysis of biomass — the RTI process 1999;51:23–37.

[78] Bentzen JD, Gøbel B. Dynamisk model af totrins-forgasningsprocessen. 1995.

[79] Mani T, Murugan P, Mahinpey N. Pyrolysis of oat straw and the comparison of the product yield to wheat and flax straw pyrolysis. Energy and Fuels 2011;25:2803–7. doi:10.1021/ef200546v.

[80] Channiwala SA, Parikh PP. A unified correlation for estimating HHV of solid , liquid and gaseous fuels. Fuel 2002;81:1051–63.

[81] Skoglund N, Grimm A, Öhman M, Boström D. Effects on ash chemistry when co-firing municipal sewage sludge and wheat straw in a fluidized bed: Influence on the ash chemistry by fuel mixing. Energy and Fuels 2013;27:5725–32. doi:10.1021/ef401197q.

[82] Ren Q, Li L. Co-combustion of Agricultural Straw with Municipal Sewage Sludge in a Fluidized Bed: Role of Phosphorus in Potassium Behavior. Energy and Fuels 2015;29:4321–7. doi:10.1021/acs.energyfuels.5b00790.

[83] Cha JS, Park SH, Jung SC, Ryu C, Jeon JK, Shin MC, et al. Production and utilization of biochar: A review. J Ind Eng Chem 2016;40:1–15. doi:10.1016/j.jiec.2016.06.002.

[84] Sigurjonsson HÆ, Elmegaard B, Clausen LR, Ahrenfeldt J. Climate effect of an integrated wheat production and bioenergy system with Low Temperature Circulating Fluidized Bed gasifier. Appl Energy 2015;160:511–20. doi:10.1016/j.apenergy.2015.08.114.

[85] Kurkela, E., Laatikainen-Luntama, J., Ståhlberg, P. & Moilanen A. Pressurised fluidised-bed gasification experiments with biomass, peat and coal at VTT, VTT in 1991-–1994. Part 3. Gasification of Danish wheat straw and coal. Espoo, Finland: VTT Publications; 1996.

[86] Skrifvars BJ, Hupa M, Moilanen A, Lundqvist R. Characterization of biomass ashes. In: Baxter L, DeSollar R, editors. Appl. Adv. Technol. to ash-related Probl. Boil., New York: Plenum Press; 1996, p. 383–98.

[87] Andritz, Carbona. Carbona Gasification Technologies - Biomass Gasification Plant in Skive. October 2010:28–9.

[88] Hofbauer H, Rauch R. Stoichiometric Water Consumption of Steam Gasification by the FICFB-Gasification Process. Prog Thermochem Biomass Convers 2008:199–208.

doi:10.1002/9780470694954.ch14.

[89] Hofbauer H, Rauch R, Loeffler G, Kaiser S, Fercher E, Tremmel H. Six years experience with the FICFB-gasification process. 12th Eur Conf Technol Exhib Biomass Energy, Ind Clim Prot 2002:982–985.

[90] Rhyner U, Kienberger T, Zuber C, Schildhauer TJ, Rabou LPLM, Van der Drift B, et al. Synthetic Natural Gas from Coal, Dry Biomass, and Power-to-Gas Applications. First edit. John Wiley & sons Ltd; 2016. doi:10.1002/9781119191339.

[91] Jenbacher type 6 gas engines n.d. https://powergen.gepower.com/products/reciprocating-engines/jenbacher-type-6.html (accessed March 29, 2017).

Appendix - model data

Fixed bed system

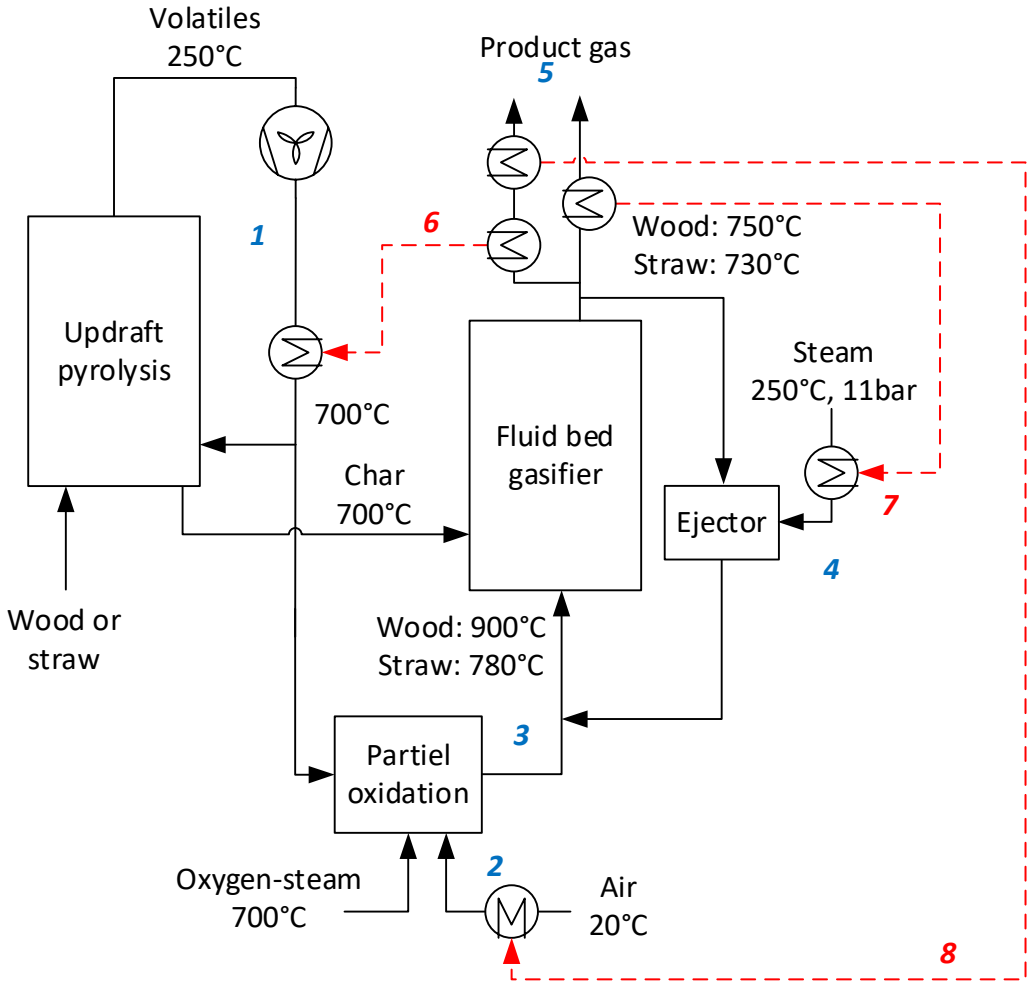

Table A1 – Fixed bed system product gas compositions and lower heating values

	H_2	CO_2	CO	CH_4	H2O	N_2	LHV_{wet}	LHV_{dry}
	[v%]	[v%]	[v%]	[v%]	[v%]	[v%]	[MJ/kg]	[MJ/kg]
Air, wood	27.1	13.2	8.0	0.0	34.4	17.2	4.482	6.542

Air, straw	24.8	12.4	4.3	0.0	51.0	7.4	3.902	7.767
Oxygen, wood	32.2	15.3	8.6	0.0	43.9	0.0	5.783	10.47
Oxygen, straw	26.7	13.2	4.5	0.0	55.6	0.0	4.381	10.16

Table A2 – Data values

Data point	Value	Unit
Air-blown, wood		
1	259	[°C]
2	328	[°C]
3	1395	[°C]
4	574	[°C]
5	300	[°C]
6	4.53	[MW_{th}]
7	2.57	[MW_{th}]
8	0.76	[MW_{th}]
Oxygen-blown, wood		
1	259	[°C]
2	700	[°C]
3	1585	[°C]
4	571	[°C]
5	306	[°C]
6	4.53	[MW_{th}]
7	2.68	[MW_{th}]
8	-	[MW_{th}]
Air-blown, straw		
1	261	[°C]
2	285	[°C]
3	1339	[°C]
4	574	[°C]
5	300	[°C]
6	4.74	[MW_{th}]
7	4.44	[MW_{th}]
8	0.39	[MW_{th}]
Oxygen-blown, straw		
1	260	[°C]
2	700	[°C]
3	1462	[°C]
4	564	[°C]
5	305	[°C]
6	4.74	[MW_{th}]
7	4.34	[MW_{th}]
8	-	[MW_{th}]

Slow fluid bed system

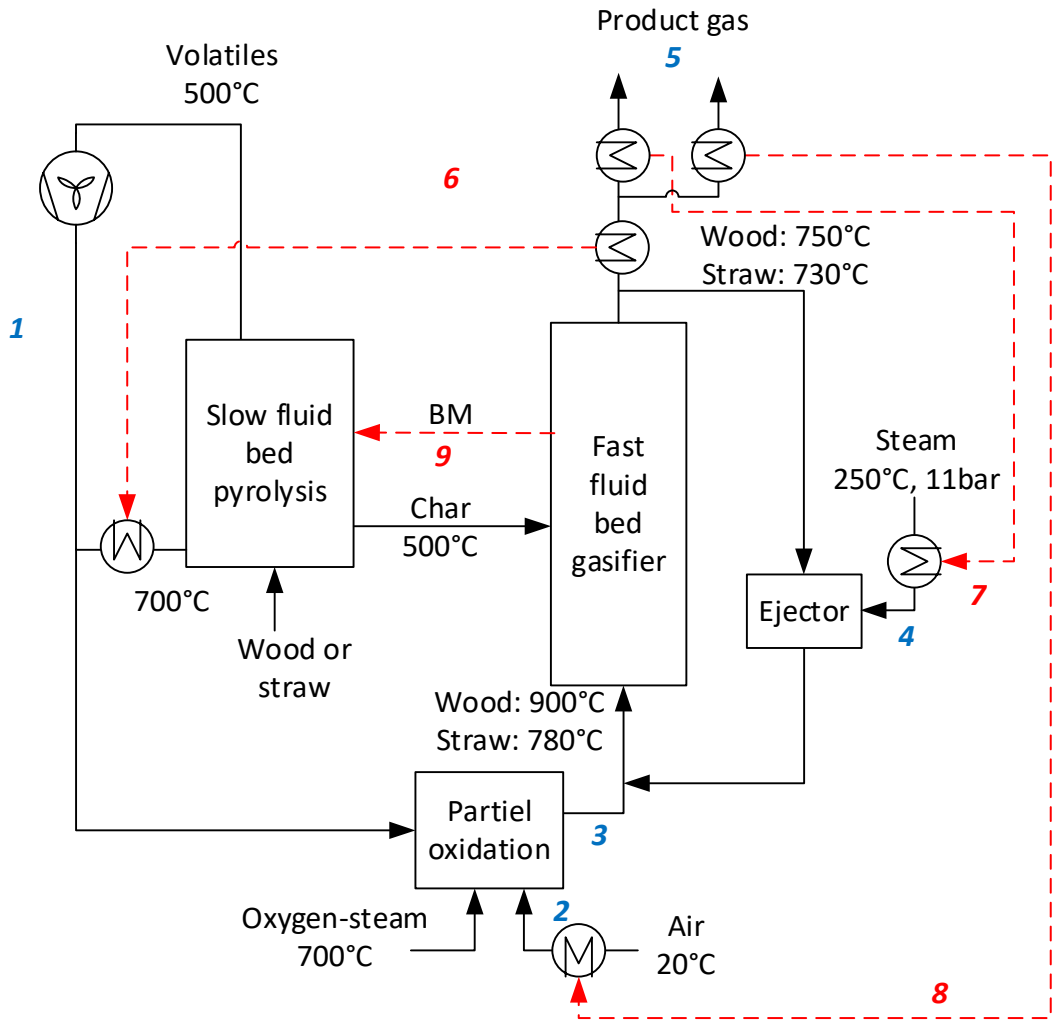

Table A3 – Slow fluid bed system product gas compositions and lower heating values

	H_2	CO_2	CO	CH_4	H2O	N_2	LHV_{wet}	LHV_{dry}
	[v%]	[v%]	[v%]	[v%]	[v%]	[v%]	[MJ/kg]	[MJ/kg]
Air, wood	28.4	12.4	11.0	0.0	26.5	21.4	4.999	6.567
Air, straw	19.6	11.9	3.1	0.0	53.7	11.7	2.871	5.701
Oxygen, wood	33.6	15.2	10.8	0.0	40.4	0.0	6.318	10.75
Oxygen, straw	21.4	12.9	3.1	0.0	62.5	0.0	3.322	8.666

Table A4 – Data values

Data point	Value	Unit
Air-blown, wood		
1	538	[°C]
2	538	[°C]
3	1236	[°C]
4	538	[°C]
5	371	[°C]
6	2.88	[MW_{th}]
7	1.53	[MW_{th}]
8	1.76	[MW_{th}]
9	0.68	[MW_{th}]
Oxygen-blown, wood		
1	538	[°C]
2	-	[°C]
3	1413	[°C]
4	538	[°C]
5	461	[°C]
6	2.86	[MW_{th}]
7	1.83	[MW_{th}]
8	-	[MW_{th}]
9	0.70	[MW_{th}]
Air-blown, straw		
1	545	[°C]
2	578	[°C]
3	1291	[°C]
4	578	[°C]
5	367	[°C]
6	2.98	[MW_{th}]
7	5.48	[MW_{th}]
8	1.83	[MW_{th}]
9	1.12	[MW_{th}]
Oxygen-blown, straw		
1	545	[°C]
2	-	[°C]
3	1454	[°C]
4	573	[°C]
5	415	[°C]
6	2.98	[MW_{th}]
7	5.56	[MW_{th}]
8	-	[MW_{th}]
9	1.12	[MW_{th}]

Fast fluid bed system

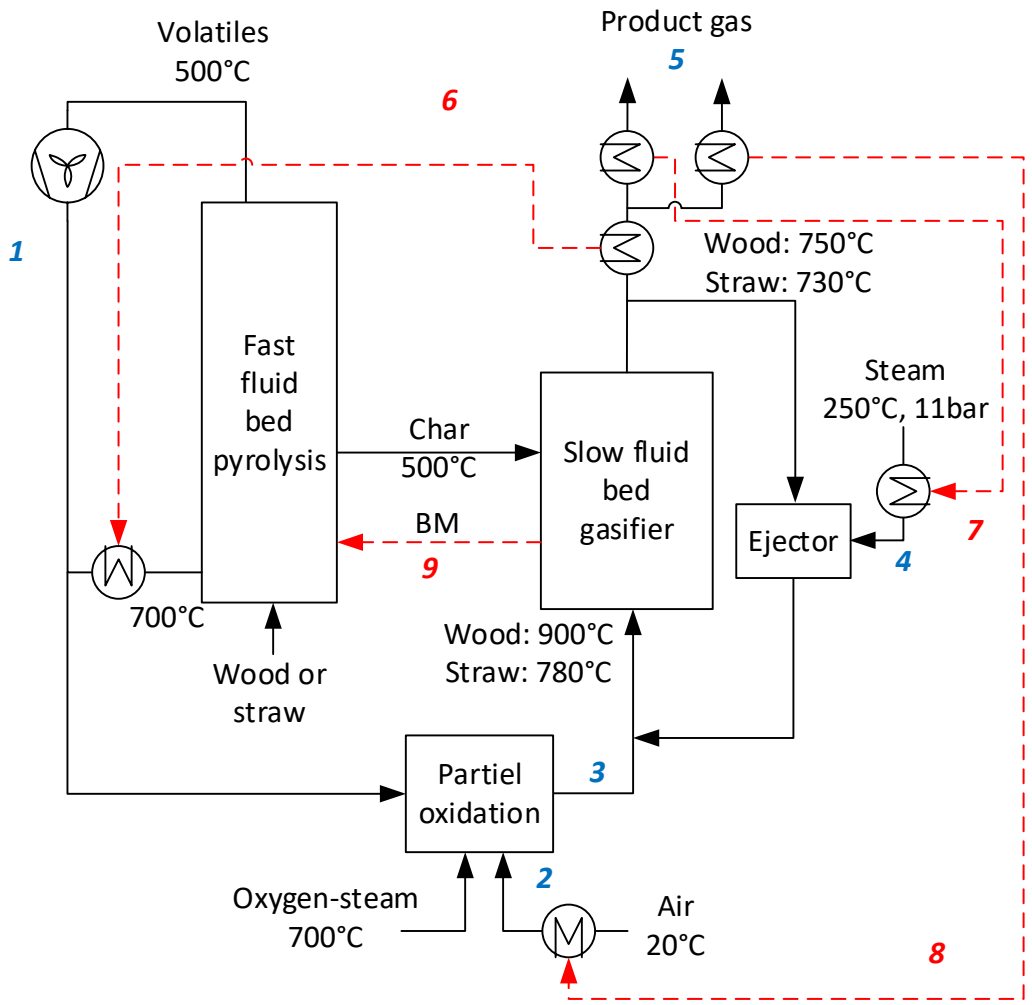

Table A5 – Fast fluid bed system product gas compositions and lower heating values

	H_2	CO_2	CO	CH_4	H2O	N_2	LHV_{wet}	LHV_{dry}
	[v%]	[v%]	[v%]	[v%]	[v%]	[v%]	[MJ/kg]	[MJ/kg]
Air, wood	26.6	11.7	16.3	0.8	18.9	25.3	5.572	6.652
Air, straw	25.4	13.7	9.3	0.6	26.4	24.3	4.428	5.732
Oxygen, wood	32.0	15.5	13.7	0.2	38.6	0.0	6.454	10.40
Oxygen, straw	32.6	17.4	10.1	0.1	39.4	0.4	5.906	9.364

Table A6 – Data values

Data point	Value	Unit
Air-blown, wood		
1	537	[^{o}C]
2	614	[^{o}C]
3	1050	[^{o}C]
4	614	[^{o}C]
5	411	[^{o}C]
6	2.11	[MW_{th}]
7	1.19	[MW_{th}]
8	2.06	[MW_{th}]
9	0.83	[MW_{th}]
Oxygen-blown, wood		
1	536	[^{o}C]
2	-	[^{o}C]
3	1200	[^{o}C]
4	435	[^{o}C]
5	557	[^{o}C]
6	2.07	[MW_{th}]
7	1.90	[MW_{th}]
8	-	[MW_{th}]
9	0.90	[MW_{th}]
Air-blown, straw		
1	531	[^{o}C]
2	551	[^{o}C]
3	1050	[^{o}C]
4	306	[^{o}C]
5	454	[^{o}C]
6	2.13	[MW_{th}]
7	0.28	[MW_{th}]
8	2.10	[MW_{th}]
9	1.12	[MW_{th}]
Oxygen-blown, straw		
1	529	[^{o}C]
2	-	[^{o}C]
3	1200	[^{o}C]
4	235	[^{o}C]
5	585	[^{o}C]
6	2.14	[MW_{th}]
7	0.0	[MW_{th}]
8	-	[MW_{th}]
9	1.12	[MW_{th}]

Thermodynamic analysis of upscaled TwoStage gasifier concepts

Rasmus Østergaard Gadsbøll*[,1], Lasse Røngaard Clausen[2], Jesper Ahrenfeldt[1], Ulrik Birk Henriksen[1]
[1]Technical university of Denmark, Department of chemical and biochemical engineering, Frederiksborgvej 399, 4000 Roskilde, Denmark
[2]Technical university of Denmark, Department of mechanical engineering, Nils Koppels Allé 403, 2800 Kgs. Lyngby, Denmark
*Corresponding author, Tel: +4560668815, E-mail: rgad@kt.dtu.dk

Abstract
The TwoStage biomass gasification process has been developed for many years at the Technical University of Denmark and efforts are being made to upscale the system to 10-100MW_{th}. By applying the principles of: 1) separate pyrolysis and gasification, 2) high internal tar conversion, and 3) effective heat integration, it is expected that large-scale systems with very high efficiencies capable of generating gas with very low tar concentrations can be designed. Four designs are presented and subsequently modeled - two fixed bed and two fluid bed designs. Build on assumptions based on previous experimental work, the results of the modeling show very high cold gas efficiencies of 84.7-93.4% with very limited downstream gas cleaning to obtain a near tar-free gas. This is significantly more efficient than several commercialized medium- and large-scale biomass gasifiers while also applying simpler gas cleaning.

Keywords: Biomass, Gasification, Plant design, Thermodynamic analysis, Two-stage gasifier

1. Introduction
It is desired to design larger gasification plants in order to impact the transition to a green and sustainable energy system via lower specific costs and larger capacities. Several larger gasification plants have shown successful operation, but are associated with relatively complex gas cleaning of tars (if the gas is to be used in a gas engine or fuel synthesis) and/or lower cold gas efficiencies in comparison to efficient small-scale systems such as the TwoStage gasifier concept [1][2][3][4].

The TwoStage biomass gasification concept has been developed for many years at the Technical University of Denmark. It is a staged gasification system with separate pyrolysis and gasification and a partial oxidation (POX) in between. The process has been heavily investigated and documented at smaller scales up to ≈1.5MW_{th} and has displayed its superiority to other systems within several aspects; especially the low tar content of <15mg/Nm^3 [5][6][7][8] and its cold gas efficiency of 93% (wet basis) [5] are key parameters for the system. The current TwoStage design uses an indirectly heated screw conveyer for pyrolysis, in which hot product gas or engine exhaust (depending on design) heats up the wood fuel to 600°C through a metal jacket. Following the pyrolysis, the gases are exposed to a POX with air that increases the temperature to >1100°C. The hot products are then led through a downdraft char bed resting on a grate in order to gasify the char. See Figure 1 for an overview of the TwoStage 'Viking' gasifier. The gasification concept is amongst best performing systems available (see e.g. Table 4 or [9]), which is namely due to two design features: 1) the combination of the separate POX and char bed causes the outlet tar content to be negligibly low and

simplifies the gas cleaning greatly; 2) by converting tars internally and utilizing the sensible heat from product gas/engine exhaust, the resulting cold gas efficiency becomes high and is state-of-the-art.

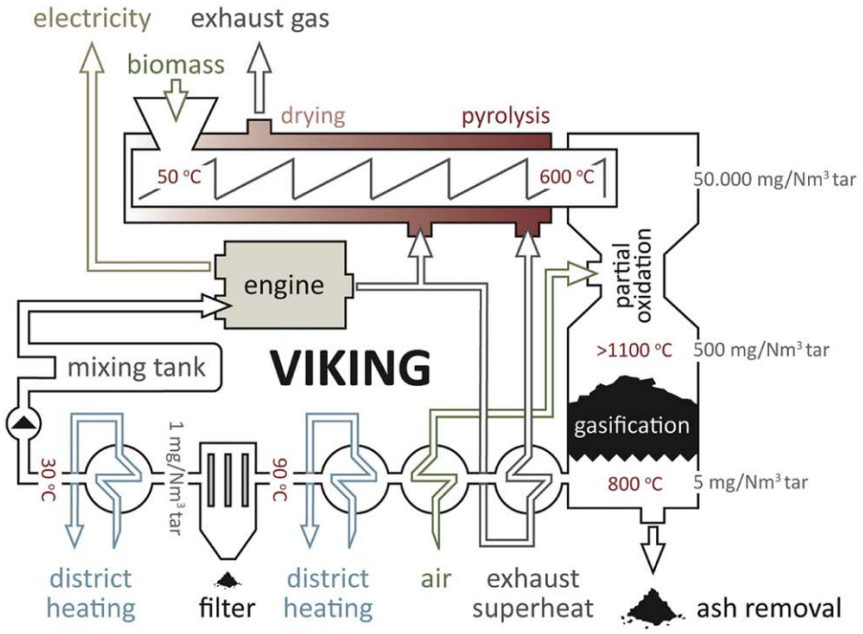

Figure 1 - Flow diagram of the TwoStage Viking gasifier at the Technical University of Denmark with approximate tar concentrations [1]

It is desired to upscale the TwoStage gasification process, but its current design might not scale well as the currently applied reactor technologies are severely challenged both with regards to scaling and fuel flexibility. The indirect heat transfer in the pyrolysis reactor is relatively inefficient and will either require a very large heat transfer surface in a single reactor or multiple reactors, which is likely not feasible when approaching larger scales – it is estimated that the feasible range is <10MW_{th} with in the current design constraints [10]. The downdraft char bed has its limitations with regards to operational control and fuel flexibility, as build-up of fines can cause the pressure drop to increase steeply and either cause a low carbon conversion and/or shut down of the gasifier. Thus the downdraft configuration has strict fuel requirements and is dependent on very well-defined fuel such as wood chips if stable and efficient operation is to be maintained.

1.1 Previuos TwoStage gasifier designs

The two-stage gasification concept has been designed for upscaling three times prior. Initially, an upscaling from around 100kW_{th} to 1.5MW_{th} was carried out during commercialization of the system – see Figure 2. The other two upscalings were redesigns of the concept, for which both applied a fluid bed system with two beds and a POX in between – both are seen in Figure 3. Hansen et al. [11] operated the system in Figure 3 (left) in which fuel was fed into a bubbling bed pyrolyzer, fluidized by recirculated pyrolysis gas, which proved to be an effective process without dilution or combustion losses from air addition. The pyrolysis gasses was then led via a combustion chamber at 1025^{o}C to a gasification reactor where it fluidizes and gasifies the char in a sand bed [11]. The other system in Figure 3 (right), called Low-Tar Biomass Integrated Gasifier (LT-BIG), described by Bentzen et al. [10], featured two fluid bed reactors fluidized by superheated steam, where the pyrolysis gases were led via a POX zone at 1000-1100^{o}C to the gasification reactor bed surface where it contacted the char in a spout. At the spout, the hot POX products

mix with the char at 850°C. The system did however have a tar concentration of around 1g/Nm^3 due to poor contact [4]. It was however shown that the gasifier could produce a near tar-free product gas of 1mg/Nm^3 by using a bag filter and an active carbon filter [4], with a modelled cold gas efficiency around 81% [10].

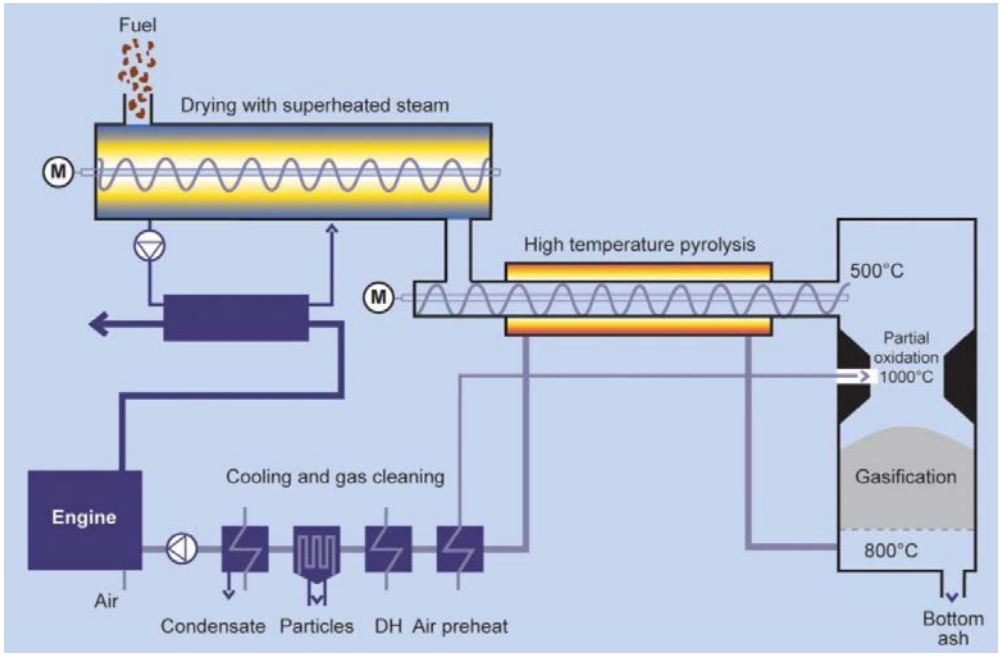

Figure 2 – Design of the upscaled TwoStage gasifier with screw conveyers for separate steam drying and pyrolysis, and a downdraft char bed [9]**.**

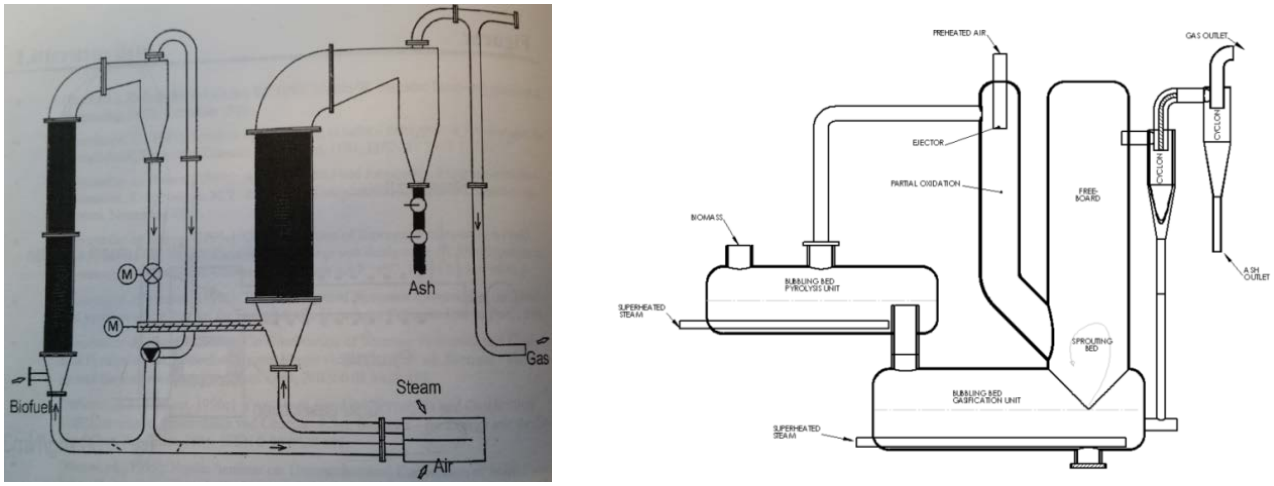

Figure 3 – Fluid bed designs of upscaled TwoStage gasifiers. Left: two-stage fluid bed pyrolysis and gasification unit [11]**. Right: LT-BIG gasifier system** [10]**.**

This study seeks to address these issues and explore alternatives to the current design via implementation of novel concepts and thermodynamic analysis. The framework of the designs is:

- Scalability of ≥10-100MW$_{th}$ as this is the estimated current limit
- Air-blown operation with wet wood chips (50% moisture) for comparison with the current design
- Low tar content of the product gas of ≤1g/Nm^3 in order to limit gas cleaning

- Cold gas efficiency of ≥85% in order to compete with existing gasifier systems and previously upscalings of the system

Through careful analysis and evaluation, four conceptual upscaled TwoStage gasifier designs have been made. These are concepts and not polished or finally optimized designs, as this would require knowledge on specifics such as product gas applications and economics. Hence this paper seeks to lay a developmental foundation for the next generation of TwoStage gasifiers in larger scales and get insight into thermodynamic mechanisms related to the presented designs. The paper presents the basis for design, thermodynamically models of the concepts and evaluation on an energy and exergy basis.

2. Considerations and system designs

2.1 Design basis

The conversion steps of TwoStage gasification concept are: drying, pyrolysis, POX and char gasification. These steps are utilized as the stepping stone for the development of the upscaled designs, which will include novel takes on the physical mechanisms, heat integrations and reactor configurations. Based on various analysis and creative sessions, the following configurations are suggested for the subprocesses.

Drying

Drying requires heat at relatively low temperatures and while it might be found within the gasification plant (sensible heat in pyrolysis or product gas), the high moisture contents applied for this process makes integration with exhaust from the product gas application (e.g. engine) more applicable – this is also applied in current design in Figures 1 and 2. Drying has been shown to effectively integrate with excess heat downstream from e.g. engine/turbine exhaust or synthesis reactors – as seen in previous modeling work on the TwoStage gasifier [12][13][14][15]. In order to limit the study, drying will not be discussed in detail and no reactor suggestions has been made – the suggested configurations for the pyrolysis would however likely be applicable with lower temperatures.

Pyrolysis

Pyrolysis requires a heat amount corresponding to 4-7% of the input fuel-LHV [16] and is mainly complete around 600^{o}C, but only a negligible tar content remains in the fuel around 500^{o}C [17]. Due to the temperature match and coherence, the sensible heat in the product gas should be applied. This can effectively be done at large scales via direct heat transfer via a heat carrier. It is suggested that this could be via recirculated pyrolysis gas or by making the process steam-blown – in the latter case, utilization of drying steam would be an obvious opportunity. If multiple fluid bed systems are applied, the heat requirement can also be supplied by hot bed material flowing from the gasification to the pyrolysis reactor.

Partial oxidation and char conversion

The POX serves two agendas: secure sensible heat sufficient to convert the char and convert tars. The necessary amount of air/ temperature in the POX should therefore be partially determined by the char yield from the pyrolysis unit, which cause larger yields to require higher temperatures and more air. The temperature should naturally consider the char reactor, which will have outlet condition requirements to secure sufficient char reactivity and conversion throughout the reactor, and temperature constraints related to the fuel ashes and materials. Sufficent conversion of char will depend on several factors including

residence time, fuel, reactor etc., but a limit is set at 750°C [18][19] and ≥5vol% steam based on the research groups experiences and estimates.

Partial oxidation and tar conversion

POX is an effective measure to remove tars and often 95-99% of the tars can be converted under proper conditions. As seen in Table 1, the tar concentration can be reduced to 1.0-1.2g/Nm^3 after at the conditions of the current TwoStage and the LT-BIG design (≈1100-1200°C). The table also show that the tar level is approaching negligible levels at 1300°C and above. If high temperatures effectively, the pyrolysis gases should be diluted as little as possible.

Temperature [°C]	Stoichiometric air ratio	Tar content [mg/Nm^3,dry][a]	Reactor conditions	Reference
900	0.5	115	POX	[20]
900	0.34	960	POX	[21]
900	-	2844	POX	[22]
1050	0.4	≈846[b]	POX	[23]
1100	0.34	1000	POX	[24]
1100	-	1150	POX	[25]
1100	0.5	1200	POX	[26]
1100-1200	-	1220	POX	[27]
1200-1300	-	≈100	POX	[25]
1000	0	5000	Thermal treatment	[20]
1100	0	8000	Thermal treatment	[24]
1200	0	385	Thermal treatment	[28]
1250	0	50	Thermal treatment	[28]

Table 1 - Overview of experimental partial oxidation and thermal treatment studies. [a]Based on 2.6nm3/kg gas production from biomass, as for the TwoStage gasifier [26]**. [b]Estimate.**

After the POX, a second conversion step for tars should be implemented, which can be either in the gasification bed or in a separate reactor. In current TwoStage design, the partially oxidized gases are led through the char bed, which couples well with partial oxidation as the char can convert heavier tars that form at the high POX temperatures [26][29][30]. Tar reduction over char is proven for fixed beds where 95-99% of the tars can be converted at 850°C and 0.3-1.2 s of residence time [26][29]. In fluid beds, char is relatively unproven, as it exhibits low mechanical strength and suffers from a high attrition rate. But tests with fluid beds by El-Rub et al. [29] with char as the only bed material have shown reductions of 70-80% when naphthalene was employed as a synthetic tar at 900°C. Bubble formation that prevented tar-char mixing was thought to be the main reason for the relatively low tar conversion.

Two cheap and proven alternatives to char is suggested: dolomite and olivine. Dolomite is a cheap mineral rock, $CaMg(CO_3)_2$ [31] that in fixed bed reactors can convert 95-99% of the tars at 800-900°C at similar residence times as for char [31][32]. It is also shown by e.g. Vassilatos et al. [33] that naphthalene is reduced up to 99% at 900°C. As it is for char, attrition is a challenge in fluid beds that therefore requires continuous feeding of dolomite to the reactor and increased dust cleaning equipment [34].
Oivine is similarly a cheap and widely applied mineral rock, $(MgFe)_2SiO_4$ [29]. Compared to dolomite, it has a lower, but still high catalytic activity at ≥800°C. It has a significantly higher mechanical strength than dolomite and char, and compares to that of sand [34] and is therefore a preferred catalyst for fluid bed.

Olivine might however not provide high reductions of heavier tars such as naphthalene, as Devi et al. [35] reported that olivine only reduced naphthalene 50-80% at 900°C and a residence time of 0.3 s.

The conversion steps can hence be schematically summarized into Figure 4.

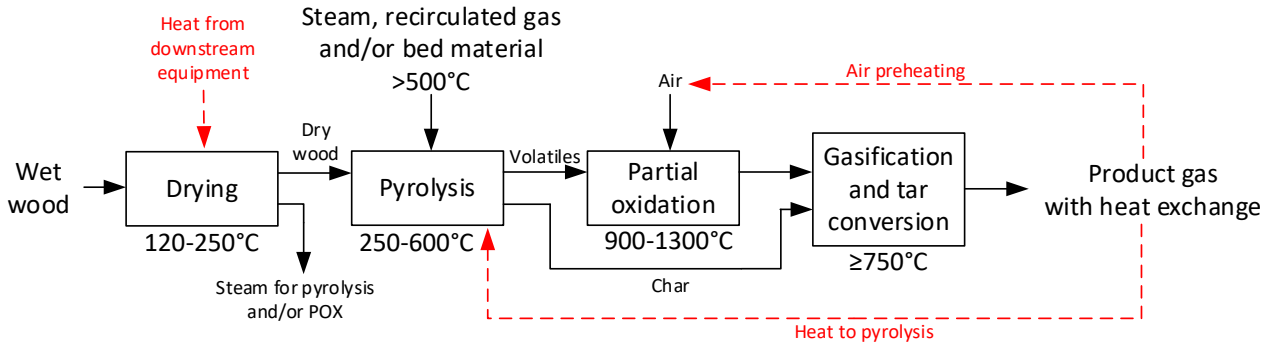

Figure 4 – Design basis for system design, shown as process diagram with process temperature ranges. Tar reduction can also be applied prior to or after the char gasification step.

Reactors

Based on a broad analysis of reactors in the >10MW_{th}-range, it is suggested to apply these reactors in the concepts: fixed bed downdraft and updraft, and fluid bed. Only a very short overview is given here.

Fixed beds offer very high gas-solid contact that is favorable for high tar and char conversion. Some of the drawbacks are limited tolerance to fines and at larger scales: 1) securing decent fuel distribution in the reactors and; 2) managing a potentially large grate area. While updraft reactors has been upscaled to hundreds of MW_{th} with coal, pressurization and use of oxygen [36][37], biomass-based systems should scale in the range of 5-90MW_{th} being suggested [38]. Downdraft reactors can be very efficient when coupled with a partial oxidation as tar and char conversion rates are very high at the entry point of the bed because of the high temperature. The main disadvantage of downdraft beds is their high intolerance to fines, as these can build up and cause large pressure drops. Updraft reactors are efficient as they has the advantage of processing the fuel in efficient countercurrent flow and being more tolerant to fines than the downdraft. At higher inlet temperatures, ash sintering and grate construction has to be considered, as the combination of physical and thermal stresses can cause mechanical collapse. A maximum inlet temperature should be set based on limited sintering, expected lifetime and stability – 950°C is suggested as feasible for this study.

In fluid beds, the fuel is processed in a bed with a large thermal capacity and it offers a very high level of mixing that a high process control. This enables the bed to process a wide range particle sizes and fuels [39], and allows scaling up to hundreds of MW_{th} [38]. Wood-based fluid beds operate typically at ≤900°C as the bed material can initiate agglomeration at this point [4][39][40][41]. The key drawback, as touched upon in the tar conversion-section, is the lesser gas-solid contact compared to fixed beds. This is namely due to the higher velocities and (potentially) bubbles in the beds, that causes char attrition and some degree of tar slip in the bubble phase [29]. This causes the carbon and tar conversion to be lower than fixed beds.

2.2 System designs

It was chosen to analyze two fixed and two fluid bed designs to effectively investigate the upscaling possibilities. Initially, the basic designs and constraints are discussed. Note that a steam dryer will be implemented, but are not shown here in the gasifier-centric design phase.

The fixed bed designs are shown in Figure 5. Both concept are based on a novel updraft pyrolysis reactor with gas recirculation that was identified as a promising subproces [11][42]. The countercurrent flow and recirculation of gas enables: 1) an effective heat exchange between gas and fuel; 2) does not cuase dilution of the pyrolysis gas and; 3) enables the use of various heat sources. The fuel is fed at the top of the reactor and is then processed through the reactor to at least 500°C to secure tar release [17]. The produced char is then transported to the gasifier, possibly with a screw conveyer. At the top of the pyrolysis reactor, it is vital that the temperature is high enough to suppress tar condensation – 250°C is chosen based on previous tests [42] that showed stable operation of a similar reactor at that temperature. Should the tars condense they will either form deposits on the reactor walls or the fuel, and can in turn form aerosols that can damage downstream equipment. The gaseous components from the reactor are then led through a blower that should overcome the pressure drop associated with the bed.

The Downdraft concept on Figure 5 (left) is primarily generated as a link to compare the current TwoStage gasifier design with the other systems, as it does not address the issue of increased fuel flexibility. At the top of the downdraft char reactor, a POX with preheated air will convert most of the tars and provide the necessary sensible heat for char conversion. This concept is expected to perform nearly identical to the current TwoStage gasifier. The Updraft concept on Figure 5 (right) is interesting as it more tolerant to fines. It does however have its limitations with regards to maximum inlet temperature to the char reactor at the grate. As a solution, a steam ejector is implemented to recirculate product gas to the hot POX gases before the gasifier grate via pressurized steam. This will ensure cooling for the grate and provide an increased steam content that will promote gasification reactions. The ejector does however also carry a penalty as a relatively ineffective component that has a significant heat demand for steam generation, but this will be limited as the pressure drop across the gasification reactor will be relatively low. With a high-temperature POX and subsequent high tar conversion from 950-750°C in the char bed, tar concentration are expected to be in the same range as the Downdraft concept.

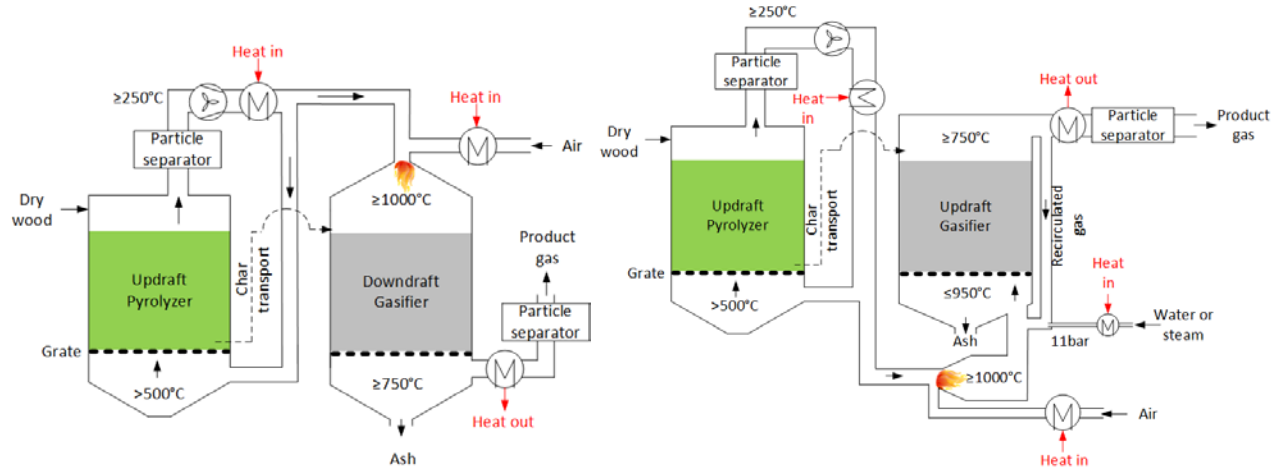

Figure 5 - Fixed bed designs. Left: Downdraft concept. Right: Updraft concept. Note that a drying system is not shown.

The designs for the fluid bed concepts are shown in Figure 6. As fluid bed reactors has significant advantages, it is desired to analyze if the proposed Updraft concept can be designed with fluid bed reactors and still maintain high efficiency and tar conversion – see Figure 6 (left). Fluid beds do however have a much higher pressure drop than fixed beds, which will increase blower consumption, as well as the steam consumption of the ejector. The pyrolysis reactor should operate at 500°C to ensure tar release, but this means that the gas entering the blower will be similiarly hot. This will stress the blower and will require specialized equipment[1]. After the pyrolysis, the gases are led to a POX, and then cooled by recirculated or other gas to 900°C to avoid agglomeration and sent through a fluid bed char gasifier. A steam source could prove to be more efficient for POX cooling than an ejector, as the larger pressure drop over the fluid bed will cause a high ejector steam consumption. The char transport from the pyrolysis reactor to the gasification reactor will likely be through a loop seal or similar that will transport the top char-rich layer with a minimum of sand as discussed in e.g. [43] – as a simplification this concept will not include bed material/heat transport between the reactors and hence assumes that pure char is transported to the gasifier.

In a more simple fluid bed design (Figure 6, right), the pyrolysis reactor is designed as a steam-blown fluid bed in order to avoid high-temperature blowers. Due to the increased heat capacity/steam content of the pyrolysis gases, the POX will be carried out at 900°C and led through a fixed dolomite bed in order to convert tars effectively and avoid cooling prior to the gasifier. This pyrolysis configuration will however have a relatively high steam consumption due to the smaller temperature difference from 700-500°C (heat exchange assumed limited by a 50°C pinch point between product gas at 750°C) and thus circulation of bed material between gasifier and pyrolyzer might very well be a more effective solution to limit the steam flow. The amount of bed material circulated should be a compromise between available downstream heat for steam generation and the heat demand for char gasification. Based on previous tests with POX [26][23][44][22], the tar concentration is estimated to 2-3g/Nm^3 at 900°C, and by assuming a 99% tar reduction over the dolomite bed a concentration around 20-30mg/Nm^3 is achived in the product gas.

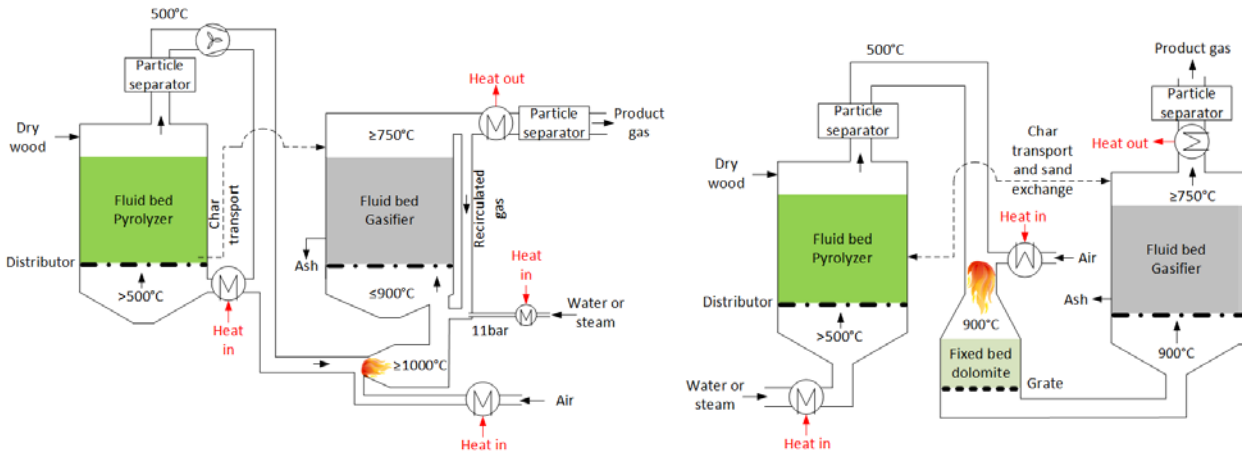

Figure 6 – Fluid bed designs. Left: Fluid bed recirculation concept. Right: Steam-blown fluid bed concept. Note that a drying system is not shown.

[1] Examples of high-temperature blowers can be found e.g. [66][67]

3. Modeling

The systems and all there components were modelled using zero-dimensional components in the DNA software [45][46]. Assumptions for the systems are listed in Table 2. The modeled systems are evaluated on their cold gas efficiencies, η_{cg}, and total effiencies, η_{total}, as seen in Equation 2 and Equation 3 – where *PG* denotes product gas and $\dot{W}$ is the electricity consumption of blowers.

Fuel	Wood chips with 50% moisture
Steam dryer	Inlet steam temp. 250°C, outlet steam temp. 120°C, 4wt% of the moisture remains in liquid state in the fuel (corresponding to a fuel moisture of 3.8wt%, pressureloss is 30mbar [42]
Pyrolyzer	Heat loss = 1% fuel input LHV, fixed bed pressure loss = 30mbar [42], fluid bed pressure loss = 146mbar[a], fixed and fluid bed volatiles are assumed to have a H_2 content of 20v% and 10v% respectively [44][47]
Gasifier	Heat loss = 1% fuel input LHV. Assumes that the water-gas shift reaction is in equilibrium at the outlet temperature. Carbon conversions are 99% and 95% for fixed [18] and fluid bed [19][40] models respectively. The methane content in the gas from the POX is assumed inert through the gasifier. Similar to the pyrolyzer the pressure loss is 146mbar[a]
Bed material recirculation	The flow is modeled as a heat flow from the gasifier to the pyrolyzer assuming that the bed material is sand (c_p=0.83kJ/(kg-°C)) and that the heat flow can be estimated via the temperature difference of the beds (outlet temperature).
Ejector	Assumed efficiency of 20% and 11bar motive pressure [48] and calculated via Equation 1 [49] (States 1 and 2 are the motive and gas fluid respectively and 3 is the resulting)
Heat exchangers	50K pinch point, 10mbar pressure loss, no heat loss
Blowers	40% isentropic efficiency, 95% combined mechanical and electrical efficiency

Table 2 – Main modeling parameters. [a]Calculated for a minimum fluidization conditions for a sand (density = 2600kg/m3) bed height of 0.95m with a distributor loss of 20%[40], voidage fraction of 50% [43] and a temperature of 700°C.

$$\eta_{ej} = \frac{\dot{V}_2 P_2 \ln(P_3/P_2)}{\dot{V}_1 (P_1 - P_3)}$$

Equation 1

$$\eta_{cg} = \frac{\dot{m}_{PG} \cdot LHV_{PG}}{\dot{m}_{fuel} \cdot LHV_{fuel}}$$

Equation 2

$$\eta_{total} = \frac{\dot{m}_{PG} \cdot LHV_{PG} - \dot{W}}{\dot{m}_{fuel} \cdot LHV_{fuel}}$$

Equation 3

3.1 Steam dryer

To optimize the systems, a steam drying unit is applied to all systems. The steam dryer features a loop of superheated steam at 250°C that heats the fuel to 120°C and evaporates the moisture using a screw conveyer, fixed bed, rotary drier or similar. By keeping these temperatures, only a few percentages of the organic matter will contaminate the steam [50]. The necessary heat for drying is not accounted for in these

designs, as it is expected that sufficient excess heat is available from the downstream gas conversion (e.g. gas engine or synthesis reactor) – this has been shown feasible up to 70% moisture in similar/related modeling studies [13][15][51].

3.2 Pyrolyzer

As the conditions are typically different in fixed and fluid beds, with slow and fast pyrolysis respectively, the pyrolysis model is adjusted to either fixed or fluid bed. The fixed and fluid bed processes are based on tests in [52] and [53] respectively, and compositions of biomass and char for the given studies are shown in Table 2. The composition of the released volatiles are calculated based on char yield and composition, by using mass balance for C,H,O,N and by assuming that pyrolysis is a balanced reaction (heating value in = heating value out).

Tars were not modeled as specific components of the volatiles, but are represented by methane (CH_4) and n-hexane (C_6H_{14}) – other compounds could have been chosen as well, but the study is simplified to these. The composition of the volatiles is therefore not the real gas composition, but a composition with the right heating value that satisfies the above mentioned atomic balances.

	C [wt%]	H [wt%]	O [wt%]	N [wt%]	S [wt%]	Ash [wt%]	Char yield [wt%]	HHV (dry) [MJ/kg]
Fixed bed								
Beech wood	48.1	6.40	44.8	0.08	0*	0.62	25	18.3
Char	90.7	2.10	4.53	0.22	0*	2.45	-	33.6
Fluid bed								
Beech wood	51.3	5.7	40.5	0.21	0	2.29	12	19.0
Char	57.0	3.30	20.3	0.40	0	19.0	-	20.9**

Table 3 – Measured composition of biomass and char for fixed and fluid bed pyrolysis. From [52] and [53]. *Under detection limit. **Calculated based on chemical composition via Equation 4 [54].

$$HHV = 0.3491C + 1.1783H + 0.1005S - 0.1034O - 0.0151N - 0.0211A\ [MJ/kg]$$

Equation 4

3.3 Partial oxidation

The POX is simulated via a premixing of reactants and a subsequent gibbs minimization reactor that produces a gas flow at a specified equilibrium outlet temperature – method described in [14][55]. The methane content after POX is calculated based on: 1) the methane content from pyrolysis, which is measured for dry pyrolysis gas to be 13.97vol% and 5.85vol% for slow and fast pyrolysis respectively [47], and 2) the temperature of the POX. Instead of calculating the methane content after POX directly, the methane content of the dry gas from pyrolysis is adjusted based on Equation 5. The adjusted methane content is then assumed inert through the POX. The equation results in a maximum slip of methane of 25% at a POX temperature of 900°C, and then a liniear reduction of the slip until the temperature reaches 1300°C [28][44]. At a POX temperature of 1300°C and above the methane content after POX is assumed to be zero.

$$\boldsymbol{vol\%_{CH4} = y \cdot 0.25 \frac{1300^0C - T}{1300^0C - 900^0C}}$$

Equation 5

, *y* is the methane content after pyrolysis (13.97vol% or 5.85vol%), *T* is the POX temperature which is defined between 900 C and 1300°C.

3.4 Gasifier

The char and POX gases are led to the gasification reactor, where the carbon conversion and outlet equilibrium temperature are given as input. The gas composition is calculated by chemical equilibrium via the water-gas shift reaction.

3.5 Auxiliary equipment

Pumps needed for pressurization of water for ejector and beds are neglegted, as their power consumption will be very small.

The particle filters and the dolomite bed (used in the Steam-blown concept) is assumed to be thermodynamically inert components with no heat flows, pressure drops, mass flow seperation or reactions taking place in the model. All fluid beds are assumed to be equipped with cyclone separators and are not shown – it is however assumed that the fluid bed concepts will require additional particle separation of the product gas following the heat exchangers (either via high-temperature ceramic filters or low-temperature bag filters).

3.6 Exergy

The exergy is calculated using the DNA software and is based on the method described in Bejan et al. [56]. The exergetic efficiencies for the gasifier system, η_{ex}, is described by Equation 6 – *PG* denotes productgas and $\dot{E}_{steam,dryer}$ is the exergy flow of the steam coming from the dryer. If it is assumed that saturated steam (instead of 20°C water) is available from the downstream equipment, then an exergetic efficiency, $\eta_{ex,evap}$, can be formulated via Equation 7 [2].

The reference state is T_0= 20°C and p_0 = 1bar. The exergy of the heat flows to or from the fluid, $\dot{E}_Q$, in the heat exchangers are estimated via the carnot efficiency at an average temperature T_{ave} of the fluid at the (in- and outlet) and the reference state T_0 [57] – see Equation 8.

$$\eta_{ex} = \frac{\dot{E}_{PG}}{\dot{E}_{fuel} + \dot{E}_{power} + \dot{E}_{air} + \dot{E}_{water} + \dot{E}_{steam,dryer}}$$

Equation 6

$$\eta_{ex,evap} = \frac{\dot{E}_{PG}}{\dot{E}_{fuel} + \dot{E}_{power} + \dot{E}_{air} + \dot{E}_{steam,dryer} + \dot{E}_{steam,ext}}$$

Equation 7

[2] This efficiency is added because the Updraft concept needs additional steam (besides that from the dryer) to drive its ejector. As the concept cannot generate the steam within the boundaries, saturated steam is supplied. The Steam-blown concept also requires additional steam, but can provide the necessary evaporation heat. This efficiency will therefore make these two concepts directly comparable, as it will substract the relatively large losses associated with the evaporation process in the Steam-blown concept, and allow them to compete on equal terms.

$$\dot{E}_Q = \dot{Q}\left(1 - \frac{T_0}{T_{ave}}\right)$$

Equation 8

4. Results and discussion

4.1 System performance

The 4 systems were modeled and optimized with regards to cold gas efficiency. The resulting flow sheets can be seen in Figure 7-10. Product gas compositions and efficiencies are given in Table 4 and Table 5, respectively.

The highest performance is achieved by the Downdraft and Updraft concepts, which is namely due to their expected due to their higher carbon conversion, input temperature tolerances and effective updraft pyrolyzer heat exchange. The updraft heat exchange lowers the recirculated flow significantly, which combined with the lower pressure drop and temperature results in 4-7 times lower blower consumption compared to the Fluid bed recirculation concept. The POX temperatures are high for both fixed bed designs and will for the Downdraft concept result in almost complete conversion of tars prior to the gasifier. If required, the POX temperatures can be modified by adjusting the steam purge of the dryer. This effect enables the use of alternative gasification reactor types (e.g. fluid beds) that might not obtain the same tar conversion, but has other operational advantages. It is seen that the cold gas efficiencies of both fixed bed concepts are similar to that of the current TwoStage gasifier.

The Updraft concept has a penalty with regards to inlet temperatures of the gasification reactor and the cooling driven by the ejector is seen to be very energy intense because of a high steam consumption. The heat required to generate the ejector steam corresponds to approximately a third of the steam dryer heat consumption. However, the evaporation heat needed by the ejector can be removed in several ways: 1) by redirecting the drying steam so that it cools the POX gas prior to the ejector, which will allow the product gas to generate the necessary steam, but reduces the cold gas efficiency by 3.1%; 2) by compressing the drying steam and using it as the automotive fluid in the ejector, which increases the cold gas efficiency by 1.8%, but also requires 0.7MW_e consumption and a specially build compressor [3]; 3) by utilizing downstream, cooled and slightly compressed product gas as the ejector motive fluid. The heat needed for ejector steam generation is however assumed to be available in the downstream equipment as assumed for the steam dryer (see Section 3.1), but the chosen scenario should depend on the specific application applied. The high external heat demand of the Updraft concept could impact the total plant efficiency if the downstream gas conversion (to electricity or fuel) produces to little waste heat to cover the demand.

[3] The compressor is assumed to utilize drying steam at 120°C and a discharge temperature of 350°C at 5.2bar (example shown in [68]) with an isentropic efficiency of 80%.

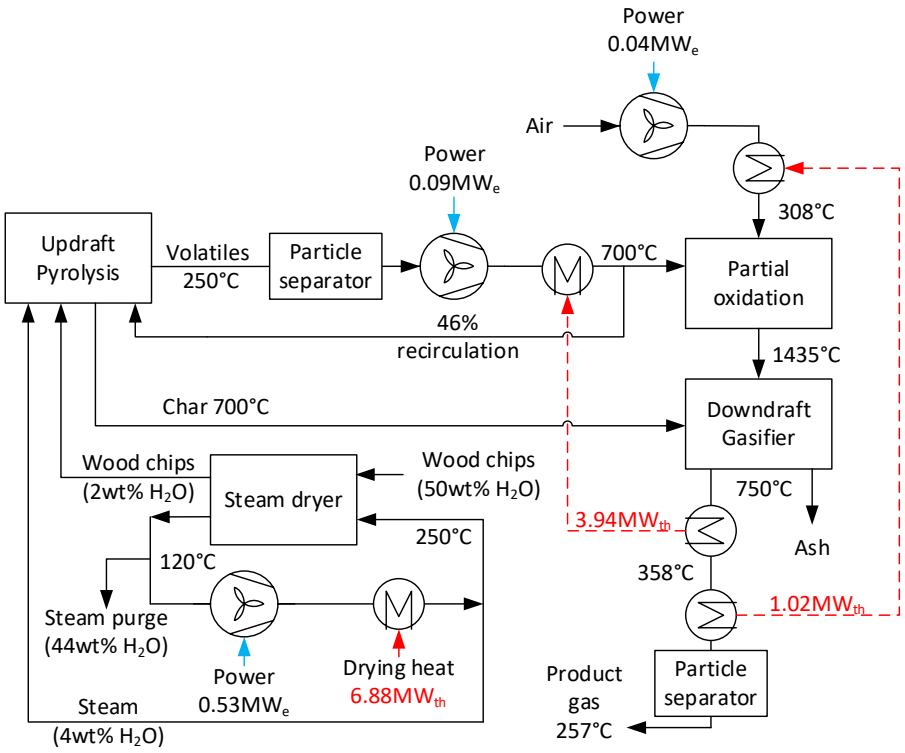

Figure 7 – Model of 50MW$_{th}$ (dry basis) Downdraft concept with relevant state values.

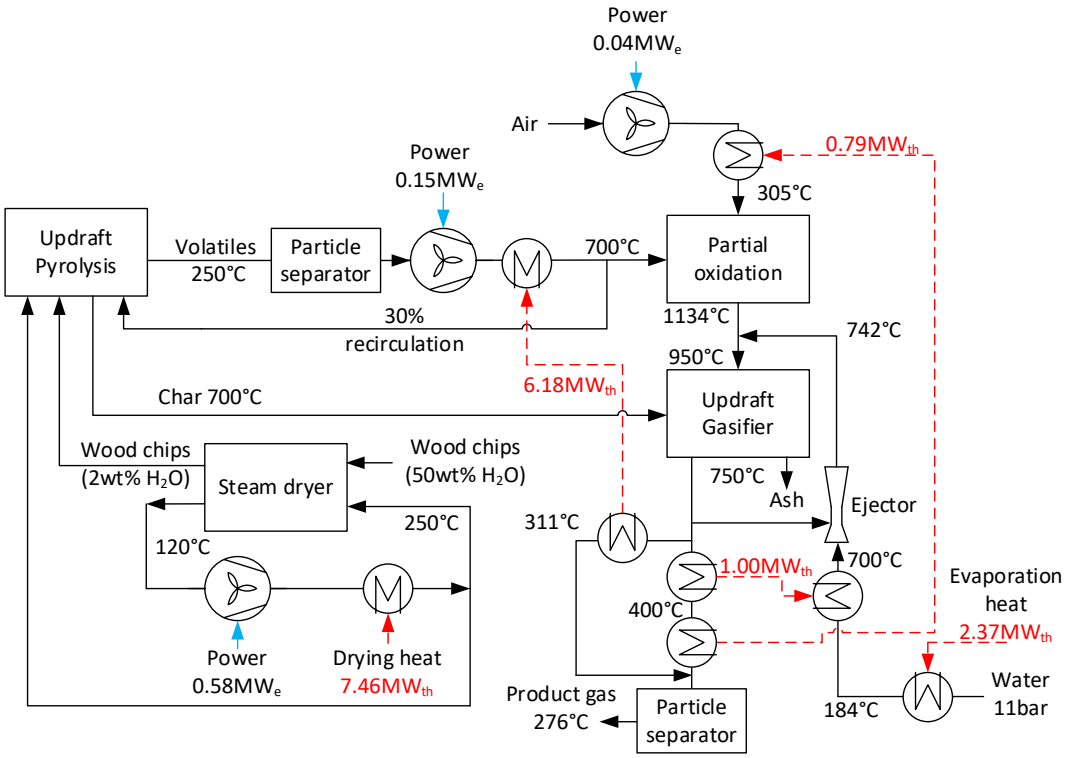

Figure 8 - Model of 50MW$_{th}$ (dry basis) Updraft concept with relevant state values and energy flows

The Fluid bed recirculation concept is seen to achieve a lower cold gas efficiency than the Updraft concept. And while no additional heat is needed - as the drying steam is sufficient for cooling the POX gas – the

system is especially limited by the pyrolysis unit. The applied temperatures here stresses the blower, require a large recirculating flow of gas and causes the product gas temperature to be higher than the 750^{o}C that is applied in the other designs – all of which will lead to lower efficiency. Due to the lower char yield, the POX is significantly cooler than the fixed bed concepts. It is estimated that the tar concentration will be between the ones used for the Updraft and Steam-blown fluid bed concepts: 1.2-2.0g/Nm^3. Hence it is suggested to utilize olivine in the char gasifier bed in order to reduce the tar content – a conservative 50% tar conversion is projected [35], which will result in 0.6-1.0g/Nm^3 that can be removed by using e.g. active carbon filters as shown with LT-BIG concept [4] or a guard bed as proposed with the Steam-blown concept below. In order to heighten the POX temperature, measures to increase the char yield could be considered. The efficiency of the concept could be improved by preheating the steam used for quenching: heating to 380^{o}C by heat exchange with the product gas, increases the cold gas efficiency by 0.5%-points, but is not chosen in order to lower costs/complexity. The product gas do contain enough energy to provide the necessary heat for evaporating the quenching steam (≈2.3MW$_{th}$ can be found by cooling to 179^{o}C), which could cause the concept to utilize fuels with lower moisture contents or by using dry fuels and removing the steam dryer. It should however be noted that a certain tar level is expected, which could limit the use of low-temperature heat exchangers.

The Steam-blown fluid bed concept differs from the other concepts, as no gas recirculation or high-temperature POX is applied. This high steam content causes the heat flows within the systems to be high. The high steam flow is however beneficial when applying tar catalysts and converting char, but causes significant losses in the heat exchange. This is especially true for the unmatched temperatures in the evaporator. In order to minimize the steam flow, the concept is optimized by letting a heat flow run from the gasifier to the pyrolyzer – which is achived by bed material (sand) circulating between the two reactors – where the sand temperature is assumed equal to the product gas temperature. The high steam requirement might be covered entirely by the steam dryer if a fuel with sufficient moisture is used. The Steam-blown concept achieves the lowest cold gas efficiency, but because of the lack of a high-temperature blower, the total efficiency is in range of the Fluid bed recirculation concept. If the electricity consumption in the Fluid bed recirculation concept is converted to chemical energy by assuming a 50% electric efficiency, the total efficiencies of the two fluid bed concepts are practically equal. The Steam-blown concept could therefore be relevant to use in a large highly efficient power plant, because of the more simple design compared with the Fluid bed recirculation concept.

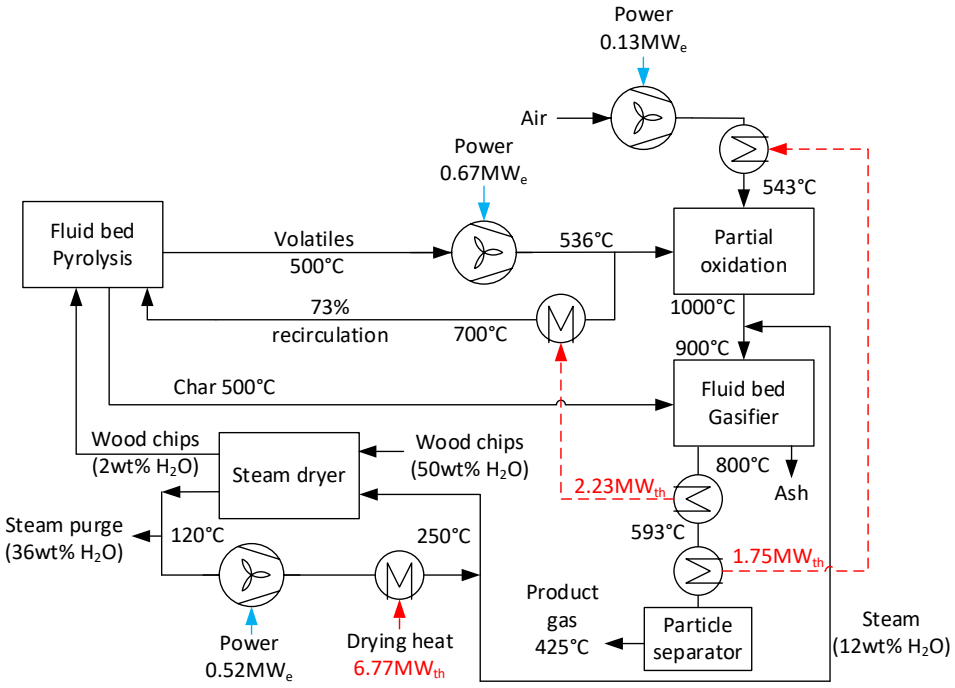

Figure 9 - Model of 50MW_{th} (dry basis) Fluid bed recirculation concept with relevant state values.

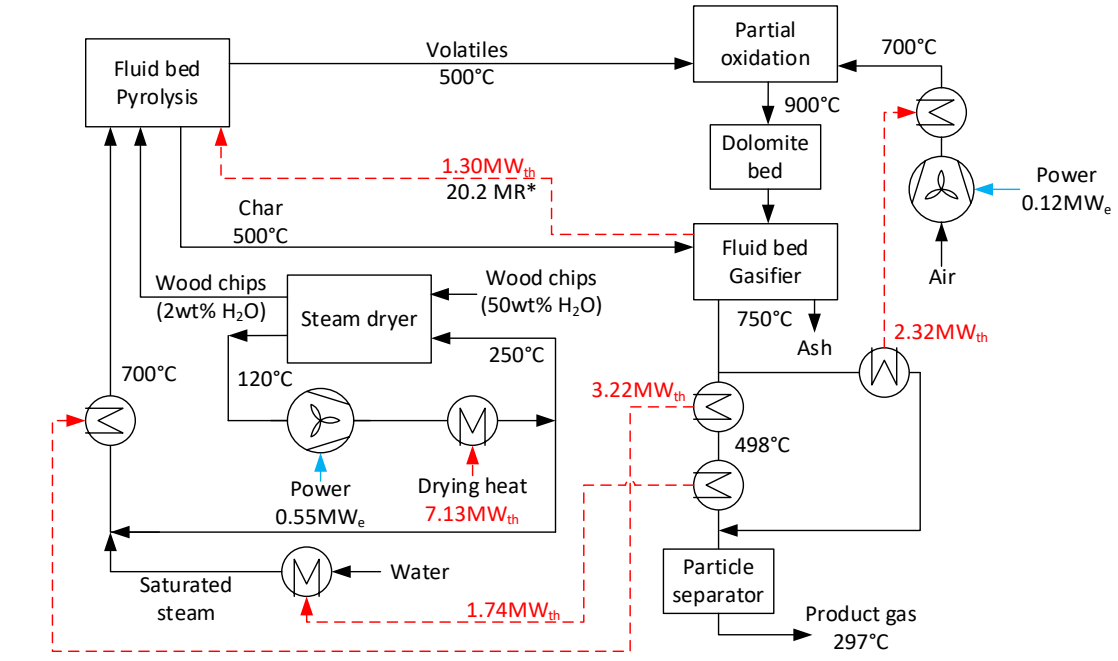

Figure 10 – Model of 50MW_{th} (dry basis) Steam-blown fluid bed concept with relevant state values. *Mass Ratio of sand-to-char from pyrolysis - bed material mass flow calculated based on the 1.30MW_{th} heat flow from gasifier to pyrolyzer with bed temperatures of 750°C and 500°C respectively and assuming sand as bed material.

	H_2 [vol%]	CH_4 [vol%]	CO [vol%]	CO_2 [vol%]	N_2 [vol%]	H_2O [vol%]	LHV_{wet} [MJ/kg]	LHV_{dry} [MJ/kg]

Downdraft	29.2	0.0	29.0	6.5	30.0	5.0	7.27	7.61
Updraft	28.2	0.7	9.0	13.5	16.2	32.2	5.07	7.20
Fluid bed recirculation	26.9	0.9	24.6	8.8	29.5	8.9	6.63	7.16
Steam-blown fluid bed	25.5	1.0	8.9	13.9	20.2	30.2	4.65	6.33

Table 4 – Gas compositions and LHV's for the 4 designs.

	η_{cg} [%]	η_{total} [%]	η_{ex} [%]	$\eta_{ex,evap}$ [%]
Downdraft	93.4	92.1	84.9	84.9
Updraft	92.6*	91.1*	84.4*	84.4
Fluid bed recirculation	87.9	85.2	81.5	81.5
Steam-blown fluid bed	84.7	83.4	79.6	80.9

Table 5 – Cold gas, total and exergetic efficiencies of the concepts (see definitions in section 3). All concepts assume that low-temperature heat for drying is availbale from downstream gas conversion (to electricity or fuel) *The updraft concept assumes that additional low-temperature heat is availbale from downstream gas conversion to satisfy the steam consumption of the ejector.

4.2 Exergy analysis

An overview of the exergy flows are shown for each concept in Sankey-diagrams in Figure 11 and the exergy efficiencies were given in Table 5. If the concepts are ranked in terms of exergy efficiency, it can be seen that the Downdraft concept has the highest efficiency and the Steam-blown fluid bed the lowest. This is the same order as when ranking the concepts in terms of energy efficiencies. It is however seen, that if the Steam-blown fluid bed is allowed to use externally generated steam as the Updraft concept, then the two fluid beds are practically equal ($\eta_{ex,evap}$). This stresses the need to: 1) optimize the water evaporator heat exchange; or 2) limit the use of steam by adding heat to the pyrolysis unit in alternative ways for the Steam-blown concept. Comparing the exergetic efficiencies for all the systems, the ash/char fraction from the gasifier is seen to be the key factor, as the fluid bed concepts have a efficiency penalty of around 3.3% compared to the fixed beds because of the lower carbon conversion (99% vs 95%). Thus, if char is considered a valued product the efficiencies are practically equal across the four concepts.

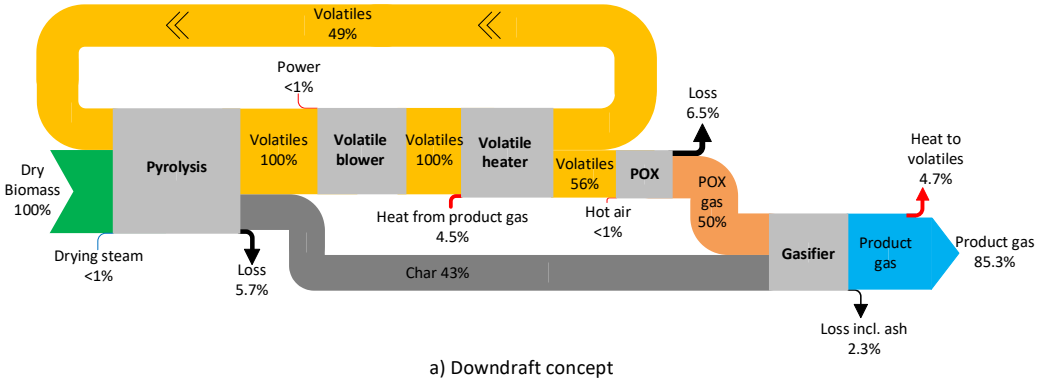

a) Downdraft concept

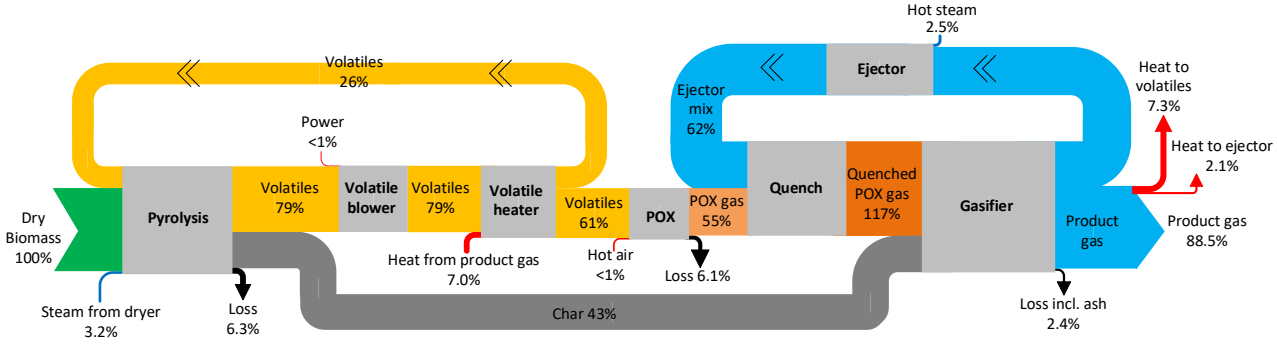

b) Updraft concept

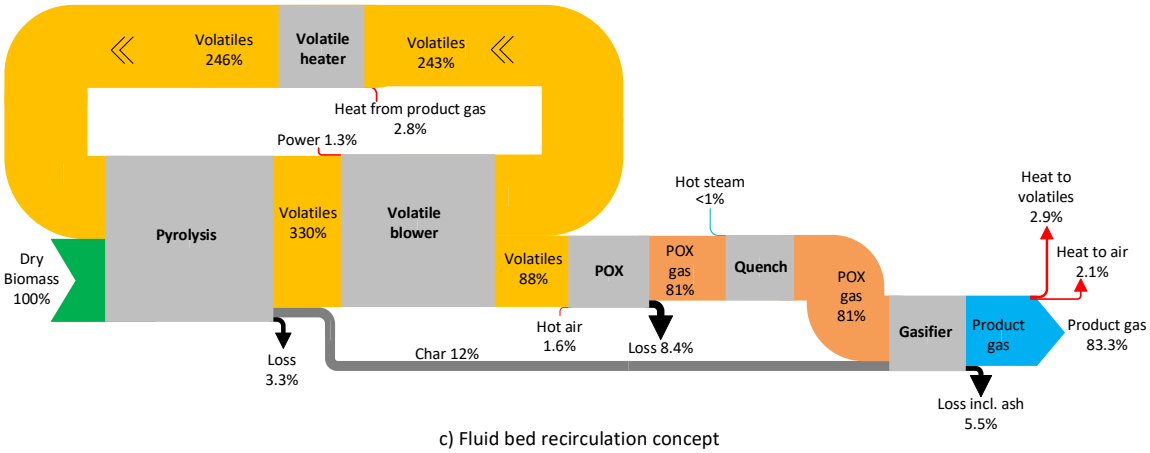

c) Fluid bed recirculation concept

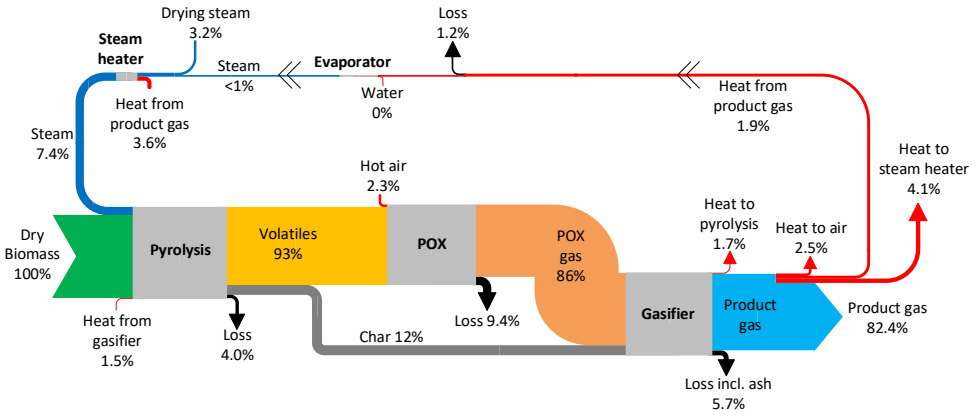

d) Steam-blown fluid bed concept

Figure 11 – Sankey diagram of exergy flows in the concepts. Losses and heat flows under 1% not shown. Note that the visual scaling of the recirculating volatiles in the Fluid bed recirculation concept (c) has been modified to compress the figure.

The three main losses in all of the concepts are the pyrolyzer, POX and gasifier which are responsible for 89-95% of all losses. The efficiency (inputs to outputs) for all three subprocesses are shown in Figure 12. It is clear that most of the exergy is destroyed in the POX. While the Downdraft concept provide the lowest POX efficiency, the fixed beds achieve lower absolute POX losses, due to smaller gas flows (via lower volatile yield) through the subprocess. This indicates that pyrolysis gases should be diluted as little as possible prior to the oxidation and that a higher char yield could prove more feasible.
The fluid bed pyrolysis is seen to be slightly more effective than the fixed bed version, likely because of the larger fuel conversion that the high heating rate causes.
The gasifier losses of the fixed beds are minor compared to the fluid beds, as the realtively small difference in carbon conversion and reactor types are seen to be the determining. Thus it will be up to the operator whether the ash/char is considered a product or not when evaluating the gasifier systems.

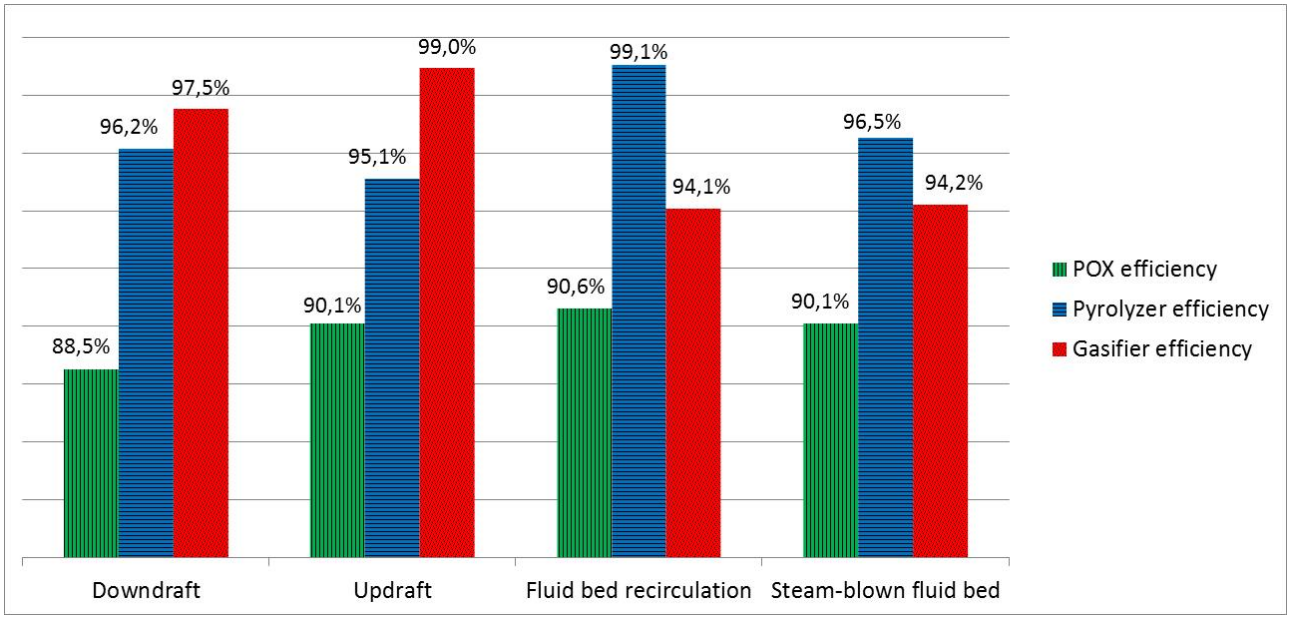

Figure 12 - Exergetic efficiencies of selected subprocesses

4.3 Perspectives

The 4 concepts are designed for medium to large scale (10-100 MW_{th}), for high cold gas efficiency with limited gas cleaning requirements. The concept efficiencies, expected tar concentrations and complexity of gas cleaning are given in Table 6 and compared with the Viking gasifier, LT-BIG and relevant medium- and large-scale state-of-the-art gasifiers. The designed concepts, along with the Viking gasifier, are seen to have a cold gas efficiencies that are 6-22%-points higher, while only applying little gas cleaning. The Steam-blown and the recirculation fluid bed concepts outperform the other direct air-blown fluid bed gasifiers: LT-BIG and Skive – of which the Skive gasifier utilizes extensive gas cleaning, but on the other hand only employs a single reactor for fuel conversion. The indirect gasifiers MILENA and FICFB produces a nitrogen-free product gas, but with the penalty of significantly lower efficiency and more complex gas cleaning. The Carbo-V

process is build on some of the same principles as the TwoStage gasifier by using separate pyrolysis and gasification and a POX, but lacks the heat integration by not using the hot product gas for heating the pyrolysis. While the designs does not compare directly to several of the state-of-the-art gasifiers, the developed designs can be technically feasible for the medium-large-scale market.

	η_{cg}	Tar content	Gas cleaning	Reference
Downdraft	93.4%	0.1mg/Nm^3	• Particle filter	This study
Updraft	92.6%	0.1mg/Nm^3	• Particle filter	This study
Fluid bed recirculation	87.9%	1mg/Nm^3	• Active carbon filter • Particle filter	This study
Steam-blown fluid bed	84.7%	4-6mg/Nm^3	• Dolomite reactor • Particle filter	This study
TwoStage Viking gasifier (moving and fixed bed)	87-90%[a]	0.1mg/Nm^3	• Particle filter	[5][58]
LT-BIG (fluid beds)	81%	1mg/Nm^3	• Active carbon filter • Particle filter	[15]
Skive gasifier (fluid bed)	77%[b]	Dew point <30^{o}C	• Dolomite bed material • Tar reformer • Particle filter • Scrubber	[59]
MILENA gasifier (fluid beds)	78%	25-63mg/Nm^3	• Catalytic bed material • Scrubber • Particle filter	[60][61]
FICFB (fluid beds)	55-75%	20mg/Nm^3	• Catalytic bed material • Scrubber • Particle filter	[3][62]
Carbo-V (moving bed and entrained flow)	49[a]-71%	Below detection limit	• Scrubber	[63]

Table 6 – Comparison of cold gas efficiencies and gas cleaning of the TwoStage gasifier concept to relevant medium- and large-scale systems. Tar concentrations and dew points are after gas cleaning. [a]Experimental data (dry basis). [b]Based on 19.5MW$_{th}$ and 6MW$_e$ assuming 40% gas-to-power engine efficiency [64].

While the fixed bed concepts achieve the highest performance parameters and the Updraft concept has some fuel flexibility with regards to particle size, the fluid bed concepts will be much more fuel flexible and are therefore of special interest for further optimization, as especially medium-scale (and possibly large-scale) systems will likely require local and low-value biomass to be competitive [65]. Especially if the ash/char is considered a valued product.

As the gas quality with regards to tars and inorganics is expected to be relatively high when using wood, the gas is most likely suited for processes that require such a quality, such as chemical synthesis, fuel cell and gas turbine/combined cycle plants. In order to gain more insight into the market possibilities and applications it would be ideal to investigate the concepts further. Points of interest are:

- Providing a higher level of detail of the physical design: char transport mechanisms between reactors; dimensioning of reactors etc.

- Converting the concepts to oxygen-blown operation to avoid nitrogen dilution which lowers the cost of liquid fuel synthesis and enables production of synthetic natural gas.
- The technical feasibility of using alternative and cheap fuels with low ash-sintering temperatures such as straw.

5. Conclusions

Designs of upscaled TwoStage gasifiers with very high tar conversion and efficiencies has been presented, modeled and evaluated on energy and exergy basis. With relatively simple measures and components, the 4 concepts have shown excellent efficiencies including cold gas efficiencies of 84.7-93.4% and low expected tar levels using only limited gas cleaning. Especially interesting is the 1) favourable performance of pyrolysis applied with gas recirculation that allow an effective heat exchange between fuel and product gas, while minimizing dilution of the pyrolysis gas; and 2) the integration of a steam drying unit that can either function as a fluidization medium or partial oxdation quench and allow effective heat integration and high-temperature tar conversion, respectively. The use of partial oxidation is a very effective meaure to reduce tars and the hot gas is effectively used for the endothermic char conversion, which also reduces the tar content even further. Several options for integrating the hot product gas in the pyrolysis and partial oxdidation has been presented, with the use of drying steam or recirculated gas proving to be effective. The 4 designs are still in an early development phase, but an overview of large-scale state-of-the-art gasifiers indicates that the high-performing systems can be technically feasible in the medium- and large-scale market.

6. Ackknowledgements

The authors would like to thank the ForskVE-programme of Energinet.dk for financial support through the Biomass Gasification Polygeneration project (ForskVE-12205).

7. References

[1] Ahrenfeldt J, Thomsen TP, Henriksen U, Clausen LR. Biomass gasification cogeneration - A review of state of the art technology and near future perspectives. Appl Therm Eng 2013;50:1407–17. doi:10.1016/j.applthermaleng.2011.12.040.

[2] Fjellerup J, Ahrenfeldt J, Henriksen U, Gøbel B. Formation, decomposition and cracking of biomass tars in gasification. 2005.

[3] Hofbauer H, Rauch R. Stoichiometric Water Consumption of Steam Gasification by the FICFB-Gasification Process. Prog Thermochem Biomass Convers 2008:199–208. doi:10.1002/9780470694954.ch14.

[4] Knoef H, editor. Handbook Biomass Gasification. BTG biomass technology group; 2005.

[5] Ahrenfeldt J, Henriksen UB, Jensen TK, Gøbel B, Wiese L, Kather A, et al. Validation of a continuous combined heat and power (CHP) operation of a Two-Stage biomass gasifier. Energy & Fuels 2006;20:2672–80.

[6] Gadsbøll RØ, Sarossy Z, Jørgensen L, Ahrenfeldt J, Henriksen UB. Oxygen-blown operation of the TwoStage gasifier. Energy 2018. doi:10.1016/j.energy.2018.06.071.

[7] Henriksen U, Ahrenfeldt J, Jensen TK, Gøbel B, Bentzen JD, Hindsgaul C, et al. The design, construction and operation of a 75 kW two-stage gasifier. Energy 2006;31:1542–53. doi:10.1016/j.energy.2005.05.031.

[8] Gadsbøll RØRØ, Thomsen J, Bang-Møller C, Ahrenfeldt J, Henriksen UBUB. Solid oxide fuel cells powered by biomass gasification for high efficiency power generation. Energy 2017;131:198–206. doi:10.1016/j.energy.2017.05.044.

[9] Ahrenfeldt J, Thomsen TP, Henriksen U, Clausen LR. Biomass gasification cogeneration – A review of state of the art technology and near future perspectives. Appl Therm Eng 2013;50:1407–17. doi:10.1016/j.applthermaleng.2011.12.040.

[10] Bentzen JD, Hummelshøj R, Henriksen UB, Gøbel B, Ahrenfeldt J, Elmegaard B. Upscale of the Two-Stage Gasification. Proc. 2nd world Conf. Technol. Exhib. biomass energy Ind., 2004.

[11] Houmøller S, Hansen M, Henriksen UB. Two-Stage Fluid Bed Pyrolysis and Gasification Unit. 9th Eur. Bioenergy Conf., Elsevier; 1996, p. 1347–52.

[12] Clausen LR, Elmegaard B, Ahrenfeldt J, Henriksen U. Thermodynamic analysis of small-scale dimethyl ether (DME) and methanol plants based on the efficient two-stage gasifier. Energy 2011;36:5805–14. doi:10.1016/j.energy.2011.08.047.

[13] Clausen LR. Energy efficient thermochemical conversion of very wet biomass to biofuels by integration of steam drying, steam electrolysis and gasification. Energy 2017;125:327–36. doi:10.1016/j.energy.2017.02.132.

[14] Bang-Moeller C. Design and Optimization of an Integrated Biomass Gasification and solid oxide fuel cell system. Technical University of Denmark, 2010.

[15] Andersen L, Elmegaard B, Qvale B, Henriksen U. Modeling the low-tar BIG gasification concept. Proc. 16. Int. Conf. Effic. Cost, Optim. Simulation, Environ. Impact Energy Syst., 2003, p. 7.

[16] Fock F, Thomsen K. Optimering af koncepter for medstrømsforgasning. Technical university of Denmark, 2000.

[17] Ahrenfeldt J, Henriksen UB, Gøbel B, Fjellerup J. Experimental characterisation of residual-tar in wood char. 2005.

[18] Gøbel B, Henriksen U, Ahrenfeldt J, Jensen TK, Hindsgaul C, Bentzen JB, et al. Status - 2000 Hours of Operation with The Viking Gasifier 2003:3–6.

[19] Thomsen TP, Sárossy Z, Gøbel B, Stoholm P, Ahrenfeldt J, Jappe F, et al. Low temperature circulating fluidized bed gasification and co-gasification of municipal sewage sludge . Part 1 : Process performance and gas product characterization. Waste Manag 2017;66:123–33. doi:10.1016/j.wasman.2017.04.028.

[20] Brandt P, Henriksen U. Decomposition of tar in pyrolysis gas by partial oxidation and thermal cracking. Part 2. Proc Conf 10th Eur Conf Technol Exhib Biomass Energy Ind 1998:1616–9.

[21] Su Y, Luo Y, Chen Y, Wu W, Zhang Y. Experimental and numerical investigation of tar destruction under partial oxidation environment. Fuel Process Technol 2011;92:1513–24. doi:10.1016/j.fuproc.2011.03.013.

[22] Zhao S, Luo Y, Zhang Y, Long Y. Experimental investigation of the synergy effect of partial oxidation and bio-char on biomass tar reduction. J Anal Appl Pyrolysis 2015;112:262–9. doi:10.1016/j.jaap.2015.01.016.

[23] Ahrenfeldt J, Egsgaard H, Stelte W, Thomsen T, Henriksen UB. The influence of partial oxidation mechanisms on tar destruction in TwoStage biomass gasification. Fuel 2013;112:662–80. doi:10.1016/j.fuel.2012.09.048.

[24] Wu WG, Luo YH, Chen Y, Su Y, Chen L, Wang Y. Experimental Investigation of Tar Destruction Under Partial Oxidative Condition in a Continuous Reactor 2011:900.

[25] Bentzen JD, Hummelshøj R, Henriksen U, Ahrenfeldt J. Storskala trinopdelt forgasning. 2004.

[26] Brandt P, Larsen E, Henriksen U. High tar reduction in a two-stage gasifier. Energy and Fuels 2000;14:816–9. doi:10.1021/ef990182m.

[27] Gerun L, Paraschiv M, Vîjeu R, Bellettre J, Tazerout M, Gøbel B, et al. Numerical investigation of the partial oxidation in a two-stage downdraft gasifier. Fuel 2008;87:1383–93. doi:10.1016/j.fuel.2007.07.009.

[28] Brandt P, Henriksen U. Decomposition of tar in gas from updraft gasifier by thermal cracking. 1st World Conf Biomass Energy Ind 2000:3.

[29] El-Rub A, Kamel Z. Biomass char as an in-situ catalyst for tar removal in gasification systems. Twente university, 2008.

[30] Fuentes-Cano D, Gómez-Barea A, Nilsson S, Ollero P. Decomposition kinetics of model tar compounds over chars with different internal structure to model hot tar removal in biomass gasification. Chem Eng J 2013;228:1223–33. doi:10.1016/j.cej.2013.03.130.

[31] Dayton D. A review of the literature on catalytic biomass tar destruction. Natl Renew Energy Lab 2002:28. doi:10.2172/15002876.

[32] Delgado J, Aznar MP, Corella J. Biomass gasification with steam in fluidized bed: effectiveness of CaO, MgO, and CaO-MgO for hot raw gas cleaning. Ind Eng Chem Res 1997;36:1535–43. doi:10.1021/ie960273w [doi].

[33] Vassilatos V, Taralas G, Sjostrom K, Bjornbom E. Catalytic cracking of tar in biomass pyrolysis gas in the presence of calcined dolomite. Can J Chem Eng 1992;70:1008–13.

[34] Devi L, Ptasinski KJ, Berends RH, Padban N, Beesteheerde J, Veringa HJ. Primary measures to reduce tar formation in fluidised-bed biomass gasifiers. 2004.

[35] Devi L, Craje M, Thüne P, Ptasinski KJ, Janssen FJJG. Olivine as tar removal catalyst for biomass gasifiers: Catalyst characterization. Appl Catal A Gen 2005;294:68–79. doi:10.1016/j.apcata.2005.07.044.

[36] Corporation AS. Industrial Size Gasification Applications Using the BGL 1000 Gasifier Module. Ind. Size Gasif. Appl. Using BGL 1000 Gasifier Modul., 2006, p. 1–22.

[37] Phillips J. Different types of gasifiers and their integration with gas turbines. Gas Turbine Handb 2006:67–77.

[38] International Renewable Energy Agency. Renewable energy technologies: cost analysis series.

Biomass for Power Generation. 2012.

[39] Basu P. Biomass Gasification, Pyrolysis and Torrefraction. Second Edi. Dalhouse University: Elsevier Inc.; 2013.

[40] Basu P. Combustion and gasification in fluidized beds. Taylor & Francis; 2006.

[41] Ohman M, Pommer L, Nordin A. Bed Agglomeration Characteristics and Mechanisms during Gasification and Combustion of Biomass Fuels. Energy & Fuels 2005;19:1742–8.

[42] Jensen TK, Maigaard P, Noes J. Pyrolyse af træflis ved recirkulering af pyrolysegas. 1996.

[43] Kunii D, Levenspiel O. Fluidization Engineering. 2nd ed. Butterworth-Heinemann; 1991.

[44] Iversen HL, Ahrenfeldt J, Egsgaard H, Henriksen UB. Partial oxidation mechanisms of tar destruction [Confidential]. 2006.

[45] Elmegaard B, Houbak N. DNA – A General Energy System Simulation Tool. DNA – A Gen. Energy Syst. Simul. Tool, SIMS 2005 and Tapir Academic Press; 2005, p. 43–52.

[46] Technical University of Denmark. Homepage of the thermodynamic simulation tool DNA. DNA - A Therm Energy Syst Simulator 2009. http://orbit.dtu.dk/en/publications/id(b76040a4-5a29-4b04-a898-12711391c933).html (accessed March 24, 2017).

[47] Thomsen T, Hauggaard-Nielsen H, Bruun E, Ahrenfeldt J. the potential of pyrolysis technology in climate change mitigation. 2011.

[48] GEA Wiegand GmbH. GEA product catalogue. Jet pumps, mixers, heater, vacuum systems. 2017. doi:10.1002/ejoc.201200111.

[49] Wendel CH, Kazempoor P, Braun RJ. Novel electrical energy storage system based on reversible solid oxide cells : System design and operating conditions. J Power Sources 2015;276:133–44. doi:10.1016/j.jpowsour.2014.10.205.

[50] Svoboda K, Martinec J, Pohořelý M, Baxter D. Integration of biomass drying with combustion/gasification technologies and minimization of emissions of organic compounds. Chem Pap 2009;63:15–25. doi:10.2478/s11696-008-0080-5.

[51] Sigurjonsson HÆ, Clausen LR. Solution for the future smart energy system: A polygeneration plant based on reversible solid oxide cells and biomass gasification producing either electrofuel or power. Appl Energy 2018;216:323–37. doi:10.1016/j.apenergy.2018.02.124.

[52] Gøbel B. Dynamisk modellering af forgasning i fixed koksbed. Technical University of Denmark, 1999.

[53] Trinh TN, Jensen PA, Kim DJ, Knudsen NO, Sørensen HR, Hvilsted S. Comparison of lignin, macroalgae, wood, and straw fast pyrolysis. Energy and Fuels 2013;27:1399–409. doi:10.1021/ef301927y.

[54] Channiwala SA, Parikh PP. A unified correlation for estimating HHV of solid , liquid and gaseous fuels. Fuel 2002;81:1051–63.

[55] Elmegaard B. Simulation of boiler dynamics - Development, evaluation and application of a general energy system simulation tool. Technical University of Denmark, 1999.

[56] Bejan A, Tsatsaronis G, Moran M. Thermal design & optimization. John Wiley & sons Ltd; 1996.

[57] Kotas TJ. The exergy method of thermal plant analysis. First edit. Exergon publishing company UK Ltd; 2012.

[58] Bentzen JD, Brandt P, Gøbel B, Henriksen UB, Hindsgaul C. Optimering af 100 kW totrinsforgasningsanlæg på DTU: Resultater fra forsøg i uge 37 1998. 1999.

[59] Andritz, Carbona. Carbona Gasification Technologies - Biomass Gasification Plant in Skive. October 2010:28–9.

[60] Meijden CM van der, Veringa HJ, Vreugdenhil BJ, Drift B van der. Bioenergy II: Scale-Up of the Milena Biomass Gasification Process. Int J Chem React Eng 2009;7. doi:10.2202/1542-6580.1898.

[61] Rhyner U, Kienberger T, Zuber C, Schildhauer TJ, Rabou LPLM, Van der Drift B, et al. Synthetic Natural Gas from Coal, Dry Biomass, and Power-to-Gas Applications. First edit. John Wiley & sons Ltd; 2016. doi:10.1002/9781119191339.

[62] Hofbauer H, Rauch R, Loeffler G, Kaiser S, Fercher E, Tremmel H. Six years experience with the FICFB-gasification process. 12th Eur Conf Technol Exhib Biomass Energy, Ind Clim Prot 2002:982–985.

[63] Bundesministerium für Ehrnärung Landwirtschaft und Verbraucherschutz. Schriftenreihe “Nachwachsende Rohstoffe”. Band 29. Analyse und Evaluierung der thermo-chemischen Vergasung von Biomass. 2006.

[64] Jenbacher type 6 gas engines n.d. https://powergen.gepower.com/products/reciprocating-engines/jenbacher-type-6.html (accessed March 29, 2017).

[65] International Energy Agency. Technology Roadmap - Bioenergy for Heat and Power. 2012.

[66] Spencerturbine.com. Spencer - custom blowers and gas boosters for air and gas handling applications n.d. http://www.spencerturbine.com/wp-content/uploads/2014/11/510C_Spencer_Custom-Blowers-and-Gas-Boosters.pdf (accessed June 12, 2018).

[67] Illinoisblower.com. Illinois blower product offerings n.d. http://www.illinoisblower.com/content/product-line-offering (accessed June 12, 2018).

[68] Siemens. Siemens Process Compressors n.d. http://m.energy.siemens.com/us/pool/hq/compression/downloads/Portfolio_Compressor_EN.pdf (accessed May 11, 2017).